This is to certify that the
thesis entitled

INSIGHTS INTO *ACTINOBACILLUS SUCCINOGENES*
FERMENTATIVE METABOLISM

presented by

James B. McKinlay

has been accepted towards fulfillment
of the requirements for the

Ph.D. degree in Microbiology and Molecular Genetics

Major Professor's Signature

12/13/06

Date

MSU is an Affirmative Action/Equal Opportunity Institution

DATE DUE	DATE DUE	DATE DUE

INSIGHTS INTO *ACTINOBACILLUS SUCCINOGENES* FERMENTATIVE METABOLISM

By

James B. McKinlay

A DISSERTATION

Submitted to
Michigan State University
in partial fulfillment of the requirements
for the degree of

DOCTOR OF PHILOSOPHY

Department of Microbiology and Molecular Genetics

2006

ABSTRACT

INSIGHTS INTO *ACTINOBACILLUS SUCCINOGENES* FERMENTATIVE METABOLISM

By

James B. McKinlay

Bio-based succinate production is receiving increasing attention as a potential intermediary feedstock for replacing a large petrochemical-based bulk chemical market. The economical and environmental benefits of a bio-based succinate industry have motivated research and development of organisms that produce succinate. *Actinobacillus succinogenes* is one of the best succinate-producing organisms ever reported, however it also produces unwanted formate, acetate, and ethanol. Thus, it is desirable to engineer *A. succinogenes* metabolism to produce succinate as the sole fermentation product. Metabolic engineering of *A. succinogenes* has been impeded by a relatively limited knowledge of its physiology and metabolism, and a lack of genetic tools.

^{13}C-metabolic flux analysis methods were chosen to obtain a detailed knowledge of *A. succinogenes* metabolic pathways, the fluxes through these pathways, and how these fluxes respond to perturbations. ^{13}C metabolic flux analysis is informative when different pathways result in different labeling patterns in metabolic products (e.g., proteinaceous amino acids). A chemically defined *A. succinogenes* growth medium, which included only the required amino acids (i.e., cysteine, methionine and glutamate), was developed to ensure that amino acids are labeled from ^{13}C-labeled substrate. Glutamate auxotrophy was determined to be due to an inability to made α-ketoglutarate,

indicating at least two missing tricarboxylic acid cycle-associated activities. A ^{13}C-labelling experiment was performed with [1-^{13}C]glucose in the defined medium to delineate *A. succinogenes* metabolic pathways and quantify in vivo fluxes. NADPH was produced by pyruvate and formate dehydrogenases coupled with transhydrogenase and by malic enzyme rather than by the oxidative pentose phosphate pathway. A C_4-decarboxylating activity shunted flux from the succinate-producing C_4 pathway to the formate-, acetate-, and ethanol-producing C_3 pathway, likely through both malic enzyme and oxaloacetate decarboxylase. ^{13}C-labelling experiments were then conducted under either N_2 or H_2 atmospheres with a mixture of [1-^{13}C]glucose, [U-^{13}C]glucose, and either 25 or 100 mM $NaHCO_3$. The labeling conditions revealed exchange fluxes in the C_3 pathway and between the C_3 and C_4 pathways. The effects of $NaHCO_3$ and H_2 concentrations on *A. succinogenes* fermentations went beyond their roles as C_4 pathway substrates for succinate production. $NaHCO_3$ concentration affected the amount of flux shunted from the C_4 to the C_3 pathway. Fluxes within the C_3 pathway changed to compensate for different reductant demands at different $NaHCO_3$ concentrations. H_2 also affected the C_3 pathway fluxes by alleviating the need for NADH production by pyruvate and formate dehydrogenases. ^{13}C-metabolic flux analyses were complemented by *A. succinogenes* draft genome sequence information. The genome sequence was also analyzed for its industrially relevant features. In summary, *A. succinogenes* metabolism is complex with flux distribution to succinate versus alternative fermentation products occurring at four different nodes. The metabolism is also flexible as fluxes change to meet the reductant demands at different $NaHCO_3$ and H_2 concentrations.

ACKNOWLEDGEMENTS

This dissertation owes much to interactions I have had with the kind and helpful individuals that embody the cooperative, creative, and productive atmosphere at MSU. I acknowledge past and present Zeikus lab members, with whom I shared the daily joys and frustrations that accompany the pursuit of discoveries. I am grateful to Pil Kim, the postdoc from whom I inherited this project, for constantly discussing his results and ideas with me despite my lack of knowledge and experience at the time. He was a true friend and a wonderfully amusing, though somewhat seedy, ambassador of Korean culture. I am also grateful to Maris Laivenieks for his advice, training and friendship. Harini Krishnamurthy was a great friend with whom I discussed all matters of life and research. She put up with my jokes, which were usually at her expense, and my positive experience in the lab owes much to her. I am grateful to Suil Kang, Hoon Song, Yoshi Sasaki, Karla Ziegelman-Fjeld, and Bryan Schindler for their friendship in the lab. I was fortunate to have worked with bright undergraduate researchers Andy Boyle, Kirk Burkart, Greg Costakes, Adam Edmunds and Vicki Harkins, from whom I learned more in attempting to train them than they likely learned from me. The independence given to me by my mentor Greg Zeikus, and his constant support of my research directions/tangents, have been an important part of my professional development. I am honored to make a contribution to his rich history of scientific achievements. I am indebted to my co-mentor Claire Vieille, who allowed me to work independently and always gave thoughtful consideration to even the smallest of my ideas or concerns, even when she was burdened by the enormous task of writing multiple grants. She has been an ideal mentor and a great

friend and I am confident that her versatility, creativity, and leadership will earn her a well-deserved position to continue the exciting and applied projects the lab is known for. I thank my committee members, Drs. Michael Bagdasarian, John Breznak, C. Adinarayana Reddy, and Yair Shachar-Hill for their guidance, advice, and thought-provoking questions. I additionally acknowledge Dr. Breznak whose notoriously infectious enthusiasm for research somehow had its effect on me during a technical conversation about gas chromatography at a time of low morale during my Masters project. I have carried his enthusiasm ever since. I also acknowledge Dr. Shachar-Hill who devoted considerable time and thought to develop my metabolic flux analysis skills. I attribute my success in securing a postdoc position largely to his thoughtful advice. I am indebted to the Shachar-Hill and Ohlrogge labs, particularly to a group of inspired and resourceful postdocs: Drs. Doug Allen, Ana Alonso, Eva Collakova, Fernando Goffman, Igor Libourel, and Jörg Schwender. I especially thank Dr. Schwender, who devoted hours of his time on short notice to help me prepare for my comprehensive exam, and Dr. Allen, who gave every one of my emails or concerns much thought and a prompt reply. I thank Peter Bergholz for being a good friend and for helpful advice on the manual genome sequence annotation. I thank Trevor Wagner for sharing the knowledge accumulated from his tireless trials in making gene knockouts. I thank all the friends I have made at MSU, whose names and attributes deserve mention but would add a volume to this dissertation. I acknowledge my family of self-proclaimed homebodies, who endure my anomalous travels from home to study strange bacteria. Finally, I thank Nastya Gridasova, who brought renewed joy to things in life I had long taken for granted. What a perfect time to learn to take a second look at what's in front of you.

TABLE OF CONTENTS

LIST OF TABLES

LIST OF FIGURES

SYMBOLS AND ABBREVIATIONS

AcCoA, acetyl-coenzymeA

Ace, acetate

ADH, alcohol dehydrogenase

AK, acetate kinase

Cit, citrate

CL, citrate lyase

C_4dec, C_4-decarboxylating flux

ED, Entner Doudoroff pathway

EMP, Embden-Meyerhoff-Parnas or glycolysis

EtOH, ethanol

E4P, erythrose-4-phosphate

For, formate

ForDH, formate dehydrogenase

Fm, fumarase

FR, fumarate reductase

Fum, fumarate

F6P, fructose-6-phosphate

Glc, glucose

Glxt, glyoxylate

G3P, glyceraldehyde-3-phosphate

G6P, glucose-6-phosphate

ICL, isocitrate lyase

Mal, malate

MDH, malate dehydrogenase

ME, malic enzyme

Msyn, malate synthase

OAA, oxaloacetate

OAAdec, oxaloacetate decarboxylase

OPP, oxidative pentose phosphate pathway

PEP, phosphoenolpyruvate

Pyr, pyruvate

PEPCK, PEP carboxykinase

PFL, pyruvate formate-lyase

PK, pyruvate kinase

ppp1 and 2, transketolase

ppp3, transaldolase

PyrDH, pyruvate dehydrogenase

PTS, PEP:sugar phosphotransferase system

R5P, pentose-phosphates

Suc, succinate

S7P, sedoheptulose-7-phosphate

upt, glucose phosphorylation by hexokinase and PTS.

Chapter 1

Prospects for an *Actinobacillus succinogenes*-based succinate industry

1.1 Introduction

Most bulk and specialty chemicals are derived from crude oil. Declining reserves, rising prices, and concerns over the environmental impacts of oil-based industries have prompted a movement towards bio-based processes. Succinate is currently produced petrochemically to satisfy a specialty chemical market, but it could also be produced by microbial fermentations. More importantly, succinate could serve as the starting material for producing bulk chemicals such as 1,4-butanediol (a precursor to "stronger-than-steel" and biodegradable plastics), ethylene diamine disuccinate (a biodegradable chelator), diethyl succinate (a "green" solvent replacement for methylene chloride), and adipic acid (a nylon precursor) (104). Bio-based succinate production also involves CO_2 fixation. Thus, in addition to being based on renewable resources, succinate production also has the environmental benefit of using a greenhouse gas as a substrate. For bio-based succinate to serve as an intermediary chemical feedstock for bulk chemicals, its production cost must be made competitive with petrochemical alternatives (e.g., maleic anhydride). Creating a bio-based succinate industry will require advances on several fronts, including strain engineering, medium optimization, and succinate purification.

For reasons discussed later in this chapter, *Actinobacillus succinogenes* is one of the best candidate organisms for industrial succinate-production. However, it also produces unwanted formate, acetate, and ethanol. Eliminating these fermentation byproducts would allow for efficient substrate conversion into succinate, and for less

complicated succinate purification procedures. Thus, *A. succinogenes* must be metabolically engineered towards a homosuccinate fermentation. The purpose of this chapter is four-fold: (i), to describe the bulk chemical market targeted by bio-based succinate production, and the obstacles that must be overcome; (ii), to compare *A. succinogenes* to other industrially relevant succinate-producing bacteria; (iii), to provide a background on ^{13}C-labeling studies and their usefulness for understanding microbial metabolism and guiding metabolic engineering; and (iv), to outline the objectives of the work described in this dissertation.

1.2. The succinate market and the petrochemical competition

Succinate is currently used as a surfactant, an ion chelator, and in the pharmaceutical and food industries. However, this specialty chemical market is relatively small at 33 M lb in the US (69). The research and development of bio-based succinate production is targeting a much larger commodity chemical market. In 1999, Zeikus et al. described a $15 billion network of bulk chemicals, mostly solvents, resins, and plastics, that could be produced from succinate as an intermediary feedstock (104). Here I revisit a number of these chemicals that could be derived from succinate with respect to their current markets:

1,4-Butanediol (BDO). The demand for BDO (equaling production plus imports minus exports) increased from 700 M lb in 1999 to 900 M lb in 2004, and it is projected to reach 1,055 M lb in 2008 (2). BDO's price has also increased from 1999-2004 from $1.00 to $1.25 per lb. Fifty-one percent of BDO is used to make tetrahydrofuran (THF); twenty

percent is used to make γ -butyrolactone (GBL); while another twenty percent is used to make polybutylene terephthalate high-performance resins for the automotive and electronics industries. BDO can be produced from succinate in a two-step process (69).

THF. Most THF is used to manufacture thermoplastic urethane elastomers and polyurethane fibers, but it is also an important solvent (3). A process for making a mixture of BDO, THF, and GBL from succinate in a single step has been described (69).

GBL. New regulations on volatile organic chemical usage have resulted in new markets for solvents such as GBL and its primary derivative, N-methyl-2-pyrrolidone, for replacing methylene chloride. The US market size for N-methyl-2-pyrrolidone is 80 M lb. GBL can also be converted to 2-pyrrolidone, a plasticizer and solvent with a US market size in excess of 65 M lb (69). Succinate can be converted to GBL as the sole product or to GBL-containing mixtures as mentioned above (69).

Succinate salts. About 210 M lb of salt are used each year as deicers. Succinate salts could replace current salts by offering improved performance characteristics and more neutral effects on surfaces and the environment (69).

Adipic acid. Adipic acid is primarily used to make nylon 6/6. The current US market for adipic acid is ~ 2 M lb (69). Benzene is currently the main feedstock for adipic acid production and benzene prices have increased dramatically from $1.53 per gallon in 2003 (89) to $3.85 in 2005 (5). Two alternative methods for making adipic acid involve

succinate. One method uses succinate as a ligand in a 'green' production method that uses hydrogen peroxide instead of nitric acid, to avoid toxic nitrous oxide emissions (13, 18). The other method, although not yet competitive with the petrochemical manufacture, hydrogenates succinate to BDO, which is then carbonylated to adipic acid (13, 69, 104). Succinate, adipic acid, BDO, and ethylene glycol can also be combined to make the biodegradable plastic, Bionelle (24).

Succinate can currently be produced by fermentation for about 25-50 ¢/lb (69). At this production cost, the succinate-derived chemicals described above (with the exception of succinate salts and adipic acid), are competitive or nearly competitive with the current petrochemical manufacture costs (69). As a result, succinate-producing facilities are beginning to emerge. Mitsubishi Chemical (Japan) is planning to make enough bio-based succinate to produce 30,000 M tons/yr of the biodegradable polymer polybutylene succinate (100). Another Japanese initiative, the Research Institute of Innovative Technology for the Earth and Showa Highpolymer Co., Ltd. is moving towards industrial succinate production using a genetically modified strain of *Corynebacterium glutamicum.* The group plans to produce 50,000 tons succinate/yr using wastepaper as the feedstock (www.tifac.org.in/offer/tsw/japenv.htm). DSM (Netherlands) and Diversified Natural Products (East Lansing, MI) have also agreed to commercialize bio-based succinate-derived products (100).

These bio-based succinate-production facilities are targeting specialized markets, but large-scale production for bulk chemical synthesis is still a distant prospect. Unlike other bio-based industrial chemicals (e.g., citrate, glutamate, and lysine), for which biological routes had clear economic advantages over petrochemical routes (99), bio-

based succinate targets a thriving petrochemical market, particularly that of maleic anhydride. Rising oil prices are resulting in record high petrochemical prices, including that of butane from which maleic anhydride is derived. However, maleic anhydride is in high demand thanks to strong housing and construction markets as well as increasing utilization by the auto and marine craft industries (8). In response to this demand, Huntsman Corp. (Salt Lake City, UT), which currently operates a 235 M lb maleic anydride plant, is increasing its production capacity by building a new 100 M lb capacity plant (8, 9). Lanxess corp. (Germany) is also increasing its US maleic anhydride capacity to 160 M lb (4). Thus, while high oil prices are drawing interest to bio-based chemicals, bio-based succinate production has yet to be made competitive with a booming petrochemical market.

Bio-based succinate production facilities will have to be constructed where the feedstock (e.g., corn or agricultural waste) is produced to minimize transport costs. Further savings could be made by producing high-value co-fermentation products. Succinate was suggested as a suitable co-product to improve the economics of industrial ethanol fermentations (58). An alternative process that is more focused on large-scale succinate production is to produce ethanol and succinate in separate fermentations but in the same facility. This process would allow CO_2 waste from the ethanol fermentation to be used as substrate for succinate production (104).

Considerable production cost is associated with succinate purification. Several methods have been described to purify succinate from fermentation broth. Succinic acid was purifyied from 80-l *Anaerobiospirillum succiniciproducens* cultures by electrodialysis (6) followed by processing on a bipolar, water-splitting membrane stack to

produce succinic acid from succinate, then ion exchange chromatographies (21). The recovered succinic acid (80% of recovered dry wt.) was almost entirely free of nitrogenous material, but acetic acid was present at 20% of the recovered dry weight (21). Electrodialysis methods are also inherently expensive (7). Another succinate purification method from 80-l *A. succiniciproducens* cultures resulted in higher succinic acid purity (94% of recovered dry wt.) but still contained acetic acid (5% recovered dry wt.) and protein (1% of recovered dry wt.) (14). The method involved adding $Ca(OH)_2$ to control the fermentation pH and precipitate succinate. Succinic acid was released from the precipitate by adding sulfuric acid, then purified by ion exchange chromatographies (14). While this method resulted in a higher succinate purity, it also produced commercially unusable $CaSO_4$ (gypsum) (7). A cheaper method for purifying succinic acid focused on using lower quantities of reagents, and thereby produced less byproducts (7). This method involved producing di-ammonium succinate while maintaining the fermentation pH (e.g., by adding NH_4OH), then reacting the material with ammonium bisulfate to form ammonium sulfate and succinic acid. Sulfuric acid was added to decrease the pH below 2, causing succinic acid to crystallize. After collecting by filtration, succinic acid was dissolved in methanol, which also precipitates contaminating sulfates. The methanol was evaporated, condensed, and recycled, and the ammonium sulfate was converted to ammonium bisulfate for reuse by cracking at 300°C. This method was demonstrated using *Escherichia coli* AFP-111, and succinic acid accounted for over 90% of the recovered dry weight, close to the theoretical yield of ~ 95% (7). Reactive extraction is another method that was used to purify succinic acid from fermentation broths. Tri-*n*-octylamine extracts only undissociated carboxylic acids. Thus, by controlling the pH of

the extraction, undesired organic acids (e.g., acetic and pyruvic acids) were extracted, leaving succinic acid and residual glucose behind. The residual glucose was removed by a low pH crystallization at 4°C. This technique was demonstrated on *Mannheimia succiniciproducens* fermentation broths (31, 32) achieving a final succinic acid yield of 73.1% and a purity of 99.8% (32). The large-scale economics of using tri-*n*-octylamine, and whether it can be reused, have not yet been addressed, or at least not reported. Regardless of the method, purifying succinic acid is a significant portion of the total cost. Thus, using an organism that produces succinate at near-maximum theoretical yields with little or no byproducts will contribute to cost-effectiveness.

1.3. Succinate-producing bacteria

Bio-based succinate will be produced from the most abundant sugars in plant biomass (i.e., glucose, fructose, arabinose, and xylose). Glucose is the most commonly used substrate for research related to industrially relevant fermentations. Theoretically, ~1.71 mol succinate could be produced per mol glucose, based on the available electrons and given additional CO_2 (i.e., 24 electrons in glucose divided by 14 electrons in succinate):

$$\text{glucose} + 0.86\ HCO_3^- \rightarrow 1.71\ \text{succinate}^{2-} + 1.74\ H_2O + 2.58\ H^+ \qquad \Delta G^{o'}\ -173\ \text{kJ/mol}$$

In the presence of both CO_2 and additional reducing power, (e.g., H_2), the theoretical yield increases to 2 mol succinate per mol glucose:

$$\text{glucose} + 2\ HCO_3^- + 2H_2 \rightarrow 2\ \text{succinate}^{2-} + 2H_2O + 2\ H^+ \qquad \Delta G^{o'}\ -317\ \text{kJ/mol}$$

These theoretical yields are the targets sought for bacterial succinate production. Experimental yields will be constrained by the pathways used and by the carbon diverted

to biomass and alternative products. Succinate titers and productivities aim to be similar to those obtained in industrial glutamic acid production: ~150g l^{-1} at 5 g l^{-1} h^{-1}.

A wide variety of bacteria and fungi excrete succinate (86), but only a few produce enough to be considered for industrial succinate production. These organisms have either been engineered to produce high succinate concentrations or do so naturally. This section focuses on five of the most promising bacteria for industrial succinate production. For each bacterial species, the metabolic routes used for succinate production are described along with their advantages and disadvantages.

1.3.1 *Escherichia coli*

E. coli naturally produces succinate from the reductive branch of the tricarboxylic acid (TCA) cycle when fermenting glucose, but only as a minor product of a mixed acid fermentation (Fig. 1.1A). Because *E. coli* is one of the best-understood bacteria, and because it can be genetically engineered with relative ease, there has been considerable effort to engineer *E. coli* for succinate production. Early efforts focused on increasing phosphoenolpyruvate (PEP) and pyruvate carboxylations to redirect carbon flux to the reductive TCA branch. By overexpressing *E. coli* PEP carboxylase (PEPC), succinate yields were improved 3.75 times to 10.7 g l^{-1} (61). Succinate production was also enhanced in strains overexpressing *Sorghum vulgare* PEPC (56). Overexpressing *E. coli* PEP carboxykinase (PEPCK) was originally shown to have no effect on succinate production in a medium containing 15 g $MgCO_3$/l (61), but when $NaHCO_3$ (more soluble than $MgCO_3$) was used, succinate concentrations increased (45). Overexpressing *A. succinogenes* PEPCK in a *ppc*$^-$ *E. coli* strain also improved succinate production (40).

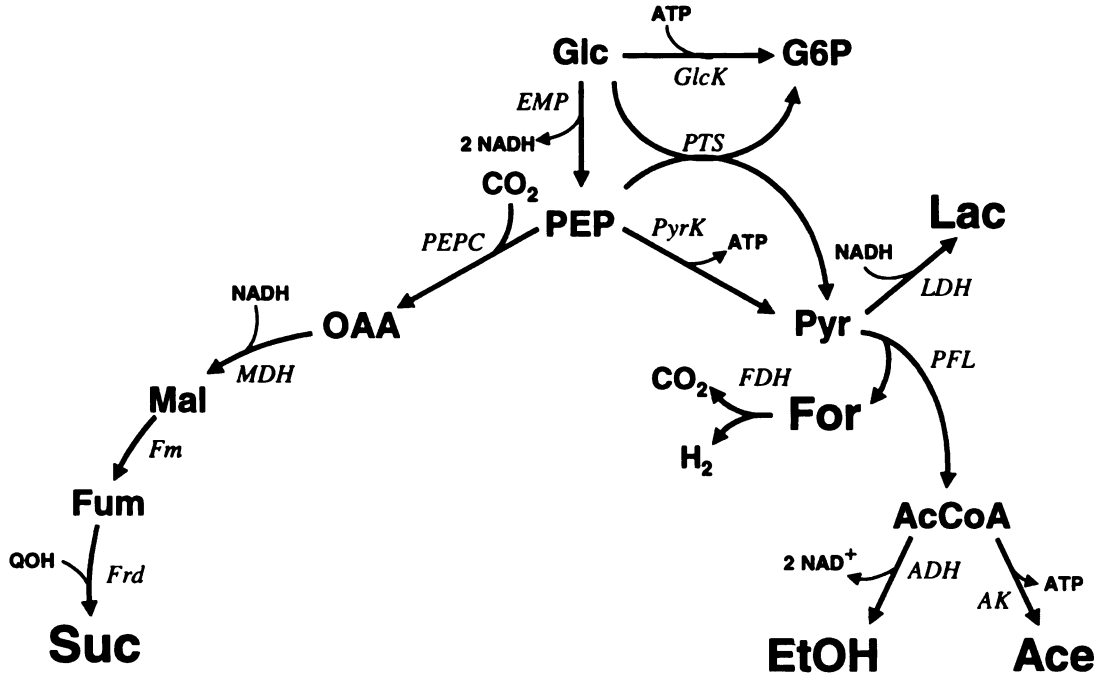

Figure 1.1A. Simplified metabolic map of wild-type *E. coli* mixed acid fermentation. The pentose phosphate pathway is not shown. Metabolites: AcCoA, acetyl-CoA; Ace, acetate; EtOH, ethanol; For, formate; Fum, fumarate; G6P, glucose-6-phosphate; Glc, glucose; Lac, lactate; Mal, malate; OAA, oxaloacetate; PEP, phosphoenolpyruvate; Pyr, pyruvate; Suc, succinate; and QOH, menaquinol. Reactions: *ADH*, alcohol dehydrogenase; *AK*, acetate kinase; *EMP*, Embden-Meyerhoff-Parnas pathway; *FDH*, formate dehydrogenase; *Fm*, fumarase; *Frd*, fumarate reductase; *GlcK*, glucokinase; *LDH*, lactate dehydrogenase; *MDH*, malate dehydrogenase; *PEPC*, PEP carboxylase; *PFL*, pyruvate formate-lyase; *PTS*, PEP:glucose phosphotransferase system; and *PyrK*, pyruvate kinase.

Increased pyruvate carboxylation leading to improved succinate production was achieved by overexpressing pyruvate carboxylase (PYC) from *Lactococcus lactis* (56) or *Rhizobium etli* (23). Succinate production in strains overexpressing PEPC or PYC was further enhanced by overexpressing *E. coli* pantothenate kinase and supplying pantothenic acid to increase intracellular acetyl-CoA levels (57). Acteyl-CoA is an activator of PEPC and PYC. Increased pyruvate carboxylation was also achieved using the *E. coli* mutant NZN111. In this strain, pyruvate is a fermentation product due to

insertional mutations in the pyruvate formate-lyase and lactate dehydrogenase genes (29, 62, 88). When *E. coli* NAD^+-dependent malic enzyme is overexpressed in NZN111, pyruvate is carboxylated, and succinate is produced as the major fermentation product (29, 62, 88). Unfortunately, NZN111 does not grow fermentatively on glucose and produces succinate slowly when overexpressing malic enzyme (88).

A major breakthrough in *E. coli* succinate production was the isolation of a spontaneous mutant of NZN111, AFP111, that grows fermentatively on glucose, produces succinate as the main fermentation product, and consumes glucose and other sugars simultaneously (10). The AFP111 mutation was found in the *ptsG* gene, encoding part of the glucose-specific phosphotransferase system (10). This mutant produces up to 50 g succinate/l using light steep water as an inexpensive alternative to yeast extract and tryptone (62). Using AFP111 expressing *R. etli* PYC, the effects of fermentation conditions on succinate production were explored by using an aerobic growth phase followed by an anaerobic succinate production phase (94). From these studies, Vemuri et al. discovered a new route for succinate production involving the glyoxylate shunt, which was activated during aerobic growth (94). The glyoxylate shunt can partially alleviate the reductant limitation associated with using the reductive TCA branch for succinate production. If all reductant comes from glycolysis (i.e., 2 NADH/glucose) then only one succinate can be produced per glucose by the reductive TCA branch (Fig. 1.1A). Glyoxylate shunt flux complements reductive-TCA branch flux by using less reductant. Use of the glyoxylate shunt might even generate reductant through if acetyl-CoA production (used by the glyoxylate shunt for making citrate) is accompanied by formate oxidation or if pyruvate dehydrogenase is used in place of pyruvate-formate lyase (Fig.

1.1B). After an aerobic growth phase, AFP111 produced 99.2 g succinic acid l^{-1} in an anerobic fed batch fermentation (93), one of the highest succinate titers ever reported (Table 1.1).

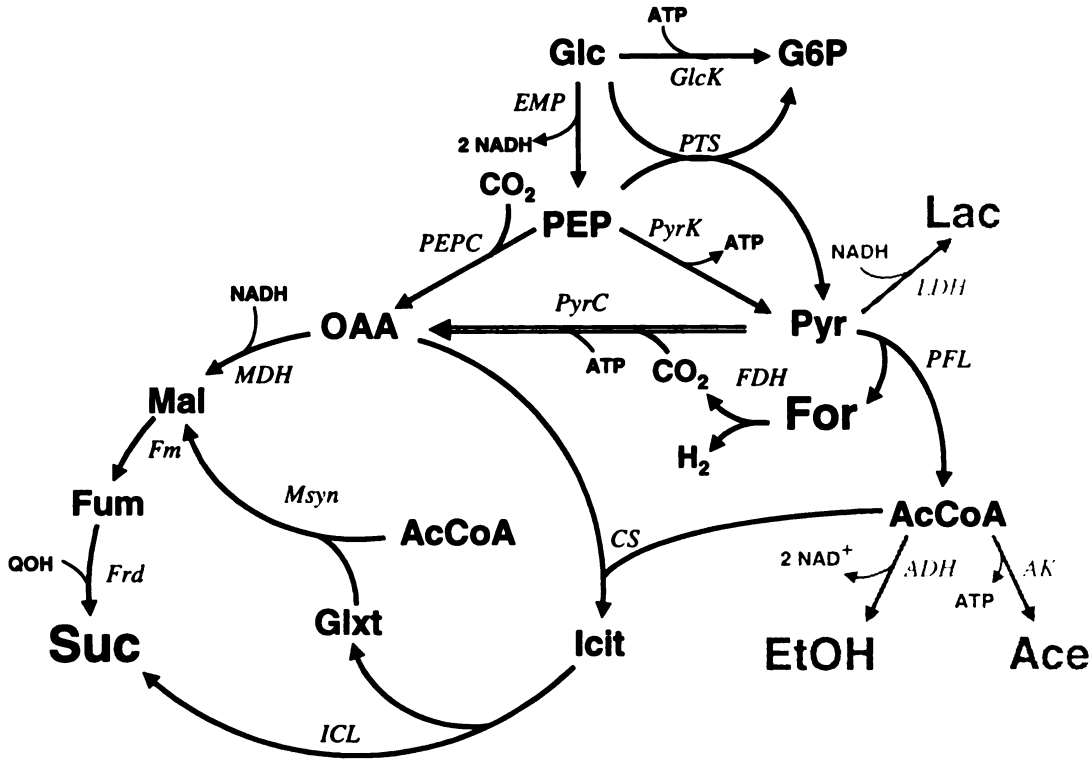

Figure 1.1B. Simplified metabolic map of engineered *E. coli* anaerobic succinate-producing metabolism (80). Grey arrows indicate missing enzyme activities due to gene deletions. The double-lined arrow indicates introduced activity. Metabolites: Glxt, glyoxylate; and Icit, citrate/isocitrate. Reactions: *CS*, citrate synthase and aconitase; *ICL*, isocitrate lyase; *Msyn*, malate synthase; and *PYC*, pyruvate carboxylase. See Fig. 1A for other abbreviations.

With a knowledge of complementary pathways for succinate production, wild-type *E. coli* was re-engineered to eliminate fermentation byproducts and guarantee glyoxylate shunt flux (Fig. 1.1B). The *ldhA*, *adhE*, and *ack-pta* deletions prevented lactate, ethanol and acetate productions, and deleting *iclR* (encodes the transcriptional repressor of the glyoxylate cycle) ensured the expression of glyoxylate cycle enzymes

(80). As was observed with AFP111 (94), though, the *iclR* deletion was not required for glyoxylate shunt flux (80). Finally, *L. lactis* PYC was overexpressed to divert flux from pyruvate to oxaloacetate (OAA), a precursor to both succinate producing pathways (80). This strain, SBS550MG/pHL413, produced 66 g succinate/l with a 1.6 mol succinate per mol glucose yield (80). This yield is the maximum yield predicted by elementary flux mode analysis of the engineered metabolic network (12). One drawback of using the glyxoylate shunt to produce succinate is that it wastes carbon through CO_2 production. Three PEP are required to generate the 1 OAA + 2 acetyl-CoA needed to produce 2 succinate using glyoxylate shunt, as opposed to 1 PEP for 1 succinate using the reductive TCA branch, given ample reductant and CO_2. Sanchez et al. showed that, for succinate production, the optimal flux partitioning at OAA to the glyoxylate (i.e., to form citrate) and reductive TCA pathways is 0.32: 0.68 (79). Thus, while the theoretical yield decreases to 1.6 succinate/glucose (12), the optimal flux through this metabolic network still results in net CO_2 consumption.

E. coli was also engineered to produce succinate aerobically (55) (Fig. 1.1C). By deleting *sdhA*, encoding succinate dehydrogenase, succinate became the terminal product of the oxidative TCA-branch. By deleting *iclR* (the transcriptional repressor of the glyoxylate cycle), the glyoxylate cycle formed a second route to succinate. Deleting *poxB* and *ackA-pta* prevented acetate production. When *ptsG* was inactivated and *S. vulgare* PEPC was overexpressed, a 1 mol succinate per glucose yield was achieved, the maximum yield predicted from elementary flux mode analysis of this metabolic network (12). In fed batch aerobic cultures, the strain produced 58.3 g succinate l^{-1} at a rate of 1.1 g l^{-1} h^{-1}, opening the possibility for aerobic succinate production (54). This aerobic

system has several disadvantages, though. First, the maximum theoretical yield of 1 succinate per glucose is less efficient than anaerobic processes. And second, maximum succinate yields result in a net CO_2 production, rather than CO_2 fixation (12). Thus, one of the environmental benefits of succinate production is not fulfilled.

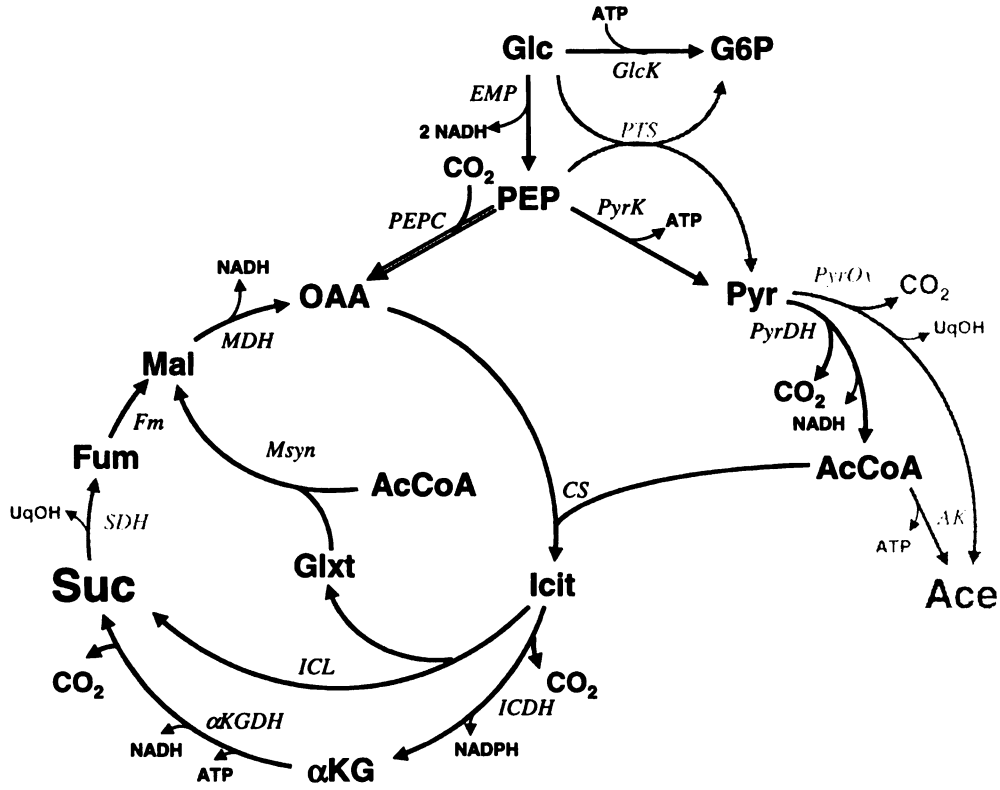

Figure 1.1C. Simplified metabolic map of engineered *E. coli* aerobic succinate-producing metabolism (54). Grey arrows indicate missing enzyme activities due to gene deletions. The double-lined arrow indicates introduced activity. Metabolites: αKG, α-ketoglutarate and UqOH, ubiquinol. Reactions: *αKGDH*, αKG dehydrogenase and succinyl-CoA synthetase; *ICDH*, isocitrate dehydrogenase; *PyrDH*, pyruvate dehydrogenase; and *PyrOx*, pyruvate oxidase. See Fig. 1.1A for other abbreviations.

The progress made in engineering *E. coli* to produce succinate is an excellent example of successful metabolic engineering. *E. coli* strains can now produce succinate at

concentrations comparable to those attained by natural succinate producers, and with high succinate product ratios (Table 1.1). However, *E. coli*-based succinate production has several disadvantages. First, the specific productivities of the engineered strains are generally lower than those of natural succinate producers (Table 1.1). One of the lower *E. coli* specific productivities is actually that of the aerobic succinate producing strain, HL27659k/pKK313 (Table 1.1), which had been engineered to overcome the low productivities of anaerobic fermentations (54). Second, dual-phase fermentations and medium aeration introduce additional production costs. Third, with the exception of AFP111 in light steep water (62), all *E. coli* strains have been studied in media containing tryptone and yeast extract, which are too expensive for large-scale use. And fourth, all strains overexpressing enzymes have used isopropyl-beta-D-thiogalactopyranoside to induce expression, which is also too expensive for large-scale use. Continued research and development of *E. coli*-based succinate production should focus on increasing specific productivity, be characterized in industrially relevant media, and use constitutive expression systems or inexpensive induction methods to overexpress enzymes.

1.3.2 *Corynebacterium glutamicum*

C. glutamicum is primarily known as the bacterium used for industrial amino acid production. Intensive research from several groups has aimed to understand and improve its amino acid production abilities. As a result, robust genetic tools exist for *C. glutamicum*, and a wealth of knowledge is available, including genome sequence, microarray, proteomic, and flux analysis data (95). Although not traditionally considered as a succinate producer, *C. glutamicum* is now poised to produce succinate on an

industrial scale (www.tifac.org.in/offer/tsw/japenv.htm). This advance was not the result of genetic engineering but rather resulted from modifying its environment. In anoxic conditions with bicarbonate, non-growing *C. glutamicum* converts glucose to succinate and lactate with acetate as a minor product (33). This mixed acid fermentation reached succinate and lactate titers of 23 g l^{-1} and 95 g l^{-1}, respectively (65). At high cell densities (60 g dry cell weight [DCW] l^{-1}) succinate was produced at 11.7 g l^{-1} h^{-1} (65), with a specific productivity of ~200 mg g DCW^{-1} h^{-1}. To increase the range of lignocellulose-based sugars to be used as feedstock, *C. glutamicum* was engineered to consume xylose. By completing the partial xylose catabolizing pathway with *E. coli* xylose isomerase, and by overexpressing *E. coli* xylulokinase, *C. glutamicum* concomitantly converted glucose and xylose to succinate and lactate (39). Succinate titer and specific productivity from glucose and xylose were similar to those from glucose alone.

The *C. glutamicum* succinate-producing pathway (Fig. 1.2) was determined from in vitro enzyme assays and multiple gene knockouts (33). OAA is converted to succinate by the reductive TCA cycle branch. The glyoxylate shunt was not necessary for succinate production, but it was not ruled out as a possible contributing route (33). OAA is produced primarily from PEP by PEPC, with PEPCK and PYC perhaps making minor contributions to OAA generation. When lactate dehydrogenase activity was impaired, succinate and acetate were the sole endproducts but were not produced at higher titers. By overexpressing PYC in an *ldhA* mutant, succinate and acetate production increased ~two-fold (33).

Guided by the vast knowledge on its metabolism and its reliable genetic tools, *C. glutamicum* succinate production has moved from a research setting to an industrial

Strain; Genotype	Succinic acid titer ($g\ l^{-1}$)	Prod.[a] ($g\ l^{-1}\ h^{-1}$)	Specific productivity[b] ($mg\ g\ DCW^{-1}\ h^{-1}$)	Succinate yield ($g\ g^{-1}$)	Molar succinate product ratio[c]	Cell Conc. ($g\ l^{-1}$)	Time (h)	Fermentation; Medium[d]	Ref.
A. succiniciproducens									
wildtype	50.3	2.1	Unk.	0.90	1.2	Unk.	24	B; Csl	(21)
FA-10; ?	34.1	0.8–1.1	Unk.	0.66	0.97	Unk.	44.5	B; Csl	(25)
A. succinogenes									
130Z; wildtype	68, 79	1.2 – 1.7	Unk.	0.68–0.87	1.7	Unk.	36-39	B; Csl, Ye	(27)
130Z; wildtype	6.6	0.4	270	0.77	0.97	0–1.6	15	B; Def.	(60)
FZ53; *pflB*?	94–106	2.0-2.8	Unk	0.78–0.82	1.6	Unk	34–52	B; Csl, Ye	(26)
C. glutamicum									
R; wildtype	23	3.8	130	0.19	0.2	30	6	F-B[e]; Def.	(65)
E. coli									
SBS550MG/pHL413; Δ*adhE*, Δ*ldhA*, Δ*iclR*, Δ*ack-pta*::Cm^R pyc^+	65.8	0.56–1.9	70-230	1.57	8.7–12.6	8.2[g]	95	F-B[e]; Ye,Trn	(80)
HL27659k/pKK313; Δ*sdhAB*, Δ*ackA-pta*, Δ*poxB*, Δ*iclR*, Δ*ptsG*, *pepc*$^+$	58.3	1.1	70-90	0.94	4.1	16.8[g]	59	F-B[f]; Ye, Trn	(54)
AFP111/pTrc9A-*pyc*; Δ*pflAB*::Cm^R, *ldhA*::Km^R, *ptsG*, pyc^+	99.2	1.3	140	1.10	1.95	10.2–13.0	76	F-B[e]; Ye, Trn	(93)
M. succiniciproducens									
MBEL55E; wildtype	13.5–18.8	1.8	530	0.70–1.04	1.05	0–3.4		B; Ye, Ppn	(48)
LPK7; *ldhA*::Km^R *pflB*::Cm^R *pta-ack*A::Sp^R	52.4	1.8	690	0.76	1.8	0-2.6	29	F-B; Ye, Ppn	(53)

Table 1.1. Comparison of succinate fermentations from glucose by different bacterial species.

[a] Volumetric productivity.

[b] Calculated using: $r_{suc} = dc_{suc} / dt \times 1/x$; where r_{suc} is the specific succinate production rate, dc_{suc} is the change in succinate concentration, dt is the change in time, and x is the amount of biomass at time t (87).

[c] Ratio of succinate to other fermentation products.

[d] B, batch; F-B, fed-batch; CFH, corn fibre hydrolysate; Csl, corn steep liquor; Ppn, polypeptone; Trn, Tryptone; Def., defined; Ye, yeast extract

[e] After transitioning from aerobic growth phase to anaerobic production phase

[f] Aerobic conditions.

[g] Dry cell weights calculated using a value of 480 mg l^{-1} for an OD_{660} of 1.0 (22)

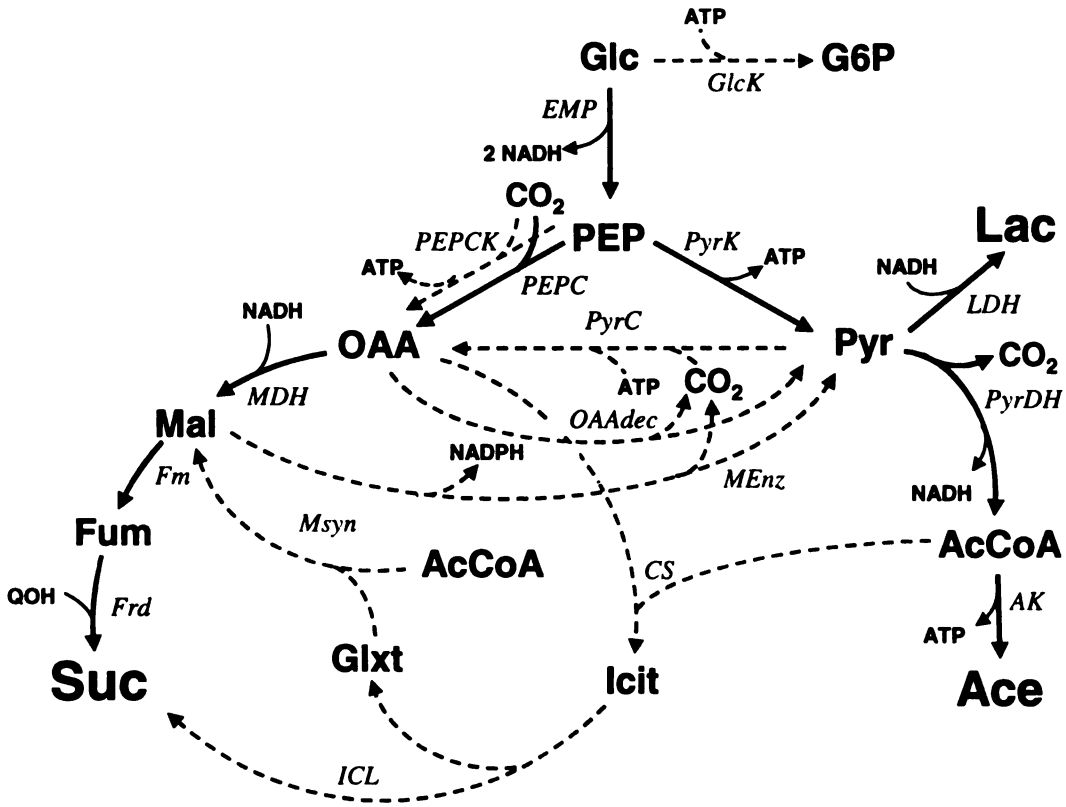

Figure 1.2. Simplified map of wild-type *C. glutamicum* succinate-producing metabolism. Dotted lines indicate enzyme activities with unknown in vivo contributions. *MEnz*, malic enzyme; *OAAdec*, OAA decarboxylase, *PEPCK*, PEP carboxykinase. See Fig. 1.1A for additional abbreviations.

setting within a relatively short time frame. Despite this rapid utilization of *C. glutamicum*-based succinate production technology, there is still much to be understood and improved.

As shown in Figure 1.2, there are several pathways whose contribution to organic acid production is unknown. Specific succinate productivities by *C. glutamicum* are also relatively low (Table 1.1). Most importantly, there are no reports of a *C. glutamicum* strain that efficiently produces succinate in great majority to alternative products. As a result, succinate titers and product ratios are relatively low (Table 1.1). The resulting

product mixture may also require more complicated and expensive purification procedures, the details of which have not been reported.

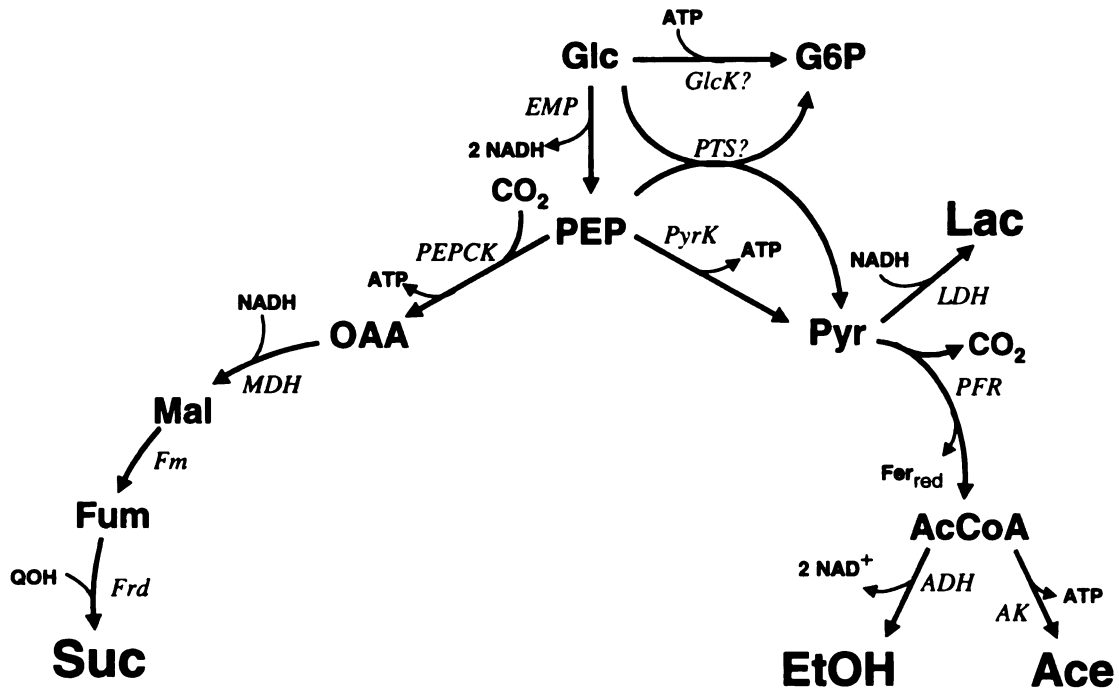

Figure 1.3. Simplified map of wild-type *A. succiniciproducens* succinate-producing metabolism. *PFR*, pyruvate ferredoxin oxidoreductase; Fer_{red}, reduced ferredoxin. See Fig. 1.1A and Fig. 1.2 for additional abbreviations.

1.3.3 *Anaerobiospirillum succiniciproducens.*

A. succiniciproducens, isolated from the feces of humans and animals (85), naturally produces succinate as its major fermentation product. The earliest metabolic studies on *A. succiniciproducens* demonstrated the effects of pH and CO_2 availability on the succinate:lactate ratio (21, 78). High CO_2 concentrations and a pH near 6, rather than 7, shifted metabolism entirely away from lactate to succinate and acetate at a ratio of 1.8:1 (21, 78). Enzyme activities detected in cell extracts suggested that glucose was metabolized to PEP by glycolysis. Pyruvate-ferredoxin oxidoreductase was found to convert pyruvate to acetyl-CoA. PEPCK was implicated as the major CO_2-fixing enzyme,

generating OAA that was then converted to succinate by the reductive TCA branch (Fig. 1.3). Both *A. succiniciproducens* pyruvate-ferredoxin oxidoreductase and PEPCK activities responded to pH and CO_2 concentration changes (78). The energy-conserving role of PEPCK is unlike its more commonly known role in gluconeogenesis and, at the time, there were few examples of PEPCK having this role, except during propionate fermentation by *Bacteroides* species from the rumen (82) and human intestine (59). *A. succiniciproducens* PEPCK was purified and characterized (73). It has been characterized extensively by site-directed mutagenesis and x-ray crystallography (11, 34-38). *A. succiniciproducens* can also use H_2 as an additional electron source, and supplying H_2 favors succinate production (102). Pyruvate-ferredoxin oxidoreductase activity also decreased significantly in the presence of H_2 (102).

A. succiniciproducens's fermentation characteristics were analyzed in industrially relevant media. Taking advantage of *A. succiniciproducens* ability to consume lactose, whey was examined as a cheap substrate source in batch, fed-batch, and continuous culture conditions (50, 77). Corn-steep liquor (77), or both yeast extract and peptone (50) were added to the whey media as nitrogen sources. Under fed-batch and batch conditions, succinate yields over 91 % were achieved (50, 77). When glucose was included in whey fermentations, lactose consumption did not occur until glucose was first consumed, indicating that *A. succiniciproducens* will not naturally co-metabolize sugars (50). Wood hydrolysate was also explored as a cheap substrate source with yeast extract, peptone, or corn-steep liquor as nitrogen sources. Succinate yields near 90% were achieved in all cases (49). Glycerol is a byproduct of fatty-acid producing industries, including bio-diesel production. Although glycerol is more expensive than glucose, its price is expected

to drop as bio-diesel production increases. It is also an attractive substrate for succinate production because it has the same number of available electrons as succinate (both glycerol and succinate yield 14 electrons when completely oxidized to CO_2), thus no additional source of reducing power would be needed to produce succinate from glycerol and CO_2. *A. succiniciproducens* can naturally convert glycerol to succinate with little acetate production. Succinate:acetate ratios from glycerol were 26:1 compared to 4:1 from glucose (51). Glycerol and glucose could also be co-utilized resulting in improved succinate productivity, but lower succinate:acetate ratios (51).

A. succiniciproducens is an attractive candidate for bio-based succinate production because it naturally produces high succinate concentrations, and its fermentation characteristics have been examined in several industrially relevant media. However, there are several disadvantages to *A. succiniciproducens*-based succinate production. There is only one mention of an improved succinate-producing strain. Strain FA-10 was obtained by using fluoroacetate as selective pressure and displayed significantly less acetate production (25). However, pyruvate was produced in place of acetate (25). FA-10 produced succinate titers between 25 and 55 g l^{-1} (25). Developing genetic tools for *A. succiniciproducens* to eliminate fermentation byproducts and allow for co-utilization of different sugars would greatly benefit its fermentation characteristics. Furthermore, relatively little is known about its metabolism. The number of reactions shown in Figure 1.3 merely reflects the amount of knowledge accumulated on *A. succiniciproducens* metabolism and does not necessarily reflect the simplicity of its metabolic pathways. *A. succiniciproducens* is also a strict anaerobe, so special procedures are required to avoid exposure to oxygen. Another potential disadvantage is that *A.*

succiniciproducens can cause bacteremia in humans (85). Although infections are rare and typically occur in immuno-compromised patients, the potential virulence of *A. succiniciproducens* cannot be ignored.

1.3.4 Rumen *Pasteurellaceae: Actinobacillus succinogenes* and *Mannheimia succiniciproducens*

Succinate is an important metabolic intermediate in the rumen. Several rumen bacteria obtain energy by decarboxylating succinate to propionate, which then serves as a nutrient for the ruminant (77, 83, 92). Many succinate-producing bacteria have been isolated from the rumen. The two currently receiving the most attention for industrial succinate production are *A. succinogenes* and *M. succiniciproducens*.

A. succinogenes and *M. succiniciproducens* were both isolated from the bovine rumen, *A. succinogenes* from a Michigan State University cow and *M. succiniciproducens* from a Korean cow. Both organisms belong to the *Pasteurellaceae* and their genome sequences are more similar to each other than to any other genome sequence (Chapter 5). Not surprisingly, the two bacteria share many metabolic traits. Both consume a wide variety of carbon and energy sources, including the most abundant plant sugars: glucose, fructose, xylose (28, 48, 91), and arabinose (28, 91) (arabinose consumption has not yet been reported for *M. succiniciproducens*). As with *A. succiniciproducens*, succinate production is enhanced in each strain by increased availability of CO_2 and H_2 (30, 91). Providing electrically-reduced neutral red, as an alternative to H_2 improved *A. succinogenes* succinate yields and product ratios during glucose fermentations (67). It was shown that neutral red, a redox dye, could serve as an

electron donor for fumarate reductase (67). Unlike with *A. succiniciproducens*, *A. succinogenes* and *M. succiniciproducens* fermentation product profiles are remarkably stable at different pH values (30, 91), and at least *A. succinogenes* can simultaneously consume multiple sugars (26). Furthermore, *A. succinogenes* can tolerate glucose concentrations as high as 150 g l^{-1} (27) whereas *A. succiniciproducens* does not grow well above carbohydrate concentrations exceeding 100 g l^{-1} (21). *A. succinogenes* and *M. succiniciproducens* also show metabolic differences. For example, *A. succinogenes* consumes sorbitol whereas *M. succiniciproducens* does not, and *M. succiniciproducens* produces lactate whereas *A. succinogenes* does not (48, 91).

An understanding of the *A. succinogenes* pathways responsible for succinate production was obtained primarily from in vitro enzyme assays (91), whereas *M. succiniciproducens* pathways were largely inferred from its genome sequence (30). In both species, succinate production occurs in a manner similar to that in *A. succiniciproducens*, with PEP being carboxylated to OAA by PEPCK, then OAA being converted to succinate by the reductive TCA branch (Fig. 1.4). PEPC does not appear to be important for converting PEP to OAA. Indeed, insertional inactivation of PEPC in *M. succiniciproducens* did not affect product distributions, whereas the insertional inactivation PEPCK severely impaired growth and production of all organic acids (53). Unlike *A. succiniciproducens*, pyruvate-ferredoxin oxidoreductase is not responsible for converting pyruvate to acetate and ethanol in either *A. succinogenes* or *M. succiniciproducens*. Instead, pyruvate formate-lyase was implicated in this role (30, 91). Despite often being depicted as a simple branched metabolism from PEP to succinate and alternative products, other enzyme activities suggest that flux distribution to products

could occur at metabolite nodes other than PEP. Malic enzyme and OAA decarboxylase activities were detected in *A. succinogenes* cell extracts (91). These enzymes were also identified in genomic and proteomic analyses of *M. succiniciproducens* (30, 46). Insertional inactivation of malic enzyme did not affect *M. succiniciproducens* product distributions, but compensating alternative pathways cannot be ruled out (53).

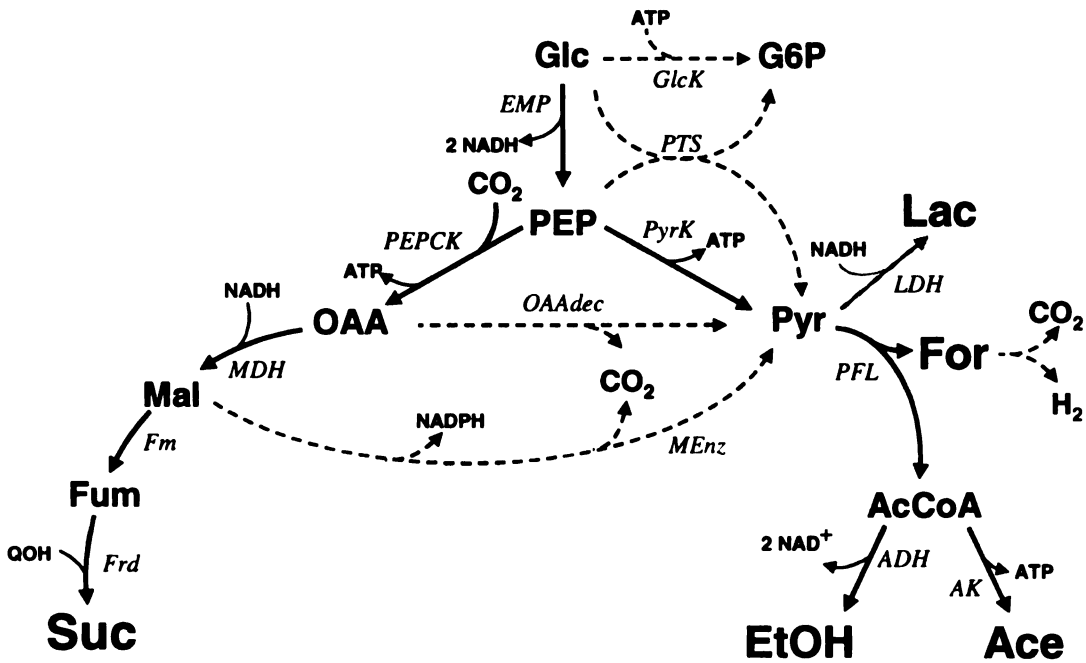

Figure 1.4. Simplified map of wild-type *A. succinogenes* and *M. succiniciproducens* succinate-producing metabolism. Dotted lines indicate enzyme activities with unknown in vivo contributions. The grey *LDH* arrow indicates that lactate production is unique to *M. succiniciproducens*. See Fig. 1.1A and Fig. 1.2 for abbreviations.

Both bacterial species have been characterized in industrially relevant media. *M. succiniciproducens* was grown in batch and continuous cultures with whey and corn steep liquor together. Succinate yields and productivities were 71% at 1.2 g l^{-1} h^{-1} and 69% at 3.9 g l^{-1} h^{-1} in batch and continuous cultures, respectively (47). In a medium containing corn steep liquor, yeast extract, and glucose, *A. succinogenes* produced 80 g succinate l^{-1} (27), a remarkable titer for a wild-type strain. Many of the described succinate purification procedures involve making succinate salts (see section 2). *A. succinogenes*

will grow and ferment in the presence of 96 g l^{-1} disodium succinate or 130 g l^{-1} magnesium succinate, whereas *A. succiniciproducens* will not (27).

A. succinogenes and *M. succiniciproducens* naturally produce high concentrations of succinate and have among the highest specific productivities reported (Table 1.1). *A. succinogenes* has a specific succinate productivity of 430 mg g^{-1} l^{-1} in batch fermentations with 5 g l^{-1} yeast extract (McKinlay et al. unpublished data). Therefore, these bacterial species are excellent starting points for engineering an industrial strain. Of the two strains, *A. succinogenes* has the highest succinate yields reported. It is worth noting, though, that *M. succiniciproducens* has not been grown under the same conditions, and no side-by-side comparative fermentation with these two bacteria has been reported. Only a few genetic engineering efforts have been reported for these two species. Fluoroacetate resistant mutants of *A. succinogenes* were obtained that, like *A. succiniciproducens* FA-10, produce pyruvate (26). The fluoroacetate resistance and altered metabolism of these strains is thought to be due to an inactive pyruvate formate-lyase (66). Despite producing pyruvate, the mutant strains generally had improved succinate yields, with one strain, FZ53, reaching a final titer of 106 g succinate/l in a medium containing corn steep liquor, yeast extract, and glucose (26). This is the highest succinate titer ever reported from a fermentation. Because of a lack of genetic tools, the fluoroacetate-resistant strains are the only known *A. succinogenes* mutants. On the other hand, several genes have been insertionally inactivated in *M. succiniciproducens* using a *sacB*-based sucrose counter selection system (53). This knock-out system was used to disrupt flux to lactate, formate, and acetate by insertionally inactivating lactate dehydrogenase, pyruvate formate-lyase, phosphotransacetylase, and acetate kinase,

creating the mutant LPK7. Lactate, formate, and acetate productions were severely limited, but pyruvate and malate were produced instead and batch succinate titers only improved from 10.5 g l^{-1} to 13.4 g l^{-1} as a result of the extensive engineering. However, the mutants were only tested under electron-limiting conditions with glucose, yeast extract, and peptone as electron sources. If all reductant is formed from glycolysis, there is only enough NADH produced to form one succinate per glucose. Interestingly, LPK7 only achieved one succinate per glucose (53). LPK7, and the other mutants described in the study, should be characterized in electron rich conditions (e.g., by adding H_2). Under electron limiting fed-batch conditions, a succinate titer of 52.4 g l^{-1} was achieved by *M. succiniciproducens* LPK7 (Table 1.1).

Overall, both rumen bateria are important organisms to be studied and engineered for industrial succinate production. However, several hurdles must be overcome. In contrast to *E. coli* and *C. glutamicum*, little is known about the physiology and genetics of these bacteria, and there is still much to be learned about their metabolism. Progress in engineering *A. succinogenes* has been relatively slow, hindered by a lack of genetic tools and system-wide analyses. Progress with *M. succiniciproducens*, on the other hand, has been rapid with the genome sequence (30), a proteomic analysis (46), and gene knockout technology (53) described within five years of the first published characterization of the organism (48). Despite the availability of genetic tools and system-wide approaches, the engineering efforts with *M. succiniciproducens* have thus far focused on inherently obvious targets, namely those activities leading to alternative endproducts (53). Only recently were oxaloacetate decarboxylase and an acetate-forming aldehyde dehydrogenase identified as potentially important targets after a *M. succiniciproducens*

proteomics study (46). These genes were either overlooked or ignored during the *M. succiniciproducens* genome annotation, and the in vivo contribution of these enzymes to flux distribution remains unknown. It is also important to note that both bacteria are related to several well-known pathogens, including *A. actinomycetemcomitans, A. pleuropneumoniae, Haemophilus influenzae, M. haemolytica,* and *Pasteurella multocida.* While *M. succiniciproducens* is reported to have no leukotoxin or capsule production genes, a detailed analysis of *M. succiniciproducens* or *A. succinogenes* for virulence traits has not been performed. Non-pathogenicity should be established before these strains are used on an industrial scale.

1.4. Backgound on ^{13}C-metabolic flux analysis

Successful metabolic engineering of microbes is usually reported as being based on a logical rationale for the genetic manipulations made that result in the expected metabolic effects. Usually not reported are the majority of engineering efforts that result in unexpected or undesired phenotypes (20, 87). However, these unpublished results are important to highlight the current limitations in accurately predicting the metabolic effects of genetic perturbations.

Even with *E. coli* the metabolic effects of genetic manipulations can be unexpected. For example, to improve succinate production, *E. coli*'s metabolism was engineered to resemble that of the natural succinate-producer, *M. succiniciproducens* (52). After several gene disruptions, the resulting mutants had few favorable characteristics over the wild type strain. The authors then used a computer modeling approach to predict the effects of different combinatorial gene knockouts. The

simulations correctly predicted the ineffectiveness of some of the mutations already made. They also predicted that knocking out *pykA*, *pykF*, and *ptsG* would benefit anaerobic succinate production. These genes were knocked out, resulting in a seven fold increase in succinate titer (52).

Using computer simulations in an effort to guide *E. coli* metabolic engineering is possible owing to a well-annotated genome and knowledge of active pathways. However, such detailed information is not available for all industrially relevant organisms. For example, the *A. succinogenes* draft genome sequence was only recently made available (http://genome.ornl.gov/microbial/asuc/). Furthermore, the robust genetic tools available for *E. coli*, make it practical to test the effects of multiple mutations in a relatively short period of time. These mutations are important not only for engineering production strains, but also for understanding metabolism and physiology. Other industrially relevant organisms, including *A. succinogenes*, are not so easily engineered. Thus, when genetic engineering is time-consuming and laborious, it is especially important to have other means by which to study metabolism, and to be able to accurately predict the metabolic effects of genetic manipulations.

Part of the current limitation in predicting the metabolic effects of genetic manipulations is due to past inabilities to assess the response of intermediary fluxes to genetic and environmental perturbations. For example, under certain conditions, both *E. coli* pyruvate kinase isoenzymes can be insertionally inactivated with no observable effect on growth parameters (74). In other conditions, inactivating one or both enzymes seemingly results only in a decreased growth rate (74). These results were surprising because pyruvate kinase is a central metabolic enzyme as the last step in glycolysis. By

using PTS deficient mutants it was inferred that the PTS could supply adequate pyruvate to support growth in the absence of pyruvate kinase activity (74). However, other metabolic changes could not be observed from this approach. Experiments with [1-^{14}C]glucose, showed that pyruvate kinase knockout mutants had increased oxidative pentose phosphate pathway (OPPP) flux (75). However, it was not until ^{13}C-labeling studies were performed that it was realized that PEP carboxylase and malic enzyme were compensating for the pyruvate kinase deficiency (1, 19) and that the OPPP and TCA cycle fluxes varied with growth conditions (19). These discoveries were made without relying on genomic analyses or further genetic manipulations. This example demonstrates the usefulness of ^{13}C-labeling experiments for revealing the global metabolic effects of perturbations, which could not otherwise be observed by measuring extracellular fluxes.

With knowledge of the enzymes involved in the metabolism under study, and with global analyses of how metabolism responds to genetic or environmental perturbations, one should be able to better predict the metabolic effects of genetic manipulations. As illustrated above, ^{13}C-labeling studies are an effective method for obtaining global metabolic data. These techniques are often referred to as ^{13}C-metabolic flux analysis (MFA), because, in addition to identifying which intermediary metabolic pathways are active, fluxes through these pathways can be quantified. MFA evolved from a mass balance approach, or flux balance analysis (FBA). FBA relies on a metabolic steady state, where the fluxes into a metabolite pool equal the fluxes out of that pool. Intermediary metabolic fluxes are estimated within the constraints of a stoichiometric metabolic network model using measurements of extracellular fluxes (i.e., substrate consumption and product formation rates, where products include biomass components).

Because FBA only uses consumption and production rate measurements, it has several limitations (84, 96). Fluxes through alternative pathways to a common product (without the production of a unique byproduct from one of those pathways) cannot be distinguished. Fluxes through cyclic pathways and bi-directional fluxes also cannot be determined. FBA analyses must therefore rely on assumptions about metabolism to estimate intermediary fluxes. For example, cofactor balances or demands, such as those for NADH and NADPH, can be used to estimate fluxes through various pathways, but the presence of enzymes like transhydrogenase make these assumptions ineffective.

Using ^{13}C-labeled substrates in combination with FBA overcomes these limitations. In addition to requiring metabolic steady state, MFA also requires (at least until recently [63, 64]) an isotopic steady state, where the proportion of labeled atoms in subtrate and metabolites is constant with time. The equations used in MFA to determine fluxes from labeling patterns describe metabolic and isotopic steady states so it is important that these conditions are met (97). Metabolic flux information is obtained from MFA when a labeled substrate is processed by different pathways, resulting in different labeling patterns, or isotopomers, in metabolic intermediates (96). These labeling patterns are imprinted on the metabolic products (e.g., proteinaceous amino acids) that are made from these metabolic intermediates and that can be measured by gas chromatography-mass spectrometry (GC-MS) and nuclear magnetic resonance spectroscopy (NMR). The ratios of the different labeling patterns can then be compared to determine the relative fluxes through the pathways that produced them. An example of this approach is illustrated in Figure 1.5, where forward glycolytic fluxes produce singly labeled 3-phosphoglycerate from [1-^{13}C]glucose, whereas OPPP flux produces unlabeled 3-

phosphoglycerate. The labeling pattern is imprinted on serine, which is then incorporated into protein. After protein hydrolysis, serine is derivatized and analyzed by GC-MS. After correcting for natural abundances of mass isotopes the relative fluxes through each pathway can be determined from the ratio of labeled to unlabeled serine.

Complex labeling patterns and reversible fluxes through multiple pathways can make manual interpretation of labeling patterns time-consuming and difficult. As a result, sophisticated software suites, such as *13C-Flux* (98), have been developed to estimate fluxes from isotopomer data (76). The process by which *13C-Flux*, and similar software, obtain values for metabolic fluxes from an experimental data set is illustrated in Figure 1.6. *13C-Flux* uses a metabolic network, substrate isotopomers conditions, and an arbitrary set of fluxes, to simulate an isotopomer data set. This simulated data set is compared to the measured data set, and the similarity between the two is scored by a sum of squared residuals (SS_{res}), weighted by the standard deviation of each measurement:

$$SS_{res} = \sum \left(\frac{\text{measured value} - \text{simulated value}}{\text{measured standard deviation}} \right)^2$$

The arbitrary fluxes are then adjusted in an iterative process until a set of fluxes is found that results in a simulated isotopomer data set that closely resembles the measured data set; an optimized fit. The quality of the fit can be statistically assessed by a χ^2 test. Statistical assessment of individual fluxes can also be performed (98).

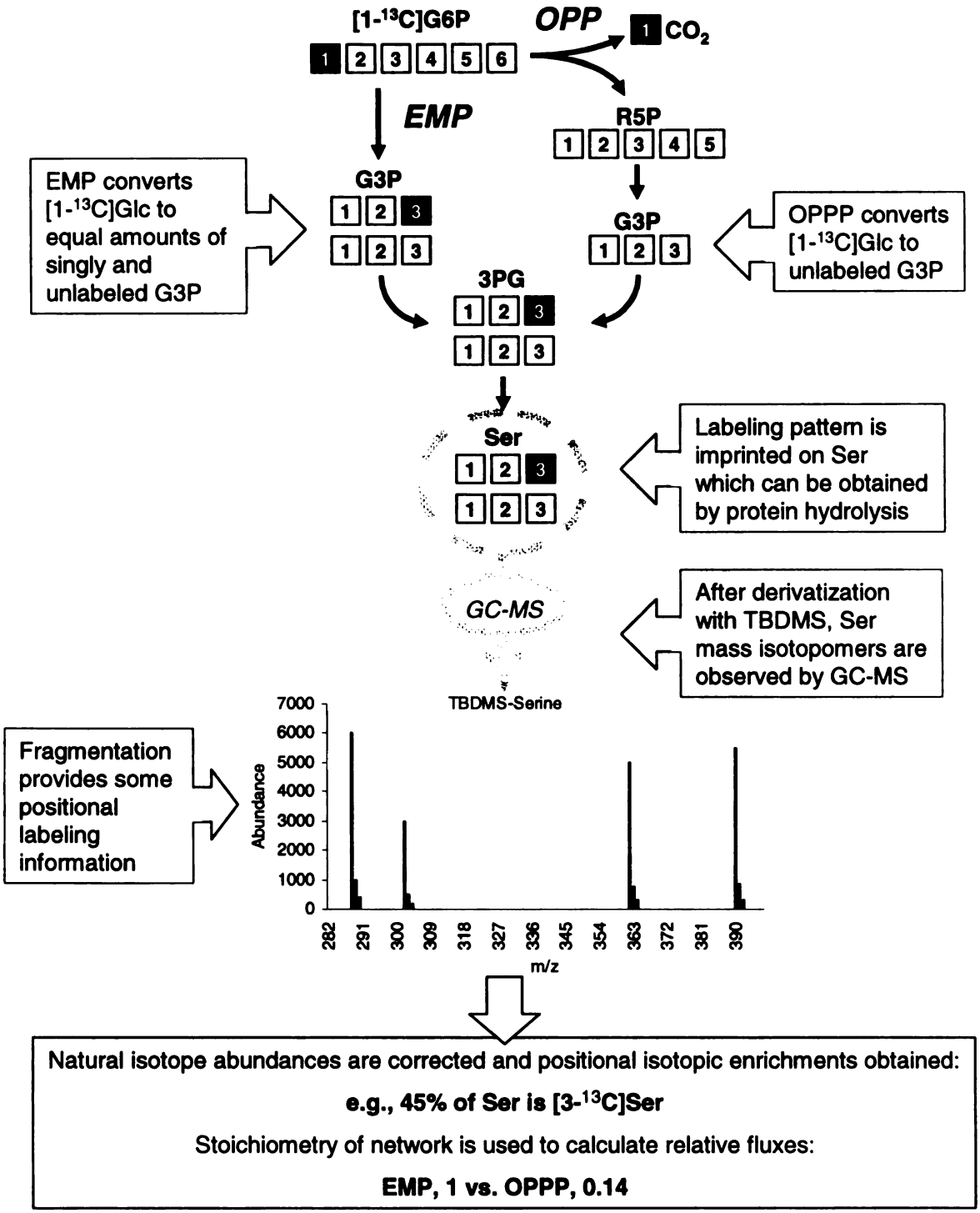

Figure 1.5. Determining relative EMP and OPPP fluxes from GC-MS measurements of serine. 3PG, 3-phosphoglycerate; G3P, glyceraldehyde-3-phosphate; G6P, glucose-6-phosphate; R5P, ribulose-5-phosphate TBDMS, tert-butyldimethylsilsyl.

MFA has been used to guide the engineering of industrially important organisms, such as lysine-producing *C. glutamicum*, as reviewed by Koffas and Stephanopoulos (41). Lysine is synthesized from OAA and pyruvate. FBA studies indicated that anaplerotic flux to OAA was limiting lysine production (90). Illustrating the limitationsof FBA, fluxes from PEP and pyruvate to OAA could not be distinguished, and OAA was thought to originate entirely from PEP carboxylation (90). Later, ^{13}C-labeling studies indicated that a pyruvate carboxylating activity was the principal C_3-carboxylating flux (68, 72). The PYC responsible for this flux was cloned, and confirmed to play a role in metabolism through genetic manipulations (42, 43, 70, 71). Overexpressing PYC favored either growth or lysine production depending on the aspartate concentration in the cell. This trend suggested that aspartate kinase flux was also important for balancing the lysine and biosynthesis demands on OAA (42). A metabolic control analysis study also indicated that aspartate kinase activity had a large influence on lysine production (101). By overexpressing both PYC and aspartate kinase, lysine specific productivity was increased by 44% on glucose, without growth defects. The increased PYC flux likely compensated for the drain of OAA from the TCA cycle to aspartate kinase. Thus, there was enough OAA supply the lysine synthesis pathway and the TCA cycle, which provides intermediates for biosynthesis (44).

Improving riboflavin-production by *Bacillus subtilis* is another example of metabolic engineering being guided by knowledge obtained from MFA. MFA performed under different growth conditions showed that different OPPP fluxes did not affect the riboflavin yield, indicating that neither precursor supply nor NADPH limited riboflavin production (16, 17, 81). MFA also identified a significant PEPCK flux from OAA to

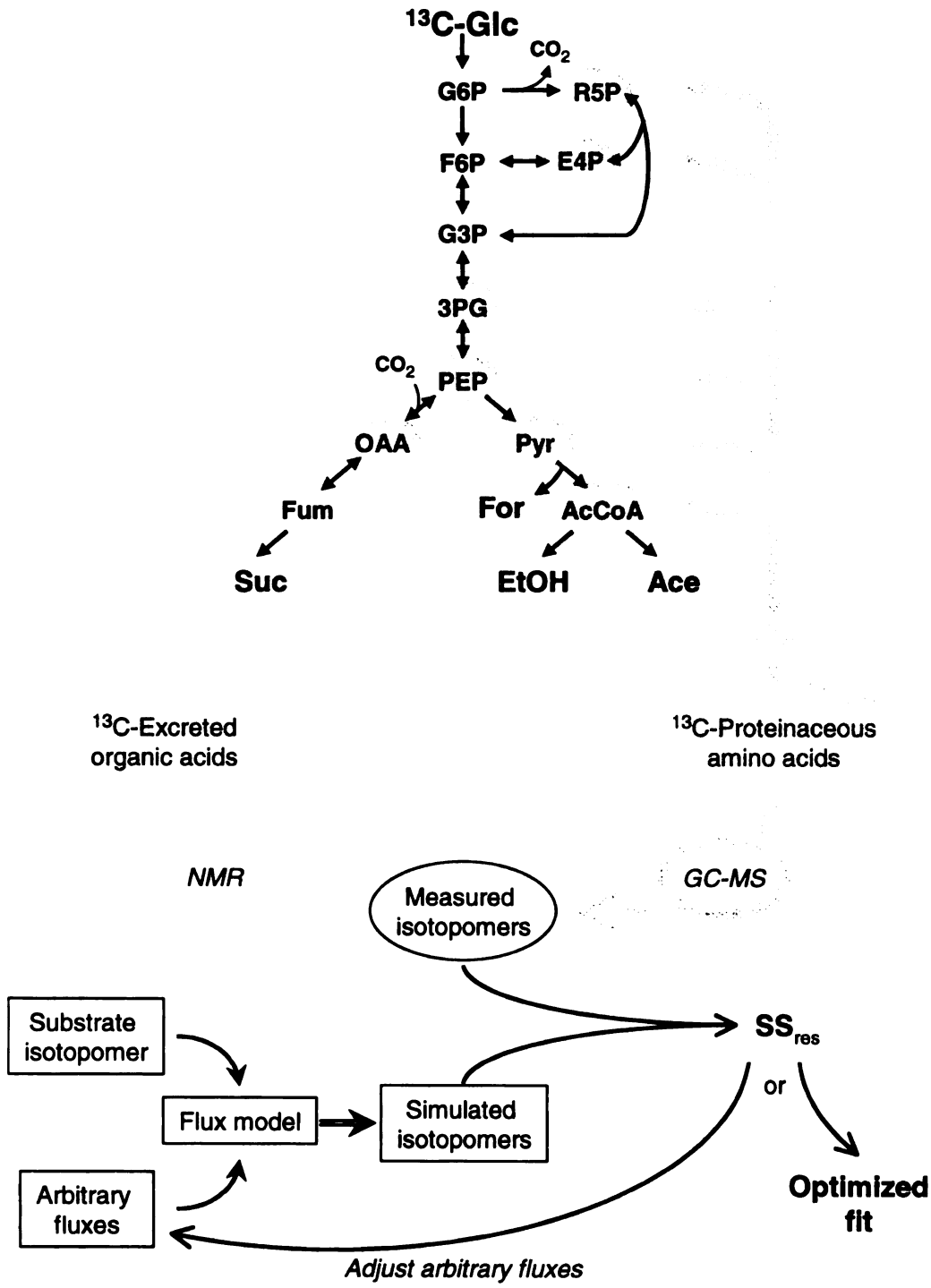

Figure 1.6. Estimation of intermediary metabolic fluxes from product isotopomers using *13C-FLUX*. E4P, erythrose-4-phosphate; F6P, fructose-6-phosphate; and SS_{res}, weighted sum of squared residuals. See Figure 1.1A and Figure 1.5 for other abbreviations. Dark gray ovals signify intermediates used for amino acid synthesis. Light gray ovals signify excreted organic acids.

PEP, completing an ATP-dissipating futile cycle from PEP → pyruvate → OAA → PEP (15-17, 81). Flux analyses carried out with carbon sources known to affect the ATP/ADP balance in the cell indicated that excess ATP was mostly being consumed in cell maintenance and energy-dissipating reactions (16). Those substrate mixtures resulting in the highest ATP/ADP ratios also resulted in the highest riboflavin yields (16). Guided by this understanding of the riboflavin-producing metabolism, the engineering focused on respiration efficiency and maintenance metabolism. By genetically disrupting the electron transport chain *bd* oxidase, which only pumps one H^+ per electron transfer, the bacterium had to rely on the more efficient aa_3 oxidase for respiration, which pumps two H^+ per electron transfer (103). The more efficient respiration decreased the energetic maintenance coefficient by ~40%, and subsequently improved riboflavin yields by ~30% (103). These examples with *C. glutamicum* and *B. subtilis* demonstrate the insights into microbial metabolism that can be gained from MFA, and how the information obtained can be used to guide successful metabolic engineering strategies. These examples also illustrate how carbon fluxes, determined in the absence of cofactor balance constraints, can provide an understanding of potentially important cofactor fluxes.

5. Objectives

A. succinogenes is a promising candidate for industrial succinate production, having the highest succinate titer, the highest substrate and product tolerance, and one of the highest specific succinate productivities (430 mg g^{-1} l^{-1}; McKinlay et al. unpublished data). However, relatively little is known about the organism, including its metabolism. This dissertation gives insight into *A. succinogenes* metabolism by accomplishing three objectives: (i), determine active metabolic pathways in *A. succinogenes*; (ii), determine

the fluxes through these pathways; and (iii), determine how fluxes respond to environmental perturbations. The resulting information is expected to be essential for guiding the metabolic engineering of *A. succinogenes*. ^{13}C-MFA was an attractive approach for studying *A. succinogenes* metabolism, because *A. succinogenes* is currently difficult to genetically manipulate, and until recently, no genome sequence was available.

^{13}C-MFA analyzes the labeling patterns in metabolic products. A chemically-defined medium was required to ensure that metabolic products (e.g., amino acids) were synthesized from ^{13}C-glucose rather than being obtained from unlabeled carbon sources (e.g., yeast extract). Chapter 2 describes the development of a chemically defined *A. succinogenes* growth medium, containing only the amino acids required for growth. This medium was also used without ^{13}C to address the existence of *A. succinogenes* TCA-associated fluxes. Chapter 3 describes the use of [1-^{13}C]glucose in the defined medium to establish the first *A. succinogenes* metabolic flux model. The *A. succinogenes* metabolic map was refined, and an understanding of the pathways responsible for generating anabolic reducing power and for distributing flux to succinate and alternative products was obtained. Chapter 4 describes MFA experiments performed under different $NaHCO_3$ and H_2 conditions with a more informative substrate isotopomer than was used in Chapter 3. Exchange fluxes were identified that could not be observed from using [1-^{13}C]glucose alone. A new understanding of how $NaHCO_3$ and H_2 perturbations affect *A. succinogenes* intermediary metabolic fluxes was obtained. In all cases, the MFA studies were complemented by *A. succinogenes* draft genome sequence information. An analysis of the industrially relevant features of the genome is described in Chapter 5. Chapter 6 summarizes the insights made into *A. succinogenes* metabolism. The results are used to

discuss possible future research for understanding and engineering *A. succinogenes* metabolism. Chapter 6 also emphasizes the importance of *A. succinogenes* gene knock-out and knock-in technologies and discusses possibilities for developing these tools.

1.6 References.

1. Al Zaid Siddiquee, M. J. A.-B. K., and K. Shimizu. 2004. Metabolic flux analysis of *pykF* gene knockout *Escherichia coli* based on ^{13}C-labeling experiments together with measurements of enzyme activities and intracellular metabolite concentrations. Appl. Microbiol. Biotechnol. 63:407-417.

2. Anonymous. 2005. 1,4-Butanediol, p. 42, Chemical Market Reporter, vol. 268.

3. Anonymous. 2002. BASF increases prices for 1,4-butanediol and derivatives, p. 8, Chemical Market Reporter, vol. 262.

4. Anonymous. 2005. Lanxess ups maleic anhydride capacity, p. 4, Chemical Market Reporter, vol. 267.

5. Anonymous. 2005. Prices & People, p. 16, Chemical Market Reporter, vol. 267.

6. Berglund, K. A., P. Elankovan, and D. A. Glassner. 1991. Carboxylic acid purification and crystallization process. U.S. patent 5,034,105.

7. Berglund, K. A., S. Yedur, and D. D. Dunuwila. 1999. Succinic acid production and purification. U.S. patent 5,958,744.

8. Brown, R. 2005. Housing sector boosts maleic anhydride, p. 24, Chemical Market Reporter, vol. 267.

9. Chang, J. 2006. Huntsman picks La. site, p. 4, Chemical Market Reporter, vol. 269.

10. Chartterjee, R., C. S. Millard, K. Champion, D. P. Clark, and M. I. Donnelly. 2001. Mutation of the *ptsG* gene results in increased production of succinate in fermentation of glucose by *Escherichia coli*. Appl. Environ. Microbiol. 67:148-154.

11. Cotelesage, J. J., L. Prasad, J. G. Zeikus, M. Laivenieks, and L. T. Delbaere. 2005. Crystal structure of *Anaerobiospirillum succiniciproducens* PEP carboxykinase reveals an important active site loop. Int. J. Biochem. Cell. Biol. 37:1829-1837.

12. Cox, S. J., S. Shalel Levanon, A. M. Sanchez, H. Lin, B. Peercy, G. N. Bennett, and K. Y. San. 2006. Development of a metabolic network design and optimization framework incorporating implementation constraints: a succinate production case study. Metab. Eng. 8.

13. Dake, S. B., R. V. Gholap, and R. V. Chaudhari. 1987. Carbonylation of 1,4-butanediol diacetate using rhodium complex catalyst: a kinetic study. Ind. Eng. Chem. Res. 26:1513-1518.

14. Datta, R., D. A. Glassner, M. K. Jain, and J. R. Vick Roy. 1992. Fermentation and purification process for succinic acid. U.S. patent 5,168,055.

15. Dauner, M., J. E. Bailey, and U. Sauer. 2001. Metabolic flux analysis with a comprehensive isotopomer model in *Bacillus subtilis*. Biotechnol. Bioeng. 76:144-156.

16. Dauner, M., M. Sonderegger, M. Hochuli, T. Szyperski, K. Wuthrich, H. P. Hohmann, U. Sauer, and J. E. Bailey. 2002. Intracellular carbon fluxes in riboflavin-producing *Bacillus subtilis* during growth on two-carbon substrate mixtures. Appl. Environ. Microbiol. 68:1760-1771.

17. Dauner, M., T. Storni, and U. Sauer. 2001. *Bacillus subtilis* metabolism and energetics in carbon-limited and excess-carbon chemostat culture. J. Bacteriol. 183:7308-7317.

18. Deng, Y., Z. Ma, K. Wang, and J. Chen. 1999. Clean synthesis of adipic acid by direct oxidation of cyclohexene with H_2O_2 over peroxytungstate-organic complex catalysts. Green Chem. 275:275-276.

19. Emmerling, M., M. Dauner, A. Ponti, J. Fiaux, M. Hochuli, T. Szyperski, K. Wuthrich, J.E. Bailey, and U. Sauer. 2002. Metabolic flux responses to pyruvate kinase knockout in *Escherichia coli*. J. Bacteriol. 184:152-164.

20. Fell, D. 1997. Understanding the control of metabolism. Portland Press, London and Miami.

21. Glassner, D. A., and R. Datta. 1992. Process for the production and purification of succinic acid. U.S. patent 5,143,834.

22. Gokarn, R. R., M. A. Eiteman, and E. Altman. 2000. Metabolic analysis of *Escherichia coli* in the presence and absence of the carboxylating enzymes phosphoenolpyruvate carboxylase and pyruvate carboxylase. Appl. Environ. Microbiol. 66:1844-1850.

23. Gokarn, R. R., J. D. Evans, J. R. Walker, S. A. Martin, M. A. Eiteman, and E. Altman. 2001. The physiological effects and metabolic alterations caused by the expression of *Rhizobium etli* pyruvate carboxylase in *Escherichia coli*. Appl. Microbiol. Biotechnol. 56:188-195.

24. Gross, R. A., and B. Kalra. 2002. Biodegradable polymers for the environment. Science 297:803-807.

25. Guettler, M. V., and M. K. Jain. 1996. Method for making succinic acid, *Anaerobiospirillum succiniciproducens* varients for use in process and methods for obtaining varients. U.S. patent 5,521,075.

26. Guettler, M. V., M. K. Jain, and D. Rumler. 1996. Method for making succinic acid, bacterial variants for use in the process, and methods for obtaining variants. US Patent 5,573,931 patent 5,573,931.

27. Guettler, M. V., M. K. Jain, and B. K. Soni. 1996. Process for making succinic acid, microorganisms for use in the process and methods of obtaining the microorganisms. US Patent 5,504,004 patent 5,504,004.

28. Guettler, M. V., D. Rumler, and M. K. Jain. 1999. *Actinobacillus succinogenes* sp. nov., a novel succinic-acid-producing strain from the bovine rumen. Int. J. Syst. Bacteriol. 49:207-216.

29. Hong, S. H., and S.Y. Lee. 2001. Metabolic flux analysis for succinic acid production by recombinant *Escherichia coli* with amplified malic enzyme activity. Biotechnol. Bioeng. 74:89-95.

30. Hong, S. H., J. S. Kim, S. Y. Lee, Y. H. In, S. S. Choi, J. K. Rih, C. H. Kim, H. Jeong, C. G. Hur, and J. J. Kim. 2004. The genome sequence of the capnophilic rumen bacterium *Mannheimia succiniciproducens*. Nat. Biotechnol. 22:1275-1281.

31. Huh, Y. S., Y. K. Hong, W. H. Hong, and H. N. Chang. 2004. Selective extraction of acetic acid from the fermentation broth produced by *Mannheimia succiniciproducens*. Biotechnol. Lett. 26:1581-1584.

32. Huh, Y. S., J. Y-S., Y. K. Hong, H. Song, S. Y. Lee, and W. H. Hong. 2006. Effective purification of succinic acid from fermentation broth produced by *Mannheimia succiniciproducens*. Process Biochem. 41:1461-1465.

33. Inui, M., S. Murakami, S. Okino, H. Kawaguchi, A. A. Vertes, and H. Yukawa. 2004. Metabolic analysis of *Corynebacterium glutamicum* during lactate and succinate productions under oxygen deprivation conditions. J. Mol. Microbiol. Biotechnol. 7.

34. Jabalquinto, A. M., F. D. Gonzalez-Nilo, M. Laivenieks, M. Cabezas, J. G. Zeikus, and E. Cardemil. 2004. *Anaerobiospirillum succiniciproducens* phosphoenolpyruvate carboxykinase. Mutagenesis at metal site 1. Biochimie 86:47-51.

35. Jabalquinto, A. M., M. Laivenieks, M. Cabezas, J. G. Zeikus, and E. Cardemil. 2002. The effect of active site mutations in the oxaloacetate decarboxylase and pyruvate kinase-like activities of *Anaerobiospirillum succiniciproducens* phosphoenolpyruvate carboxykinase. J. Protein. Chem. 21:443-445.

36. Jabalquinto, A. M., M. Laivenieks, F. D. Gonzalez-Nilo, M. V. Encinas, G. Zeikus, and E. Cardemil. 2003. *Anaerobiospirillum succiniciproducens*

phosphoenolpyruvate carboxykinase: mutagenesis at metal site 2. J. Protein. Chem. 22:515-519.

37. Jabalquinto, A. M., M. Laivenieks, F. D. Gonzalez-Nilo, A. Yevenes, M. V. Encinas, J. G. Zeikus, and E. Cardemil. 2002. Evaluation by site-directed mutagenesis of active site amino acid residues of *Anaerobiospirillum succiniciproducens* phosphoenolpyruvate carboxykinase. J. Protein. Chem. 21:393-400.

38. Jabalquinto, A. M., M. Laivenieks, J. G. Zeikus, and E. Cardemil. 1999. Characterization of the oxaloacetate decarboxylase and pyruvate kinase-like activities of *Saccharomyces cerevisiae* and *Anaerobiospirillum succiniciproducens* phosphoenolpyruvate carboxykinases. J. Protein. Chem. 18:659-664.

39. Kawaguchi, H., A. A. Vertes, S. Okino, M. Inui, and H. Yukawa. 2006. Engineering of a xylose metabolic pathway in *Corynebacterium glutamicum*. Appl. Environ. Microbiol. 72:3418-3428.

40. Kim, P., M. Laivenieks, C. Vieille, and J.G. Zeikus. 2004. Effect of overexpression of *Actinobacillus succinogenes* phosphoenolpyruvate carboxykinase on succinate production in *Escherichia coli*. Appl. Environ. Microbiol. 70:1238-1241.

41. Koffas, M., and G. Stephanopoulos. 2005. Strain improvement by metabolic engineering: lysine production as a case study for systems biology. Curr. Opin. Biotechnol. 16:361-366.

42. Koffas, M. A., G. Y. Jung, J. C. Aon, and G. Stephanopoulos. 2002. Effect of pyruvate carboxylase overexpression on the physiology of *Corynebacterium glutamicum*. Appl. Environ. Microbiol. 68:5422-5428.

43. Koffas, M. A., R. Ramamoorthi, W. A. Pine, A. J. Sinskey, and G. Stephanopoulos. 1998. Sequence of the *Corynebacterium glutamicum* pyruvate carboxylase gene. Appl. Microbiol. Biotechnol. 50:346-352.

44. Koffas, M. A. G., G. Y. Jung, and G. Stephanopoulos. 2003. Engineering metabolism and product formation in *Corynebacterium glutamicum* by coordinated gene overexpression. Metab. Eng. 5:32-41.

45. Kwon, Y. D., S. Y. Lee, and P. Kim. 2006. Influence of gluconeogenic phosphoenolpyruvate carboxykinase (PCK) expression on succinic acid fermentation in *Escherichia coli* under high bicarbonate condition. J. Microbiol. Biotechnol. 16:1448-1452.

46. Lee, J. W., S. Y. Lee, H. Song, and J. S. Yoo. 2006. The proteome of *Mannheimia succiniciproducens*, a capnophilic rumen bacterium. Proteomics 6:3550-3566.

47. Lee, P. C., S. Y. Lee, S. H. Hong, and H. N. Chang. 2003. Batch and continuous cultures of *Mannheimia succiniciproducens* MBEL55E for the production of succinic acid from whey. Bioprocess. Biosyst. Eng. 26:63-67.

48. Lee, P. C., S. Y. Lee, S. H. Hong, and H. N. Chang. 2002. Isolation and characterization of a new succinic acid-producing bacterium, *Mannheimia succiniciproducens* MBEL55E, from bovine rumen. Appl. Microbiol. Biotechnol. 58:663-668.

49. Lee, P. C., S. Y. Lee, S. H. Hong, H. N. Chang, and S. C. Park. 2003. Biological conversion of wood hydrolysate to succinic acid by *Anaerobiospirillum succiniciproducens*. Biotechnol. Lett. 25:111-114.

50. Lee, P. C., W. G. Lee, S. Kwon, S. Y. Lee, and H. N. Chang. 2000. Batch and continuous cultivation of *Anaerobiospirillum succiniciproducens* for the production of succinic acid from whey. Appl. Microbiol. Biotechnol. 54:23-27.

51. Lee, P. C., W. G. Lee, S. Y. Lee, and H. N. Chang. 2000. Succinic acid production with reduced by-product formation in the fermentation of *Anaerobiospirillum succiniciproducens* using glycerol as a carbon source. Biotechnol. Bioeng. 72:41-48.

52. Lee, S. J., D.-Y. Lee, T. Y. Kim, B. H. Kim, J. Lee, and S. Y. Lee. 2005. Metabolic engineering of *Escherichia coli* for enhanced production of succinic acid, based on genome comparison and in silico gene knockout simulation. Appl. Environ. Microbiol. 71:7880-7887.

53. Lee, S. J., H. Song, and S. Y. Lee. 2006. Genome-based metabolic engineering of *Mannheimia succiniciproducens* for succinic acid production. Appl. Environ. Microbiol. 72:1939-1948.

54. Lin, H., G. N. Bennett, and K. Y. San. 2005. Fed-batch culture of a metabolically engineered *Escherichia coli* strain designed for high-level succinate production and yield under aerobic conditions. Biotechnol. Bioeng. 90:775-779.

55. Lin, H., G. N. Bennett, and K. Y. San. 2005. Metabolic engineering of aerobic succinate production systems in *Escherichia coli* to improve process productivity and achieve the maximum theoretical succinate yield. Metab. Eng. 7:116-127.

56. Lin, H., K. Y. San, and G. N. Bennett. 2005. Effect of *Sorghum vulgare* phosphoenolpyruvate carboxylase and *Lactococcus lactis* pyruvate carboxylase coexpression on succinate production in mutant strains of *Escherichia coli*. Appl. Microbiol. Biotechnol. 67:515-523.

57. Lin, H., R. V. Vadali, G. N. Bennett, and K. Y. San. 2004. Increasing the acetyl-CoA pool in the presence of overexpressed phosphoenolpyruvate carboxylase or

pyruvate carboxylase enhances succinate production in *Escherichia coli.* Biotechnol. Prog. 20:1599-1604.

58. Lynd, L. R., C. Wyman, M. Laser, D. Johnson, and R. Landucci. 2002. Strategic biorefinery analysis: analysis of biorefineries. National Renewable Energy Laboratory.

59. Macy, J. M., L. G. Ljungdahl, and G. Gottschalk. 1978. Pathway of succinate and propionate fromation in *Bacteroides fragilis.* J. Bacteriol. 134:84-91.

60. McKinlay, J. B., Y. Shachar-Hill, J. G. Zeikus, and C. Vieille. 2006. Determining *Actinobacillus succinogenes* metabolic pathways and fluxes by NMR and GC-MS analyses of ^{13}C-labeled metabolic product isotopomers. Metab. Eng. In press.

61. Millard, C. S., Y.-P. Chao, J. C. Liao, and M. I. Donnelly. 1996. Enhanced production of succinic acid by overexpression of phosphoenolpyruvate carboxylase in *Escherichia coli.* Appl. Environ. Microbiol. 62:1808-1810.

62. Nghiem, N., M. Donnelly, C.S. Millard, and L. Stols. 1999. Method for the production of dicarboxylic acids. U.S. patent 5,869,301.

63. Noh, K., A. Wahl, and W. Wiechert. 2006. Computational tools for isotopically instationary ^{13}C labeling experiments under metabolic steady state conditions. Metab. Eng. 8:554-577.

64. Noh, K., and W. Wiechert. 2006. Experimental design principles for isotopically instationary ^{13}C labeling experiments. Biotechnol. Bioeng. 94:234-251.

65. Okino, S., M. Inui, and H. Yukawa. 2005. Production of organic acids by *Corynebacterium glutamicum* under oxygen deprivation. Appl. Microbiol. Biotechnol. 68:475-480.

66. Park, D. H., M. Laivenieks, M. V. Guettler, M. K. Jain, and J. G. Zeikus. 1999. Microbial utilization of electrically reduced neutral red as the sole electron donor for growth and metabolite production. Appl. Environ. Microbiol. 65:2912-2917.

67. Park, D. H., and J. G. Zeikus. 1999. Utilization of electrically reduced neutral red by *Actinobacillus succinogenes*: physiological function of neutral red in membrane-driven fumarate reduction and energy conservation. J. Bacteriol. 181:2403-2410.

68. Park, S. M., C. Shaw-Reid, A. J. Sinskey, and G. Stephanopoulos. 1997. Elucidation of anaplerotic pathways in *Corynebacterium glutamicum* via ^{13}C-NMR spectroscopy and GC-MS. Appl. Microbiol. Biotechnol. 47:430-440.

69. Paster, M., J. L. Pellegrino, and T. M. Carole. 2003. Industrial bioproducts: today and tomorrow. Energetics, Incorporated.

70. Peters-Wendisch, P. G., C. Kreutzer, J. Kalinowski, M. Patek, H. Sahm, and B. J. Eikmanns. 1998. Pyruvate carboxylase from *Corynebacterium glutamicum*: characterization, expression and inactivation of the *pyc* gene. Microbiology 144 915-927.

71. Peters-Wendisch, P. G., B. Schiel, V. F. Wendisch, E. Katsoulidis, B. Mockel, H. Sahm, and B. J. Eikmanns. 2001. Pyruvate carboxylase is a major bottleneck for glutamate and lysine production by *Corynebacterium glutamicum*. J. Mol. Microbiol. Biotechnol. 3:295-300.

72. Petersen, S., A. A. de Graaf, L. Eggeling, M. Mollney, W. Wiechert, and H. Sahm. 2000. *In vivo* quantification of parallel and bidirectional fluxes in the anaplerosis of *Corynebacterium glutamicum*. J. Biol. Chem. 275:35932-35941.

73. Podkovyrov, S. M., and J. G. Zeikus. 1993. Purification and characterization of phosphoenolpyruvate carboxykinase,a catabolic CO_2-fixing enzyme, from *Anaerobiospirillum succiniciproducens*. J. Gen. Microbiol. 139:223-228.

74. Ponce, E., N. Flores, A. Martinez, F. Valle, and F. Bolivar. 1995. Cloning of the two pyruvate kinase isoenzyme structural genes from *Escherichia coli*: the relative roles of these enzymes in pyruvate biosynthesis. J. Bacteriol. 177:5719-5722.

75. Ponce, E., A. Martinez, F. Bolivar, and F. Valle. 1997. Stimulation of glucose catabolism throught the pentose pathway by the absence of the two pyruvate kinase isoenzymes in *Escherichia coli*. Biotechnol. Bioeng. 58:292-295.

76. Ratcliffe, R. G., and Y. Shachar-Hill. 2006. Measuring multiple fluxes through plant metabolic networks. Plant J. 45:490-511.

77. Samuelov, N. S., R. Datta, M. K. Jain, and J. G. Zeikus. 1999. Whey fermentation by *Anaerobiospirillum succiniciproducens* for production of a succinate-based animal feed additive. Appl. Environ. Microbiol. 65:2260-2263.

78. Samuelov, N. S., R. Lamed, S. Lowe, and J. G. Zeikus. 1991. Influence of CO_2-HCO_3 levels and pH on growth, succinate production, and enzyme activities of *Anaerobiospirillum succiniciproducens*. Appl. Environ. Microbiol. 57:3013-3019.

79. Sanchez, A. M., G. N. Bennett, and K. Y. San. 2006. Batch culture characterization and metabolic flux analysis of succinate-producing *Escherichia coli* strains. Metab. Eng. 8:209-226.

80. Sanchez, A. M., G. N. Bennett, and K. Y. San. 2005. Novel pathway engineering design of the anaerobic central metabolic pathway in *Escherichia coli* to increase succinate yield and productivity. Metab. Eng. 7:229-239.

81. Sauer, U., V. Hatzimanikatis, J. E. Bailey, M. Hochuli, T. Szyperski, and K. Wuthrich. 1997. Metabolic fluxes in riboflavin-producing *Bacillus subtilis*. Nat. Biotechnol. 15:448-452.

82. Scardovi, V., and M. G. Chiappini. 1966. Studies in rumen bacteriology. V. Carboxylation of phosphoenolpyruvate in some rumen bacterial strains and in the cell-free extract of the total rumen flora. Ann. Microbiol. Enzymol. 16:119-127.

83. Scheifinger, C. C., and M. J. Wolin. 1973. Propionate formation from cellulose and soluble sugars by combined cultures of *Bacteroides succinogenes* and *Selenomonas ruminantium*. Appl. Environ. Microbiol. 26:789-795.

84. Schmidt, K., A. Marx, A.A. de Graaf, W. Wiechert, H. Sahm, J. Nielsen, and J. Villadsen. 1998. ^{13}C tracer experiments and metabolite balancing for metabolic flux analysis: comparing two approaches. Biotechnol. Bioeng. 58:254-257.

85. Secchi, C., V. V. Cantarelli, S. Pereira Fde, H. H. Wolf, T. C. Brodt, M. C. Amaro, and E. Inamine. 2005. Fatal bacteremia due to *Anaerobiospirillum succiniciproducens*: first description in Brazil. Braz. J. Infect. Dis. 9:169-172.

86. Song, H., and S. Y. Lee. 2006. Production of succinic acid by bacterial fermentation. Enzyme Microbial Technol. 39:353-361.

87. Stephanopoulos, G., A. A. Aristidou, and J. Nielsen. 1998. Metabolic Engineering: Principles and Methodologies. Academic Press, London.

88. Stols, L., and M. I. Donnelly. 1997. Production of succinic acid through overexpression of NAD^+-dependent malic enzyme in an *Escherichia coli* mutant. Appl. Environ. Microbiol. 63:2695-2701.

89. Tilton, H. 2003. Prices & People, p. 20, Chemical Market Reporter, vol. 264.

90. Vallino, J. J., and G. Stephanopoulos. 1993. Metabolic flux distributions in *Corynebacterium glutamicum* during growth and lysine overproduction. Biotechnol. Bioeng. 41:633-646.

91. van der Werf, M. J., M. V. Guettler, M. K. Jain, and J. G. Zeikus. 1997. Environmental and physiological factors affecting the succinate product ratio during carbohydrate fermentation by *Actinobacillus sp.* 130Z. Arch. Microbiol. 167:332-342.

92. van Gylswyk, N. O. 1995. *Succiniclasticum ruminis* gen. nov., sp. nov., a ruminal bacterium convering succinate to propionate as the sole energy-yielding mechanism. Int. J. Syst. Bacteriol. 45:297-300.

93. Vemuri, G. N., M. A. Eiteman, and E. Altman. 2002. Succinate production in dual-phase *Escherichia coli* fermentations depends on the time of transition from aerobic to anaerobic conditions. J. Ind. Microbiol. Biotechnol. 28:325-332.

94. Vemuri, G. N., M.A. Eiteman, and E. Altman. 2002. Effects of growth mode and pyruvate carboxylase on succinic acid production by metabolically engineered strains of *Escherichia coli.* Appl. Environ. Microbiol. 68:1715-1727.

95. Wendisch, V. F., M. Bott, J. Kalinowski, M. Oldiges, and W. Wiechert. 2006. Emerging *Corynebacterium glutamicum* systems biology. J. Biotechnol. 124:74-92.

96. Wiechert, W. 2001. ^{13}C Metabolic flux analysis. Metab. Eng. 3:195-206.

97. Wiechert, W., and A. A. de Graaf. 1997. Bidirectional reaction steps in metabolic networks: I. Modeling and simulation of carbon isotope labeling experiments. Biotechnol. Bioeng. 55:101-117.

98. Wiechert, W., M. Mollney, S. Petersen, A. A. de Graaf, and 2001. A universal framework for ^{13}C metabolic flux analysis. Metab. Eng. 3:265-283.

99. Wilke, D. 1999. Chemicals from biotechnology: molecular plant genetics will challenge the chemical and fermentation industry. Appl. Microbiol. Biotechnol. 52:135-145.

100. Wood, A. 2004. Bioprocessing, p. 15-17, Chemical Week, vol. 166.

101. Yang, C., Q. Hua, and H. Shimizu. 1999. Development of a kinetic model for L-lysine biosynthesis in *Corynebacterium glutamicum* and its application to metabolic control analysis. J. Biosci. Bioeng. 88:393-403.

102. Yoo, J. Y., and J. G. Zeikus. 1996. Modulation of phosphoenolpyruvate metabolism of *Anaerobiospirillum succiniciproducens* ATCC 29305. J. Microbiol. Biotechnol. 6:43-49.

103. Zamboni, N., N. Mouncey, H. P. Hohmann, and U. Sauer. 2003. Reducing maintenance metabolism by metabolic engineering of respiration improves riboflavin production by *Bacillus subtilis*. Metab. Eng. 5:49-55.

104. Zeikus, J. G., M. K. Jain, and P. Elankovan. 1999. Biotechnology of succinic acid production and markets for derived industrial products. Appl. Environ. Microbiol. 51:545-552.

Chapter 2

Insights into *Actinobacillus succinogenes* fermentative metabolism in a chemically defined growth medium

McKinlay, J. B., J. G. Zeikus, and C. Vieille. 2005. Insights into *Actinobacillus succinogenes* fermentative metabolism in a chemically defined growth medium. Applied and Environmental Microbiology. **71:**6651-6656.

2.1 ABSTRACT

Chemically defined media allow for a variety of metabolic studies that are not possible in undefined media. A defined medium, AM3, was created to expand the experimental opportunities for investigating the fermentative metabolism of succinate-producing *Actinobacillus succinogenes*. AM3 is a phosphate-buffered medium containing vitamins, minerals, NH_4Cl as the main nitrogen source, and glutamate, cysteine, and methionine as required amino acids. *A. succinogenes* growth trends and endproduct distributions in AM3 and rich medium fermentations were compared. The effect of $NaHCO_3$ concentration in AM3 on endproduct distribution, growth rate, and metabolic rates were also examined. The *A. succinogenes* growth rate was 1.3 to 1.4 times higher at 25 mM $NaHCO_3$ than at any other $NaHCO_3$ concentration, likely because both energy-producing metabolic branches (i.e., the succinate-producing branch and the formate, acetate, and ethanol-producing branch) were functioning at relatively high rates in the presence of 25 mM bicarbonate. To improve the accuracy of the *A. succinogenes* metabolic map, the reasons for *A. succinogenes* glutamate auxotrophy were examined by enzyme assays and by testing the ability of glutamate precursors to support growth. Enzyme activities were detected for glutamate synthesis that required glutamine or α-ketoglutarate. The inability to synthesize α-ketoglutarate from glucose indicates that at least two tricarboxylic acid cycle-associated enzyme activities are absent in *A. succinogenes*.

2.2 INTRODUCTION

Bio-based chemical production is a growing multi-billion dollar industry converting renewable resources into valuable products (20, 21). A US $15 billion market could be based on succinate for producing bulk chemicals such as 1,4-butanediol (a precursor to "stronger-than-steel" plastics), ethylene diamine disuccinate (a biodegradable chelator), diethyl succinate (a green solvent for replacement of methylene chloride), and adipic acid (nylon precursor) (24). However, the cost of bio-based succinate is not yet competitive with petrochemical-based alternatives such as maleic anhydride. The development of a cost-effective industrial succinate fermentation will rely on organisms able to produce high concentrations of succinate and at high rates.

Actinobacillus succinogenes is a capnophilic, facultatively anaerobic, gram negative bacterium that naturally produces high concentrations of succinate as a fermentation endproduct in addition to formate, acetate, and ethanol (4-6, 18). *A. succinogenes* converts glucose to phosphoenolpyruvate (PEP), at which point metabolism splits into two branches: (i) the formate, acetate and ethanol-producing C3 pathway, and (ii) the succinate producing C4 pathway (Fig. 1). Metabolic engineering of *A. succinogenes* has begun, with the aim of achieving a homosuccinate fermentation. The most notable success has arisen from inactivation of pyruvate-formate lyase (PFL) by selecting mutants resistant to fluoroacetate (4, 13). *A. succinogenes* PFL mutants have increased succinate yields, however significant amounts of pyruvate are also formed.

Modern, efficient metabolic engineering strategies rely on a thorough understanding of the metabolism under study, and of how metabolism responds to environmental and genetic perturbations (2, 16). This understanding can be obtained by using ^{13}C-labeling

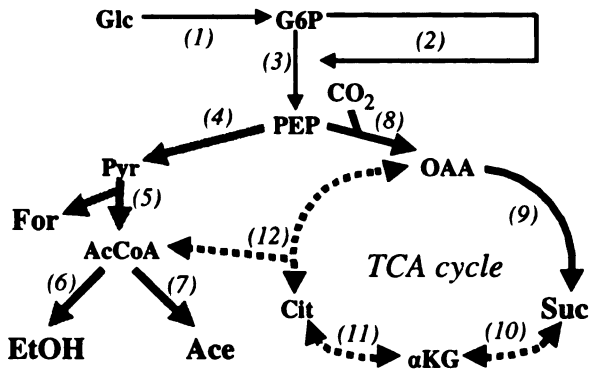

Figure 2.1. Simplified metabolic map of *A. succinogenes* central metabolism. Thin black arrows are glucose uptake, pentose phosphate pathway (PPP), and Embden-Meyerhoff-Parnas pathway (EMP) reactions. Grey arrows are C3 pathway reactions. Thick black arrows are C4 pathway reactions. Dashed arrows are TCA-associated reactions that have not been tested. 1. hexokinase or PEP: glucose phosphotransferase; 2. PPP; 3. EMP; 4. pyruvate kinase and PEP: glucose phosphotransferase; 5. pyruvate-formate lyase; 6. acetaldehyde dehydrogenase and alcohol dehydrogenase; 7. phosphotransacetylase and acetate kinase; 8. PEP carboxykinase; 9. malate dehydrogenase, fumarase, and fumarate reductase; 10 succinyl-CoA synthetase, αKG dehydrogenase, and αKG synthase; 11. isocitrate dehydrogenase and aconitase; 12. citrate lyase and citrate synthase. Metabolites: Glc, glucose; G6P, glucose-6-phosphate; Pyr, pyruvate; For, formate; AcCoA, acetyl-CoA; EtOH, ethanol; Ace, acetate; OAA, oxaloacetate; Suc, succinate; Cit, citrate.

experiments to measure intracellular metabolic fluxes. These experiments require a defined growth medium so that cell components (e.g., amino acids) are synthesized from labeled substrate (e.g., ^{13}C-glucose) and not from complex media components such as yeast extract. Furthermore, an accurate metabolic map is essential for metabolic flux analyses. A defined medium, AM3, for growing wild-type *A. succinogenes* is described. A common experiment for succinate-producing capnophiles is conducted in AM3 with different $NaHCO_3$ concentrations that provides new insights into *A. succinogenes* metabolism. Finally, we improve the *A. succinogenes* metabolic map in the poorly characterized region of its TCA-cycle by using experiments made possible by one of *A. succinogenes* amino acid auxotrophies and by the advent of AM3.

2.3 MATERIALS AND METHODS

2.3.1 Chemicals, bacteria, and culture conditions. All chemicals were purchased from Sigma-Aldrich (St. Louis, MO) unless otherwise stated. *Escherichia coli* K12 (ATCC 10798) and *A. succinogenes* type strain 130Z (ATCC 55618) were obtained from the American Type Culture Collection. All liquid cultures were incubated at 37°C and shaken at 250 rpm. Cultures were inoculated with cell suspensions that were harvested in late log phase, washed twice in sterile saline, and resuspended in an appropriate volume of sterile saline to give a starting OD_{660} of 0.1 after inoculation.

2.3.2 Identification of a defined growth medium, AM3. The defined medium was based on the phosphate buffer of the rich medium, Medium A, commonly used to grow *A. succinogenes* (13, 14, 18), and it contained per liter: 15.5 g K_2HPO_4, 8.5 g $Na_2HPO_4*H_2O$, 1 g NaCl, 2 g NH_4Cl, and 10 ml mineral mix. This basal solution was aliquoted into 28-ml anaerobic test tubes. The tubes were then sealed with rubber bungs and aluminum crimps, and repeatedly flushed and evacuated with N_2. After autoclaving, each tube received filter-sterilized vitamin mix, kanamycin, amino acids, glucose, and $NaHCO_3$ to final respective concentrations of 2 ml/L, 10 μg/ml, 0.08 %, 50 mM, and 30 mM. Concentrations of basal solution and supplement stocks were adjusted to give total culture volumes of 10 ml. Soluble $NaHCO_3$ was used instead of insoluble $MgCO_3$ (4, 5, 18) to facilitate growth measurements by optical density. One M $NaHCO_3$ stock solutions under 100 % CO_2 atmosphere were prepared as described (19). An equal volume of sterile 100 % CO_2 was used to replace any volume of $NaHCO_3$ taken from the stock

solutions. The final medium pH was 6.9 – 7.1, depending on the amount of $NaHCO_3$ added. The mineral mix was based on Lovley (11) and contained per liter: 1.5 g nitrilotriacetic acid, 3 g $MgSO_4*7H_2O$, 0.5 g $MnSO_4*H_2O$, 0.1 g $FeSO_4*7H_2O$, 0.1 g $CaCl_2*2H_2O$, 0.1 g $CoCl_2*6H_2O$, 13 mg $ZnCl_2$, 10 mg $CuSO_4*5H_2O$, 10 mg $AlK(SO_4)_2*12H_2O$, 10 mg H_3BO_3, 25 mg Na_2MoO_4, 25 mg $NiCl_2*6H_2O$, 25 mg $Na_2WO_4*2H_2O$, and 10 mg $NaSeO_3$. The vitamin mix was based on Wolin et al. (22) and contained per liter: 10 mg biotin, 10 mg folic acid, 50 mg pyridoxine HCl, 25 mg thiamine HCl, 25 mg riboflavin, 25 mg nicotinic acid, 25 mg pantothenic acid, 0.5 mg cyanocobalamin, 25 mg P-aminobenzoic acid, and 25 mg thioctic acid.

The inoculum was *A. succinogenes* 130Z grown from glycerol frozen stocks in 10 ml of BBL trypticase soy broth (TSB; Becton Dickinson, Sparks, MD) containing 50 mM glucose, 30 mM $NaHCO_3$, and 10 μg/ml kanamycin in 15-ml screw cap glass tubes with air as headspace. The defined medium was inoculated with 0.5 ml of washed cell suspension. The original defined medium supporting growth contained 12 amino acids (i.e., glutamate, aspartate, cysteine, tyrosine, phenylalanine, serine, alanine, isoleucine, valine, arginine, leucine, and methionine) that were chosen based on literature for *Haemophilus influenzae* defined media (7, 8). Cells grown in this medium were washed and used to inoculate various defined media containing 11 amino acids, each medium missing one of the initial 12 amino acids. This procedure was repeated with fewer and fewer amino acids until the amino acids required for growth were identified. The defined medium with the fewest amino acids still supporting growth was called AM3.

2.3.3 Growth of *A. succinogenes* on AM3 solid agar medium. AM3 agar was prepared as for the liquid medium, with the addition of 1.5% Bacto agar (Becton Dickinson) and with or without 10 g/L $MgCO_3$ prior to autoclaving. $NaHCO_3$ was added to some preparations after autoclaving to a final concentration of 30 mM. *A. succinogenes* was grown in liquid AM3 and washed as described. After aerobic inoculation, plates were incubated at 37°C in an anaerobic jar with a CO_2 headspace.

2.3.4 Determination of growth trends and fermentation balances in AM3 and Medium A.

Anoxic Media A and AM3 (11 ml final volume in 28-ml test tubes) were inoculated with 0.25 ml of washed cells grown in identical media. Medium A differs from AM3 by having 5 g/L yeast extract in place of the vitamins, minerals, amino acids, NaCl, and NH_4Cl in AM3. Both media contained 150 mM $NaHCO_3$. Growth was monitored throughout log phase by measuring OD_{660} with a Spectronic 20 (Bausch and Lomb, Rochester, NY), which does not require culture sampling. Growth rates were determined from 4 – 6 measurements. Samples (< 1 ml) were collected at the beginning of incubation, once during log phase (0.6 – 1.0 OD_{660}), and at the end of log phase. The optical densities of these samples were determined using a DU 650 spectrophotometer (Beckman, Fullerton, CA). These OD_{660} values (more precise than those obtained with the Spectronic 20) were used to calculate final OD, and in carbon and electron balances. Glucose and metabolic endproducts in the sample supernatants were separated by HPLC (Waters, Milford, MA) on a 300 x 7.8 mm Aminex HPX-87H column (Bio-Rad, Hercules, CA) at 23°C with 4 mM H_2SO_4 as the eluent, at a flow rate of 0.6 ml/min.

Glucose and ethanol were quantified using a Waters 410 differential refractometer, and organic acids were quantified using a Waters 2487 UV detector at 210 nm.

2.3.5 Determination of fermentation balances, growth rates, and product formation rates in AM3 with different $NaHCO_3$ concentrations. Anoxic AM3 was prepared as described but with $NaHCO_3$ concentrations ranging from 5 to 150 mM. The inoculum was 0.25 ml of washed culture grown in AM3 of identical $NaHCO_3$ concentration. Sample collection and determination of cell densities, growth rates, and endproduct concentrations were performed as described above. CO_2 was detected by transferring 1 ml of culture headspace and 0.3 ml of liquid cultures to separate bung-sealed 13-ml serum vials. The liquid sample was acidified with 50 µl of 3.2 N H_2SO_4. Vial headspaces were sampled using a pressure syringe and injected into a Series 750 gas chromatograph (GOW-MAC, Bethlehem, PA) equipped with a Carbosphere column, methanizer, and flame ionization detector. Specific rates were calculated as described for batch cultures (15, 16). For example, to calculate a specific product formation rate the equation $r_p = Y_{XP}\mu$, was used, where r_p is the specific product formation rate, Y_{XP} is the amount of product produced per gram of biomass, and μ is the growth rate.

2.3.6 Preparation of crude cell extracts and enzyme assays. *A. succinogenes* 130Z was grown in 450 ml Medium A containing 33 mM glucose and 15 mM $NaHCO_3$ in 1 L spherical flasks with an N_2 headspace. Cultures were harvested in log phase by centrifugation, washed once with 200 ml 0.1 M Tris-HCl (pH 7.7), and resuspended in 20 ml 0.1 M Tris-HCl (pH 7.7). Cells were lysed by two passages through a French press at

1,200 -1,400 lb under an N_2 headspace. Cell extracts were stored at -20°C before assays. The cell extract protein concentration (i.e., 1.8 mg protein /ml) was quantified by the bicinchoninic acid assay (Pierce, Rockford, IL) with bovine serum albumin as the standard (12).

Enzyme activities were assayed by measuring the oxidation or reduction of NADP(H) using a Cary 300 spectrophotometer (Varian, Palo Alto, CA). An extinction coefficient of 6.23 cm^{-1} mM^{-1} at 340 nm was used for NADPH (18). Reagents were dissolved in 0.1 M Tris-HCl (pH 8.0), and reactions were carried out in triplicate in 1 ml volumes at 37°C. The reaction mixture for the glutamate dehydrogenase assay contained 40 mM NH_4Cl, 5 mM α-ketoglutarate (αKG), 0.3 mM NADPH, 1 mM $CaCl_2$, and 25 µl cell extract. The reaction was started by the addition of αKG. Glutamate synthase activity was tested in the presence of 5 mM glutamine, 5 mM αKG, 0.3 mM NADPH, 1 mM $CaCl_2$, and 25 µl cell extract. The reaction was started by the addition of glutamine. Isocitrate dehydrogenase was assayed using anoxic reagents in rubber-stoppered cuvettes that were evacuated and flushed with N_2 as described (23). The reaction mixture contained 0.1 M NaCl, 5 mM $MgCl_2$, 1 mM dithiothreitol, 0.3 mM $NADP^+$, 50 µl cell extract, and 5 mM isocitrate (17). Cell extracts (15.2 mg protein/ml) from *E. coli* K12 aerobically grown in LB with 25 mM glucose were used as a positive control. The reaction was started with the addition of isocitrate. No enzyme activity was detected in any assay when NAD(H) was used in place of NADP(H).

2.3.7 Test of potential glutamate precursors to support growth. Anoxic defined medium was prepared as described for AM3, but glutamate and/or NH_4Cl were omitted

where appropriate. Filter-sterilized stock solutions of potential glutamate precursors (i.e., αKG, glutamine, aspartate, isocitrate, and citrate) were added to the autoclaved medium to 15 mM final concentration. The inoculum was 0.25 ml of *A. succinogenes* grown in AM3 and washed as described. The culture volume was 12 ml. The turbidity was monitored until stationary phase was reached or for five days using a Spectronic 20. If growth occurred, cells were washed as before and used to inoculate identical medium to ensure that growth was not due to nutrient carry over.

2.4 RESULTS AND DISCUSSION

2.4.1 Creation of the defined growth medium, AM3. *A. succinogenes* grew slowly (0.06 hr^{-1}) when first transferred from TSB to defined medium containing the initial 12 amino acids, with final OD_{660} values ranging from 0.7 to 1.1. After several transfers in defined medium, growth rates increased to 0.14 hr^{-1}. This improvement could be due to a slow response in gene regulation to suit the new growth conditions or to genetic drift. After removing amino acids from the defined medium one at a time, the amino acid requirements of *A. succinogenes* were determined to be cysteine, glutamate, and methionine. To improve the *A. succinogenes* growth rate and final OD in defined medium, concentrations of amino acids, NH_4Cl, vitamin mix, and mineral mix were varied, and their effects on growth rate and final OD were determined. Mineral mix, vitamin mix, and amino acids were required for anaerobic growth on glucose. Increasing the vitamin concentration from 2 ml/L to 10 ml/L doubled the growth rate and tripled the final OD. *A. succinogenes* grew without NH_4Cl when glutamate, cysteine, and methionine were present but the growth rate (0.03 ± 0.00 hr^{-1}) and final OD_{660} (0.44 ± 0.07) were poor. The improved medium, called AM3, contained per liter: 15.5 g K_2HPO_4, 8.5 g $Na_2HPO_4*H_2O$, 1 g NaCl, 2 g NH_4Cl, 0.15 g L-glutamate, 0.08 g L-cysteine-HCl, 0.08 g L-methionine, 10 ml mineral mix, 10 ml vitamin mix, 30 mmol $NaHCO_3$, and 50 mmol glucose.

A. succinogenes also grew on solid AM3 agar. One-mm sized colonies developed after 2 - 4 days of incubation under CO_2 gas phase at 37°C. Colonies developed with and without $MgCO_3$ or $NaHCO_3$.

2.4.2 Growth trends and fermentation balances in AM3 and Medium A. In a defined medium, bacteria are forced to synthesize a number of cellular building blocks that would otherwise be available from rich medium components. For this reason, growth rates were lower in AM3 (0.24 ± 0.01 hr^{-1}) than in Medium A (0.43 ± 0.01 hr^{-1}). The final OD_{660} in AM3 (2.82 ± 0.05) was slightly lower than in Medium A (3.03 ± 0.14). Since most of the succinate is produced during log phase, fermentation balances were based on log phase samples. While carbon and electron recoveries for cultures grown in AM3 were near 100%, recoveries for cultures grown in Medium A exceeded 100% (Table 1) likely because carbon and electron recoveries only take into account the glucose consumed. The yeast extract carbon in Medium A is ~50% that of the supplied glucose, according to the BD Diagnostic Systems website (http://www.bd.com/diagnostics/microservices/regulatory) and Doyle et al. (1). Thus, there is ample carbon in yeast extract to explain a 117% carbon recovery in Medium A. Yeast extract may also have contributed to the higher formate and acetate yields and to the lower succinate product ratio in Medium A compared to AM3. With no undefined carbon sources to track in AM3, the comparison of fermentation balances in AM3 and Medium A illustrates how a chemically defined medium facilitates metabolic studies.

2.4.3 Effect of AM3 $NaHCO_3$ concentration on fermentation balances, growth rates, and metabolic rates. Succinate production by *A. succinogenes* requires CO_2, presumably as a substrate for PEP carboxykinase (9, 18) (Fig.1). We previously showed that *A. succinogenes* produces more succinate and less alternative endproducts when the $MgCO_3$

Medium	mmol product / 100 mmol glucose consumed					Carbon Recovery[b] (%)	Electron Recovery[c] (%)	Succinate product ratio[d]
	Succinate	Formate	Acetate	Ethanol	Biomass[a]			
Defined (AM3)	70 ± 1	61 ± 3	64 ± 2	9 ± 2	166 ± 5	97 ± 2	106 ± 2	0.97 ± 0.02
Rich (Medium A)	70 ± 1	99 ± 6	80 ± 3	16 ± 4	199 ± 5	117 ± 1	117 ± 0	0.73 ± 0.02

Table 2.1. Log phase fermentation balances of *A. succinogenes* in AM3 and Medium A

Data are means ± standard deviation from triplicate cultures.

[a] mmol Biomass was determined using assumed values of 567 mg dry cell weight / ml per OD_{660} and a cell composition of $CH_2O_{0.5}N_{0.2}$ (24.967 g/mol) (18).

[b] Carbon in product / carbon in glucose consumed. An assumption was made that one mole of CO_2 was fixed per mole succinate produced (18). Therefore, $C_3H_6O_2$ was used as the chemical composition of succinate derived from glucose consumed.

[c] Electron recoveries are based on available hydrogen (3).

[d] Succinate / (acetate + ethanol). It was assumed that all formate is formed from PFL and is accounted for in the sum of acetate and ethanol. Production of less formate than the sum of acetate and ethanol may be due to pyruvate dehydrogenase activity, however this has not yet been proven for *A. succinogenes*.

concentration was increased in Medium A (18). To confirm that this trend holds in AM3, we compared endproduct distributions in AM3 with different $NaHCO_3$ concentrations. Indeed, increasing the $NaHCO_3$ concentration in AM3 increased the succinate product ratio (Table 2). In addition to confirming this trend, we also wanted to determine an optimal $NaHCO_3$ concentration for succinate production in AM3. In our previous study, the maximum $MgCO_3$ concentration tested was equimolar to that of the supplied glucose (i.e., 55 mM) (18). Here we tested $NaHCO_3$ concentrations up to 3 times the molar concentration of supplied glucose. As seen in Table 2, the succinate production ratio plateaued at $NaHCO_3$ concentrations above 75 mM. Although not quantitatively precise, CO_2 was detected in all cultures at the time of log phase sampling (data not shown). Therefore, the reported succinate yields are not due to complete CO_2 consumption. While CO_2 was not completely consumed, the endproduct distributions suggest that $NaHCO_3$, at 5 and 25 mM, may be limiting succinate production.

As shown in Table 2, the average growth rate was statistically higher at 25 mM $NaHCO_3$ than at any other $NaHCO_3$ concentration (*t*-test, 2-tail, equal variance, $p = 0.001$). This high growth rate can be explained by the metabolic rates shown in Table 3. At 5 mM $NaHCO_3$, C3 flux (estimated from specific acetate and ethanol formation rates) is high, while C4 flux (i.e., the specific succinate formation rate) is low. At 25 mM $NaHCO_3$, C3 flux remains high, with a maximum acetate formation rate, and C4 flux reaches a maximum. At 75 mM $NaHCO_3$ and above, C4 flux remains high, while C3 flux decreases by about half. ATP can be derived from PEP conversion to succinate via the C4 pathway (1.67 mol ATP), and from ethanol (1 mol ATP) or acetate (2 mol ATP) productions via the C3 pathway. With high C3 and C4 fluxes at 25 mM $NaHCO_3$, more

$NaHCO_3$ concn. (mM)	mmol product / 100 mmol glucose consumed					Carbon Recovery (%)	Electron Recovery (%)	Succinate product ratio	Growth rate (hr^{-1})
	Succinate	Formate	Acetate	Ethanol	Biomass				
5	33 ± 1	117 ± 1	72 ± 1	51 ± 7	146 ± 6	101 ± 1	109 ± 2	0.27 ± 0.02	0.24 ± 0.01
25	52 ± 2	91 ± 1	68 ± 1	28 ± 3	169 ± 4	101 ± 2	110 ± 2	0.54 ± 0.03	0.32 ± 0.01
75	67 ± 1	58 ± 5	61 ± 3	14 ± 1	199 ± 10	102 ± 4	113 ± 4	0.90 ± 0.03	0.25 ± 0.00
125	71± 1	60 ± 2	64 ± 1	10 ± 3	176 ± 1	100 ± 2	110 ± 2	0.96 ± 0.05	0.23 ± 0.01
150	70 ± 0	61 ± 3	64 ± 2	9 ± 2	166 ± 5	97 ± 2	106 ± 2	0.97 ± 0.02	0.24 ± 0.01

Table 2.2. Effect of $NaHCO_3$ concentration on endproduct distribution and growth rate in AM3

Data are means ± standard deviation from triplicate cultures. Biomass, carbon recovery, electron recovery, and succinate product ratio were calculated as described in Table 1.

ATP is generated for biosynthesis, explaining the high growth rate in these conditions. The maximum succinate formation rate at 25 mM $NaHCO_3$ also indicates that $NaHCO_3$ is not limiting succinate production, unlike what Table 2 endproduct distributions suggest.

It is also worth noting that the high specific product formation rates at 25 mM $NaHCO_3$ are allowed by a high glucose consumption rate (Table 3). This high glucose uptake rate (and expected corresponding high glycolytic flux) should be able to support a succinate formation rate higher than the observed 4 mmol x g biomass^{-1} x hr^{-1}. Not enough is known at this stage to identify the regulatory mechanism or mechanisms behind this observation. Among the possible explanations are that (i) high $NaHCO_3$ concentrations inhibit the C3 pathway and that the C4 pathway cannot process substrate faster than 4 mmol x g biomass^{-1} x hr^{-1}. This bottleneck would in turn inhibit glucose uptake and glycolysis. (ii) Another possibility is that $NaHCO_3$ (or CO_2) inhibits glucose uptake and/or glycolysis. Any of these mechanisms would have important implications for the metabolic engineering of *A. succinogenes* succinate production. Future metabolic flux analyses, in which genetic or environmental perturbations individually affect individual pathway branches, will focus on identifying what limits the succinate production rate in *A. succinogenes*.

2.4.4 *A. succinogenes* is missing at least two TCA cycle-associated enzyme activities.

A. succinogenes was found to be auxotrophic for cysteine, methionine and glutamate. Glutamate auxotrophy was initially surprising since *A. succinogenes* cell extracts have aspartate: glutamate transaminase activity (18). Figure 2 shows possible enzyme activities leading to glutamate, not all of which are known to be present in *A.*

$NaHCO_3$ concn. (mM)	Specific rates (mmol x g biomass $^{-1}$ x hr $^{-1}$)							
	Glucose consumption	Succinate formation or C4 flux	Formate formation	Acetate formation	Ethanol formation	Estimated C3 flux[a]	Estimated net ATP formation[b]	Estimated glycolytic flux[c]
5	6.6 ± 0.0	2.2 ± 0.1	7.8 ± 0.1	4.8 ± 0.0	3.4 ± 0.4	8.2 ± 0.5	16.6 ± 0.4	10.4 ± 0.4
25	7.7 ± 0.0	4.0 ± 0.2	7.0 ± 0.1	5.3 ± 0.1	2.2 ± 0.2	7.4 ± 0.2	19.4 ± 0.5	11.4 ± 0.3
75	5.0 ± 0.2	3.4 ± 0.1	2.9 ± 0.1	3.1 ± 0.0	0.7 ± 0.1	3.8 ± 0.1	12.5 ± 0.2	7.2 ± 0.1
125	5.3 ± 0.2	3.7 ± 0.1	3.2 ± 0.1	3.4 ± 0.1	0.5 ± 0.1	3.9 ± 0.2	13.5 ± 0.3	7.6 ± 0.2
150	5.7 ± 0.3	4.0 ± 0.1	3.5 ± 0.1	3.6 ± 0.1	0.5 ± 0.1	4.2 ± 0.2	14.5 ± 0.4	8.2 ± 0.4

Table 2.3. Effect of $NaHCO_3$ concentration on specific metabolic rates and estimated fluxes.

[a] Estimated C3 flux = specific acetate formation rate + specific ethanol formation rate.

[b] Estimated net ATP formation: Estimated ATP formation – estimated ATP consumption flux in central metabolism. The assumptions of ATP consumption and formation by central metabolic pathways are as follows: (i) glucose uptake consumes 1 ATP either by ATP-utilizing hexokinase or by PEP:glucose phosphotransferase system preventing ATP production by pyruvate kinase, (ii) 1 ATP is consumed by phosphofructokinase, (iii) pyruvate kinase, acetate kinase, and PEP carboxykinase each produce 1 ATP, and (iv) fumarate reductase produces 0.67 ATP per reaction (10).

[c] Estimated glycolytic flux = specific succinate production rate + estimated C3 flux.

succinogenes. Several glutamate precursors (i.e., αKG, isocitrate, citrate, succinate) are TCA cycle intermediates. It is still unclear whether *A. succinogenes* has a complete TCA cycle (Fig. 1). Because a complete TCA cycle would mean at least two pathways for succinate production and/or consumption, we used *A. succinogenes*'s glutamate auxotrophy to our advantage to study a poorly characterized region of the *A. succinogenes* central metabolic map. Table 4 shows that αKG can replace glutamate in the growth medium when NH_4Cl is present, indicating *in vivo* glutamate dehydrogenase activity. Aspartate plus αKG also supported growth, while aspartate alone did not. These results suggest that aspartate: glutamate transaminase is functional *in vivo*. Alternatively, aspartase activity could convert aspartate to fumarate and NH_4^+, and then NH_4^+ used with αKG by glutamate dehydrogenase to produce glutamate. Growth on glutamine indicates the presence of a glutamine deaminating activity (e.g., glutamine synthetase or carbamoyl phosphate synthetase). *In vitro* enzyme activity assays suggested that glutamate dehydrogenase (1,100 ± 180 nmol x min^{-1} x mg $protein^{-1}$) and glutamate synthase (30 ± 10 nmol x min^{-1} x mg $protein^{-1}$) are also functional in *A. succinogenes*. Taken together, these results suggest that all the enzyme activities (i.e., 3, 6, 7, and 8) below αKG in Figure 2 are present in *A. succinogenes*.

These results also point to a single reason for *A. succinogenes*'s glutamate auxotrophy: *A. succinogenes* cannot synthesize αKG from glucose. This inability means that enzymes are absent or inactive in two pathways: (i) between succinate and αKG in the reverse TCA cycle (especially since *A. succinogenes* produces ample succinate), and (ii) in the TCA cycle from acetyl-CoA and oxaloacetate to citrate to αKG (Fig. 1). This conclusion is supported in part by the fact that no *in vitro* isocitrate dehydrogenase

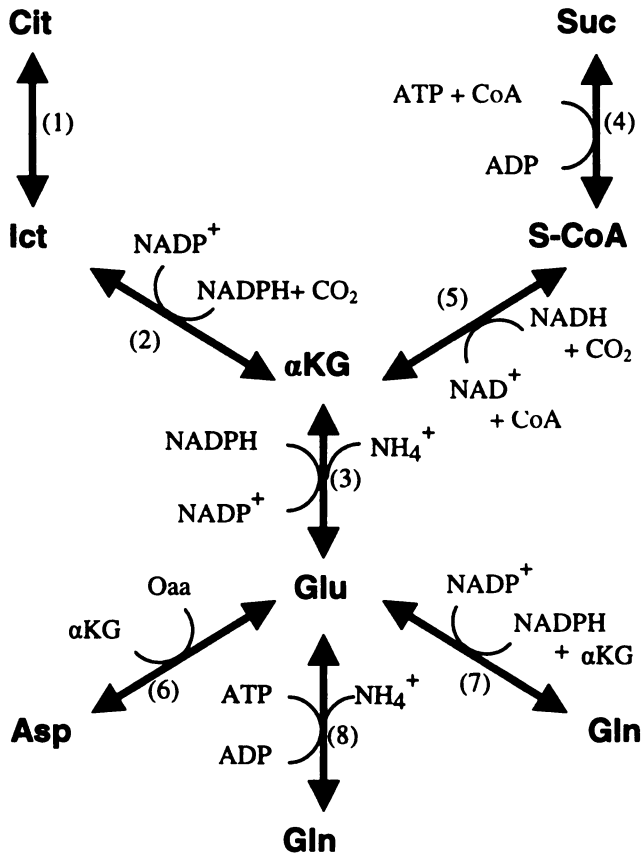

Figure 2.2. Possible enzyme activities leading to glutamate synthesis. 1, aconitase; 2, isocitrate dehydrogenase; 3, glutamate dehydrogenase; 4, succinyl-CoA synthetase; 5, αKG dehydrogenase; 6, aspartate:glutamate transaminase; 7, glutamate synthase; 8, glutamine synthetase. Metabolites: Ict, isocitrate; S-CoA, succinyl-CoA.

	Supplement					
	NH_4^+	NH_4^+ + Glu	NH_4^+ + αKG	Gln	Asp	Asp + αKG
Growth[a]	-	+	+	+	-	+

Table 2.4. Ability of glutamate precursors to support growth of *A. succinogenes* in AM3. [a] Growth (+) is defined as > 1.5 OD_{660} within 24 hours. No growth (-) is defined as no OD_{660} increase within 5 days after inoculation. Tests were performed at least in duplicate.

activity could be detected in anaerobically and aerobically grown *A. succinogenes* cell extracts, while it was detected in *E. coli* cell extracts as a positive control (70 ± 10 nmol NADP(H) min^{-1} mg $protein^{-1}$). Growth experiments on citrate or isocitrate were not informative (*A. succinogenes* did not grow when citrate or isocitrate were supplied with NH_4Cl or aspartate, data not shown) for at least two reasons: (i) it is not known whether citrate and isocitrate are taken up by *A. succinogenes* cells; and (ii) citrate prevented *A. succinogenes* growth at concentrations above 3 mM in the presence of glutamine or glutamate (data not shown). This inhibition was countered by adding extra minerals (data not shown), suggesting that citrate binds essential minerals (e.g., iron) and prevents mineral acquisition.

A. succinogenes is a promising catalyst for bio-based production of succinate and potentially other chemicals (e.g., malate, fumarate, 5-aminolevulinate, αKG, and glutamate). We have described a chemically defined medium for growing *A. succinogenes* and studying its metabolism. $NaHCO_3$ concentration had pronounced effects on fermentation end product distributions between 5 and 75 mM but not at higher concentrations. *A. succinogenes* had an optimal growth rate at 25 mM $NaHCO_3$, where both energy producing pathways displayed their highest fluxes. αKG could be used in place of glutamate to support growth, indicating that at least two TCA cycle-associated enzyme activities are absent. The defined medium made testing growth on glutamate precursors possible. The discovery that *A. succinogenes* lacks a full TCA cycle is a key information for the construction of an accurate *A. succinogenes* metabolic map that will be essential in future metabolic flux analyses and practical metabolic engineering designs for *A. succinogenes*-based chemical production.

2.5 ACKNOWLEDGEMENTS

This work was supported by the National Science Foundation grant #BES-0224596. James McKinlay was supported by a Michigan State University Quantitative Biology and Modeling Initiative fellowship. We thank Dr. John Breznak, Dr. Yair Shachar-Hill, Harini Krishnamurthy, and Maris Laivenieks for helpful discussions.

2.6 REFERENCES

1. Doyle, A., M. N. Weintraub, and J. P. Schimel. 2004. Persulfate digestion and simultaneous colorimetric analysis of carbon and nitrogen in soil extracts. Soil Sci. Soc. Am. J. 68:669-676.

2. Fell, D. 1997. Understanding the control of metabolism. Portland Press, London.

3. Gottschalk, G. 1986. Bacterial Metabolism, 2nd ed. Springer-Verlag, New York.

4. Guettler, M. V., M. K. Jain, and D. Rumler. 1996. Method for making succinic acid, bacterial variants for use in the process, and methods for obtaining variants. U.S. patent 5,573,931.

5. Guettler, M. V., M. K. Jain, and B. K. Soni. 1996. Process for making succinic acid, microorganisms for use in the process and methods of obtaining the microorganisms. U.S. patent 5,504,004.

6. Guettler, M. V., D. Rumler, and M. K. Jain. 1999. *Actinobacillus succinogenes* sp. nov., a novel succinic-acid-producing strain from the bovine rumen. Int. J. Syst. Bacteriol. 49:207-216.

7. Herroitt, R. M., E. M. Meyer, and M. Vogt. 1970. Defined nongrowth media for stage II development of competence in *Haemophilus influenzae*. J. Bacteriol. 101:517-524.

8. Herroitt, R. M., E. Y. Meyer, M. Vogt, and M. Modan. 1970. Defined medium for growth of *Haemophilus influenzae*. J. Bacteriol. 101:513-516.

9. Kim, P., M. Laivenieks, C. Vieille, and J. G. Zeikus. 2004. Effect of overexpression of *Actinobacillus succinogenes* phosphoenolpyruvate carboxykinase on succinate production in *Escherichia coli*. Appl. Environ. Microbiol. 70:1238-1241.

10. Kroger, A., S. Biel, J. Simon, R. Gross, G. Unden, and C. R. D. Lancaster. 2002. Fumarate respiration of *Wolinella succinogenes*: enzymology, energetics and coupling mechanism. Biochim. Biophys. Acta. 1553:23-28.

11. Lovely, D. 2000. Dissimilatory Fe(III)-and Mn(IV)-Reducing Prokaryotes. *In* Martin Dworkin (ed.), The Prokaryotes. Springer-Verlag [Online.] http://141.150.157.117:8080/prokPUB/index.htm. Accessed December 2003.

12. McKinlay, J. B., and J. G. Zeikus. 2004. Extracellular iron reduction is mediated in part by neutral red and hydrogenase in *Escherichia coli*. Appl. Environ. Microbiol. 70:3467-3474.

13. Park, D. H., M. Laivenieks, M. V. Guettler, M. K. Jain, and J. G. Zeikus. 1999. Microbial utilization of electrically reduced neutral red as the sole electron donor for growth and metabolite production. Appl. Environ. Microbiol. 65:2912-2917.

14. Park, D. H., and J. G. Zeikus. 1999. Utilization of electrically reduced neutral red by *Actinobacillus succinogenes*: physiological function of neutral red in membrane-driven fumarate reduction and energy conservation. J. Bacteriol. 181:2403-2410.

15. Sauer, U., D. R. Lasko, J. Fiaux, M. Hochuli, R. Glaser, T. Szyperski, K. Wüthrich, and J. E. Bailey. 1999. Metabolic flux ratio analysis of genetic and environmental modulations of *Escherichia coli* central carbon metabolism. J. Bacteriol. 181:6679-6688.

16. Stephanopoulos, G., A. A. Aristidou, and J. Nielsen. 1998. Metabolic Engineering: Principles and Methodologies. Academic Press, London.

17. Thorsness, P. E., and D. E. Koshland, Jr. 1987. Inactivation of isocitrate dehydrogenase by phosphorylation is mediated by the negative charge of the phosphate. J Biol Chem 262:10422-10425.

18. van der Werf, M. J., M. V. Guettler, M. K. Jain, and J. G. Zeikus. 1997. Environmental and physiological factors affecting the succinate product ratio during carbohydrate fermentation by *Actinobacillus sp.* 130Z. Arch. Microbiol. 167:332-342.

19. Widdel, F., and F. Bak. 1992. Gram-negative mesophilic sulfate-reducing bacteria., p. 3358-3378. *In* A. Balows, H. G. Truper, M. Dworkin, W. Harder, and K. H. Schleifer (ed.), The Prokaryotes, 2nd ed, vol. 4. Springer-Verlag, New York.

20. Wilke, D. 1999. Chemicals from biotechnology: molecular plant genetics will challenge the chemical and fermentation industry. Appl. Microbiol. Biotechnol. 52:135-145.

21. Wilke, D. 1995. What should and what can biotechnology contribute to chemical bulk production? FEMS Microbiol. Rev. 16:89-100.

22. Wolin, E., M. Wolin, and R. Wolfe. 1963. Formation of methane by bacterial extracts. J. Biol. Chem. 238:2882-2886.

23. Zeikus, J. G., G. Fuchs, W. Kenealy, and R. K. Thauer. 1977. Oxidoreductases involved in cell carbon synthesis of *Methanobacterium thermoautotrophicum*. J. Bacteriol. 132:604-613.

24. Zeikus, J. G., M. K. Jain, and P. Elankovan. 1999. Biotechnology of succinic acid production and markets for derived industrial products. Appl. Environ. Microbiol. 51:545-552.

Chapter 3

Determining *Actinobacillus succinogenes* metabolic pathways and fluxes by NMR and GC-MS analyses of ^{13}C-labeled metabolic product isotopomers

McKinlay, J. B., Y. Shachar-Hill, J. G. Zeikus, and C. Vieille. 2006. Determining *Actinobacillus succinogenes* metabolic pathways and fluxes by NMR and GC-MS analyses of ^{13}C-labeled metabolic product isotopomers. Metabolic Engineering. In press, doi:10.1016/j.ymben.2006.10.006.

3.1 ABSTRACT

Actinobacillus succinogenes is a promising candidate for industrial succinate production. However, in addition to producing succinate, it also produces formate and acetate. To understand carbon flux distribution to succinate and alternative products we fed *A. succinogenes* [1-^{13}C]glucose and analyzed the resulting isotopomers of excreted organic acids, proteinaceous amino acids, and glycogen monomers by gas chromatography-mass spectrometry and nuclear magnetic resonance spectroscopy. The isotopomer data, together with the glucose consumption and product formation rates and the *A. succinogenes* biomass composition, were supplied to a metabolic flux model. Oxidative pentose phosphate pathway flux supplied, at most, 20% of the estimated NADPH requirement for cell growth. The model indicated that NADPH was instead produced primarily by the conversion of NADH to NADPH by transhydrogenase and/or by NADP-dependent malic enzyme. Transhydrogenase activity was detected in *A. succinogenes* cell extracts, as were formate and pyruvate dehydrogenases, which the model suggested were contributing to NADH production. Malic enzyme activity was also detected in cell extracts, consistent with the flux analysis results. Labeling patterns in amino acids and organic acids showed that oxaloacetate and malate were being decarboxylated to pyruvate. These are the first in vivo experiments to show that the partitioning of flux between succinate and alternative fermentation products can occur at multiple nodes in *A. succinogenes*. The implications for designing effective metabolic engineering strategies to increase *A. succinogenes* succinate production are discussed.
Keywords: *Actinobacillus succinogenes*, succinate, metabolic flux analysis, biomass composition, oxaloacetate decarboxylase, malic enzyme, transhydrogenase

3.2 INTRODUCTION

Declining oil reserves, rising petrochemical prices, and the environmental impact of oil-based industries have prompted the development of bio-based processes for fuel and chemical production (64, 65). Industrial-scale microbial processes are meeting the global demands for a variety of amino acids, organic acids, vitamins, and antibiotics (64). Succinate is produced petrochemically from butane to satisfy a specialty chemical market, but it can also be produced from microbial fermentations (69). More importantly, bio-based succinate could replace a large petrochemical-based commodity chemical market for making bulk chemicals including 1,4-butanediol (a precursor to "stronger-than-steel" and biodegradable plastics), ethylene diamine disuccinate (a biodegradable chelator), diethyl succinate (a "green" solvent replacement for methylene chloride), and adipic acid (a nylon precursor) (69). In addition to being based on renewable resources, bio-based succinate production has the additional environmental benefit of using CO_2, a greenhouse gas, as a substrate. Developing a more cost-effective industrial succinate fermentation to replace the butane-based commodity maleic anhydride will require advances on several fronts. In particular, it will require developing organisms that produce high succinate concentrations at high rates.

The capnophilic bacterium, *Actinobacillus succinogenes*, is a promising biocatalyst for industrial succinate production. While *A. succinogenes* produces some of the highest succinate concentrations ever reported (15, 16), it does so as part of a mixed acid fermentation, producing high concentrations of formate and acetate as well. Therefore, it is desirable to genetically engineer *A. succinogenes* to produce succinate as the sole fermentation end product.

Metabolic engineering is most effective when it is based on an understanding of the pathways involved and of how the fluxes through those pathways are controlled (12, 51). Knowledge of *A. succinogenes* metabolism comes from fermentation balances, from in vitro enzyme assays (34, 55), and, more recently, from its genome sequence (McKinlay et al., manuscript in preparation., http://genome.ornl.gov/microbial/asuc/). A simplified map of *A. succinogenes* central metabolism is depicted in Figure 1. Previous data suggest that *A. succinogenes* ferments glucose to phosphoenolpyruvate (PEP) by glycolysis and the oxidative pentose phosphate pathway (OPPP) (55). PEP is thought to serve as the branchpoint between the formate-, acetate-, and ethanol-producing pathway (C_3 pathway), and the succinate-producing (C_4) pathway. Malic enzyme and oxaloacetate (OAA) decarboxylase activities measured in vitro (55) suggest that malate and OAA can also serve as branch points between the C_3 and C_4 pathways. The presence of these activities and others in vivo, such as those of the Entner Doudoroff (ED) and glyoxylate pathways (for which questionable in vitro activities were detected [(55)]), must be determined to develop effective *A. succinogenes* engineering strategies.

^{13}C-labeling studies are a useful approach for understanding the in vivo workings of metabolism (42, 60). Knowledge resulting from these techniques has been used to guide the metabolic engineering of industrial microbes, such as vitamin-producing *Bacillus subtilis* (7, 46, 68) and amino acid-producing *Corynebacterium glutamicum* (26, 38, 40). ^{13}C-labeling studies can distinguish fluxes through different pathways when these fluxes result in different positional isotopic enrichments in metabolic intermediates. These labeling patterns are imprinted on metabolic products (e.g., proteinaceous amino acids and excreted organic acids) and can be analyzed by gas chromatography-mass

Figure 3.1. *A. succinogenes* metabolic pathways addressed in this study. Solid lines: pathways or reactions for which enzyme activity was detected in vitro; dotted lines: pathways or reactions where no activity or uncertain activity was detected in vitro (55). Unidirectional arrows: fluxes considered to be unidirectional (all other fluxes are considered to be reversible). The C_4 pathway is defined as: PEP → OAA → Mal → Fum → Suc. The C_3 pathway is defined as: PEP → Pyr → AcCoA → Ace + EtOH. Alternative PPP reactions, cysteine and methionine degradation pathways, and amino acid synthesis pathways are not shown (Supplementary material). It was assumed that 0.67 ATP is produced per fumarate reductase reaction based on data from *Wolinella succinogenes* (27). Metabolites: AcCoA, acetyl-coenzymeA; Ace, acetate; Cit, citrate; EtOH, ethanol; E4P, erythrose-4-phosphate; For, formate; Fum, fumarate; F6P, fructose-6-phosphate; Glc, glucose; Glxt, glyoxylate; G3P, glyceraldehyde-3-phosphate; G6P, glucose-6-phosphate; Mal, malate; OAA, oxaloacetate; PEP, phosphoenolpyruvate; Pyr, pyruvate; R5P, pentose-phosphates, Suc, succinate; S7P, sedoheptulose-7-phosphate. Pathways and reactions: *ADH*, alcohol dehydrogenase; *AK*, acetate kinase; *CL*, citrate lyase; *ED*, Entner Doudoroff pathway; *empl*, 2, and *3*, Embden-Meyerhoff-Parnas (EMP) or glycolytic reactions; *Fm*, fumarase; *FR*, fumarate reductase; *ICL*, isocitrate lyase and aconitase; *MDH*, malate dehydrogenase; *ME*, malic enzyme; *Msyn*, malate synthase; *OAAdec*, oxaloacetate decarboxylase; *OPP*, oxidative pentose phosphate pathway; *PEPCK*, PEP carboxykinase; *PFL*, pyruvate formate-lyase; *PK*, pyruvate kinase and PEP:glucose phosphotransferase system (PTS); *ppp1* and *2*, transketolase; *ppp3*, transaldolase; *PyrDH*, pyruvate dehydrogenase or PFL coupled with formate dehydrogenase; *upt*, glucose phosphorylation by hexokinase and PTS.

Figure 3.1 (cont'd)

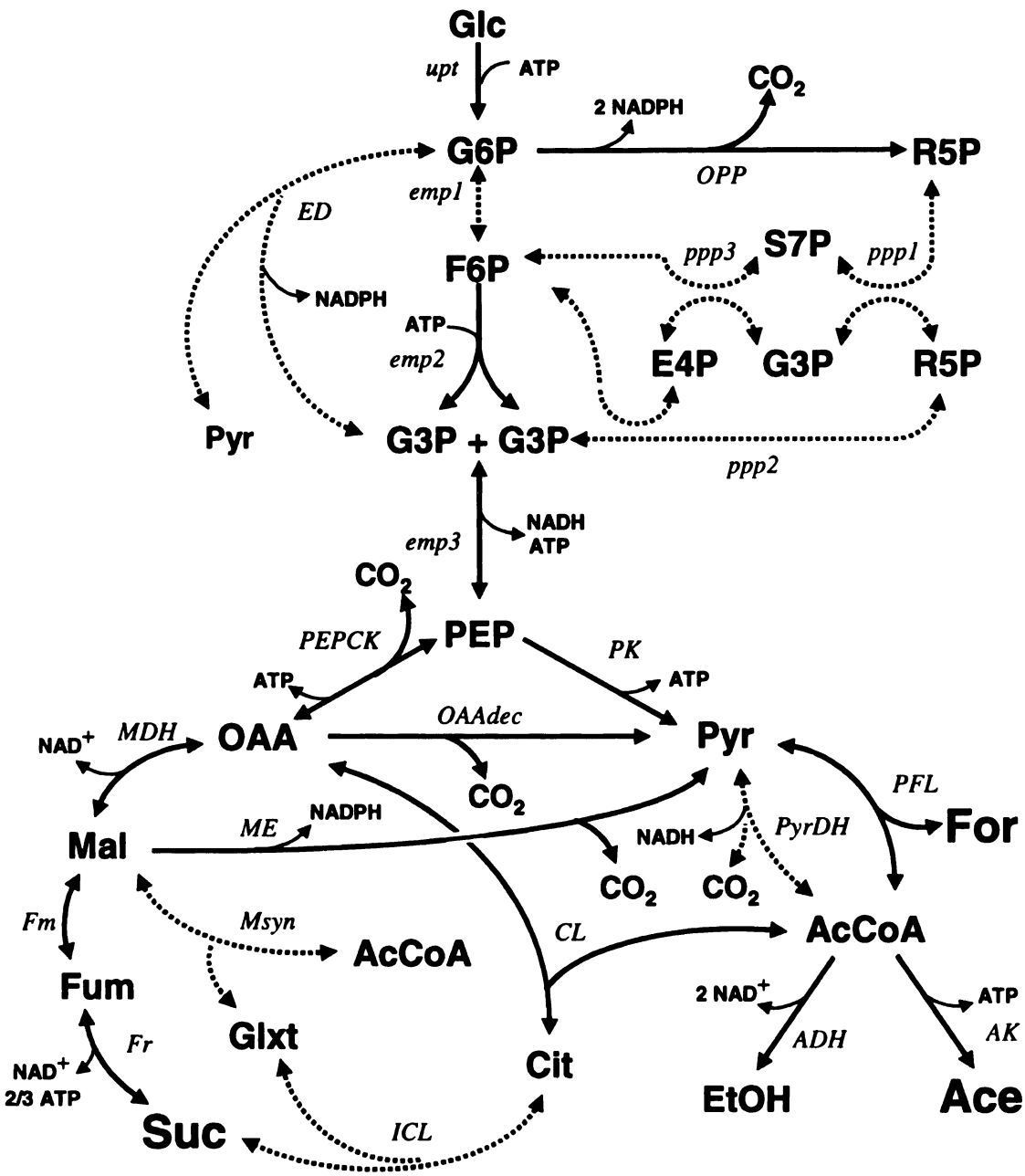

spectrometry (GC-MS) and nuclear magnetic resonance spectroscopy (NMR). We recently developed a chemically defined growth medium that makes ^{13}C-labeling experiments with *A. succinogenes* possible (34). Here we describe the use of [1-^{13}C]glucose to obtain an *A. succinogenes* metabolic flux map based on analyses of its cell composition, extracellular fluxes, and isotopomers of amino acids, organic acids, and glycogen monomers.

3.3 MATERIALS AND METHODS

3.3.1 Chemicals, bacteria, and culture conditions. All chemicals were purchased from Sigma-Aldrich (St. Louis, MO) unless stated otherwise. *A. succinogenes* type strain 130Z (ATCC 55618) was purchased from the American Type Culture Collection (Manassas, VA) and adapted to growth in AM3 as described (34). AM3 is a chemically defined medium containing Cys, Met, and Glu, which are required for *A. succinogenes* growth. Cultures were grown in 11-ml volumes of AM3 in 28-ml anaerobic test tubes or in 60-ml volumes in 150-ml serum vials. Anoxic AM3 contained 150 mM $NaHCO_3$ and 50 mM glucose, and was prepared as described (34). Cultures were incubated at 37°C with shaking at 250 rpm.

3.3.2 Growth and sampling conditions in the presence of [1-^{13}C]glucose. A starter culture was grown from a glycerol frozen stock in AM3 to an OD_{660} of 1.0. The starter culture was harvested, washed once, and resuspended in an equal volume of the AM3 phosphate buffer. Nine 11-ml volumes of AM3 containing 50 mM [1-^{13}C]glucose (99%, Cambridge Isotope Laboratories, Cambridge, MA), instead of unlabeled glucose, were each inoculated with 0.1 ml of the cell suspension to give a starting OD_{660} of ~0.01. Unlabeled biomass accounted for only 0.5 – 1.8% of the total biomass at the time of harvesting. Growth was monitored using a Spectronic 20 spectrophotometer (Bausch and Lomb, Rochester, NY) to calculate growth rates. A 1-ml sample was taken 4.5 hours into growth to serve as a '0 time point' sample, rather than at the time of inoculation to account for any lag phase. This sample was used for a more accurate OD_{660} measurement using a Beckman DU 650 spectrophotometer (Fullerton, CA). It was also analyzed by

high performance liquid chromatography (HPLC) to determine glucose and product concentrations. Culture growth was stopped by chilling on ice as follows: three tubes were stopped at 0.5 OD_{660}, three at 1.0 OD_{660}, and three at 1.5 OD_{660}. Cell densities were recorded, then cultures were harvested by centrifugation at 4°C. The supernatants were stored at –70°C, as was the biomass after two washes with 0.9% NaCl at 4°C.

3.3.3 HPLC analysis of glucose and products and GC analysis of headspace gas. HPLC was performed on culture supernatants as described (34). A negative HCO_3^- peak interfered with ethanol peak integration. To improve the ethanol measurement accuracy, subsamples were mixed 1:1 with 150 mM H_2SO_4 to release HCO_3^- as CO_2 before analysis. Untreated samples were used to quantify glucose, succinate, formate, acetate, and fumarate. GC was used to analyze culture headspace for H_2 using a Shimadzu GC-2014 (Columbia, MD) equipped with an 80/100 Porapak Q column and a thermal conductivity detector.

3.3.4 Determination of extracellular fluxes. Specific glucose consumption and product formation rates (i.e., extracellular fluxes) were calculated as described (48) using the equation $r_p = Y_{XP}\mu$, where r_p is the specific product formation rate, Y_{XP} is the amount of product produced per gram of biomass, and μ is the growth rate. The same equation was used for glucose consumption. All flux data were obtained during exponential growth, during which the growth rate and extracellular fluxes are constant.

3.3.5 GC-MS analysis of amino acids and organic acids. Amino acid preparation and GC-MS analysis were based on the methods of Schwender et al. (50) and Dauner and Sauer (6). All drying and evaporation steps were performed under a stream of N_2. Each cell pellet from 8.4 ml of culture was resuspended in 1 ml of distilled water and lysed by six freeze-thaw cycles (–70°C/30°C). The lysates were centrifuged, then 600 µl aliquots of supernatant were then transferred to 1.5-ml screw-cap conical tubes and concentrated to 100 µl under vacuum. Proteins were hydrolyzed by adding 333 µl of 6 N HCl to each sample and incubating at 110°C for 24 h under Ar. HCl was then evaporated to near-dryness at 55°C, then samples were diluted with 1 ml of 0.01 N HCl, and applied to a Dowex 50Wx8-100 cation exchange column. Amino acids were eluted with 1 N NH_4OH and dried at 55°C. Samples were then dissolved in 0.1 ml of 0.01 N HCl. Amino acid concentrations were estimated by spotting 10- and 100-fold dilutions of the samples and an amino acid standard onto silica gel plates and comparing the color intensities after staining with ninhydrin spray solution and incubating at 80°C for 10 min. Volumes containing 100–200 µg of amino acids were transferred to glass vials and dried at 25°C. To derivatize the amino acids for GC-MS analysis, 800 µl of methylene chloride was added to each sample and evaporated to remove trace amounts of water. Acetonitrile and *N*-(*tert*-butyldimethylsilyl)-*N*-methyl-trifluoroacetamide (MTBSTFA) (200 µl each) were then added to the samples under Ar. Vials were capped and incubated at 25°C for 30 min, then at 120°C for 1 h. Samples were evaporated to near dryness at 25°C before being diluted with 400 µl of 20:1 acetonitrile: MTBSTFA, and run on GC-MS. Succinate and fumarate in supernatants were derivatized by the same method but without column purification, and concentrations were determined by HPLC.

GC-MS was performed using an Agilent 5973 inert MSD benchtop quadrapole mass spectrometer (Palo Alto, CA) at the MSU Mass Spectrometry facility. Derivatized compounds in 1-µl injections were separated on a 60-m DB5MS column. The inlet temperature was 280°C. The oven temperature started at 100°C for 4 min, was then raised by 5°C/min to 200°C, then by 10°C/min to 300°C, and held at 300°C for 10 min. *Tert*-butyldimethylsilyl (TBDMS)-amino acid and organic acids were identified using described fragmentation patterns (6) and unlabeled standards.

3.3.6 NMR analysis of organic acids, alanine, and glucose monomers from glycogen. Prior to NMR analysis, organic acids were separated from glucose and ethanol on a Dowex 1X8-200 anion exchange column. Organic acids were eluted with 1 M $HClO_4$. The eluate was made alkaline by adding K_2CO_3 until CO_2 bubbles stopped forming. The $KClO_4$ precipitate was pelleted by centrifugation and the supernatant was lyophilized and dissolved in D_2O. Amino acids were obtained from hydrolyzed proteins as described above but, prior to hydrolysis, the proteins were precipitated with trichloroacetic acid (25 % final concentration) on ice for 30 min, pelleted by centrifugation, washed twice with ice-cold acetone, air-dried, and resuspended in 100 µl water. After hydrolysis, amino acids were partially purified, dried, and dissolved in D_2O. Glucose monomers were prepared from glycogen by resuspending the pellets from centrifuged cell lysates in 50 mM sodium acetate (pH 4.5), boiling for 5 min, then digesting with *Pseudomonas amyloderamosa* isoamylase (E.C. 3.2.1.68) and *Aspergillus niger* amyloglucosidase (E.C. 3.2.1.3) for 24 h at 40°C with occasional mixing. Cell debris was pelleted by centrifugation, and the supernatant was applied to a Dowex 1X8-200 anion exchange column. The flow-through was lyophilized and redissolved in D_2O.

All compounds were analyzed by ^{1}H-NMR and ^{1}H-decoupled ^{13}C-NMR using a Varian VXR 500 MHz spectrometer with a 5-mm ^{13}C-^{1}H switchable probe at the MSU Max T. Rodgers NMR facility. For ^{13}C-NMR, ^{1}H-decoupling was applied only during acquisition, and recycle times were 60 -120 s to allow for full relaxation. After determining that there were no statistical differences in the relative ^{1}H-NMR peak intensities between samples originating from different cell concentrations (see Results), the organic acid samples originating from all OD_{660} 0.5 and OD_{660} 1.0 cultures were combined into a single sample to decrease ^{13}C-NMR run times. Organic acid samples originating from the OD_{660} 1.5 cultures were not pooled for ^{13}C-NMR. All samples were pooled for glucose and Ala measurements. NMR peak assignments were based on spectra found at www.aist.go.jp/RIODB/SDBS/ (Japanese National Institute of Advanced Industrial Science and Technology, Dec 2005) and on spectra of unlabeled standards.

3.3.7 Metabolic modeling and flux analysis. The initial *A. succinogenes* metabolic model (Fig.1) is based on *A. succinogenes* enzyme activities (55), and on sequences in the *A. succinogenes* draft genome sequence. The tricarboxylic acid (TCA) cycle was omitted because it was shown that *A. succinogenes* cannot synthesize α-ketoglutarate when grown in AM3, indicating at least two missing TCA cycle enzyme activities (34). Glucose uptake was not constrained to the conversion of PEP to pyruvate (i.e., by the PEP:glucose phosphotransferase system [PTS]) to allow for glucokinase activity. Both PTS and glucokinase activities were detected in *A. succinogenes* (55), and the PTS does not appear to be the main glucose uptake mechanism at high glucose concentrations (24). Pyruvate carboxylating activities were omitted, because no pyruvate carboxylase gene

was found in any *Pasteurellaceae* genome sequence, and *A. succinogenes* pyruvate formate-lyase mutants excrete pyruvate (15), suggesting that *A. succinogenes* cannot carboxylate pyruvate. Redox balance constraints were omitted to allow for transhydrogenase activity.

AM3 contains unlabeled Glu, Cys, Met, and vitamins that could potentially enter amino acid or central metabolic pathways and affect our interpretation of the isotopomer data set. Glu cannot affect the isotopomer data set for several reasons. First, it is normally catabolized via α-ketoglutarate, which is disconnected from central metabolism in *A. succinogenes* (34). Second, there is only enough Glu supplied to meet the biosynthetic requirements for Glu and its derivatives, Gln, Pro, Arg, and polyamines (estimated from Table 1 values). While unlabeled Glu directly affects the isotopomer distribution of Gln, Pro, and Arg (Glx and Pro are ~100% unlabeled, Table 2), these amino acid isotopomers are not used in our flux analysis, and not enough Glu is provided to affect other metabolic pathways. The amount of vitamins supplied is also too low to impact our isotopomer measurements, representing only 0.28% of the carbon consumed as glucose by the lowest cell density culture and 0.07% of that consumed by the highest cell density culture. Cys and Met are supplied at 4- and 5-fold excess, respectively, and together account for 1.3% of the total supplied carbon. For this reason, we included Cys and Met degradation pathways in our model based on those found at Metacyc (i.e., Cys → pyruvate; Met → oxobutanoate → Thr → Asp → OAA; www.metacyc.com).

The model is simplified for flux analysis by grouping metabolites that are assumed to be in rapid equilibrium (e.g., pentose phosphates in the pentose phosphate pathway [PPP]), or that are undistinguishable by labeling (e.g., all metabolites in

Table 3.1. *A. succinogenes* metabolic intermediate and cofactor requirements for biosynthesis.

[a] ATP needs for polymerization reactions were assumed to be the same as in *E. coli* (22), but adjusted for percentage of dry cell weight.

[b] Gln and Asn were oxidized to Glu and Asp during hydrolysis and Cys and Trp were destroyed. Cys and Trp values were based on *E. coli* values (22). A correction factor was applied to Tyr to account for average recoveries of 70%.

[c] The values were derived using an RNA NTP composition based on that of *A. succinogenes* ribosomal RNA.

[d] The values were derived using a DNA dNTP composition based on the GC content of *A. succinogenes* (17).

[e] The phospholipid composition was assumed to be 25 % phosphatidylglycerol and 75% phosphatidylethanolamine. The values were derived using the *A. succinogenes* fatty acid composition, which was measured to be (in percent of total lipid mass): 14:0, 11; 3-OH-14:0, 3; 16:0, 35; 16:1, 37; 18:0, 1; 18:1, 3; and 18:2, 10.

[f] The polyamine requirement was assumed to be the same as for *E. coli* (22).

[g] A stoichiometry of 1 ATP per NH_3, PO_4^{2-}, or amino acid transported was assumed. The ATP requirement for K^+ transport was assumed to be 190 μmol per g biomass^{-1} (52).

[h] Unaccounted for biomass is assumed to be composed of metabolites and inorganic ions. Table 1 values were corrected for Glu, Cys, and Met, which are supplied in AM3.

Table 3.1 (cont'd)	Percent of dry cell wt.[h]	µmols per g biomass													
		ATP[a]	NADH	NADPH	NH_3	G6P	F6P	R5P	E4P	G3P	3PG	PEP	Pyr	AcCoA	OAA
Protein	56.8	22,689													
Ala	6.0			671	671								671		
Arg	2.5	1,009	-144	432	432										
Asx[b]	5.6	634		423	634										423
Cys[b]	0.9														
Glx[b]	6.0	203			203										
Gly	5.8		-768	768	768						768				
His	1.1	435	-218	73	218			73							
Ile	3.1	480		1201	240								240		240
Leu	4.9		-374	747	374								747	374	
Lys	3.9	528		1056	528								264		264
Met	1.1														
Phe	2.3	139		277	139				139			277			
Pro	2.3	196		392	196										
Ser	2.2		-211	211	211						211				
Thr	2.9	492		737	246										246
Trp[b]	0.6	149	-60	90	60			30	30			30			
Tyr[b]	1.4	75	-75	150	75				75			150			
Val	4.3			727	363								727		
RNA[c]	14.2	4,304	-583	317	1,536			415			194				221
DNA[d]	4.4	1,670	-195	274	498			135			65				70
Glycogen	6.6	366				366									
Lipid[e]	8.8	2,081	-99	3688	99					66	99			2,098	
LPS	4.7	1,073	0	817	33	44	49	33		33	33	33		457	
PG	3.5	192		269	230		77					38	115	77	38
Polyamines[f]	0.4	119		119	59										
Uptake[g]: NH_3		7,813													
PO_4^{2-}		1,108													
K^+		190													
Amino acids		985													
		ATP	NADH	NADPH	NH_3	G6P	F6P	R5P	E4P	G3P	3PG	PEP	Pyr	AcCoA	OAA
TOTAL	99.5	46,930	-2,727	13,439	7,813	410	126	686	244	99	1,370	528	2,764	3,006	1,502

Table 3.2. Mass isotopomer distributions of TBDMS-amino acid and -organic acid fragments

[a] Negative values are the result of correcting for natural abundances and can be treated as having zero value. The distributions shown were corrected as described in the methods and also for natural ^{13}C abundance in the amino and organic acid backbones using an excel macro developed by Joerg Schwender (Brookhaven National Laboratory, Upton, NY) based on correction matrices described by Lee et al. (30). Simulated values resulting from the optimized set of fluxes (i.e., Figure 3 fluxes) are in parentheses.

[b] Data for Phe's highest mass fragments were omitted from the table.

* Values were omitted from the fitting procedure.

Table 3.2 (cont'd)			Mass isotopomer distributions[a] (% of product population)					
Product	Fragment	Carbons	X+0	X+1	X+2	X+3	X+4	X+5
Ala	M-57	1-3	54.0 ± 0.4 (52.0)	45.8 ± 0.3 (48.0)	0.1 ± 0.0 (0.0)	0.1 ± 0.1*		
	M-85	2-3	53.8 ± 1.3 (52.2)	46.0 ± 1.2 (47.8)	0.4 ± 0.1 (0.0)			
Asx	M-57	1-4	51.4 ± 0.5 (51.8)	47.5 ± 0.4 (48.0)	0.6 ± 0.2 (0.2)	0.4 ± 0.1*	0.2 ± 0.0*	
	M-85	2-4	52.5 ± 0.5 (52.0)	47.4 ± 0.4 (47.9)	0.1 ± 0.2 (0.1)	0.1 ± 0.1*		
	M-159	2-4	52.9 ± 0.6 (52.0)	46.8 ± 0.5 (47.9)	-0.2 ± 0.1 (0.1)	0.5 ± 0.1*		
	f302	1-2	93.7 ± 1.2 (93.4)	6.6 ± 0.8 (6.6)	-0.3 ± 0.1 (0.0)			
Glx*	M-57	1-5	101.2 ± 1.1	0.1 ± 0.0	-0.2 ± 0.7	-1.3 ± 2.4	0.2 ± 1.0	0.1 ± 0.1
	M-85	2-5	101.0 ± 0.2	-0.2 ± 0.0	-0.4 ± 0.2	0.1 ± 0.3	-0.5 ± 0.5	
	M-159	2-5	99.8 ± 0.2	0.0 ± 0.0	0.3 ± 0.1	0.0 ± 0.0	-0.1 ± 0.1	
Gly	M-57	1-2	98.7 ± 0.3 (98.8)	1.2 ± 0.2 (1.2)	0.0 ± 0.0 (0.0)			
	M-85	2	99.3 ± 0.3 (99.1)	0.7 ± 0.1 (0.9)				
Ile	M-85	2-6	27.8 ± 0.5 (27.1)	49.1 ± 0.4 (49.8)	23.7 ± 0.3 (23.0)	0.1 ± 0.2 (0.1)	-0.8 ± 0.7*	0.1 ± 0.3*
	M-159	2-6	27.4 ± 0.3 (27.1)	48.9 ± 0.2 (49.8)	23.5 ± 0.2 (23.0)	0.2 ± 0.0 (0.1)	0.1 ± 0.0*	-0.0 ± 0.0*
Leu	M-85	2-6	17.7 ± 0.8 (15.5)	38.5 ± 0.4 (40.1)	33.7 ± 0.4 (34.5)	10.0 ± 0.1 (9.9)	0.0 ± 0.0*	0.1 ± 0.1*
	M-159	2-6	16.6 ± 0.4 (15.5)	38.2 ± 0.3 (40.1)	34.1 ± 0.3 (34.5)	10.4 ± 0.1 (9.9)	0.2 ± 0.0*	0.5 ± 0.2*
Met*	M-57	1-5	97.6 ± 0.9	0.4 ± 0.0	-0.4 ± 0.2	0.6 ± 0.3	0.6 ± 0.2	1.2 ± 0.3
	M-85	2-5	99.4 ± 0.6	0.4 ± 0.0	-0.5 ± 0.1	0.2 ± 0.1	0.4 ± 0.2	
Phe[b]	M-57	1-9	22.8 ± 0.4 (22.5)	42.7 ± 0.7 (46.0)	26.0 ± 0.4 (27.5)	3.8 ± 0.2 (4.0)	0.1 ± 0.1 (0.0)	1.5 ± 0.5*
	M-85	2-9	24.4 ± 0.6 (22.6)	44.9 ± 1.1 (46.0)	28.1 ± 1.3 (27.4)	4.0 ± 0.2 (4.0)	-1.6 ± 2.6 (0.0)	-0.0 ± 0.2*
	f302	1-2	98.1 ± 0.3 (98.2)	1.8 ± 0.1 (1.8)	0.1 ± 0.1 (0.0)			
Pro*	M-159	2-5	99.1 ± 1.1	0.2 ± 0.0	0.4 ± 0.2	0.2 ± 0.2	0.2 ± 0.4	
Ser	M-57	1-3	54.4 ± 5.4 (50.3)	45.5 ± 0.8 (48.6)	0.1 ± 0.1 (1.1)	2.3 ± 0.1*		
	M-85	2-3	53.2 ± 1.2 (51.0)	46.7 ± 1.2 (48.4)	0.1 ± 0.1 (0.5)			
	M-159	2-3	53.9 ± 0.9 (51.0)	45.0 ± 0.8 (48.4)	1.1 ± 0.1 (0.5)			
	f302	1-2	98.5 ± 0.1 (98.8)	1.2 ± 0.0 (1.2)	0.3 ± 0.1 (0.0)			
Thr	M-57	1-4	52.5 ± 0.5 (51.8)	47.7 ± 0.3 (48.0)	-0.0 ± 0.2 (0.2)	-0.1 ± 0.2*	-0.0 ± 0.0*	
	M-85	2-4	50.9 ± 0.3 (52.0)	47.3 ± 0.4 (47.9)	1.0 ± 0.2 (0.1)	0.8 ± 0.2*		
Val	M-57	1-5	26.1 ± 0.2 (27.1)	48.1 ± 0.8 (49.9)	24.8 ± 0.1 (23.0)	1.3 ± 0.2*	0.0 ± 0.1*	-0.2 ± 0.3*
	M-159	2-5	26.6 ± 0.6 (27.2)	46.8 ± 1.7 (49.9)	22.4 ± 1.0 (22.9)	3.7 ± 3.0*	0.5 ± 0.3*	
Fum	M-57	1-4	51.5 ± 1.0 (51.8)	50.1 ± 0.6 (48.0)	-0.7 ± 0.5 (0.2)	-0.9 ± 0.5*	0.1 ± 0.4*	
Suc	M-15	1-4	50.7 ± 0.2 (51.8)	49.2 ± 0.2 (48.0)	0.1 ± 0.0 (0.2)	0.0 ± 0.0*	-0.0 ± 0.0*	
	M-57	1-4	51.1 ± 0.4 (51.8)	49.8 ± 0.2 (48.0)	-0.1 ± 0.5 (0.2)	-0.1 ± 0.2*	-0.7 ± 0.3*	

glycolysis between glyceraldehyde-3-phosphate [G3P] and 3-phosphoglycerate). Anabolic fluxes were based on the *A. succinogenes* biomass composition (Table 1). The standard deviation for all anabolic fluxes was set to 10% of the flux value, which is the average standard deviation determined from replicate samples for all measured biomass components, and which takes into account the standard deviation for the dry cell weight determination. The biosynthetic origin of amino acid carbon atoms from their metabolic precursors was based on constraints described by Szyperski (53).

Extracellular fluxes, and NMR and GC-MS data sets used were averages of measurements on all nine cultures with the exception of a few samples that were pooled for NMR analyses (see NMR methods section). Mass isotopomer standard deviations for individual amino acid fragments from all nine cultures were typically < 1%. To more closely reflect biological variability, standard deviations for mass isotopomers were raised to 2.6%. This value was the standard deviation between mass isotopomers that are expected to be identical (i.e., between Ala, Asp, Ser, and Thr M-57 fragment x+0 mass isotopomers). The averaged data were applied to several versions of an *A. succinogenes* metabolic model (Fig. 1) using *13C-Flux* software (62). The model variations were: the presence and absence of ED and glyoxylate pathways, and alternative PPP reactions (25, 56), as well as grouping or separating OAA and malate pools. *13C-Flux* uses a metabolic network (specified by the user) and an arbitrary set of starting values for the free fluxes to simulate a data set of isotopomers and extracellular fluxes. The simulated data set is then compared to the experimental data set, and the fit between simulated and experimental data is determined by a sum of squared residuals (SS_{res}) weighted by their respective standard deviations. The free flux values are then varied until the weighted SS_{res} is

minimized, indicating an optimized fit between the two data sets. The choice of free flux starting values can affect the resulting SS_{res} value if local minima are encountered in the optimization process. We used thousands of starting values to determine if multiple solutions existed. This process was automated using a perl script, 'autoflux3.pl,' written by Hart Poskar (University of Manitoba, Canada). Natural ^{13}C abundance in the supplied glucose was included in the model. Mass distribution data were therefore corrected only for natural isotope abundances in all TBDMS atoms and all amino acid heteroatoms, and for unlabeled inoculum biomass, using software described by Wahl et al. (58). The heaviest mass isotopomers were omitted from the fitting process, since their occurrence is highly improbable when starting from a singly-labeled isotopomer (Table 2) and they are therefore likely to be overestimated due to contaminants. NMR alanine and glycogen data were corrected for the inoculum's unlabeled biomass as described (13).

3.3.8 Analytical techniques for determining *A. succinogenes* cellular composition.

A. succinogenes was grown as described above and harvested at 0.6–2.1 OD_{660}. Samples were centrifuged and washed at least once in 0.9% NaCl at 4°C prior to analysis, except for dry cell weight determination. All sample measurements were compared to the corresponding OD_{660} values by linear regression.

Dry cell weight was determined from thirteen cell suspensions, each composed of 3–5 pooled cultures. Suspensions were filtered through pre-weighed 0.45 μm HA filters (Millipore, Billerica, MA) and washed with 10 ml of 0.9% NaCl or water. The biomass-containing filters were dried to constant weight at 85°C for 24 h, and the weights recorded.

Total protein and RNA contents were determined from twelve cultures each. For protein content, cell pellets from 1-ml culture samples were resuspended in 0.5 ml water, lysed by sonication, and lysate protein (20 µl) was quantified by the bicinchoninic acid assay (Pierce) with bovine serum albumin as the standard (33). Total cell RNA quantification was based on the method of Benthin et al. (2). Cell pellets from 9-ml culture samples were resuspended in 3 ml of 0.3 M KOH and digested for 1 h at 37°C, then chilled on ice. Ice-cold 3 M $HClO_4$ (1 ml) was added to the suspension, then $KClO_4$ and insoluble cell components were pelleted by centrifugation. The supernatant was saved, and RNA was extracted from the pellet twice more with 4 ml of ice-cold 0.5 M $HClO_4$. The supernatants were pooled and brought up to 13 ml with 0.5 M $HClO_4$. Samples were neutralized with 2 M Tris-HCl (pH 7.4) and the absorbance was measured at 260 and 280 nm (A_{260}:A_{280} ratios were between 1.9-2.0). A correspondence of 1.0 A_{260} to 40 mg RNA/l was used (1). The accuracy of the method was confirmed by performing the RNA and dry weight determinations on six *Escherichia coli* cultures grown aerobically in modified-M9 without casamino acids (33) and obtaining the expected RNA content of 20.8% of the dry cell weight (36).

Total cell lipid was determined from six cultures using a transmethylation protocol (31). Cell pellets were resuspended in 1 ml water and volumes containing ~ 25 mg of biomass were transferred to glass screw cap tubes and dried by lyophilization. Cells were resuspended in 2 ml of fresh 5% H_2SO_4 in methanol. To this solution were added 25 µl of 0.2% butylated hydroxy toluene in methanol and 24 µl of internal standard containing 1.74 mg/ml glyceryl triheptadecanoate in a 2:1 mixture of 2,2,4-trimethylpentane:toluene. The reaction mixtures were heated and quenched, and FAMES

were extracted and analyzed by GC as described (31). Peak identities were determined from fatty acid standards GLC-10 and GLC-50.

Total glycogen was determined from eighteen cultures. Cell pellets from 6–10 ml of culture were resuspended in 1.4 ml of 50 mM sodium acetate buffer (pH 4.5) and lysed by sonication, followed by 5 min of boiling. Lysate samples (0.75 ml) were used to determine the initial glucose concentrations by HPLC. To ensure total glucose release, 6,700 U of isoamylase and 3 U of amyloglucosidase were incubated with the lysates for 20–90 h at 40°C with occasional mixing. At various time points, cell debris was pelleted by centrifugation and glucose in the supernatant was quantified by HPLC. Similar glucose yields were observed in 20 and 90 h digests. Isoamylase was required for complete digestion during this time, as determined by comparing glucose released from digests of type II glycogen from oyster with and without isoamylase (data not shown).

Peptidoglycan (PG) and lipopolysaccharide (LPS) levels were estimated from the difference in the surface area:volume ratios of *A. succinogenes* and *E. coli*, using the same PG:LPS ratio for *A. succinogenes* as for *E. coli* (36). The dimensions of 25 *A. succinogenes* and 43 *E. coli* exponential phase cells were measured by phase contrast microscopy. Volumes and surface areas were calculated assuming that each cell pole was a hemi-sphere and that the section between the hemi-spheres was a right cylinder.

To determine *A. succinogenes'* amino acid composition, lysates were prepared as described for total protein determination and centrifuged. Supernatants were dried by lyophilization, washed four times with ice-cold 80% ethanol in water to remove free amino acids, and dried under vacuum. Proteins were hydrolyzed under vacuum with 6 N

HCl at 110°C for 24 h. Amino acid analysis was performed at the MSU Macromolecular Structure Facility using a Hitachi L-8800 amino acid analyzer (San Jose, CA).

To determine the *A. succinogenes* C and N contents, cultures were harvested and washed three times with 0.9% NaCl. Pellets were resuspended in 1 ml water, boiled for 10 min, and dried by lyophilization. The C and N composition was then determined by the Duke Environmental Stable Isotope Laboratory, Duke University as described (31).

3.3.9 Enzyme assays. Cell extracts were prepared from *A. succinogenes* grown in AM3. Cell pellets were washed in 0.9% NaCl, resuspended in 100 mM Tris-HCl (pH 7.4), and lysed by sonication. Soluble cell extracts were the supernatant of centrifuged lysate while particulate cell extracts were not centrifuged. Cell extract protein was quantified using the bicinchoninic acid assay. All enzyme activities were measured in at least triplicate using a Cary 300 spectrophotometer (Varian, Palo Alto, CA) in final volumes of 1 ml at 37°C. All reactions were started by adding the substrate, except for OAA decarboxylase, which was started by adding cell extract after the spontaneous OAA degradation rate was measured. Any background activity before adding the substrate was subtracted from the activity detected after adding the substrate. Extinction coefficients (mM^{-1} cm^{-1}) used were: 3-acetylpyridine adenine dinucleotide, 6.1 (57); benzyl viologen (BV), 8.65; OAA, 0.95; NAD^+ and $NADP^+$, 6.23.

Formate dehydrogenase was assayed by monitoring BV reduction at 578 nm or NAD^+ reduction at 340 nm in a mixture containing 100 mM Tris-HCl (pH 7.4), 2 mM BV or NAD^+, 5 mM sodium formate, and 0.2 μg/ml particulate cell extract protein. The reaction was made anoxic by flushing solutions with N_2 for 10 min, sealing cuvettes with

rubber stoppers, and injecting the substrate through the stopper. Malic enzyme was assayed by monitoring $NADP^+$ reduction at 340 nm in a mixture containing 75 mM Tris-HCl (pH 8.1), 4 mM $MnCl_2$, 1 mM dithiothreitol, 1 mM $NADP^+$, 40 mM disodium malate, 20 μg/ml soluble cell extract protein, and in the presence or absence of 2 mM NH_4Cl. To confirm that NH_4Cl did not activate other NADPH-producing activities, reactions were stopped by cooling on ice, then products were analyzed by HPLC. OAA decarboxylase was assayed by monitoring OAA removal at 265 nm (8) in a mixture containing 75 mM Tris-HCl (pH 7.4), 1 mM potassium OAA, 85 μg/ml particulate or 20 μg/ml soluble cell extract protein, in the presence or absence of 15 mM NaCl. OAA decarboxylation to pyruvate was confirmed by analyzing the reaction products by HPLC. Pyruvate dehydrogenase was assayed as described (35) in a mixture containing 750 μg/ml soluble cell extract protein. Transhydrogenase was assayed as described (44) in a mixture containing 170 μg/ml particulate cell extract protein.

3.4 RESULTS

3.4.1 Determining *A. succinogenes*' cellular composition. Knowing the requirements for metabolic intermediates for biosynthesis is essential for accurately quantifying metabolic fluxes and for estimating ATP and redox balances. This knowledge can be obtained by quantifying cell components or by assuming a cell composition similar to that of *E. coli*, and relating the values to central metabolism through anabolic pathway stoichiometries (19, 22, 28, 32, 47). We determined the *A. succinogenes* glycogen, lipid, protein, and RNA levels, which together account for ~ 86% of the dry cell weight. At an OD_{660} of 1.0 in AM3, *A. succinogenes* had a concentration of 535 ± 47 mg dry cell wt/l. *A. succinogenes* amino acid and fatty acid compositions were also determined (Table 1). DNA levels were estimated by assuming the same genome copy number for *A. succinogenes* and *E. coli* and adjusting for cells per gram of dry biomass (*A. succinogenes*, 3.3×10^{15}; *E. coli*, 1.1×10^{15} [(36)]) and for genome sizes (*A. succinogenes*, 2.1 Mb; *E. coli* K12, 4.6 Mb). LPS and PG were estimated from the differences in surface area:volume ratios between *A. succinogenes* and *E. coli*. With cell dimensions of $0.63 \times 0.63 \times 1.21$ μm (*A. succinogenes*) and $0.80 \times 0.80 \times 2.63$ μm (*E. coli*), *A. succinogenes* has a surface area:volume ratio 1.39 times that of *E. coli*. Table 1 summarizes *A. succinogenes*' cell composition and its metabolite and cofactor requirements.

3.4.2 Confirming a pseudo-metabolic steady state. Since industrial fermentations typically occur as batch processes, we decided to perform flux analysis with *A. succinogenes* under batch conditions. Figure 2, shows batch *A. succinogenes* growth and fermentation characteristics in AM3, during which the pH decreases from 7.2 to 6.4.

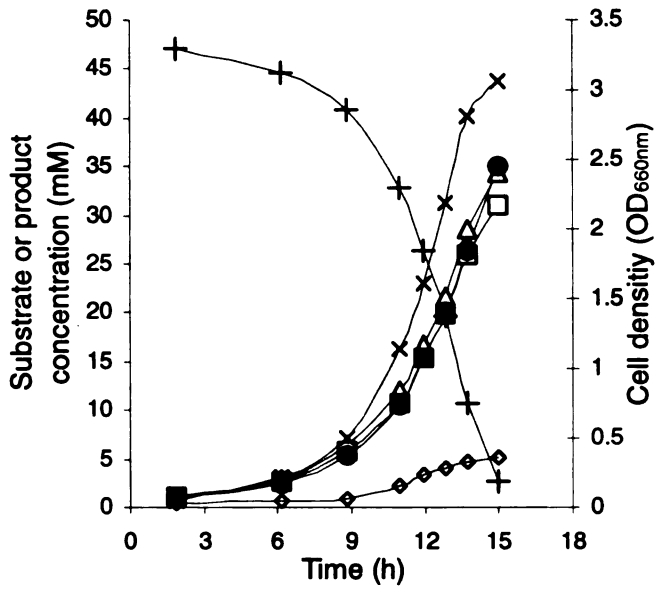

Figure 3.2. *A. succinogenes* batch fermentation characteristics in AM3. Data were obtained from triplicate 60-ml cultures rather than 11-ml cultures to avoid significant volume changes during the course of the fermentation. Data obtained from parallel 11-ml cultures sampled showed nearly identical fermentation characteristics (data not shown). Standard deviations are less than or equal to the size of the symbols. Legend: glucose, +; succinate, ●; formate, Δ ; acetate, □; ethanol, ◊; growth, ×.

Metabolic flux analysis uses equations that describe a metabolic steady state, where the fluxes into a metabolite pool equal the fluxes out of that pool. In batch cultures, however, changing cell, substrate, product, and proton concentrations can potentially affect metabolic fluxes. To confirm that *A. succinogenes* fluxes were constant during exponential growth, we first grew 11-ml cultures with unlabeled glucose and compared extracellular fluxes (specific rates of glucose consumption and product formations) at different cell densities in duplicate (i.e., at OD_{660} values of 0.5, 1.0, and 1.5) as described in the methods. The pH at the highest cell concentration sampled had only decreased to 7.0, and fermentation balances are known to be similar at pH values between 6.0 and 7.4 (55). The extracellular fluxes were similar at all cell densities (data not shown), so the experiment was repeated with nine cultures grown on [1-^{13}C]glucose as described in the

Methods section. Extracellular fluxes and positional isotopic enrichments were compared in the cultures harvested at the different cell densities using Student's *t*-tests (95% confidence, equal-variance). A statistical difference occurred about once in every 19 comparisons, which is indistinguishable from the expected frequency for false positive occurrences. Based on these results we felt confident that our batch cultures exhibited a pseudo-metabolic steady state during exponential growth, and we averaged the data across all 9 cultures for use in our metabolic flux analysis.

3.4.3 Metabolic pathway delineation and flux quantification. To better understand *A. succinogenes* in vivo pathway utilization we used our biomass (Table 1), extracellular flux (Table 3), and isotopomer data sets (Tables 2 and 4) in several variations of the metabolic model shown in Figure 1. This process was done both manually and by using

μ (h^{-1})	mmol g^{-1} h^{-1}						Carbon recovery (%)	Electron recovery (%)
	r_{Glc}	r_{Suc}	r_{Fum}	r_{For}	r_{Ace}	r_{EtOH}		
0.28 ± 0.01	7.9 ± 0.5	5.8 ± 0.3	0.2 ± 0.0	3.5 ± 0.3	4.4 ± 0.2	1.2 ± 0.2	98 ± 4	104 ± 4

Table 3.3 Growth and metabolic parameters. The carbon and electron recoveries were calculated using an assumed elemental composition of $CH_2O_{0.5}N_{0.2}$. This typical microbial composition (51) agrees with the C:N ratio for *A. succinogenes* ($CN_{0.18}$).

13C-Flux software. Where possible, the values used were the average from all nine cultures, sampled at different cell densities. The set of fluxes giving the best fit between the simulated and experimental data sets (weighted $SS_{res} = 148$) is shown in Figure 3. This model contains 28 free net fluxes and 11 free exchange fluxes (39 degrees of freedom). With a $SS_{res} > 54$, our fitting fails the χ^2 test at the 95% confidence interval, but this result is observed with most flux analysis studies of biological systems (61).

Compound / Carbon	^{13}C enrichment (%) [a]	
	^{1}H-NMR	^{13}C-NMR
Acetate / C1	5.1 ± 0.5 (4.7)[b]	4.9 ± 0.8 (4.7)
Acetate / C2	42.5 ± 1.0 (43.1)	42.5 ± 1.0 (43.1)[d]
Alanine / C2	4.9 ± 0.4 (4.7)[b,c]	5.4 ± 0.7 (4.7)
Alanine / C3	43.9 ± 0.9 (43.1)[c]	43.9 ± 0.9 (43.1)[d]
Formate	0.0 ± 0.0 (0.3)	N.D.
Glucose / C1	97.6 ± 3.3 (97.2)	97.6 ± 3.3 (97.2)[d]
Glucose / C6	N.D.	1.3 ± 0.2 (1.4)
Succinate / C1 or C4	N.D.	0.0 ± 0.0 (0.3)
Succinate / C2 or C3	24.0 ± 0.2 (23.9)	24.0 ± 0.2 (23.9)[d]

Table 3.4. Measured and simulated percent ^{13}C-enrichments in alanine, glucose, and organic acids as determined by NMR

[a] Simulated values resulting from the optimized set of fluxes (i.e., Figure 3 fluxes) are in parentheses. N.D., not determined.

[b] Long range coupling between ^{1}H and neighboring ^{13}C (i.e., acetate, $^{2}J^{1}H^{\alpha}$-^{13}C; alanine, $^{2}J^{1}H^{\beta}$-$^{13}C^{\alpha}$).

[c] While there is considerable overlapping of peaks in the ^{1}H-NMR spectra of amino acids, the peaks representing the alanine C^{3} protons are sufficiently resolved for accurate quantification.

[d] Since ^{13}C-NMR only gives relative peak intensities, the ^{1}H-NMR-determined value for this carbon was used to represent the ^{13}C-NMR peak area. The label represented by ^{13}C-NMR peaks for other carbons was then determined from the relative peak intensity.

Non-oxidative PPP models usually consist of three reactions (ppp1-3; Fig. 1). Additional reactions may exist, though, that can affect the resulting global flux values. We tested the effects of including additional PPP reactions (56) and of describing all possible PPP reactions as a simplified set of half reactions (25). These models gave nearly identical fluxes and weighted SS_{res} values (152 when including additional reactions and 154 when using half-reactions) as when only traditional PPP reactions were included. Because alternative PPP reactions have not been solidly established in vivo, and because they did not affect the resulting fluxes, we did not use alternative PPP reactions in our final model.

Figure 3.3. *A. succinogenes* metabolic fluxes in AM3 with 150 mM $NaHCO_3$ obtained after fitting of experimental and simulated data sets in *13C-Flux*. All flux values have units of mmol g^{-1} h^{-1}. Single parameter 90% confidence intervals were calculated as described (63). Net flux directions are indicated by an enlarged arrowhead. Exchange flux values are in parentheses. Exchange fluxes that could not be quantified are indicated by a bi-directional arrow without an exchange flux value. Anabolic fluxes are based on Table 1 values. Anabolic flux requirements for 3-phosphoglycerate, Tyr, and Trp are accounted for in other anabolic fluxes. The estimated ATP, NADH, and NADPH fluxes for biosynthesis and transport were –13.36, 0.78, and –3.83, respectively. Reversible citrate lyase was omitted because there was no glyoxylate shunt flux and citrate was not observed in culture supernatants.

Figure 3.3 (cont'd)

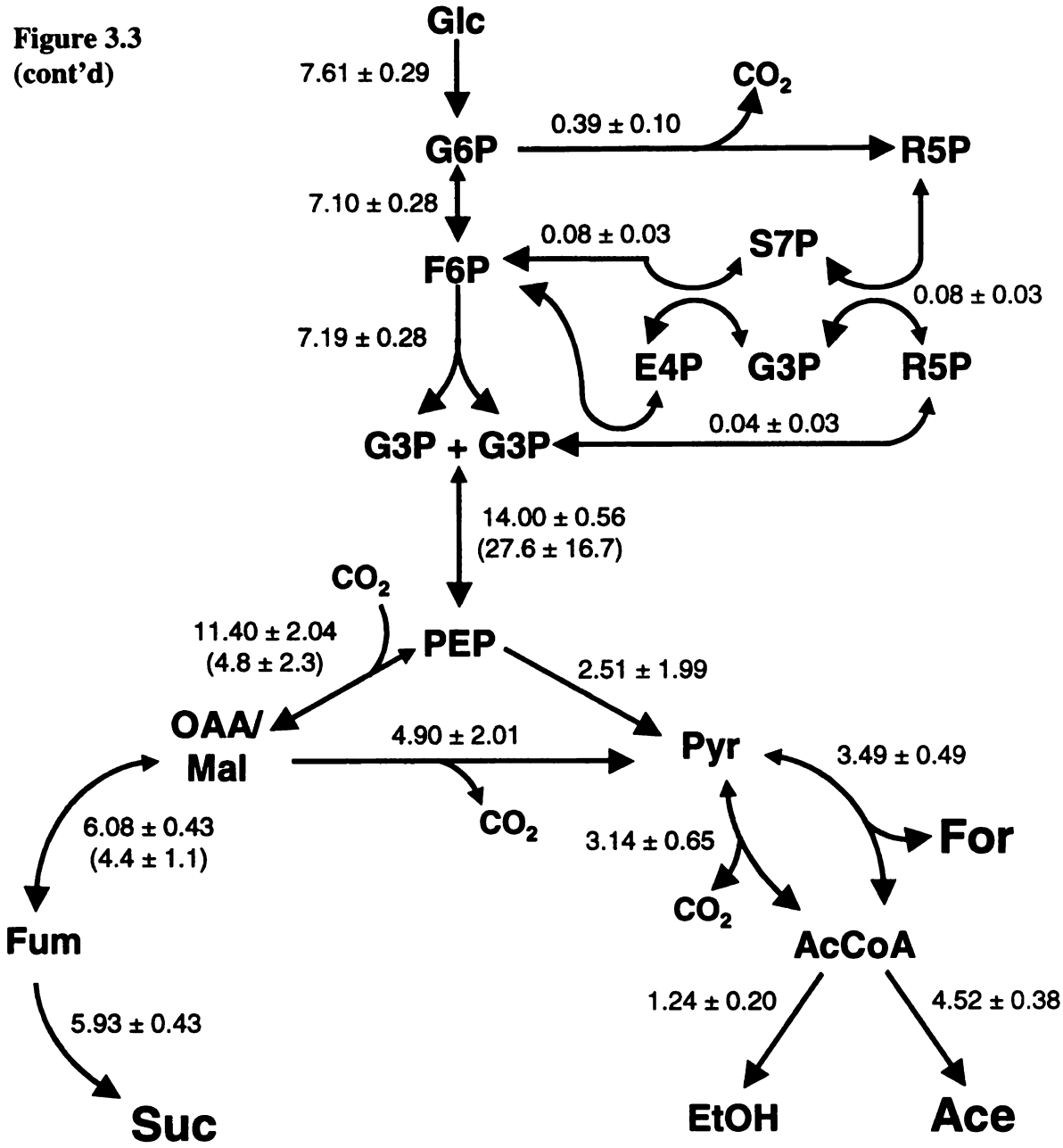

Additional net fluxes.

ATP	NADH	CO_2 uptake	Fum production
8.23	3.43	2.47 ± 0.92	0.15 ± 0.02

Net Anabolic fluxes.

G6P	F6P	R5P	E4P	G3P	PEP	Pyr	AcCoA	OAA
0.12	0.04	0.19	0.04	0.42	0.10	0.78	0.86	0.42

Our focus was to identify pathways involved in distributing flux to succinate and alternative fermentation products as well as those involved in redox balance. For this reason, and because the ATP required for cell maintenance is unknown, we did not focus on why the net ATP production is 1.6 times greater than the estimated requirement. Figure 3 is described in detail below, focusing on the pathways of interest, and explaining the progression from the metabolic model shown in Figure 1 to that shown in Figure 3.

3.4.4 The glyoxylate cycle. The glyoxylate cycle could act as a shunt between the C_3 and C_4 pathways. Because low in vitro isocitrate lyase activity was reported for *A. succinogenes* (55), we investigated the presence of a functioning glyoxylate cycle in our ^{13}C-labeling experiment. Glyoxylate shunt flux was first addressed by inspection of the isotopomer data. As seen in Figure 4, the [3-^{13}C]OAA and [2-^{13}C]acetyl-CoA produced from [1-^{13}C]glucose would generate double-labeled OAA through an active glyoxylate cycle. Table 2 shows insignificant fractions of double-labeled OAA-derived products (i.e., Asp, Thr, Fum, and Suc). These results suggest that the glyoxylate cycle, if present in *A. succinogenes*, is not active in cultures grown in AM3. Confirming our manual inspection of the data, all fittings of simulated to experimental data in *13C-Flux* indicated no forward or reverse glyoxylate cycle flux. These results agree with the fact that no *Pasteurellaceae* genome sequenced to date (complete or incomplete) contains genes showing similarity to known malate synthase and isocitrate lyase genes.

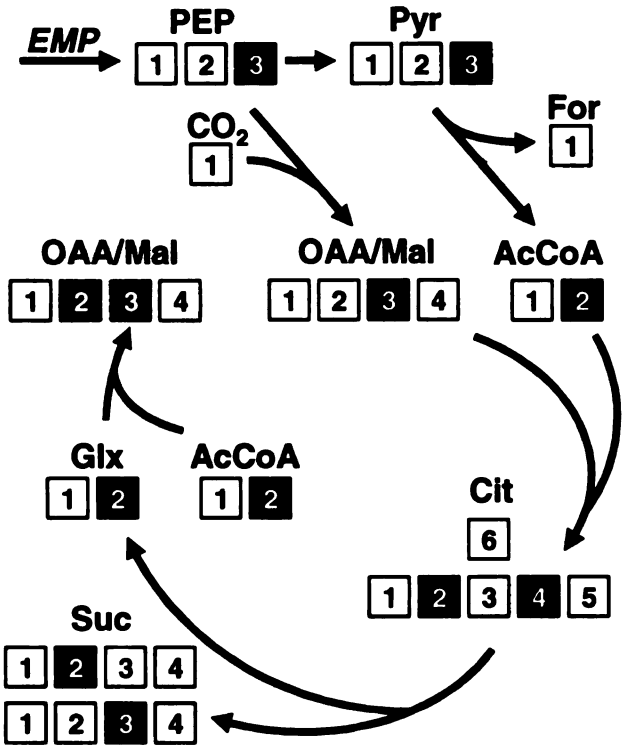

Figure 3.4. Acetyl-CoA and OAA isotopomers expected from forward glyoxylate cycle flux. Black squares, ^{13}C; white squares, ^{12}C. The shaded oval highlights the double-labeled OAA that would be generated by glyoxylate cycle flux.

3.4.5 The oxidative pentose phosphate pathway. Since succinate production from PEP requires reductant (Fig. 1), it is important to understand *A. succinogenes*' redox balance. The OPPP was thought to be important for NADPH production based on previous enzyme activity data (55). Also, the *A. succinogenes* genome sequence encodes the OPPP enzymes, glucose-6-phosphate (G6P) dehydrogenase (AsucDRAFT_0146) and 6-phosphogluconate dehydrogenase (AsucDRAFT_0141). We first addressed OPPP flux by inspecting the isotopomer data. While glycolysis converts [1-^{13}C]G6P into equal proportions of unlabeled and single-labeled G3P, the OPPP produces $^{13}CO_2$ and unlabeled G3P (Fig. 5a). Between 45.5% (in Ser) and 50.1% (in Fum) of each downstream product of G3P (i.e., Ala, Asp, Fum, Ser, Suc, and Thr) contain a single

label (Table 2). These values are close to the 50% expected from glycolytic flux alone. However, to accurately quantify the glycolytic and OPPP fluxes, the existence of [6-^{13}C]G6P should be considered. [6-^{13}C]G6P is produced by reverse flux from [6-^{13}C]fructose-6-phosphate, which is generated by triose-phosphate cycling (50) and reverse PPP reactions. NMR analysis of glycogen's glucose monomers shows that only 1.4% of G6P is labeled at carbon 6 (Table 4), indicating very little OPPP flux.

We then used *13C-Flux* to quantify the OPPP flux. Since there is a net CO_2 consumption by *A. succinogenes* fermentations, we originally only included a CO_2 influx in our model. This first model did not account for the possibility of $^{13}CO_2$ produced by the OPPP being diluted by the large amount of $^{12}CO_2$ in the medium. Without a CO_2 efflux, all fittings indicated no OPPP flux. Since most metabolites, with the exception of fumarate and succinate, indicate a small ^{13}C loss from the system (Tables 2 and 4), we included a CO_2 efflux in the model. The OPPP flux was 5% that of the glucose uptake rate, only enough to supply 20% of the estimated NADPH requirements (Fig. 3).

Like OPPP flux, Cys and Met uptake would contribute to unlabeled isotopomers. However, the fitting shown in Figure 3 indicates no Cys and Met uptake. To determine if our adjustment of the mass isotopomer standard deviations (see Methods) prevented the detection of Cys and Met uptake, we used unmodified standard deviations in the fitting process. The best fit in this case (SS_{res} of 384) showed essentially the same set of fluxes, including no Met uptake and a very small Cys uptake (1% of the glucose uptake rate). As expected, OPPP flux was lower (4% of the glucose uptake rate) in the fit showing Cys uptake. If our model underestimates the extent of Cys and Met uptakes, then it

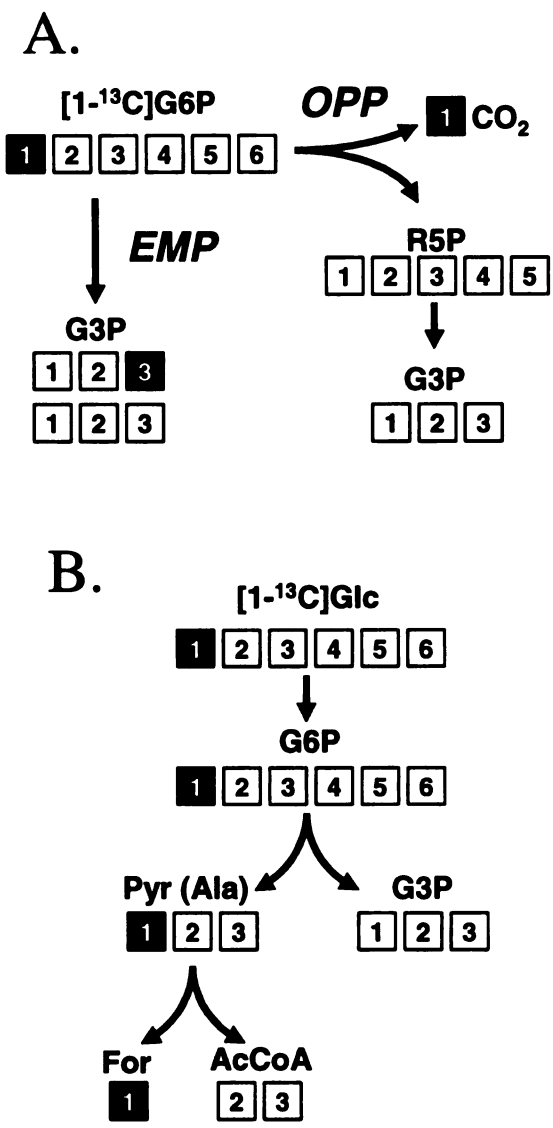

Figure 3.5. Isotopomers expected from OPPP and ED pathway fluxes. Black squares, ^{13}C; white squares, ^{12}C. A. G3P isotopomers expected from forward glycolytic and OPPP fluxes. B. Alanine and formate isotopomers expected from ED pathway flux.

overestimates the OPPP flux as well. Thus, 20% represents the upper limit of the NADPH requirements that can be supplied by the OPPP.

3.4.6 The Entner-Doudoroff pathway. With low OPPP flux, other pathways must be responsible for NADPH production. Previously, low ED pathway enzyme activities were detected in *A. succinogenes* extracts (55). The *A. succinogenes* genome encodes two proteins showing 36% and 37% identity to *E. coli* 2-keto-3-deoxy-6-phosphogluconate aldolase (AsucDRAFT_0727 and 1070) and a protein that is 27% identical to *E. coli* phosphogluconate dehydratase (AsucDRAFT_0513). For these reasons, we investigated the presence of ED pathway flux in our labeling experiment. Flux through the ED pathway would produce [1-^{13}C]pyruvate, resulting in [1-^{13}C]Ala and ^{13}C-formate (Fig 5b). As seen in Table 2, Ala M-57 fragments (containing carbons 1-3) and M-85 fragments (containing carbons 2 and 3) have almost identical mass isotopomer distributions. Since losing Ala carbon 1 does not affect the mass distribution, carbon 1 must be 100% unlabeled. Furthermore, no labeled formate was observed by ^{1}H-NMR (Table 4). These results indicate that there is negligible ED pathway flux. All *13C-Flux* fittings using models containing the ED pathway confirmed this conclusion.

3.4.7 C_3 pathway dehydrogenases and transhydrogenase. HPLC analysis of excreted products showed that 1.6 times more acetate + ethanol were excreted than formate. The expected ratio is < 1.0 since pyruvate formate-lyase produces equal amounts of formate and acetyl-CoA (Fig. 1) and some acetyl-CoA is required for biomass (Fig. 3). This observation can be explained if formate dehydrogenase (ForDH) consumes some formate

or pyruvate dehydrogenase (PyrDH) converts some pyruvate to acetyl-CoA and CO_2. The *A. succinogenes* genome encodes both PyrDH (AsucDRAFT_001-003) and ForDH (AsucDRAFT_1405-1408), and in vitro activity was detected for both enzymes (Table 5).

Enzyme assayed	Specific activity (nmol mg protein^{-1} min^{-1})
Transhydrogenase	14 ± 1
Pyruvate dehydrogenase	5 ± 1
Formate dehydrogenase[a]	7 ± 2
Malic enzyme (- NH_4^+)[b]	120 ± 10
Malic enzyme (+ NH_4^+)[b]	620 ± 50
Soluble OAA decarboxylase (- Na^+)[c]	260 ± 60
Soluble OAA decarboxylase (+ Na^+)[c]	80 ± 110
Particulate OAA decarboxylase (+ Na^+)[c]	1,080 ± 110

Table 3.5. Enzyme activities in cell extracts of *A. succinogenes* grown in AM3 with 150 mM $NaHCO_3$

[a] Activity was not detected when NAD^+ was supplied in place of BV.

[b] Since NH_4^+ is known to stimulate malic enzyme activity (43), NH_4Cl was added to the reaction to confirm that the measured activity was due to malic enzyme. The amount of NADPH produced was 94 ± 3 % that of the pyruvate produced.

[c] HPLC analysis confirmed that pyruvate was the main product formed.

ForDH is often coupled to hydrogenase in bacterial fermentations, producing H_2 rather than NADH. Here, the electron balance was 104 ± 4% (Table 3) and GC analysis showed that H_2 was absent from culture headspaces, indicating either that H_2 was not produced or that it was quickly consumed. In any case, pyruvate oxidation to acetyl-CoA without formate or H_2 production yields reductant. Our metabolic flux model (Fig. 3) indicates a 3.14 mmol g^{-1} h^{-1} flux through the PyrDH/ForDH grouped reaction, giving a total NADH production rate of 17.92 mmol g^{-1} h^{-1} (including NADH produced by G3P dehydrogenase and anabolism). Succinate and ethanol productions require a total of 14.49 mmol NADH g^{-1} h^{-1} (Fig. 3), leaving 3.43 mmol NADH g^{-1} h^{-1} to be consumed by other reactions. One possibility for an NADH-consuming reaction is transhydrogenase. The *A. succinogenes*

genome encodes a membrane-associated transhydrogenase (AsucDRAFT_0847-848). In vitro transhydrogenase activity was previously reported as diaphorase activity (37) and it was also detected in this study (Table 5). If the excess NADH is consumed entirely by transhydrogenase, it could supply 90% of the estimated NADPH requirements.

3.4.8 Malic enzyme and OAA decarboxylase. While transhydrogenase and OPPP fluxes could account for up to 110% of the estimated NADPH requirements, other NADH-consuming (i.e., malate dehydrogenase) and NADPH-producing (i.e., malic enzyme) reactions are possible. Together, the reactions catalyzed by malate dehydrogenase and malic enzyme are an alternative to transhydrogenase, resulting in the net oxidization of NADH and reduction of $NADP^+$ (Fig. 1). Besides producing NADPH, malic enzyme also bridges the C_4 and the C_3 pathways (Fig. 1). Therefore, the existence of a malic enzyme flux could dramatically influence metabolic engineering strategies. Malic enzyme activity was detected in extracts of *A. succinogenes* grown in several conditions (55), including in AM3 (Table 5). To distinguish fluxes between PEP and pyruvate from fluxes between OAA/malate and pyruvate, a unique isotopomer of pyruvate or OAA/malate must be present. As illustrated in Figure 6, a unique isotopomer, [2-^{13}C]fumarate, is formed when scrambling caused by the symmetry of fumarate generates 25% each of [3-^{13}C]fumarate and [2-^{13}C]fumarate (50% of the fumarate is unlabeled). Exchange flux in the C_4 pathway then generates 7% [2-^{13}C]OAA and 2% [2-^{13}C]PEP (determined from GC-MS analyses of Asp's and Phe's f302 fragments, respectively; Table 2). If all pyruvate were generated from PEP, as would be expected in a simple branched fermentation, pyruvate and PEP would have identical positional

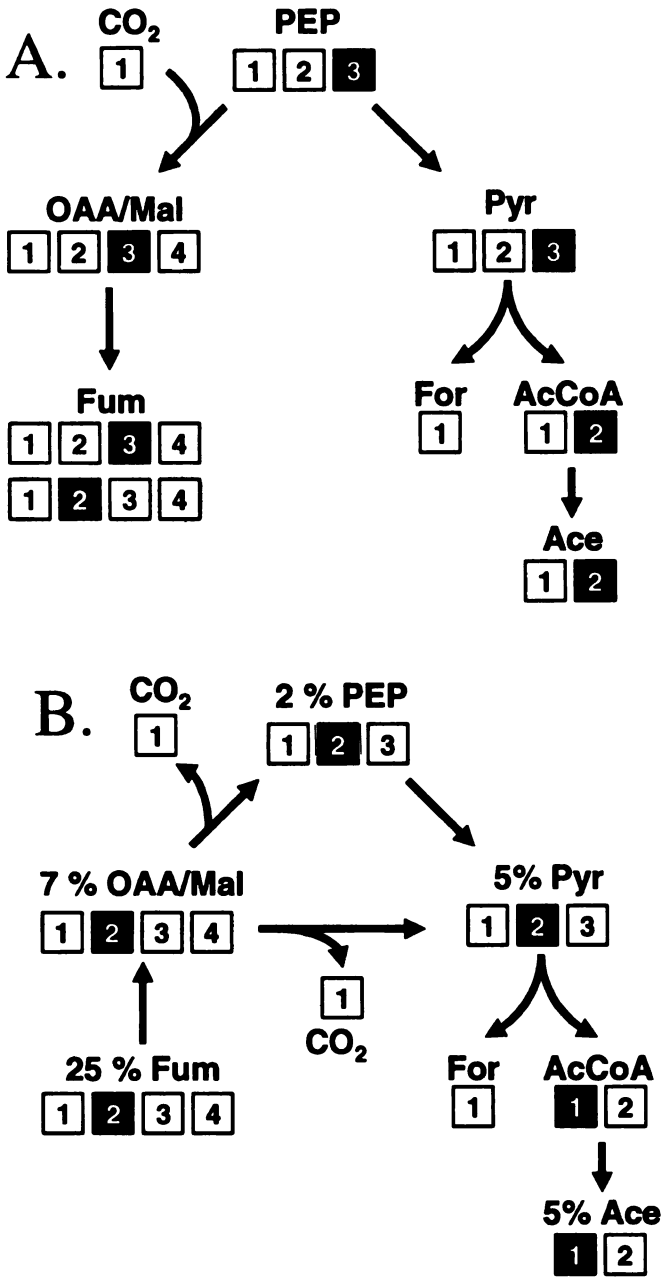

Figure 3.6. Two-step illustration of the fluxes resulting in [2-^{13}C]pyruvate. Black squares, ^{13}C; white squares, ^{12}C. **A.** Step 1: Generation of [2-^{13}C]fumarate (highlighted by the shaded oval) by forward fluxes through the C_4 pathway and fumarate's symmetry. **B.** Step 2: Isotopomers resulting from [2-^{13}C]fumarate by reverse C_4 pathway flux, C_4-decarboxylating flux, and forward C_3 pathway flux.

isotopic enrichments. NMR analyses of Ala (Table 4) show that 5%, rather than 2%, of pyruvate is labeled at the C2 position. This result indicates that a C_4-decarboxylating enzyme (i.e., malic enzyme or OAA decarboxylase) is active during growth in AM3. This conclusion is also supported by the detection of 5% [1-^{13}C]acetate (Table 4), a downstream product of [2-^{13}C]pyruvate.

Because fluxes from OAA, malate, and PEP to pyruvate give identical pyruvate isotopomers, and because different combinations of these three fluxes can result in identical pyruvate isotopomer distributions, OAA and malate decarboxylating fluxes cannot be distinguished. For this reason, malate and OAA were grouped into a single pool, as in other metabolic flux models (3, 32, 40, 59, 66). In Figure 3, PEPCK and PK net flux values were dependent on the OAAdec/ME flux (set as a free variable), explaining why PEPCK, PK, and OAAdec/ME fluxes have similar confidence intervals. These confidence intervals are large, and different values for fluxes between PEP, OAA/malate, and pyruvate were obtained in multiple fittings with little effect on the SS_{res} value. However, our fittings consistently showed that the OAAdec/ME flux was larger than the PK flux. The best fit indicates that the C_4-decarboxylating flux is 4.9 mmol g^{-1} h^{-1}, which is greater than the flux needed to convert excess NADH to NADPH (3.43 mmol g^{-1} h^{-1}). Therefore, the C_4-decarboxylating flux must represent a combination of malic enzyme and OAA-decarboxylating fluxes, since OAA decarboxylation to pyruvate does not yield reductant. An operon encoding a membrane-bound, Na^+-pumping OAA decarboxylase was identified in the genome sequence (AsucDRAFT_1557-1559). In addition to detecting a Na^+-independent OAA decarboxylase activity in soluble cell extracts, we also detected significant Na^+-dependent activity in particulate cell extracts

but not in soluble cell extracts (Table 5). From the flux analysis and enzyme activities detected, it is clear that flux distribution to succinate and alternative products can occur at OAA and malate, rather than just at PEP.

3.5 DISCUSSION

This study has described important aspects of *A. succinogenes* metabolism. Flux through the glyoxylate and ED pathways was ruled out. OPPP flux was too low to meet NADPH requirements. PyrDH and/or ForDH contribute to a net NADH production that could be converted to NADPH by transhydrogenase. Malic enzyme may also contribute to NADPH production. In addition to PEP, OAA and malate are important nodes for flux distribution to succinate and alternative fermentation products.

We assume that the excess ATP not needed for biosynthesis and transport (Table 1) is used for cell maintenance. The estimated ATP required for biosynthesis alone (10.48 mmol g^{-1} h^{-1}) is 49 % of the total ATP produced, which is not unreasonable. It was estimated that 51% of the energy produced by anaerobically growing *E. coli* is used for transport and maintenance processes (52).

Optimized fits showed a greater OAAdec/ME flux than PK flux. PK flux is composed of pyruvate kinase and the PTS. If glucose phosphorylation occurred through the PTS alone, the PK flux would be at least equal to the glucose uptake rate. Because the estimated PK flux is only 33% of the glucose uptake rate, and because most of the flux into the C_3 pathway is likely from OAA/malate rather than from PEP (Fig. 3), it is unlikely that the PTS is the main glucose phosphorylation mechanism. *A. succinogenes* was previously shown to have hexokinase activity in addition to PTS activity (55). Uptake assays with ^{14}C-glucose and a ^{14}C-glucose analogue indicated that the PTS is not the main *A. succinogenes* glucose uptake mechanism at high glucose concentrations (24).

This study identified the mechanisms responsible for NADPH production in glucose-grown *A. succinogenes* in AM3. Product isotopomer data indicated no ED

pathway flux and low OPPP flux. The lower flux to formate than to acetyl-CoA indicated, in addition to pyruvate formate-lyase activity, a pyruvate oxidizing activity (i.e., PyrDH) and/or a formate oxidizing activity (i.e., ForDH). PyrDH is often considered to be an enzyme of aerobic metabolism. However, it is expressed in anaerobically-grown *Haemophilus influenzae* (41), a bacterium closely related to *A. succinogenes*. PyrDH and ForDH activities were also detected in *A. succinogenes* cell extracts (Table 5). In either case, there is enough excess NADH to meet the NADPH requirements through transhydrogenase and/or through NADH-oxidizing malate dehydrogenase plus NADP-reducing malic enzyme. Product isotopomer data confirmed the existence of a C_4-decarboxylating flux, suggesting that malic enzyme contributes to NADPH production. NADP-dependent malic enzyme and transhydrogenase activities were detected in cell extracts (Table 5). Given the low OPPP flux, transhydrogenase and/or malic enzyme are the main NADPH-producing mechanisms, and account for at least 80% of the NADPH requirements.

Malic enzyme's contribution to NADPH production in *A. succinogenes* and other bacteria is currently unclear. Under ammonia-limiting conditions, or when pyruvate kinase is knocked out, malic enzyme flux increases in *E. coli*, but this results in excess NADPH that is oxidized by transhydrogenase (11). Transhydrogenase, on the other hand, is a significant NADPH producer in several cases. In fact, *E. coli* was recently shown to rely on transhydrogenase for up to 45% of its NADPH requirements in aerobic batch cultures (44). Transhydrogenase is even more important for *E. coli* NADPH production when the OPPP enzyme, G6P dehydrogenase, is disrupted (21, 44). Transhydrogenase is also important for NADPH production in *Rhodospirillum rubrum* and *Rhodobacter*

sphaeroides (14, 20), suggesting an important role for this enzyme across a diverse range of bacteria. While we have shown that transhydrogenase and/or malic enzyme are important for NADPH production in *A. succinogenes*, it remains to be seen how flux through these enzymes and through the OPPP respond to environmental stimuli.

Understanding the NADPH-producing mechanisms in *A. succinogenes* may also be important for devising metabolic engineering strategies. It is well known that the CO_2 concentration affects the flux distribution into the C_4 and C_3 pathways (34, 55). Here we have shown that flux to the C_3 pathway (i.e., malic enzyme) and flux through the C_3 pathway (i.e., PyrDH and ForDH) are important for NADPH production. Therefore, it is plausible that the need for NADPH also controls flux distribution between the C_4 and C_3 pathways. Under the conditions studied here, a limited quantity of reductant must be shared by the C_4 pathway and anabolism. Adding H_2 shifts the *A. succinogenes* fermentation balance toward succinate in rich media (55). Adding H_2 also, at least partially, alleviates the need for flux through C_3 pathway dehydrogenases, as shown by the fact that adding H_2 increases the formate:(acetate + ethanol) ratio in AM3-grown cultures (McKinlay et al., unpublished data). It will be important to determine whether a surplus of electrons (e.g., as H_2) will be sufficient to suppress the C_3 pathway or if genetic modifications are necessary.

The discovery of an in vivo C_4-decarboxylating flux is particularly important because it reveals that flux distribution to succinate and alternative products can occur at multiple nodes (i.e., PEP, OAA, malate, and possibly pyruvate). This discovery also implicates PEPCK as a major flux-carrying enzyme that feeds both product-forming branches rather than just the C_4 pathway. Thus, at least under the growth conditions

tested here, OAA and malate could be more important nodes than PEP in controlling flux distribution to succinate and alternative products. There is currently much interest in the fields of bacterial physiology and metabolic engineering in understanding flux distribution at these nodes (45). In the case of *A. succinogenes,* it now seems likely that redirecting flux towards succinate production will face the engineering challenges of dealing with alternative routes (e.g., pyruvate kinase vs. PEPCK and a C_4-decarboxylase) and redundant activities. In this study, malic enzyme and two OAA-decarboxylating activities were identified. The Na^+-dependent OAA decarboxylase activity was only observed in particulate cell extracts, which is consistent with the Na^+-pumping, membrane-bound OAA decarboxylase encoded in the *A. succinogenes* genome. Membrane-bound OAA decarboxylase is also expressed by closely related *Mannheimia succiniciproducens* grown anaerobically on glucose (29). While this enzyme is required for growth on citrate by other bacteria (5, 9, 67), its activity during glucose fermentation is an intriguing finding that suggests an alternative role. A role for OAA decarboxylase in Na^+-linked energetics has been suggested for several bacteria (10, 18), including in Na^+-dependent glutamate transport and drug efflux in closely related *A. actinomycetemcomitans* (18). A Na^+ gradient could also be involved in fumarate and succinate transport as was shown for *Wolinella succinogenes* (54). However, given that AM3 contains ~230 mM Na^+, the membrane-bound OAA decarboxylase may simply function to pump Na^+ out of the cell. A Na^+-independent OAA-decarboxylating activity was detected in the soluble crude extract (Table 5). Malic enzyme (43), PEPCK (23), pyruvate kinase (4), and 2-keto-3-deoxy-6-phosphogluconate aldolase (39) can also decarboxylate OAA, at least in vitro. While the in vivo contribution of these OAA

decarboxylating activities is unknown, the potential for redundant activities is considerable, and may present a challenge for metabolic engineering. On the other hand, a C_4-decarboxylating flux that only meets anabolic pyruvate and acetyl-CoA needs could be beneficial for developing a succinate-producing strain with an acceptable growth rate.

This study has provided key insights into *A. succinogenes* NADPH production and flux distribution to major fermentation products, and has raised important considerations for its metabolic engineering. ^{13}C-labeling studies of industrial organisms have not only led to strain improvements but also to a deeper understanding of metabolism. They have led to the discovery of new pathways (3, 49), and to a better understanding of anaplerosis (38, 40, 45) and of the controls effected by cofactor production and cell energetics (7, 46, 68). The effects of CO_2 and alternative carbon and electron sources on *A. succinogenes*' fermentation balance make this bacterium an excellent system for analyzing the metabolic control effects of CO_2 and reducing power on flux distribution between PEP, pyruvate, OAA, and malate using ^{13}C-labeling and other studies. While *A. succinogenes* has industrial potential, it also has unique metabolic traits whose study could contribute to a broader understanding of bacterial metabolism and its diversity.

3.6 ACKNOWLEDGEMENTS

This work was supported by the National Science Foundation grant BES-0224596 and by a grant from the Michigan State University (MSU) Research Excellence Fund. James McKinlay was supported in part by MSU Quantitative Biology and Modeling Initiative and Marvin Hensley Endowed fellowships and by an Annie's Homegrown fellowship for environmental studies.

We are indebted to Dr. Douglas Allen for valuable discussions and technical assistance. We also thank Drs. John Ohlrogge, Ana Alonso, Fernando Goffman, Igor Libourel, and Joerg Schwender for valuable discussions. We are grateful for the use of Drs. Tom Schmidt's and John Ohlrogge's GC equipment. We are also grateful for the use of the autoflux3 program written by Dr. Hart Poskar. We thank Drs. Beverly Chamberlin, Daniel Holmes, and Joe Leykam for assistance with GC-MS, NMR, and amino acid analysis, respectively.

3.7 REFERENCES

1. Ausubel, F. M., R. Brent, R. E. Kingston, D. D. Moore, J. G. Seidman, J. A. Smith, and K. Struhl. (ed.). 1998. Current Protocols in Molecular Biology. John Wiley and Sons, Inc.

2. Benthin, S., J. Nielsen, and J. Villadsen. 1991. A simple and reliable method for the determination of cellular RNA content. Biotechnol. Tech. 5:39-42.

3. Christensen, B., and J. Nielsen. 2000. Metabolic network analysis of *Penicillium chrysogenum* using ^{13}C-labeled glucose. Biotechnol. Bioeng. 68:652-659.

4. Creighton, D. J., and I. A. Rose. 1976. Oxalacetate decarboxylase activity in muscle is due to pyruvate kinase. J. Biol. Chem. 251:69-72.

5. Dahinden, P., Y. Auchli, T. Granjon, M. Taralczak, M. Wild, and P. Dimroth. 2005. Oxaloacetate decarboxylase of *Vibrio cholerae*: purification, characterization, and expression of the genes in *Escherichia coli*. Arch. Microbiol. 183:121-129.

6. Dauner, M., and U. Sauer. 2000. GC-MS analysis of amino acids rapidly provides rich information for isotopomer balancing. Biotechnol. Prog. 16:642-649.

7. Dauner, M., M. Sonderegger, M. Hochuli, T. Szyperski, K. Wüthrich, H. P. Hohmann, U. Sauer, and J. E. Bailey. 2002. Intracellular carbon fluxes in riboflavin-producing *Bacillus subtilis* during growth on two-carbon substrate mixtures. Appl. Environ. Microbiol. 68:1760-1771.

8. Dimroth, P. 1981. Characterization of a membrane-bound biotin-containing enzyme: oxaloacetate decarboxylase from *Klebsiella aerogenes*. Eur. J. Biochem. 115:353-358.

9. Dimroth, P. 1980. A new sodium-transport system energized by the decarboxylation of oxaloacetate. FEBS Lett. 122:234-236.

10. Dimroth, P., and B. Schink. 1998. Energy conservation in the decarboxylation of dicarboxylic acids by fermenting bacteria. Arch. Microbiol. 170:69-77.

11. Emmerling, M., M. Dauner, A. Ponti, J. Fiaux, M. Hochuli, T. Szyperski, K. Wüthrich, J.E. Bailey, and U. Sauer. 2002. Metabolic flux responses to pyruvate kinase knockout in *Escherichia coli*. J. Bacteriol. 184:152-164.

12. Fell, D. 1997. Understanding the control of metabolism. Portland Press, London and Miami.

13. Fischer, E., and U. Sauer. 2003. Metabolic flux profiling of *Escherichia coli* mutants in central carbon metabolism using GC-MS. Eur. J. Biochem. 270:880-891.

14. Grammel, H., E. D. Gilles, and R. Ghosh. 2003. Microaerophilic cooperation of reductive and oxidative pathways allows maximal photosynthetic membrane biosynthesis in *Rhodospirillum rubrum*. Appl. Environ. Microbiol. 69:6577-6586.

15. Guettler, M. V., M. K. Jain, and D. Rumler. 1996. Method for making succinic acid, bacterial variants for use in the process, and methods for obtaining variants. U.S. patent 5,573,931.

16. Guettler, M. V., M. K. Jain, and B. K. Soni. 1996. Process for making succinic acid, microorganisms for use in the process and methods of obtaining the microorganisms. U.S. patent 5,504,004.

17. Guettler, M. V., D. Rumler, and M. K. Jain. 1999. *Actinobacillus succinogenes* sp. nov., a novel succinic-acid-producing strain from the bovine rumen. Int. J. Syst. Bacteriol. 49:207-216.

18. Hase, C. C., N. D. Fedorova, M. Y. Galperin, and P. A. Dibrov. 2001. Sodium ion cycle in bacterial pathogens: evidence from cross-genome comparisons. Microbiol. Mol. Biol. Rev. 65:353-370.

19. Henriksen, C. M., L. H. Christensen, and J. Nielsen. 1996. Growth energetics and metabolic fluxes in continuous cultures of *Penicillium chrysogenum*. J. Biotechnol. 45:149-164.

20. Hickman, J. W., R. D. Barber, E. P. Skaar, and T. J. Donohue. 2002. Link between the membrane-bound pyridine nucleotide transhydrogenase and glutathione-dependent processes in *Rhodobacter sphaeroides*. J. Bacteriol. 184:400-409.

21. Hua, Q., C. Yang, T. Baba, H. Mori, and K. Shimizu. 2003. Responses of the central metabolism in *Escherichia coli* to phosphoglucose isomerase and glucose-6-phosphate dehydrogenase knockouts. J. Bacteriol. 185:7053-7067.

22. Ingraham, J. L., O. Maaloe, and F. C. Neidhardt. 1983. Growth of the bacterial cell. Sinauer Associates, Sunderland, MA.

23. Jabalquinto, A. M., M. Laivenieks, J. G. Zeikus, and E. Cardemil. 1999. Characterization of the oxaloacetate decarboxylase and pyruvate kinase-like activities of *Saccharomyces cerevisiae* and *Anaerobiospirillum succiniciproducens* phosphoenolpyruvate carboxykinases. J. Protein. Chem. 18:659-664.

24. Kim, P., and C. Vieille. Glucose phosphorylation mechanisms in succinate-producing *Actinobacillus succinogenes*. submitted.

25. Kleijn, R. J., W. A. van Winden, W. M. van Gulik, and J. J. Heijnen. 2005. Revisiting the ^{13}C-label distribution of the non-oxidative branch of the pentose phosphate pathway based upon kinetic and genetic evidence. FEBS J. 272:4970-4982.

26. Koffas, M. A. G., G. Y. Jung, and G. Stephanopoulos. 2003. Engineering metabolism and product formation in *Corynebacterium glutamicum* by coordinated gene overexpression. Metab. Eng. 5:32-41.

27. Kroger, A., S. Biel, J. Simon, R. Gross, G. Unden, and C. R. D. Lancaster. 2002. Fumarate respiration of *Wolinella succinogenes*: enzymology, energetics and coupling mechanism. Biochim. Biophys. Acta. 1553:23-28.

28. Lange, H. C., and J. J. Heijnen. 2001. Statistical reconciliation of the elemental and molecular biomass composition of *Saccharomyces cerevisiae*. Biotechnol. Bioeng. 75:334-344.

29. Lee, J. W., S. Y. Lee, H. Song, and J. S. Yoo. 2006. The proteome of *Mannheimia succiniciproducens*, a capnophilic rumen bacterium. Proteomics 6:3550-3566.

30. Lee, W. N., L. O. Byerley, E. A. Bergner, and J. Edmond. 1991. Mass isotopomer analysis: theoretical and practical considerations. Biol. Mass. Spectrom. 20:451-458.

31. Li, Y., F. Beisson, M. Pollard, and J. Ohlrogge. 2006. Oil content of *Arabidopsis* seeds: the influence of seed anatomy, light and plant-to-plant variation. Phytochemistry 67:904-915.

32. Marx, A., A. A. de Graaf, W. Wiechert, L. Eggeling, and H. Sahm. 1996. Determination of fluxes in the central metabolism of *Corynebacterium glutamicum* by nuclear magnetic resonance spectroscopy combined with metabolic balancing. Biotechnol. Bioeng. 49:111-129.

33. McKinlay, J. B., and J. G. Zeikus. 2004. Extracellular iron reduction is mediated in part by neutral red and hydrogenase in *Escherichia coli*. Appl. Environ. Microbiol. 70:3467-3474.

34. McKinlay, J. B., J. G. Zeikus, and C. Vieille. 2005. Insights into *Actinobacillus succinogenes* fermentative metabolism in a chemically defined growth medium. Appl. Environ. Microbiol. 71:6651-6656.

35. Millar, A. H., C. Knorpp, C. J. Leaver, and S. A. Hill. 1998. Plant mitochondrial pyruvate dehydrogenase complex: purification and identification of catalytic components in potato. Biochem. J. 334:571-576.

36. Neidhardt, F. C. 1987. *Escherichia coli* and *Salmonella typhimurium* cellular and molecular biology, vol. 1. American Society for Microbiology, Washington, D.C.

37. Park, D. H., and J. G. Zeikus. 1999. Utilization of electrically reduced neutral red by *Actinobacillus succinogenes*: physiological function of neutral red in membrane-driven fumarate reduction and energy conservation. J. Bacteriol. 181:2403-2410.

38. Park, S. M., C. Shaw-Reid, A. J. Sinskey, and G. Stephanopoulos. 1997. Elucidation of anaplerotic pathways in *Corynebacterium glutamicum* via ^{13}C-NMR spectroscopy and GC-MS. Appl. Microbiol. Biotechnol. 47:430-440.

39. Patil, R. V., and E. E. Dekker. 1992. Cloning, nucleotide sequence, overexpression, and inactivation of the *Escherichia coli* 2-keto-4-hydroxyglutarate aldolase gene. J. Bacteriol. 174:102-107.

40. Petersen, S., A. A. de Graaf, L. Eggeling, M. Mollney, W. Wiechert, and H. Sahm. 2000. *In vivo* quantification of parallel and bidirectional fluxes in the anaplerosis of *Corynebacterium glutamicum*. J. Biol. Chem. 275:35932-35941.

41. Raghunathan, A., N. , D. Price, M. Y. Galperin, K. S. Makarova, S. Purvine, A. F. Picone, T. Cherny, T. Xie, T. J. Reilly, J. R. Munson, R. E. Tyler, B. J. Akerley, A. L. Smith, B. O. Palsson, and E. Kolker. 2004. *In silico* metabolic model and protein expression of *Haemophilus influenzae* strain Rd KW20 in rich medium. Omics 8:25-41.

42. Ratcliffe, R. G., and Y. Shachar-Hill. 2006. Measuring multiple fluxes through plant metabolic networks. Plant J. 45:490-511.

43. Sanwal, B. D., and R. Smando. 1969. Malic enzyme of *Escherichia coli*. Diversity of the effectors controlling enzyme activity. J. Biol. Chem. 244:1817-1823.

44. Sauer, U., F. Canonaco, S. Heri, A. Perrenoud, and E. Fischer. 2004. The soluble and membrane-bound transhydrogenases UdhA and PntAB have divergent functions in NADPH metabolism of *Escherichia coli*. J. Biol. Chem. 279:6613-6619.

45. Sauer, U., and B. J. Eikmanns. 2005. The PEP-pyruvate-oxaloacetate node as the switch point for carbon flux distribution in bacteria. FEMS Microbiol. Rev. 29:765-794.

46. Sauer, U., V. Hatzimanikatis, J. E. Bailey, M. Hochuli, T. Szyperski, and K. Wüthrich. 1997. Metabolic fluxes in riboflavin-producing *Bacillus subtilis*. Nat. Biotechnol. 15:448-452.

47. Sauer, U., V. Hatzimanikatis, H. P. Hohmann, M. Manneberg, A. P. van Loon, and J. E. Bailey. 1996. Physiology and metabolic fluxes of wild-type and riboflavin-producing *Bacillus subtilis*. Appl. Environ. Microbiol. 62:3687-3696.

48. Sauer, U., D. R. Lasko, J. Fiaux, M. Hochuli, R. Glaser, T. Szyperski, K. Wüthrich, and J. E. Bailey. 1999. Metabolic flux ratio analysis of genetic and environmental

modulations of *Escherichia coli* central carbon metabolism. J. Bacteriol. 181:6679-6688.

49. Schwender, J., F. Goffman, J. B. Ohlrogge, and Y. Shachar-Hill. 2004. Rubisco without the Calvin cycle improves the carbon efficiency of developing green seeds. Nature 432:779-782.

50. Schwender, J., J. B. Ohlrogge, and Y. Shachar-Hill. 2003. A flux model of glycolysis and the oxidative pentose phosphate pathway in developing *Brassica napus* embryos. J. Biol. Chem. 278:29442-29453.

51. Stephanopoulos, G., A. A. Aristidou, and J. Nielsen. 1998. Metabolic Engineering: Principles and Methodologies. Academic Press, London.

52. Stouthamer, A. H. 1979. The search for correlation between theoretical and experimental growth yields. *In* J. R. Quayle (ed.), International review of biochemistry. Microbial biochemistry, vol. 21. University Park Press, Baltimore.

53. Szyperski, T. 1995. Biosynthetically directed fractional ^{13}C-labeling of proteinogenic amino acids. An efficient analytical tool to investigate intermediary metabolism. Eur. J. Biochem. 232:433-448.

54. Ullmann, R., R. Gross, J. Simon, G. Unden, and A. Kroger. 2000. Transport of C_4-dicarboxylates in *Wolinella succinogenes*. J. Bacteriol. 182:5757-5764.

55. van der Werf, M. J., M. V. Guettler, M. K. Jain, and J. G. Zeikus. 1997. Environmental and physiological factors affecting the succinate product ratio during carbohydrate fermentation by *Actinobacillus sp.* 130Z. Arch. Microbiol. 167:332-342.

56. van Winden, W., P. Verheijen, and S. Heijnen. 2001. Possible pitfalls of flux calculations based on ^{13}C-labeling. Metab. Eng. 3:151-162.

57. Venning, J. D., and J. B. Jackson. 1999. A shift in the equilibrium constant at the catalytic site of proton-translocating transhydrogenase: significance for a 'binding-change' mechanism. Biochem. J. 341:329-337.

58. Wahl, S. A., M. Dauner, and W. Wiechert. 2004. New tools for mass isotopomer data evaluation in ^{13}C flux analysis: mass isotope correction, data consistency checking, and precursor relationships. Biotechnol. Bioeng. 85:259-268.

59. Wendisch, V. F., A. A. de Graaf, H. Sahm, and B. J. Eikmanns. 2000. Quantitative determination of metabolic fluxes during coutilization of two carbon sources: comparative analyses with *Corynebacterium glutamicum* during growth on acetate and/or glucose. J. Bacteriol. 182:3088-3096.

60. Wiechert, W. 2001. ^{13}C Metabolic flux analysis. Metab. Eng. 3:195-206.

61. Wiechert, W., and A. A. de Graaf. 1997. Bidirectional reaction steps in metabolic networks: I. Modeling and simulation of carbon isotope labeling experiments. Biotechnol. Bioeng. 55:101-117.

62. Wiechert, W., M. Mollney, S. Petersen, and A. A. de Graaf. 2001. A universal framework for ^{13}C metabolic flux analysis. Metab. Eng. 3:265-283.

63. Wiechert, W., C. Siefke, A. A. de Graaf, and A. Marx. 1997. Bidirectional reaction steps in metabolic networks: II. Flux estimation and statistical analysis. Biotechnol. Bioeng. 55:118-135.

64. Wilke, D. 1999. Chemicals from biotechnology: molecular plant genetics will challenge the chemical and fermentation industry. Appl. Microbiol. Biotechnol. 52:135-145.

65. Wilke, D. 1995. What should and what can biotechnology contribute to chemical bulk production? FEMS Microbiol. Rev. 16:89-100.

66. Wittmann, C., and E. Heinzle. 2001. Application of MALDI-TOF MS to lysine-producing *Corynebacterium glutamicum*: a novel approach for metabolic flux analysis. Eur. J. Biochem. 268:2441-2455.

67. Woehlke, G., and P. Dimroth. 1994. Anaerobic growth of *Salmonella typhimurium* on L(+)- and D(-)-tartrate involves an oxaloacetate decarboxylase Na^+ pump. Arch. Microbiol. 162:233-237.

68. Zamboni, N., N. Mouncey, H. P. Hohmann, and U. Sauer. 2003. Reducing maintenance metabolism by metabolic engineering of respiration improves riboflavin production by *Bacillus subtilis*. Metab. Eng. 5:49-55.

69. Zeikus, J. G., M. K. Jain, and P. Elankovan. 1999. Biotechnology of succinic acid production and markets for derived industrial products. Appl. Environ. Microbiol. 51:545-552.

Chapter 4.

^{13}C-metabolic flux analysis of *Actinobacillus succinogenes* fermentative metabolism at different $NaHCO_3$ and H_2 concentrations

4.1 ABSTRACT

Actinobacillus succinogenes naturally produces high concentrations of succinate; a potential intermediary feedstock for bulk chemical productions. High CO_2 and H_2 concentrations make *A. succinogenes* produce more succinate and less formate, acetate, and ethanol. To determine how intermediary fluxes in *A. succinogenes* respond to CO_2 and H_2 perturbations, ^{13}C-metabolic flux analysis was performed in batch cultures at two different $NaHCO_3$ concentrations, with and without H_2, using a substrate mixture of [1-^{13}C]glucose, [U-^{13}C]glucose, and unlabeled $NaHCO_3$. The resulting amino acid, organic acid, and glycogen isotopomers were analyzed by GC-MS and NMR. In all conditions, exchange fluxes were observed through pyruvate formate-lyase, formate dehydrogenase and/or pyruvate dehydrogenase, and through malic enzyme and/or oxaloacetate decarboxylase. The detection of exchange flux between oxaloacetate, malate, and pyruvate indicated that pyruvate is also a node for flux distribution to succinate versus alternative fermentation products. High $NaHCO_3$ concentrations decreased the amount of flux shunted by C_4-decarboxylating activities from the succinate-producing C_4 pathway to the formate-, acetate-, and ethanol-producing C_3 pathway. Correspondingly, pyruvate carboxylating flux increased in response to high $NaHCO_3$ concentrations. C_3-pathway dehydrogenase fluxes responded to the different redox demands imposed by the different $NaHCO_3$ and H_2 concentrations. Overall, the metabolic flux changes allowed *A. succinogenes* to maintain a constant growth rate and biomass yield in all conditions.

4.2 INTRODUCTION

Succinate is produced as a fermentation product by a variety of bacteria and can be converted into many important commodity chemicals, including 1,4-butanediol, tetrahydrofuran, and γ –butyrolactone, which are largely used to make plastics, resins, and solvents (25, 43). These chemicals are currently produced from petrochemical feedstocks, namely from butane through maleic anhydride. By producing these chemicals from succinate, a crude oil-based industry could be replaced by one based on renewable resources. Succinate produced by fermentation has the additional environmental benefit of using CO_2, a greenhouse gas, as a substrate. To create a bio-based succinate industry, production costs must be made competitive with that of maleic anhydride, which is in increasing demand despite rising oil prices (1). Obtaining an organism that produces high succinate concentrations at high rates, with little byproduct formation, would allow for more cost effective substrate utilization and succinate purification processes.

Actinobacillus succinogenes is a capnophilic, gram-negative bacterium that naturally produces succinate as a major fermentation endproduct. After extensive engineering, *Escherichia coli* can produce nearly 100 g/l succinate in fed-batch conditions, but it requires transitioning from an aerobic growth phase to an anaerobic production phase (35). In contrast, wild-type *A. succinogenes* can grow and produce nearly 80 g/l succinate in a single batch fermentation (10). Fluoroacetate-resistant *A. succinogenes* mutants can produce over 100 g/l succinate in batch fermentations; the highest succinate concentrations ever reported (9). With evidence that the already high succinate titers obtained with the wild-type *A. succinogenes* can be improved through

genetic modifications, *A. succinogenes* is a logical starting point for engineering an industrial succinate-producing bacterium.

To engineer *A. succinogenes* effectively it is important to know which enzymes and pathways are involved in distributing flux to succinate and alternative fermentation products, and to understand how fluxes through these pathways respond to perturbations. *A. succinogenes* metabolism was first studied using in vitro enzyme assays and fermentation balances (34). Enzyme activities levels indicated that *A. succinogenes* metabolizes glucose to phosphoenolpyruvate (PEP) via glycolysis with the involvement of the oxidative pentose phosphate pathway (OPPP). PEP was thought to serve as the branch point to the formate-, acetate-, and ethanol-producing C_3 pathway and the succinate-producing C_4 pathway (Fig. 4.1).

Succinate production from PEP involves one CO_2 fixation step and two reduction steps (Fig. 4.1). Succinate yields increase with increasing CO_2 and reductant (e.g., H_2) concentrations. The reason for these increased yields was thought to simply be the increased availability of these C_4 pathway substrates (34). Oxaloacetate (OAA) decarboxylase and malic enzyme activities were also detected in *A. succinogenes* cell extracts, suggesting that, in addition to PEP, OAA and malate were nodes for flux distribution between the C_4 and C_3 pathways (34). A recent ^{13}C-metabolic flux analysis confirmed in vivo flux from OAA and malate to pyruvate (Pyr) in *A. succinogenes*, and it also indicated that more flux to Pyr came from OAA and malate than from PEP (18). This large C_4-decarboxylating flux suggests a model in which PEPCK feeds both the C_4 and C_3 pathways. In this model, CO_2 availability could affect flux through both

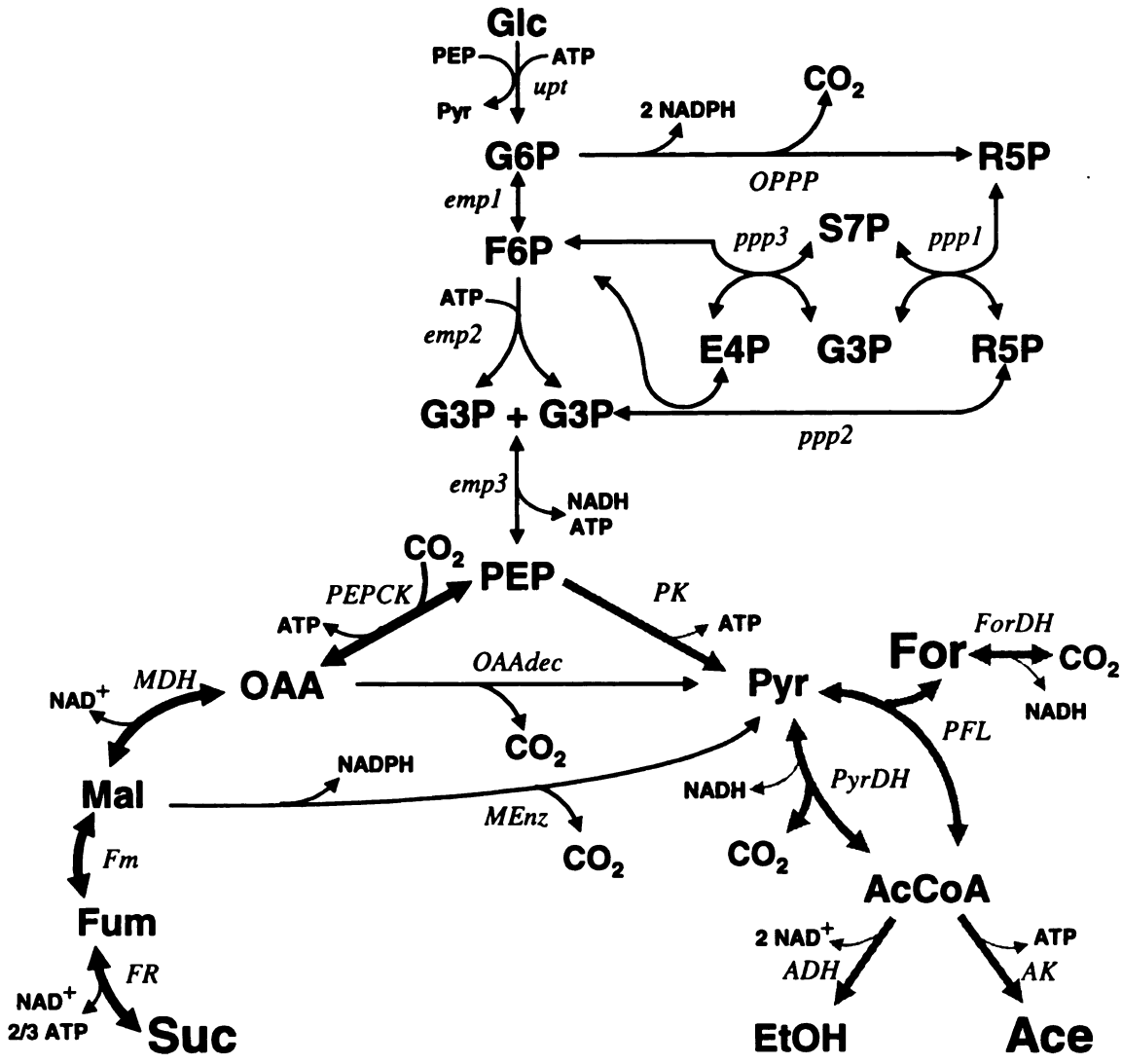

Figure 4.1. Simplified central metabolic pathways known to be active during *A. succinogenes* mixed acid fermentation (18)). Black bold lines: succinate-producing C_4 pathway. Gray bold lines: formate-, acetate-, and ethanol-producing C_3 pathway. Unidirectional arrows: fluxes considered to be unidirectional (all other fluxes are considered to be reversible). The assumption that 2/3 ATP is produced per fumarate reductase reaction is based on data from *Wolinella succinogenes* (14). Metabolites: AcCoA, acetyl-coenzyme A; Ace, acetate; EtOH, ethanol; E4P, erythrose-4-phosphate; For, formate; Fum, fumarate; F6P, fructose-6-phosphate; Glc, glucose; G3P, glyceraldehyde-3-phosphate; G6P, glucose-6-phosphate; Mal, malate; OAA, oxaloacetate; PEP, phosphoenolpyruvate; Pyr, pyruvate; R5P, pentose-phosphates; Suc, succinate; and S7P, sedoheptulose-7-phosphate. Pathways and reactions: *ADH*, alcohol dehydrogenase; *AK*, acetate kinase; *empl*, 2, and *3*, Embden-Meyerhoff-Parnas or glycolytic reactions; *Fm*, fumarase; *ForDH*, formate dehydrogenase; *FR*, fumarate reductase; *MDH*, malate dehydrogenase; *MEnz*, malic enzyme; *OAAdec*, oxaloacetate decarboxylase; *OPPP*, oxidative pentose phosphate pathway; *PEPCK*, PEP carboxykinase; *PFL*, pyruvate formate-lyase; *PK*, pyruvate kinase and PEP:glucose phosphotransferase system; *ppp1* and *2*, transketolase; *ppp3*, transaldolase; *PyrDH*, pyruvate dehydrogenase; *upt*, glucose phosphorylation by hexokinase and PEP:glucose phosphotransferase system.

pathways, rather than just the C_4 pathway. This recent ^{13}C-labeling study also indicated that little flux occurs through the OPPP (18). NADPH was instead generated by fluxes to and through the C_3 pathway (i.e., by malic enzyme and by formate and pyruvate dehydrogenases [ForDH and PyrDH] coupled with transhydrogenase) (18). Therefore, reductant availability may exert some control over C_3 pathway fluxes, in addition to directly affecting C_4 pathway flux. Here we examine the effects of CO_2 and reductant concentrations on *A. succinogenes* intermediary metabolism using ^{13}C-metabolic flux analysis in batch fermentations. $NaHCO_3$ and H_2 were used as CO_2 and reductant sources, respectively. The $NaHCO_3$ concentrations chosen were based on those shown to affect *A. succinogenes* fermentation balances in the defined medium, AM3 (20). A mixture of [1-^{13}C]glucose and [U-^{13}C]glucose was used to increase the amount of information obtained from amino acid and organic acid isotopomers over our previous flux analysis that used [1-^{13}C]glucose alone (18).

4.3 MATERIALS AND METHODS

4.3.1 Chemicals, bacteria, and culture conditions. All chemicals were purchased from Sigma-Aldrich (St. Louis, MO) unless stated otherwise. *A. succinogenes* type strain 130Z (ATCC 55618) was purchased from the American Type Culture Collection (Manassas, VA) and adapted to growth in AM3 medium as described (20). AM3 is a chemically defined medium containing Cys, Met, and Glu, which are required for *A. succinogenes* growth. For this paper's experiments, AM3 was modified by omitting the 1g/l NaCl and adjusting Cys-HCl, Met, and monosodium Glu concentrations to 17, 21, and 240 mg/l, respectively, to more closely reflect their requirements for biosynthesis (18). AM3 was prepared by distributing 8.3 ml aliquots of a 1.2X AM3 basal solution containing the phosphate buffer, NH_4Cl, monosodium Glu, and minerals, to 28-ml anaerobe tubes (Bellco, Vineland, NJ). Tubes were sealed with rubber bungs and aluminum crimps, then repeatedly evacuated and flushed with N_2 to create anaerobic conditions. In tubes to be used for growth conditions with H_2, N_2 was replaced by H_2. After autoclaving, excess pressure was released, then tubes were pressurized with 3 ml of either N_2 or H_2 at 1 ATM. The total H_2 supplied was ~0.8 mmols. CO_2-saturated 1 M $NaHCO_3$ was prepared as described (38), and 0.25 or 1 ml was then injected into each tube. Tubes receiving 0.25 ml 1M $NaHCO_3$ also received 0.75 ml 1M NaCl. Each tube also received 0.5 ml of an anoxic (under N_2) nutrient mix containing 1 M glucose, 200 ml/l vitamin mix (20), 0.2 mg/ml kanamycin, 0.34 g/l Cys-HCl, and 0.42 g/l Met. After adding 0.2 ml of inoculum, all final volumes were 10 ml with 50 mM glucose, and satisfied one of four growth conditions: A, 25 mM $NaHCO_3$ under N_2; B, 25 mM $NaHCO_3$ under H_2; C, 100 mM

$NaHCO_3$ under N_2; and D, 100 mM $NaHCO_3$ under H_2. Cultures were incubated at 37°C with shaking at 250 rpm.

4.3.2 Growth and sampling conditions in the presence of ^{13}C-glucose. The AM3 medium contained [1-^{13}C]glucose and [U-^{13}C]glucose (99% each; Cambridge Isotope Laboratories, Cambridge, MA) at a molar ratio of 1.97:1.00. Starter cultures from glycerol frozen stocks were grown in each growth condition to an OD_{660} of 0.7 – 1.1. Starter cultures were harvested by centrifugation, and washed once in an equal volume of anoxic (under N_2) 1X basal solution. Cells were resuspended in 1X basal solution to an OD_{660} of ~ 2, and 0.2 ml was inoculated into four replicates of each growth condition. Growth was monitored using a Spectronic 20 spectrophotometer (Bausch and Lomb, Rochester, NY) to calculate growth rates. A 1-ml sample was taken 2 – 2.5 hours into growth, rather than at the time of inoculation, to serve as a '0 time point' sample and account for any lag phase. This sample was used for a more accurate OD_{660} measurement using a Beckman DU 650 spectrophotometer (Fullerton, CA). It was also analyzed by high performance liquid chromatography (HPLC) to determine glucose and product concentrations. Culture growth was stopped by chilling on ice at 1.1 – 1.2 OD_{660} (conditions A and B) and at 1.5 – 1.7 OD_{660} (conditions C and D). Cell densities were recorded, then cultures were harvested by centrifugation at 4°C. Supernatants were stored at –70°C. The biomass was washed twice with 0.9% NaCl at 4°C, resuspended in 0.5 ml distilled water at 4°C, then stored at -70°C.

4.3.3 Analytical procedures. Glucose and product concentrations were determined by HPLC as described (18, 20). These values along with growth rates were used to calculate

extracellular fluxes using the Monod model as described (18, 29, 31). To obtain ^{13}C-labeled amino acids for analysis by gas chromatography-mass spectrometry (GC-MS), harvested biomass was thawed on ice, then sonicated three times. Lysates were then diluted to 1 ml with distilled water at 4°C and centrifuged. Supernatant samples (100 µl) were transferred to 1.5-ml screw cap-conical tubes and diluted to 700 µl with distilled water. Proteins were precipitated with trichloracetic acid and washed twice with acetone as described (18). Protein pellets were hydrolyzed, and amino acids partially purified, derivatized, and analyzed by GC-MS as described (18). Organic acids and glucose monomers of glycogen were prepared and analyzed by ^{1}H-NMR and ^{1}H-decoupled ^{13}C-NMR as described (18).

4.3.4 Enzyme assays. Cell extracts for enzyme assays were prepared from *A. succinogenes* grown in each of the four conditions with unlabeled glucose. Cultures were harvested at an OD_{660} of 1.0 – 1.2 by centrifugation at 4°C. Pellets were washed once in an equal volume of 100 mM Tris-HCl (pH 7.4), then resuspended in 2 ml of the same buffer. Cells were lysed by sonicating three times and lysates were stored at -70°C. After thawing, lysate subsamples were centrifuged to obtain soluble cell extracts, while particulate cell extracts were not centrifuged. Cell extract protein was quantified using the bicinchoninic acid assay (19). All assays were performed in 1-ml volumes with 3–6 replicates. All reactions were started by adding substrate or cell extract. Extinction coefficients ($mM^{-1}\ cm^{-1}$) used were: 3-acetylpyridine adenine dinucleotide, 6.1 (36); benzyl viologen, 8.65; OAA, 0.95; and NADH and NADPH, 6.23. ForDH was assayed under anoxic conditions by monitoring benzyl viologen reduction as described (18), but

with 1 mM dithiotheitol and 0.1 mg/ml particulate cell extract protein. Hydrogenase was assayed using the ForDH protocol, except that formate was excluded and reactions were initiated by replacing the N_2 headspace with H_2. Malic enzyme was assayed as described (18) with 2 mM NH_4Cl and ~20 μg/ml soluble cell extract protein. Na^+-dependent OAA decarboxylase was assayed as described (18) with ~0.1mg/ml particulate cell extract protein. PyrDH was assayed as described (22) in a mixture containing ~0.12 mg/ml soluble cell extract protein, except that Tris-HCl (pH 7.4) was used as the buffer. Transhydrogenase was assayed as described (28) in a mixture containing ~0.1 mg/ml particulate cell extract protein.

4.3.5 Metabolic modeling and flux analysis. The initial *A. succinogenes* metabolic model was based on the results obtained from a previous ^{13}C-labeling experiment (18). Modifications were then made to this model (e.g., setting some reactions as reversible) based on information obtained by including [U-^{13}C]glucose in the substrate isotopomer mixture. Thermodynamic considerations on reaction reversibility made use of $\Delta G^{\circ\prime}$ values obtained from Metacyc (2) or from the Thermodynamics of Enzyme-catalyzed Reactions Database (8). Cys uptake was removed from the model because the medium contained only enough Cys for protein synthesis. All modeling and fitting of fluxes to the experimental data sets were performed using *13C-Flux* software (40). *13C-Flux* uses a metabolic network, substrate isotopomer conditions, and an arbitrary set of fluxes to simulate an isotopomer data set. This simulated data set is then compared to the measured data set, and the similarity between the two is scored by a sum of squared residuals (SS_{res}), weighted by the standard deviation of each measurement:

$$SS_{res} = \Sigma \left(\frac{\text{measured value} - \text{simulated value}}{\text{measured standard deviation}} \right)^2$$

A fitting algorithm is then used to adjust the arbitrary fluxes in an iterative process until a set of fluxes is found that results in a simulated isotopomer data set that closely resembles the measured data set; an optimized fit. Because the substrate isotopomer mixture used in the model included natural ^{13}C abundance, amino acid and succinate fragment mass isotopomers were corrected for natural abundances in all atoms of the derivatization agent, all amino acid heteroatoms, and for unlabeled inoculum biomass. This correction procedure was performed using software described by Wahl et al. (37). For succinate mass isotopomers, there was no initial unlabeled succinate to correct for. Glucose monomers from glycogen were manually corrected for unlabeled inoculum biomass as described (7). Although mass isotopomer standard deviations were less than 1% of the mean, standard deviations between mass isotopomers that should give identical information (i.e., M-85 and M-159 fragments of the same amino acid) were usually greater (i.e., ~1.2% of the mean). To take this variability into account, mass isotopomer values with standard deviations less than 1.2% of the mean were raised to 1.2%. This adjustment did not significantly affect the fluxes nor did it greatly increase confidence intervals (data not shown). Anabolic fluxes used in the model were based on the *A. succinogenes* biomass composition (18). Because the choice of free flux starting values can affect the resulting SS_{res} value, we used ~100 different starting values for each model to determine if multiple solutions existed. This process was automated using a perl script, 'autoflux3.pl,' written by Hart Poskar (University of Manitoba, Canada).

4.4 RESULTS

4.4.1 Confirmation of pseudo-metabolic steady state and choice of substrate isotopomers. Metabolic flux analysis requires a metabolic steady state. Previously, metabolic steady state in *A. succinogenes* batch cultures was confirmed by comparing extracellular fluxes and specific isotopic enrichments at different cell densities during exponential growth (18). We measured extracellular fluxes for the four growth conditions (A, 25 mM $NaHCO_3$; B, 25 mM $NaHCO_3$ + H_2; C, 100 mM $NaHCO_3$; and D, 100 mM $NaHCO_3$ + H_2) at three different cell densities, in duplicate (i.e., two biological replicates per cell density per condition for a total of six cultures per condition). Only 2 of the 60 comparisons showed a statistical difference (2-tailed *t*-test, equal variance, $p<0.05$), as would be expected when taking into account false positive frequencies. Based on these extracellular flux data, and on our previous investigation into product isotopomer distributions at different cell densities in batch cultures (18), we felt confident that the batch cultures exhibited pseudo-metabolic steady state.

Previous ^{13}C-labeling experiments revealed a C_4-decarboxylating flux, forming a shunt from OAA and malate to Pyr (18). However, the confidence interval for this flux was large. To determine whether the C_4-decarboxylating flux could be measured with greater confidence we ran simulations with different glucose and CO_2 isotopomers using the previously determined set of fluxes (18). We then examined the resulting sensitivity matrices using the *Estimatestat* program in *13C-Flux* (40). The simulations indicated that no mixture would greatly improve our ability to quantify the C_4-decarboxylating flux. On the other hand, a practical and economical substrate isotopomer mixture consisting of [1-^{13}C]glucose, [U-^{13}C]glucose, and unlabeled $NaHCO_3$, was predicted to greatly increase

the number of isotopomers carrying information on the C_4-decarboxylating flux. Using [1-^{13}C]glucose alone, 28 measurable product isotopomers provide information on the C_4-decarboxylating flux. With the described substrate isotopomer mixture, 59 product isotopomers can be used to quantify this flux, and 56 of these isotopomers were used in this study. As before, the information on the C_4-decarboxylating flux depends on isotopomers generated by the symmetry of fumarate and by the C_4-pathway exchange flux (Fig. 4.2). When using [U-^{13}C]glucose, unlabeled CO_2 and [U-^{13}C]PEP combine to form [1,2,3-^{13}C]OAA, which is then converted to fumarate by the C_4 pathway. Label scrambing by fumarate symmetry generates a unique C_4 isotopomer that can be tracked throughout metabolism. To maximize isotopomer levels from [1-^{13}C]glucose and [U-^{13}C]glucose, they were supplied at approximately a 2:1 molar ratio.

4.4.2 Modifying the *A. succinogenes* flux model based on results from growth condition C. Growth condition C most closely resembles the 150 mM $NaHCO_3$ conditions used for the previous *A. succinogenes* ^{13}C-labeling study (18). *A. succinogenes* fermentation balances and extracellular fluxes were shown to be similar in AM3 between 75 and 150 mM $NaHCO_3$ (20). The previously established model (18) was used to fit fluxes to the condition C data set. Surprisingly, a high SS_{res} (>4500) was obtained. The weighted squared residuals (S_{res}) of each measurement (i.e., [measured value – simulated value]^2 ÷ [standard deviation]^2) were examined to identify which isotopomer measurements contributed the most to the SS_{res} (40). The highest S_{res} values were from isotopomers that provide information on C_4 pathway reversibility (i.e., mass isotopomers of Asx, Suc, and Thr M-57 fragments and Asx and Phe f302 fragments). Table 4.1 shows

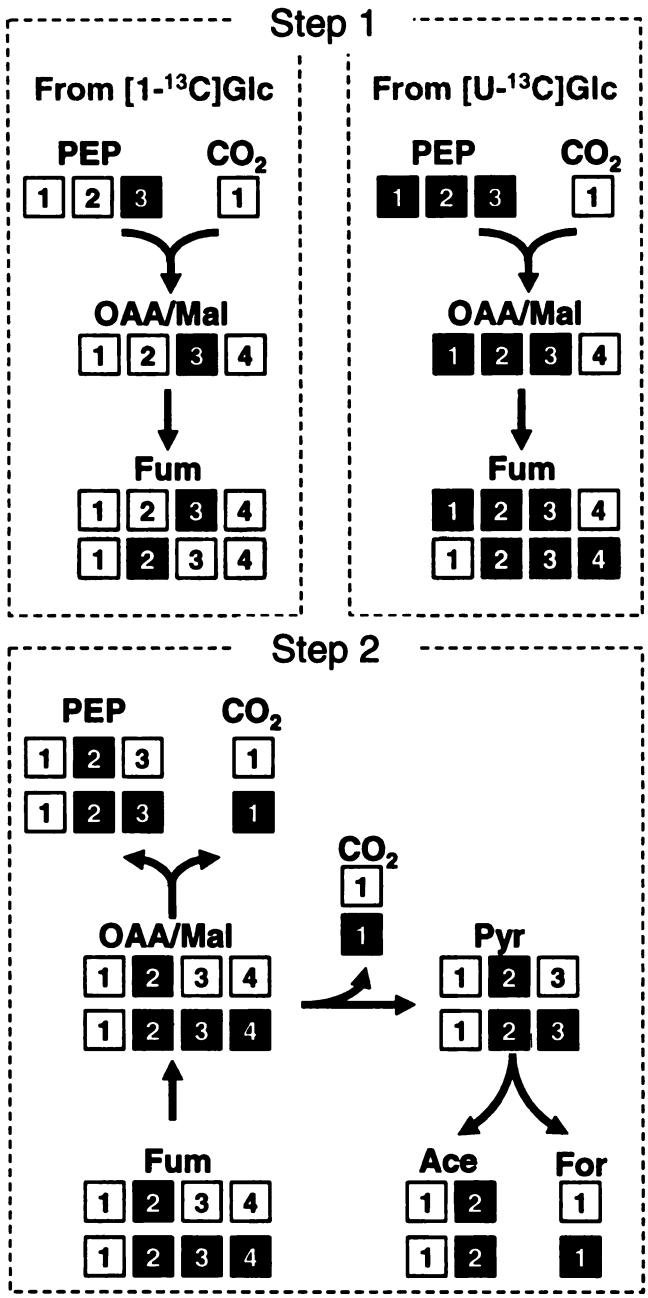

Figure 4.2. Two-step illustration of fluxes leading to isotopomers that provide information on C_4 pathway reversibility and on the C_4-decarboxylating flux. White boxes, ^{12}C; Black boxes, ^{13}C. Step 1: [2-^{13}C]fumarate and [2,3,4-^{13}C]fumarate originate in C_4 pathway fluxes from forward C_4 pathway fluxes and fumarate symmetry. Step 2: Isotopomers resulting from [2-^{13}C]fumarate and [2,3,4-^{13}C]fumarate through C_4 pathway flux and the C_4 decarboxylating flux. Abbreviations are the same as in Figure 4.1.

that ~12-13% of the C_4 compounds, Asx, Suc, and Thr M-57 fragments were double-labeled. Using multiple different starting values for C_4 pathway exchange fluxes did not result in significantly lower SS_{res} values. However, setting the C_4-decarboxylating reaction as reversible decreased the SS_{res} value from >4500 to 1520, indicating that the double-labeled C_4 isotopomers must come from Pyr. Ala M-57 fragment measurements show that there is also an unexpectedly high percentage of double-labeled Pyr (Table 4.1). We previously only considered irreversible flux from OAA and malate to Pyr because an uncharacterized *A. succinogenes* mutant that is deficient in PFL activity (23), accumulates and excretes Pyr (9), suggesting that it cannot carboxylate Pyr. The flux model indicates that, in addition to PEP, OAA, and malate, Pyr is a node for flux distrubution to succinate and alternative products.

			Mass isotopomer distributions[b] (% of product population)					
	Fragment	Carbons	X+0	X+1	X+2	X+3	X+4	X+5
Ala	M-57	1-3	29.4 ± 0.1	32.5± 0.1	20.0 ± 0.4	18.1 ± 0.3		
Asx[c]	M-57	1-4	30.3 ± 0.2	32.8 ± 0.1	12.2 ± 0.3	24.1 ± 0.1	0.6 ± 0.0	
	f302	1-2	58.3 ± 0.2	17.1 ± 0.3	24.7 ± 0.2			
Gly	M-57	1-2	64.8 ± 0.4	5.8 ± 0.4	29.4 ± 0.1			
	M-85	2	67.3 ± 0.2	32.7 ± 0.2				
Met	M-57	1-5	94.1± 0.5	3.2 ± 0.3	0.6 ± 0.8	1.9 ± 0.1	0.0 ± 0.1	0.1 ± 0.1
	M-85	2-5	95.9 ± 1.1	1.9 ± 0.2	1.9 ± 0.9	0.3 ± 0.6	0.0 ± 0.4	
Phe	f302	1-2	64.7 ± 0.1	5.2 ± 0.1	30.1 ± 0.1			
Ser	M-57	1-3	31.2 ± 0.1	34.5 ± 0.2	5.2 ± 0.1	29.1 ± 0.1		
	M-85	2-3	31.5 ± 0.1	37.2 ± 0.1	31.3 ± 0.2			
Thr	M-57	1-4	30.3 ± 0.3	32.4 ± 0.1	12.4 ± 0.3	24.4 ± 0.4	0.5 ± 0.1	
Suc	M-57	1-4	31.2 ± 0.4	32.3 ± 0.1	13.3 ± 0.3	22.7 ± 0.1	0.5 ± 0.0	

Table 4.1. Selected TBMDS[a]-amino acid and -succinate fragments obtained from *A. succinogenes* grown without H_2 in AM3 with 100 mM $NaHCO_3$ (Condition C).

[a] tert-butyldimethylsilyl. Details of fragmentation patterns for TBDMS-amino acids are described by Dauner and Sauer (4), and Wahl et al. (37).

[b] The distributions shown were corrected as described in the methods as well as for natural ^{13}C abundance in the amino and organic acid backbones using an excel macro developed by Dr. Joerg Schwender (Brookhaven National Laboratory, Upton, NY) based on correction matrices described by Lee et al. (17).

[c] Combined data for Asp and Asn since Asn is oxidized to Asp during hydrolysis.

Previously we considered the possibility of reversible PFL and PyrDH fluxes, but using [1-^{13}C]glucose alone provided no information on these exchange fluxes (18). The new isotopomer mixture indicates that both PFL and PyrDH fluxes can be reversible. These exchange fluxes allow for recombination of labeled and unlabeled formate or CO_2 with different acetyl-CoA isotopomers, generating the 20% of double-labeled Pyr (observed in Ala M-57 fragments; Table 1). PFL must be reversible to obtain low SS_{res} values. SS_{res} values are lowest when both PFL and PyrDH are made reversible. While the original model depicts PyrDH activity, it is important to note that ForDH was included in this activity. Both PyrDH and ForDH activities were detected in cell extracts, but the in vivo fluxes through these enzymes cannot be distinguished by the labeling experiments (18), thus only one of the two reactions is represented. When ForDH is substituted in the model for PyrDH, similar SS_{res} values are obtained. Furthermore, setting PyrDH or ForDH exchange fluxes to zero in models with either PyrDH or ForDH affects the S_{res} values of the same isotopomer measurements. Since the new labeling conditions are sensitive to the reversibility of these reactions, we used ForDH in the model instead PyrDH. ForDH and PFL, with $\Delta G^{\circ\prime}$ values of –15 and –17 kJ/mol, respectively, are more likely to be reversible than PyrDH, with a $\Delta G^{\circ\prime}$ value of –33 kJ/mol.

The original model (18) used Ser and Gly mass isotopomer measurements as exact imprints of G3P (the model was simplified by including 3-phosphoglycerate in the G3P pool). Fitting to the condition C data set resulted in high S_{res} values for Ser M-57 and M-85 fragment measurements. Forward fluxes from G3P to Ser should generate approximately equal percentages of Ser M-85 x+0, x+1, and x+2 mass isotopomers, even when taking into account label scrambling from the C_4 pathway. Table 4.1 shows that the

percentage of Ser M-85 x+1 mass isotopomer is higher than expected. This pattern could result from a reversible flux from Gly to Ser, combining $^{12}C_1$ with double-labeled Gly and $^{13}C_1$ with unlabeled Gly. The C_1 intermediate in Gly synthesis is 5,10-methylene-tetrahydrofolate, which can potentially inter-convert with formate through N-formyl-tetrahydrofolate or with 5-methyl-tetrahydrofolate from Met degradation. Surprisingly, a small percentage of Met is labeled (Table 4.1). Not only is there a significant percentage of Met x+1 mass isotopomer, as might be expected through C_1 exchange, but there is also a significant percentage of Met M-57 x+3 mass isotopomer. The *A. succinogenes* draft genome sequence encodes a homocysteine transmethylase (EC 2.1.1.13; Asuc_DRAFT 1212) suggesting that C_1 exchange with methionine is possible. The presence of Met x+3 mass isotopomers may indicate flux from Thr to Met. However, neither homoserine O-acetyltransferase (EC 2.3.1.31) nor homoserine O-succinyltransferase (EC 2.3.1.46) are encoded in the *A. succinogenes* draft genome sequence, thus separating methionine from central metabolism. To date, we have been unable to grow *A. succinogenes* in AM3 in the absence of Met (20). Met x+3 mass isotopomers may be an artifact. At best, ~10-20 times less Met mass isotopomers are obtained from hydrolyzed protein compared to most other amino acid mass isotopomers. Thus, Met mass isotopomer measurements may be particularly susceptible to the effects of contaminating fragments.

Ser, Gly, C_1, and Met pathways were remodeled to account for these observations, including Met x+3 mass isotopomers (Fig. 4.3). The modified model was fit to the condition C data set, and the Ser fragments' S_{res} values decreased significantly. The optimized fit indicated that little, if any, 5,10-methylene-tetrahydrofolate was derived from formate or from 5-methyl-tetrahydrofolate. Therefore, even if some Met originates

from Thr, Ser isotopomers are not affected because there is insignificant C_1 exchange between Met and Ser. The label scrambling observed in Ser is due almost entirely to the reversibility of vGly alone and to the large amount of labeled Ser C_3 (~ 66% of Ser C_3 is expected to be labeled from forward fluxes from the glucose isotopomer mixture).

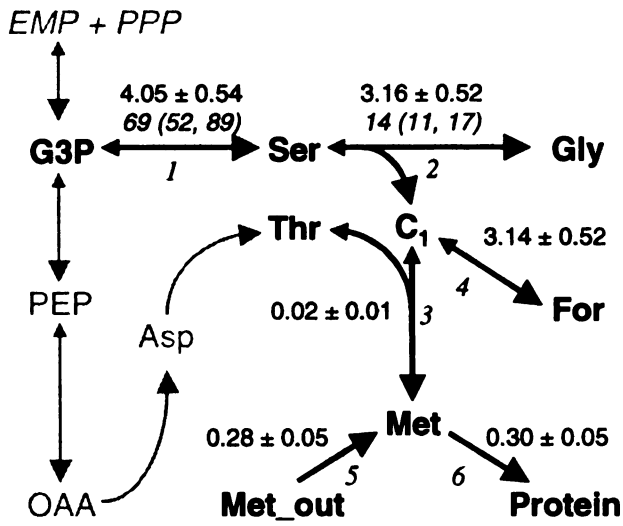

Figure 4.3. Glycine synthesis and C_1 metabolism used in the metabolic flux model. Flux units are percent of glucose uptake rate ± 90% confidence intervals. Exchange fluxes that could be determined are shown in italics with unsymmetrical exchange flux 90% confidence intervals in brackets. Confidence intervals were calculated as described (41). Exchange fluxes between OAA to Thr could not be quantified from the available isotopomers. Although the model allowed for exchange fluxes between Thr and Met and between C_1 and For (as indicated by the bidirectional arrows), the exchange fluxes were not statistically different from zero. Reactions:1, vSer (simplified serine biosynthesis pathway); 2, vGly (glycine hydroxymethyltransferase); 3 vMet1(simplified methionine biosynthesis pathway); 4, vC1 (simplified pathway from 5,10-methylene-tetrahydrofolate to formate); 5, vMet_in (methionine uptake); 6, vMet_prot (methionine incorporated into protein). Other abbreviations are the same as in Figure 1.

The described modifications to the *A. succinogenes* metabolic map are illustrated in Figure 4.4. This new model was used to fit fluxes to the growth condition C data set. The resulting fluxes were, for the most part, very similar to those obtained for growth with 150 mM $NaHCO_3$ using [1-^{13}C]glucose alone (18). Again, OPPP flux is low at ~3%

of the glucose uptake rate, compared with 5%, obtained previously. All product formation rates were similar, relative to the glucose uptake rate. The most significant differences between the two flux maps are the fluxes between PEP, OAA/Mal, and Pyr, which are all dependent on each other. The new flux map shows a C_4-decarboxylating flux (here-on referred to as C_4dec, comprised of both malic enzyme and OAA decarboxylase activities) that is 38% of the glucose uptake rate, compared to 64% obtained previously (18). [1-^{13}C]Glucose alone cannot be used to detect reversible C_4dec flux, but it does produce [3-^{13}C]Ser, which allows for label scrambling from exchange flux between Ser and Gly. To determine if the Ser and Gly pathway modifications affect the determination of the C_4dec flux, we included the reversible vSer and vGly reactions in the original model and ran the fitting algorithm with the data set obtained using [1-^{13}C]glucose alone (18). The optimized fit had an SS_{res} of 182 (compared to 148 obtained previously) and the C_4dec net flux decreased to 41% of the glucose uptake rate, a value similar to that obtained in this study. When vSer exchange flux was set to zero in the new model and used with the growth condition C data, the obtained C_4dec net flux values were between 63% and 81% of the glucose uptake rate (SS_{res} from 355-358). Therefore the modifications to the Ser and Gly pathway may have resulted in an over-estimated C_4dec flux in the previous model. However, even using the new model (Fig. 4.4) C_4dec is still a major catabolic flux in growth condition C.

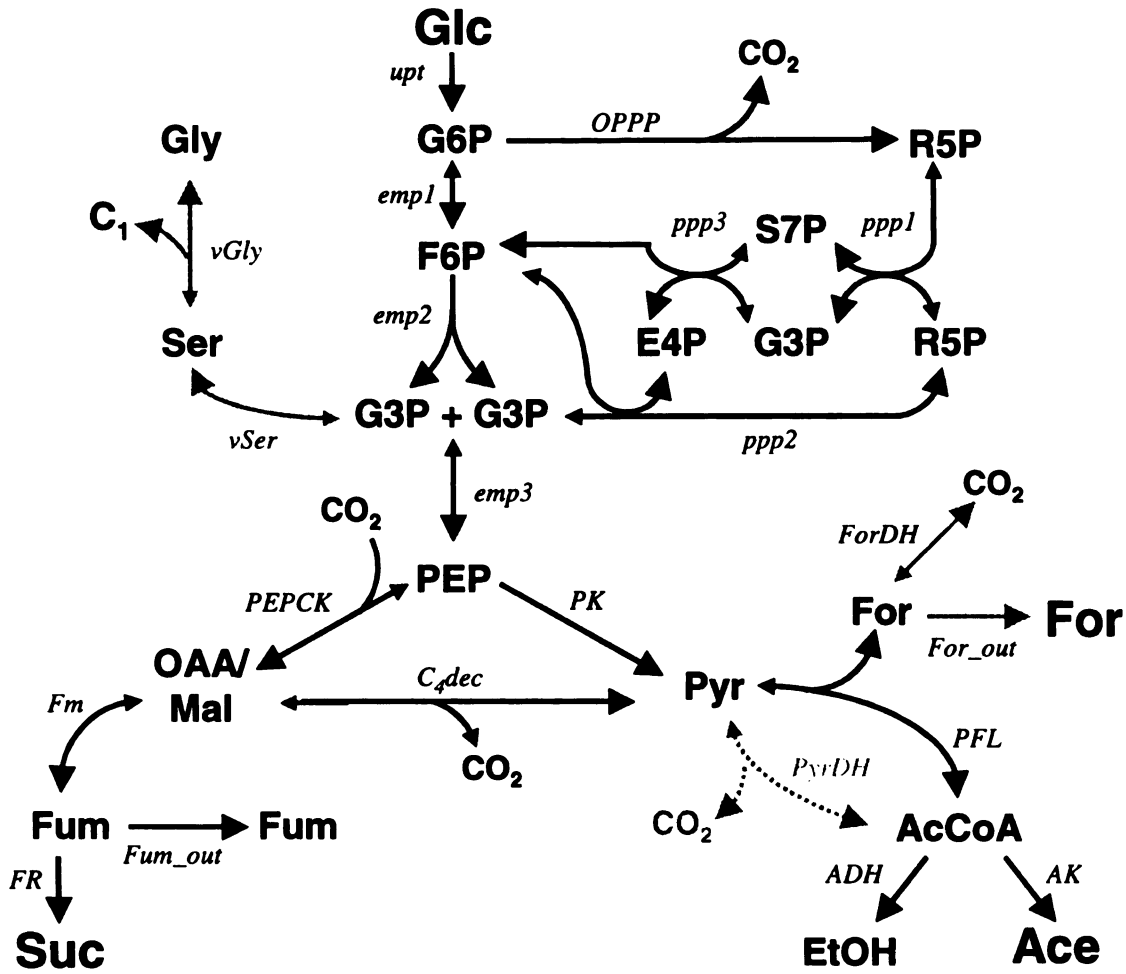

Figure 4.4. Modified metabolic flux model of *A. succinogenes* mixed acid fermentative metabolism. Net flux directions are indicated by an enlarged arrow head. Gray arrows highlight the modifications that were made. PyrDH is shown by dotted arrows to indicate that ForDH replaced it. Most amino acid synthesis pathways are not shown. See Figure 4.3 for more details on the modeling of C_1 metabolism. Reactions: *C_4dec*, OAA decarboxylase and malic enzyme; *For_out*, formate excretion; *Fum_out*, fumarate excretion. Other abbreviations are the same as in Figures 4.1 and 4.3.

4.4.3 Effects of $NaHCO_3$ and H_2 concentrations on metabolic fluxes. CO_2 and reductant were thought to affect fermentation balances through their role as substrates for succinate production in the C_4 pathway (Fig. 4.1) (20, 34). ^{13}C metabolic flux analysis of *A. succinogenes* in a single growth condition suggested that the mechanisms by which CO_2 and reductant affect fermentation balances are more complex (18). To define the effects of CO_2 and reductant on metabolism, we performed ^{13}C-metabolic flux analysis on *A. succinogenes* fermentative metabolism at two different $NaHCO_3$ concentrations in the presence and absence of H_2. Table 4.2 shows the growth parameters for the four growth conditions. Despite product formation rate changes, glucose uptake rates, growth rates, and biomass yields were similar for all conditions. During the experiment, ~ 4% and 10% of the H_2 was estimated to be consumed in conditions B and D, respectively. H_2 oxidation rates were less than succinate formation rates indicating that succinate production was only supported in part by H_2 oxidation (Table 4.2). Specific rates were normalized to the glucose uptake rate and used in *13C-Flux* flux models for each condition. The SS_{res} values for each model were: condition A, 192; condition B, 150; condition C, 233; and condition D, 163. Since all models have 42 degrees of freedom, and all SS_{res} values are >58, none of the models passed the χ^2 test at the 95% confidence interval, a common result for biological systems (39). However, these SS_{res} values are similar to that obtained previously (SS_{res} = 148) for *A. succinogenes* grown with 150 mM $NaHCO_3$ (18). Higher SS_{res} values were expected in this study because: (i) the minimum mass isotopomer standard deviation was set to 1.2% of the mean, compared to 2.6% of the mean used previously (18); and (ii) 197 measurements were used versus 127 previously (18). The estimated fluxes in each growth condition are shown in Table

Conditions			Specific rates (mmol g^{-1} h^{-1})							C. rec (%)[b]	e⁻ rec (%)[b]	μ (hr^{-1})	Y_{XS} ($g\ g^{-1}$)[c]
	$NaHCO_3$ (mM)	H_2	r_{Glc}	r_{Suc}	r_{For}	r_{Ace}	r_{Fum}	r_{EtOH}	r_{H2}[a]				
A	25	-	9.5 ± 0.4	5.8 ± 0.4	6.9 ± 0.4	6.0 ± 0.4	0.030 ± 0.002	2.2 ± 0.2		99 ± 1	106 ± 1	0.41 ± 0.02	0.24 ± 0.00
B	25	+	9.1 ± 0.3	5.9 ± 0.2	7.4 ± 0.2	5.0 ± 0.2	0.018 ± 0.001	2.3 ± 0.1	11.0 ± 0.2	99 ± 2	108 ± 3	0.40 ± 0.01	0.24 ± 0.01
C	100	-	9.4 ± 0.3	7.1 ± 0.2	4.7 ± 0.1	5.6 ± 0.1	0.093 ± 0.003	1.2 ± 0.2		99 ± 2	106 ± 2	0.39 ± 0.01	0.23 ± 0.01
D	100	+	9.4 ± 0.4	7.9 ± 0.4	6.2 ± 0.4	4.4 ± 0.3	0.042 ± 0.003	1.4 ± 0.1	18.7 ± 0.9	98 ± 2	109 ± 2	0.39 ± 0.01	0.23 ± 0.01

Table 4.2. Growth parameters observed for the different growth conditions.

[a] H_2 oxidation rates were estimated from the ratio of electron recoveries between a condition with H_2 (e.g., B) and its control (e.g., A). The percentage of excess electrons was converted into mols of electrons by multiplying the percentage by the electrons in biomass and excreted products.

[b] Carbon and electron recoveries were calculated using an assumed biomass of $CH_2O_{0.5}N_{0.2}$, which is a typical microbial composition (31) and is in agreement with the *A. succinogenes* C:N ratio of $CN_{0.18}$ (18).

[c] Biomass yield during exponential growth (grams of biomass per grams of glucose).

4.3. Unless stated otherwise, all flux descriptions refer to net fluxes. Net flux corresponds to the forward flux minus the reverse flux, and the exchange flux is the remainder (39, 40). Exchange fluxes reflect the reversibility of a reaction. Since all flux values in this study are reported as being positive in the directions indicated in Figure 4.4, an exchange flux is equal to the reverse flux, and a forward flux is the sum of the net and exchange fluxes.

In addition to similar a glucose uptake rate, growth rate, and biomass yield for all conditions (Table 4.2), the glycolytic and OPPP fluxes were also similar (Table 4.3). The one exception is the emp3 exchange flux. Large exchange fluxes (i.e. that for emp3) can generally only be determined within an order of magnitude (40, 41). The flux changes that allow *A. succinogenes* to maintain its growth parameters in the different growth conditions occur downstream of PEP. The effects of $NaHCO_3$ and H_2 on these fluxes are described in detail in the following sections.

$NaHCO_3$ effects. As expected, higher succinate formation rates (FR) and larger C_4:C_3 flux ratios were observed at 100 mM $NaHCO_3$ (C and D) than at 25 mM $NaHCO_3$ (A and B) (Table 4.3). Interestingly, fumarate formation rates were also significantly higher in conditions C and D than in conditions A and B (2-tailed *t*-test, equal variance, $p<0.01$; Table 4.2). Although ~100 times less fumarate is excreted than the major fermentation products, fumarate can be accurately quantified by HPLC because it strongly absorbs at 210 nm. $NaHCO_3$ did not drastically affect the Fm reverse flux, which was approximately proportional to the forward fluxes (i.e., 24% and 28% that of the forward flux rate in conditions A and C, respectively).

PFL flux, the central C_3 pathway flux in this model, is lower in conditions C and D than in conditions A and B, as are C_3 pathway product formation rates (i.e., formate, acetate, and ethanol; Table 4.3). PFL exchange fluxes were also lower in conditions C and D than in conditions A and B. This decreased reverse flux could be due in part to lower formate concentrations in conditions C and D, but it could also be due to lower PFL activity in general, since the reverse flux decreased proportionately to the forward flux, in all conditions. The reverse PFL flux was 72%, 72%, 69%, and 67% that of the forward flux in conditions A, B, C, and D, respectively.

It was previously suggested that the CO_2 concentration affects the flux distribution through the C_4 and C_3 pathways by increasing PEPCK flux (34). Contrary to this hypothesis, PEPCK fluxes are similar at high and low $NaHCO_3$ concentrations (Table 4.3). However, comparing PEPCK fluxes is complicated by large confidence intervals. PEPCK confidence intervals are large because PEPCK flux is dependent on the C_4dec flux, which is not well determined. PEPCK exchange fluxes are also similar in all conditions (32% to 35% that of the forward flux), and they are better determined than the net fluxes. These similar exchange fluxes indicate that the CO_2 concentration at least does not affect PEPCK reversibility. An alternative (or additional) mechanism for CO_2 to affect the fermentation balance is by influencing the amount of flux shunted from the C_4 to the C_3 pathway. The C_4dec flux is lower in conditions C and D than in conditions A and B, but again, comparisons are complicated by large confidence intervals (Table 4.3). Unlike C_4dec net fluxes, C_4dec exchange fluxes were relatively well determined. C_4dec

Fig. 4 Reactions	Fluxes (Percent of glucose uptake rate ± 90% confidence intervals) [a]			
	A	B	C	D
	25 mM HCO_3^-	25 mM HCO_3^- + H_2	100 mM HCO_3^-	100 mM HCO_3^- + H_2
Glycolysis and OPPP				
upt	100.0 ± 4.0	100.0 ± 2.5	100.0 ± 2.3	100.0 ± 4.2
OPPP	2.6 ± 1.3	6.9 ± 5.9	2.7 ± 1.2	3.7 ± 1.2
emp1	95.6 ± 4.0	91.4 ± 5.5	95.7 ± 2.5	94.6 ± 4.2
emp2	94.5 ± 3.9	93.4 ± 2.6	94.8 ± 2.3	94.3 ± 4.1
emp3	182.0 ± 7.8	181.5 ± 4.7	182.8 ± 4.6	182 ± 8.3
emp3	*1143 (616, 4606)*	*1926 (1024, 10185)*	*970 (641, 1827)*	*457 (261, 1118)*
C_3 and C_4 pathway				
PyrK	64.0 ± 21.0	51.1 ± 47.2	60.9 ± 15.1	64.0 ± 30.1
PFL	101.8 ± 6.6	97.9 ± 3.9	87.2 ± 3.6	78.0 ± 5.6
PFL	*268 (249, 288)*	*250 (232, 270)*	*190 (179, 203)*	*158 (145, 172)*
ForDH	33.1 ± 9.0	21.3 ± 4.7	40.5 ± 4.1	16.8 ± 9.4
ForDH	*30 (22, 39)*	*11 (7, 15)*	*29 (21, 37)*	*22 (16, 29)*
For_out	72.0 ± 6.2	79.8 ± 2.6	49.8 ± 2.0	64.4 ± 7.6
ADH	27.0 ± 3.5	32.0 ± 2.5	16.2 ± 2.5	18.6 ± 2.8
AK	62.1 ± 5.6	53.6 ± 2.7	58.5 ± 2.2	46.9 ± 4.7
PEPCK	115.8 ± 21.6	128.2 ± 47.2	119.8 ± 15.4	115.9 ± 30.6
PEPCK	*55 (44, 67)*	*69 (58, 82)*	*61 (52, 71)*	*58 (47, 71)*
Fm	59.9 ± 5.5	63.5 ± 2.7	75.6 ± 3.1	83.9 ± 7.0
Fm	*19 (17, 21)*	*15 (12, 17)*	*30 (28, 32)*	*17 (15, 20)*
Fum_out	0.30 ± 0.03	0.20 ± 0.01	0.99 ± 0.07	0.50 ± 0.05
FR	59.6 ± 5.5	63.3 ± 2.7	74.6 ± 3.1	83.5 ± 7.0
Other fluxes				
C_4dec	49.6 ± 21.3	58.4 ± 47.2	38.0 ± 15.2	25.6 ± 30.2
C_4dec	*105 (92, 121)*	*124 (96, 160)*	*170 (154, 187)*	*158 (130, 192)*
vSer	*67 (48, 91)*	*83 (47, 141)*	*69 (52, 89)*	*75 (58, 95)*
vGly	*12 (9, 15)*	*14 (8, 21)*	*14 (11, 17)*	*16 (13, 20)*
CO_2 uptake	24.0 ± 3.6	35.0 ± 9.9	32.1 ± 2.6	63.1 ± 14.9
H_2 oxidation		30.2 ± 0.4		50.0 ± 2.4
ATP[b]	67.2 ± 30.9	61.3 ± 52.0	79.1 ± 25.5	73.5 ± 37.7
NADH[c]	53.4 ± 13.1	23.7 ± 7.9	52.3 ± 8.2	5.5 ± 14.9
Ratios				
ForDH:PFL	0.33	0.22	0.46	0.22
ADH:AK	0.43	0.60	0.28	0.40
C_4 (Fm):C_3 (PFL)	0.59	0.65	0.87	1.08

Table 4.3. Effect of $NaHCO_3$ concentration and H_2 on net and exchange fluxes.

[a] Exchange fluxes are italicized with unsymmetrical 90% confidence intervals in parentheses. Confidence intervals were calculated as described (41). Anabolic fluxes out of metabolic intermediates were within the following ranges for all conditions: G6P, 1.7-1.8; F6P, 0.5; R5P, 2.8-3.1; E4P, 0.9; G3P, 6.1-6.2; PEP, 2.2; Pyr, 11.6-11.8; AcCoA, 12.4-12.7; and OAA, 6.2-6.4. Net fluxes involved in Ser and Gly syntheses (see Fig. 3) were similar in all conditions (data not shown). Non-oxidative pentose phosphate pathway net and exchange fluxes are not shown.

[b] Equals the net ATP flux produced by central metabolic fluxes minus the estimated ATP flux for biosynthesis and transport (~200% of the glucose uptake rate; based on the *A. succinogenes* biomass composition [18]).

[c] Includes the estimated NADH flux from biosynthesis (~11.6% of the glucose uptake rate). Net NADH is assumed to be converted to NADPH by transhydrogenase or by malate dehydrogenase coupled with malic enzyme. The estimated NADPH flux for biosynthesis was ~57.2% of the glucose uptake rate.

exchange fluxes were higher in conditions C and D than in conditions A and B, indicating that high $NaHCO_3$ concentrations stimulate reverse C_4dec flux. In vitro OAA decarboxylase activity levels were similar in all conditions (Table 4.4). Higher malic enzyme activity levels were detected in extracts from cells grown with 100 mM $NaHCO_3$ (C and D) than in those of cells grown with 25 mM $NaHCO_3$ (A and B) (Table 4.4). This malic enzyme activity trend correlates with the reverse C_4dec flux, suggesting that malic enzyme may be involved in pyruvate carboxylation.

Enzyme assayed	*n*	Specific activity (nmol mg protein^{-1} min^{-1})			
		A 25 mM $NaHCO_3$	**B** 25 mM $NaHCO_3 + H_2$	**C** 100 mM $NaHCO_3$	**D** 100 mM $NaHCO_3 + H_2$
Transhydrogenase	4	61 ± 5	64 ± 2[c]	62 ± 7	54 ± 4[a,b]
Pyruvate dehydrogenase	3	16 ± 0	14 ± 0[c]	18 ± 1[a]	15 ± 1[b]
Formate dehydrogenase	3	36 ± 4	37 ± 5	27 ± 4[a]	31 ± 4[d,e]
Hydrogenase	3	400 ± 60	290 ± 120[c]	350 ± 50	600 ± 60[a,b]
Malic enzyme	6	460 ± 20	430 ± 20[b]	520 ± 40[a]	460 ± 30[a,b]
OAA decarboxylase	3	1060 ± 110	990 ± 150	980 ± 110	970 ± 80

Table 4.4. Enzyme activities in cell extracts of *A. succinogenes* grown in different $NaHCO_3$ and H_2 conditions

[a] Statistically different from identical N_2/H_2 condition at 25 mM $NaHCO_3$ (2-tailed *t*-test, equal variance, $p < 0.01$).

[b] Statistically different from identical $NaHCO_3$ condition without H_2 (2-tailed *t*-test, equal variance, $p < 0.01$).

[c] Statistically different from identical $NaHCO_3$ condition without H_2 (2-tailed *t*-test, equal variance, $p < 0.05$)

[d] Statistically different from identical N_2/H_2 condition with 25 mM $NaHCO_3$ (2-tailed *t*-test, equal variance, $p < 0.1$).

[e] Statistically different from identical $NaHCO_3$ condition without H_2 (2-tailed *t*-test, equal variance, $p < 0.1$).

Regardless of the mechanism by which CO_2 affects flux distribution between the C_4 and the C_3 pathways, the increased succinate production at high CO_2 concentrations

requires reductant. Glycolytic flux and biomass yields were nearly identical in all growth conditions (Tables 4.2 and 4.3). Therefore, the extra reductant needed for succinate production in condition C was not generated by an increased glycolytic flux or by the C_4 pathway out-competing anabolism for reducing power. The main reductant sources for biomass and high succinate producing rate in condition C are in the C_3 pathway. In condition C, the ethanol-producing ADH flux decreased ~ 40% from that in condition A. Producing 1 ethanol from 1 AcCoA requires 2 NADH (Fig. 4.1). The flux through ForDH (and/or PyrDH) was higher in condition C than in condition A. Enzyme activity data suggest that the increased succinate producing flux in condition 3 most likely coincides with increased flux through PyrDH rather than through ForDH (Table 4.4). ForDH activity may actually be inhibited by high CO_2 conditions (Table 4.4). The combination of decreased NADH consumption and increased NADH production in the C_3 pathway meets the high electron-demand in condition 3. In fact, the net NADH production by the C_3 pathway increases just enough to compensate succinate production increase from conditions A to C, as illustrated by the similar NADH net fluxes in conditions A and C (Table 4.3). As noted previously (18), this excess NADH is likely converted to NADPH by transhydrogenase, an especially important process for biosynthesis given the low OPPP flux. Similar transhydrogenase activity levels were detected in extracts of cells grown in conditions A and C (Table 4.4). The similar net NADH fluxes in conditions 1 and 3 demonstrate the flexibility of the C_3 pathway dehydrogenase fluxes for generating enough reducing power to maintain a biomass yield in conditions with different reductant demands for succinate production.

H_2 effects. For H_2 to affect metabolism, it must be oxidized. Hydrogenase activity was previously reported in *A. succinogenes* cell extracts (23, 24). It was also detected in this study, and activity levels were higher in extracts of cells grown under H_2, at least in high CO_2 conditions (Table 4.4). Interestingly, hydrogenase activity was present even in cells grown in the absence of H_2.

In agreement with previous observations (34), growing *A. succinogenes* with H_2 increased succinate production rates (FR; Table 4.3), but more so at high $NaHCO_3$ concentrations (C vs. D). At both $NaHCO_3$ concentrations, the presence of H_2 decreased fumarate formation rates significantly (2-tailed *t*-test, equal variance, $p<0.01$; Fum_out; Table 4.3). Decreased fumarate excretion suggests that reductant availability is limiting fumarate reductase flux, and that this limitation can be relieved, at least in part, by supplying H_2. While adding H_2 generally increased the net Fm flux, it also decreased the Fm exchange flux. Adding H_2 decreased the reverse:forward Fm flux ratio from 0.24 and 0.28 (conditions A and C, respectively) to 0.19 and 0.17 (conditions B and D, respectively). Reverse C_4 pathway flux generates the isotopomers used to quantify the net C_4dec flux. Correspondingly, the conditions exhibiting the least Fm exchange flux (i.e., conditions B and D) have the largest C_4dec confidence intervals. Thus, the perturbations used to study the changes in flux distribution may also affect our ability to quantify a metabolic flux of central interest.

H_2 was hypothesized to affect flux distributions through its role as a substrate for the C_4 pathway (34). Recently, the C_3 pathway was shown to be important for generating reductant, thus leading to an additional hypothesis that H_2 can decrease C_3 pathway flux by serving as an alternative reductant source (18). Supporting the new hypothesis, there is

less central C_3-pathway flux, PFL flux, in condition D than in condition C (Table 4.3). Acetate formation rates decreased in the presence of H_2, but ethanol and formate formation rates increased (Table 4.2). H_2 is expected to stimulate ethanol production because ethanol production requires reductant (Fig. 4.1). At both $NaHCO_3$ conditions, the presence of H_2 increased the ethanol:acetate flux ratio 1.4 fold, due to the combined decreased flux to acetate and increased flux to ethanol (Table 4.3).

More than causing a decrease in the total C_3 pathway flux (at least at 100 mM $NaHCO_3$), H_2 partially alleviated the need for NADH production by ForDH and/or PyrDH. The net NADH flux is lower in the presence of H_2, and even approaches zero in condition D (Table 4.3). The decrease in ForDH flux in response to H_2 is greater than the decrease in PFL flux, as reflected by the ForDH:PFL ratios (Table 4.3), resulting in higher formate formation rates in conditions B and D than in conditions A and C. In agreement with the observed fluxes, in vitro PyrDH activity was lower in extracts of cells grown under H_2 (Table 4.4). In contrast, ForDH activity was similar in conditions 1 and 2 (25 mM $NaHCO_3$), and may have increased in the presence of H_2 at 100 mM $NaHCO_3$. With a high succinate production rate and low CO_2 production rate (i.e., through ForDH/PyrDH and C_4dec fluxes) in condition D, the net CO_2 consumption rate is 2.6 times greater than in condition A.

ForDH exchange fluxes were lower in cultures grown under H_2, and unlike what was observed with PFL, the reverse:forward ForDH flux ratio varied widely from 0.34 (condition B) to 0.57 (condition D). While $NaHCO_3$ concentration did not affect ForDH exchange fluxes in the absence of H_2 (conditions A and C), the ForDH exchange flux as much lower in condition B than in condition D. What causes these exchange flux

variations is not obvious, but could be due to disproportional effects of $NaHCO_3$ and H_2 concentrations on ForDH and PyrDH.

Malic enzyme flux is also a potentially important source of NADPH (18). According to this hypothesis, supplying H_2 could alleviate the need for malic enzyme flux if H_2 oxidation can be coupled to NADPH production. C_4dec fluxes, which contain malic enzyme flux, are best compared at high $NaHCO_3$ concentrations, however confidence intervals remain large. In these conditions (100 mM $NaHCO_3$), supplying H_2 decreased the C_4dec flux by 33% (Table 4.3). Correspondingly, in vitro malic enzyme activity was less in extracts of cells grown with H_2 at both $NaHCO_3$ concentrations (Table 4.4). The effects of H_2 on C_4dec exchange fluxes were less pronounced than those of $NaHCO_3$. Assuming that the net C_4dec fluxes are accurate, H_2 had no observable affect on the C_4dec exchange flux at 25 mM $NaHCO_3$, with the reverse flux being 68% that of the forward flux in both conditions A and B. The same effect is observed at 100 mM $NaHCO_3$, where the reverse C_4dec flux is 82% and 86% that of the forward flux in conditions C and D, respectively.

4.5 DISCUSSION

This study has made several contributions to the understanding of *A. succinogenes* fermentative metabolism: (i), the use [1-^{13}C]glucose and [U-^{13}C]glucose together brought new insights into the reversibility of some pathways; (ii), pyruvate was shown to participate as a node in the flux distribution between the C_3 and C_4 pathways; (iii) decreasing the C_4-decarboxylating flux was suggested as a new mechanism for how $NaHCO_3$ affects flux distribution; (iv) H_2 was shown to affect C_3 pathway fluxes in addition to C_4 pathway fluxes; and (v) C_3 pathway dehydrogenase fluxes were shown to be flexible to meet different reductant demands.

Product isotopomers generated from [U-^{13}C]glucose metabolism provided information on exchange fluxes (e.g., PFL exchange flux) that could not be quantified by using [1-^{13}C]glucose alone. Reversible PFL flux in *A. succinogenes* is supported by the fact that a fluoroacetate-resistant *A. succinogenes* mutant has no PFL activity (23). While fluoroacetate itself is not toxic, metabolic products of fluoroacetate, such as fluoropyruvate, are toxic. Since the fluoroacetate-resistant strain has no detectable PFL activity, it suggests that PFL is required for fluoroacetate toxicity, likely by generating fluoropyruvate through reverse flux. Reverse PFL flux is likely influenced by internal, rather than external, formate concentrations. Formate consumption was not detected, and fermentation balances were not affected, when formate was added to *A. succinogenes* cultures (34). The lowest SS_{res} values were obtained when PyrDH or ForDH were allowed to be reversible. Although usually considered to be an enzyme of aerobic metabolism, PyrDH activity was detected in extracts of *A. succinogenes* grown anaerobically (Table 4.4), and PyrDH is expressed in closely related, anaerobically

grown, *Haemophilus influenzae* (26). Based on reaction thermodynamics, ForDH ($\Delta G^{\circ\prime}$ = -15 kJ/mol) is more likely to be reversible than PyrDH ($\Delta G^{\circ\prime}$ = -33 kJ/mol). However, high CO_2 concentrations could affect PyrDH reversibility. Isocitrate dehydrogenase is commonly considered to be a unidirectional enzyme, having a $\Delta G^{\circ\prime}$ of -30 kJ/mol. However, in the high CO_2 environment of developing *Brassica napus* embryos, mitochondrial isocitrate dehydrogenase carries a net reverse flux (30). While PyrDH reversibility cannot be assessed from the current data set, it could be assessed if the same methods were applied to an *A. succinogenes* PFL-knockout strain.

The C_4-decarboxylating flux, composed of OAA decarboxylase and malic enzyme, was also shown to be reversible. The *A. succinogenes* OAA decarboxylase (AsucDRAFT_1557-1559), is believed to use the energy from OAA decarboxylation ($\Delta G^{\circ\prime}$= -29 kJ/mol) to transport Na^+ across the cytoplasmic membrane, as has been shown for the homologous *Klebsiella aerogenes* enzyme (5). The high $\Delta G^{\circ\prime}$ value suggests that OAA decarboxylase is unlikely to be reversible. However, inverted vesicles containing *K. aerogenes* OAA decarboxylase accumulated slightly more $^{22}Na^+$ in the presence of pyruvate, HCO_3^-, and $^{22}NaCl$ than with $^{22}NaCl$ alone (5). Malic enzyme typically functions as a malate decarboxylating enzyme because it has high Km values for pyruvate (~5-15mM) and CO_2 (~13-25 mM) (www.brenda.uni-koeln.de/index.php4, Accessed Nov. 2006). However, the pyruvate carboxylating direction is thermodynamically favored under standard conditions ($\Delta G^{\circ\prime}$= –8.7 kJ/mol). In fact, net pyruvate-carboxylating flux through malic enzyme has been shown in a succinate-producing *E. coli* mutant (32). While reverse flux through OAA decarboxylase cannot be ruled out, malic enzyme is likely responsible the majority of the observed C_4dec

exchange flux. The $NaHCO_3$ concentrations used in this study are near or above the reported Km values for malic enzyme. Furthermore, the C_4dec reverse flux values are higher at 100 mM $NaHCO_3$ than at 25mM $NaHCO_3$ (Table 4.3), indicating that the reverse flux is influenced by the CO_2 concentration. Potentially, malic enzymes's pyruvate carboxylating ability could be harnessed to create a net flux to malate in *A. succinogenes*, as was done for *E. coli* (32). However, observing this flux is not possible if there is significant flux through OAA decarboxylase.

Reverse flux from Pyr to malate and possibly OAA has several implications. First, it indicates that, in addition to PEP, OAA, and malate, pyruvate can also serve as a node for flux distribution between the C_3 and the C_4 pathways. Second, reverse flux from Pyr to OAA/malate increased in response to elevated $NaHCO_3$ concentrations relative to the forward flux, resulting in a decreased C_4dec net flux. Thus, CO_2 concentration may affect succinate production by determining the amount of flux shunted to the C_3 pathway. This CO_2 effect on the C_4-decarboxylating flux may work alone or in conjuction with the CO_2 effect on flux through PEPCK, which has been the prevailing hypothesis for CO_2's effects on succinate production to date.

While PEPCK flux was similar in all conditions, it could not be concluded that CO_2 does not affect PEPCK flux due to large confidence intervals (Table 4.3). Elevated CO_2 concentrations are thought to increase PEPCK flux by overcoming limiting CO_2 substrate concentrations and allowing PEPCK to out compete pyruvate kinase and the glucose:PEP phosphotransferase system for PEP. There is evidence in other bacterial systems suggesting that CO_2 affects succinate production through PEPCK flux. In succinate-producing *Anaerobiospirillum succiniciproducens*, PEPCK activity and

succinate production both increase in response to increased CO_2 concentration and decreased pH (27). However, *A. succinogenes* fermentation balances are relatively constant at different pH values and in vitro PEPCK activities are similar in extracts of cells grown with different CO_2 concentrations (34). In an *E. coli ppc*$^-$ mutant, overexpressing *A. succinogenes* PEPCK improves succinate yields, indicating that PEPCK flux is important for succinate production (13). Furthermore, *E. coli* succinate production was enhanced by overexpressing *E. coli* PEPCK, but only at high $NaHCO_3$ concentrations (15). While these *E. coli* studies did not address C_4-decarboxylating fluxes, they suggest that the CO_2 concentration affects succinate production through its effect on PEPCK flux. It would be interesting to test whether overexpressing PEPCK in *A. succinogenes* would increase flux to succinate at high $NaHCO_3$ concentrations or whether C_4 dearboxylating fluxes would counter the effect of increased PEPCK flux. Interestingly, the effects of H_2 on metabolic fluxes were more pronounced at 100 mM $NaHCO_3$ than at 25mM $NaHCO_3$ (Table 4.3). This trend suggests that sufficient CO_2 is a prerequisite for H_2 to stimulate succinate production, either by increasing PEPCK flux or by decreasing the C_4-decarboxylating flux, to make OAA and malate available for reduction to succinate.

Malic enzyme flux is a potentially important NADPH source in *A. succinogenes* (18). C_4dec fluxes and in vitro malic enzyme activity levels suggest that supplying H_2 partially alleviates the need for NADPH-producing malic enzyme flux, assuming that malic enzyme carries a net decarboxylating flux (Tables 4.4 and 4.3). However, the C_4dec confidence interval in condition D was very large and the C_4-decarboxylating flux decreased and the pyruvate carboxylating flux increased in response to elevated $NaHCO_3$

concentrations, despite the increased reductant demands by the accompanied increased succinate formation rate (A vs. C; Table 4.3). This decreased C_4dec flux suggests that transhydrogenase is more important for NADPH production than malic enzyme. However, even in the presence of H_2 optimized fittings suggest significant C_4dec flux. In vitro OAA decarboxylase activity was similar for all conditions (Table 4.4). While this enzyme is required for growth on citrate by other bacteria (3, 5, 42), its role during glucose fermentation is an intriguing finding that warrants further investigation, especially given its ability to divert flux away from succinate. OAA decarboxylase could be important for Na^+-linked energetics (6, 11). In closely related *A. actinomycetemcomitans*, OAA decarboxylase is involved in Na^+-dependent glutamate transport and drug efflux (11). A Na^+ gradient could also be involved in fumarate and succinate transport, as was shown for *Wolinella succinogenes* (33). OAA decarboxylase could also be important for maintaining osmostic balance by pumping Na^+ out of the cell. Since the C_4dec flux is composed of both malic enzyme and OAA decarboxylase, a high OAA decarboxylase flux could mask a net pyruvate carboxylating flux by malic enzyme. Modifying Na^+ concentrations in the growth medium could be an insightful perturbation to understand OAA decarboxylase's role in *A. succinogenes* and gage the contributions of OAA decarboxylase and malic enzyme to the total C_4-decarboxylating flux.

C_3 pathway dehydrogenases are important for generating NADPH in *A. succinogenes* when coupled with transhydrogenase (18). Alcohol dehydrogenase and ForDH/PyrDH fluxes responded to changes in $NaHCO_3$ concentration to maintain a net NADH flux that is likely coupled to NADPH production through transhydrogenase (Table 4.3). Therefore, flux distribution in the C_3 pathway is important for maintaining

redox balance and appears to be one the most flexible aspects of *A. succinogenes* fermentative metabolism. Ultimately, metabolic engineering of *A. succinogenes* metabolism aims to minimize C_3 pathway flux and maximize C_4 pathway flux. Given the importance of PyrDH, ForDH, and possibly malic enzyme for generating reducing power, it will be important to have an alternative reductant source if C_3 pathway flux is disrupted. Supplying H_2 partially alleviated the need for NADH generation in the C_3 pathway (Table 4.3). Supplying H_2 also decreased the fumarate formation rate, suggesting that fumarate reductase flux is limited by reductant availability. Although H_2 is an attractive electron source, H_2 oxidation is likely coupled to menaquinone reduction, since H_2 oxidation drove fumarate reduction in purified *A. succinogenes* membranes (24). Thus, although H_2 oxidation can supply reduced menaquinone for succinate production, C_3 pathway flux will remain important for biomass production if H_2 oxidation cannot be coupled to NADH or NADPH production. *A. succinogenes* can grow by fumarate respiration with H_2, a process that involves hydrogenase 2, rather than hydrogenase 1, in *E. coli* (16, 21) and the *A. succinogenes* hydrogenase operon is most similar to hydrogenase 2. Therefore, it may be necessary to overexpress a ferredoxin reducing hydrogenase to couple H_2 oxidation to NADH production and relieve the need for NADH production by C_3 pathway. Estimated H_2 oxidation rates were less than succinate formation rates in both conditions B and D, indicating that reducing power for fumarate reductase was still generated to a large extent from carbon-based reactions. Therefore it may also be worthwhile to increasing the H_2 oxidation rate by hydrogenase 2. The H_2 oxidation rate may increase naturally if ForDH and PyrDH are knocked out, or overxpressing hydrogenase 2 may be required. Alternatively, H_2 oxidation rates may

increase naturally if *A. succinogenes* is grown in bioreactors with higher dissolved H_2 concentrations. Of course, H_2 use in an industrial succinate fermentation will require an inexpensive source of H_2, perhaps from another bio-based process.

The effects of the $NaHCO_3$ and H_2 concentrations on in vitro enzyme activities, although sometimes significant, were relatively subtle in this study (<1.5 fold differences; Table 4.4). In no case was an enzyme activity or a metabolic flux shut down in response to a $NaHCO_3$ or H_2 perturbation. Perhaps most interesting was the observation of high hydrogenase activity in extracts from cells grown without H_2 (Table 4.4). Citrate lyase was detected in cell extracts of *A. succinogenes* grown in fermentative and fumarate respiration conditions (34). This activity was also surprising because citrate was not provided and citrate and isocitrate have never been observed in *A. succinogenes* culture supernatants (McKinlay et al. unpublished data). *Pasteurellaceae*, the family to which *A. succinogenes* belongs, are host-associated organisms, with few free-living examples. Even *Pasteurella multocida*, which can be isolated from water and soil, may associate with amoebae to survive in these environments (12). It is possible that the natural *A. succinogenes* ecology is restricted to the rumen, where CO_2 and H_2 are major products of other microbial fermentations. Without drastic changes to its environment, *A. succinogenes* may have evolved to have a relatively uniform metabolism.

This study has illustrated the complexities of *A. succinogenes* metabolism, with exchange fluxes in, and between, the C_3 and C_4 pathways, and four nodes involved in the distribution of flux between the two pathways. The methods presented in this paper, when combined with genetic engineering, indicate that *A. succinogenes* could be used to address issues of in vivo malic enzyme, OAA decarboxylase and pyruvate dehydrogenase

reversibility. This study also illustrated how *A. succinogenes* maintains a fixed growth rate and biomass yield in different growth conditions by modulating its metabolic fluxes. When the $NaHCO_3$ concentration is raised from 25 mM to 100 mM, the C_4dec reverse flux increases, and the PEPCK flux may also increase. The resulting increase in C_4 pathway flux, must be channeled to succinate for the cell to compensate energetically for the decreased flux to acetate (fumarate reductase is linked to an electron transport chain). The reductant demand from the increased succinate formation rate is met by increasing ForDH and PyrDH fluxes and decreasing the flux to ethanol. When H_2 is supplied, PyrDH and ForDH fluxes decrease in response to the higher reductant availability. These discoveries will be important to consider when engineering *A. succinogenes* metabolism. They should also be of general interest for the study of microbial metabolism.

4.6 REFERENCES

1. Brown, R. 2005. Housing sector boosts maleic anhydride, p. 24, Chemical Market Reporter, vol. 267.

2. Caspi, R., H. Foerster, C. A. Fulcher, R. Hopkinson, J. Ingraham, P. Kaipa, M. Krummenacker, S. Paley, J. Pick, S. Y. Rhee, C. Tissier, P. Zhang, and P. D. Karp. 2006. MetaCyc: a multiorganism database of metabolic pathways and enzymes. Nucleic Acids Res. 34:D511-D516.

3. Dahinden, P., Y. Auchli, T. Granjon, M. Taralczak, M. Wild, and P. Dimroth. 2005. Oxaloacetate decarboxylase of *Vibrio cholerae*: purification, characterization, and expression of the genes in *Escherichia coli*. Arch. Microbiol. 183:121-129.

4. Dauner, M., and U. Sauer. 2000. GC-MS analysis of amino acids rapidly provides rich information for isotopomer balancing. Biotechnol. Prog. 16:642-649.

5. Dimroth, P. 1980. A new sodium-transport system energized by the decarboxylation of oxaloacetate. FEBS Lett. 122:234-236.

6. Dimroth, P., and B. Schink. 1998. Energy conservation in the decarboxylation of dicarboxylic acids by fermenting bacteria. Arch. Microbiol. 170:69-77.

7. Fischer, E., and U. Sauer. 2003. Metabolic flux profiling of *Escherichia coli* mutants in central carbon metabolism using GC-MS. Eur. J. Biochem. 270:880-891.

8. Goldberg, R. N., Y. B. Tewari, and T. N. Bhat. 2004. Thermodynamics of enzyme-catalyzed reactions - a database for quantitative biochemistry. Bioinformatics 20:2874-2877.

9. Guettler, M. V., M. K. Jain, and D. Rumler. 1996. Method for making succinic acid, bacterial variants for use in the process, and methods for obtaining variants. U.S. patent 5,573,931.

10. Guettler, M. V., M. K. Jain, and B. K. Soni. 1996. Process for making succinic acid, microorganisms for use in the process and methods of obtaining the microorganisms. U.S. patent 5,504,004.

11. Hase, C. C., N. D. Fedorova, M. Y. Galperin, and P. A. Dibrov. 2001. Sodium ion cycle in bacterial pathogens: evidence from cross-genome comparisons. Microbiol. Mol. Biol. Rev. 65:353-370.

12. Hundt, M. J., and C. G. Ruffolo. 2005. Interaction of *Pasteurella multocida* with free-living amoebae. Appl. Environ. Microbiol. 71:5485 - 5464.

13. Kim, P., M. Laivenieks, C. Vieille, and J. G. Zeikus. 2004. Effect of overexpression of *Actinobacillus succinogenes* phosphoenolpyruvate carboxykinase on succinate production in *Escherichia coli*. Appl. Environ. Microbiol. 70:1238-1241.

14. Kroger, A., S. Biel, J. Simon, R. Gross, G. Unden, and C. R. D. Lancaster. 2002. Fumarate respiration of *Wolinella succinogenes*: enzymology, energetics and coupling mechanism. Biochim. Biophys. Acta. 1553:23-28.

15. Kwon, Y. D., S. Y. Lee, and P. Kim. 2006. Influence of gluconeogenic phosphoenolpyruvate carboxykinase (PCK) expression on succinic acid fermentation in *Escherichia coli* under high bicarbonate condition. J. Microbiol. Biotechnol. 16:1448-1452.

16. Laurinavichene, T. V., N. A. Zorin, and A. A. Tsygankov. 2002. Effect of redox potential on activity of hydrogenase 1 and hydrogenase 2 in *Escherichia coli*. Arch. Microbiol. 178:437-442.

17. Lee, W. N., L. O. Byerley, E. A. Bergner, and J. Edmond. 1991. Mass isotopomer analysis: theoretical and practical considerations. Biol. Mass. Spectrom. 20:451-458.

18. McKinlay, J. B., Y. Shachar-Hill, J. G. Zeikus, and C. Vieille. 2006. Determining *Actinobacillus succinogenes* metabolic pathways and fluxes by NMR and GC-MS analyses of ^{13}C-labeled metabolic product isotopomers. Metab. Eng. doi:10.1016/j.ymben.2006.10.006.

19. McKinlay, J. B., and J. G. Zeikus. 2004. Extracellular iron reduction is mediated in part by neutral red and hydrogenase in *Escherichia coli*. Appl. Environ. Microbiol. 70:3467-3474.

20. McKinlay, J. B., J. G. Zeikus, and C. Vieille. 2005. Insights into *Actinobacillus succinogenes* fermentative metabolism in a chemically defined growth medium. Appl. Environ. Microbiol. 71:6651-6656.

21. Menon, N. K., C. Y. Chatelus, M. Dervartanian, J. C. Wendt, K. T. Shanmugam, H. D. Peck, Jr., and A. E. Przybyla. 1994. Cloning, sequencing, and mutational analysis of the hyb operon encoding Escherichia coli hydrogenase 2. J Bacteriol 176:4416-23.

22. Millar, A. H., C. Knorpp, C. J. Leaver, and S. A. Hill. 1998. Plant mitochondrial pyruvate dehydrogenase complex: purification and identification of catalytic components in potato. Biochem. J. 334:571-576.

23. Park, D. H., M. Laivenieks, M. V. Guettler, M. K. Jain, and J. G. Zeikus. 1999. Microbial utilization of electrically reduced neutral red as the sole electron donor for growth and metabolite production. Appl. Environ. Microbiol. 65:2912-2917.

24. Park, D. H., and J. G. Zeikus. 1999. Utilization of electrically reduced neutral red by *Actinobacillus succinogenes*: physiological function of neutral red in membrane-driven fumarate reduction and energy conservation. J. Bacteriol. 181:2403-2410.

25. Paster, M., J. L. Pellegrino, and T. M. Carole. 2003. Industrial bioproducts: today and tomorrow. Energetics, Incorporated.

26. Raghunathan, A., N. , D. Price, M. Y. Galperin, K. S. Makarova, S. Purvine, A. F. Picone, T. Cherny, T. Xie, T. J. Reilly, J. R. Munson, R. E. Tyler, B. J. Akerley, A. L. Smith, B. O. Palsson, and E. Kolker. 2004. *In silico* metabolic model and protein expression of *Haemophilus influenzae* strain Rd KW20 in rich medium. Omics 8:25-41.

27. Samuelov, N. S., R. Lamed, S. Lowe, and J. G. Zeikus. 1991. Influence of CO_2-HCO_3 levels and pH on growth, succinate production, and enzyme activities of *Anaerobiospirillum succiniciproducens*. Appl. Environ. Microbiol. 57:3013-3019.

28. Sauer, U., F. Canonaco, S. Heri, A. Perrenoud, and E. Fischer. 2004. The soluble and membrane-bound transhydrogenases UdhA and PntAB have divergent functions in NADPH metabolism of *Escherichia coli*. J. Biol. Chem. 279:6613-6619.

29. Sauer, U., D. R. Lasko, J. Fiaux, M. Hochuli, R. Glaser, T. Szyperski, K. Wüthrich, and J. E. Bailey. 1999. Metabolic flux ratio analysis of genetic and environmental modulations of *Escherichia coli* central carbon metabolism. J. Bacteriol. 181:6679-6688.

30. Schwender, J., Y. Schachar-Hill, and J. Ohlrogge. 2006. Mitochondrial metabolism in developing embryos of *Brassica napus*. J. Biol. Chem. 281:34040-34047.

31. Stephanopoulos, G., A. A. Aristidou, and J. Nielsen. 1998. Metabolic Engineering: Principles and Methodologies. Academic Press, London.

32. Stols, L., and M. I. Donnelly. 1997. Production of succinic acid through overexpression of NAD^+-dependent malic enzyme in an *Escherichia coli* mutant. Appl. Environ. Microbiol. 63:2695-2701.

33. Ullmann, R., R. Gross, J. Simon, G. Unden, and A. Kroger. 2000. Transport of C_4-dicarboxylates in *Wolinella succinogenes*. J. Bacteriol. 182:5757-5764.

34. van der Werf, M. J., M. V. Guettler, M. K. Jain, and J. G. Zeikus. 1997. Environmental and physiological factors affecting the succinate product ratio during carbohydrate fermentation by *Actinobacillus sp.* 130Z. Arch. Microbiol. 167:332-342.

35. Vemuri, G. N., M. A. Eiteman, and E. Altman. 2002. Succinate production in dual-phase *Escherichia coli* fermentations depends on the time of transition from aerobic to anaerobic conditions. J. Ind. Microbiol. Biotechnol. 28:325-332.

36. Venning, J. D., and J. B. Jackson. 1999. A shift in the equilibrium constant at the catalytic site of proton-translocating transhydrogenase: significance for a 'binding-change' mechanism. Biochem. J. 341:329-337.

37. Wahl, S. A., M. Dauner, and W. Wiechert. 2004. New tools for mass isotopomer data evaluation in ^{13}C flux analysis: mass isotope correction, data consistency checking, and precursor relationships. Biotechnol. Bioeng. 85:259-268.

38. Widdel, F., and F. Bak. 1992. Gram-negative mesophilic sulfate-reducing bacteria., p. 3358-3378. *In* A. Balows, H. G. Truper, M. Dworkin, W. Harder, and K. H. Schleifer (ed.), The Prokaryotes, 2nd ed, vol. 4. Springer-Verlag, New York.

39. Wiechert, W., and A. A. de Graaf. 1997. Bidirectional reaction steps in metabolic networks: I. Modeling and simulation of carbon isotope labeling experiments. Biotechnol. Bioeng. 55:101-117.

40. Wiechert, W., M. Mollney, S. Petersen, and A. A. de Graaf. 2001. A universal framework for ^{13}C metabolic flux analysis. Metab. Eng. 3:265-283.

41. Wiechert, W., C. Siefke, A. A. de Graaf, and A. Marx. 1997. Bidirectional reaction steps in metabolic networks: II. Flux estimation and statistical analysis. Biotechnol. Bioeng. 55:118-135.

42. Woehlke, G., and P. Dimroth. 1994. Anaerobic growth of *Salmonella typhimurium* on L(+)- and D(-)-tartrate involves an oxaloacetate decarboxylase Na^+ pump. Arch. Microbiol. 162:233-237.

43. Zeikus, J. G., M. K. Jain, and P. Elankovan. 1999. Biotechnology of succinic acid production and markets for derived industrial products. Appl. Environ. Microbiol. 51:545-552.

Chapter 5.

Genomic perspective on the potential of *Actinobacillus succinogenes* for industrial succinate production

5.1 ABSTRACT

Actinobacillus succinogenes naturally converts sugars and CO_2 into high concentrations of succinic acid as part of a mixed-acid fermentation. Efforts are ongoing to maximize carbon flux to the succinate-producing pathway to generate industrial amounts of succinate. Described herein is the 2.04 Mb *A. succinogenes* draft genome sequence in the context of *A. succinogenes'* potential for: (i) chemical production, (ii) genetic engineering, and (iii) non-pathogenicity. The genome sequence indicates that *A. succinogenes* lacks a complete tricarboxylic acid cycle as well as the glyoxylate pathway. Nine potential dicarboxylate transporters and numerous sugar uptake and degradation pathways were identified. The genome sequence contains 1,458 DNA uptake signal sequence repeats and a nearly complete set of natural competence proteins, suggesting that *A. succinogenes* is, or was, capable of natural transformation. The genomes of *A. succinogenes* and its closest-known relative, *Mannheimia succiniciproducens*, were analyzed for the presence of *Pasteurellaceae* virulence factors. Neither bacterium appears to have virulence traits such as toxin production, sialic acid and choline incorporation into lipopolysaccharide, and uptake of haemoglobin and transferin as iron sources.

5.2 INTRODUCTION

Actinobacillus succinogenes is a gram negative capnophilic bacterium that was isolated from cow-rumen as part of a search for succinate-producing bacteria (26). Succinate is an important metabolic intermediate in the rumen, where several rumen bacteria obtain energy by decarboxylating succinate to propionate, which then serves as a nutrient for the ruminant (51, 56, 64). Succinate is used as a specialty chemical in food, agriculture, and pharmaceutical industries, but it has a much greater potential value for making bulk chemicals that are currently petrochemical based (73). Thus bio-based succinate production is both economically and environmentally attractive, with the potential to replace a large crude oil-based industry with one based on renewable resources. A further environmental benefit is that succinate production via fermentation uses CO_2, a greenhouse gas, as substrate.

A. succinogenes is one of the best succinate producers ever described but it also produces high formate and acetate concentrations. Flux distribution between succinate and alternative fermentation products is affected by environmental conditions. For example, increasing the available CO_2 and reductant (e.g., by supplying H_2 or by using more-reduced carbon sources than glucose) shifts the fermentation toward higher succinate yields (40, 63). However, adjusting the environmental conditions is not enough to achieve a homosuccinate fermentation, thus genetic engineering is required. *A. succinogenes'* metabolic engineering will benefit from an understanding of the enzymes and mechanisms controlling flux distribution. The *A. succinogenes* genome sequence is an important step in defining *A. succinogenes* metabolic pathways. The genome sequence

also opens the door to functional genomic approaches to address the metabolic and regulatory mechanisms controlling flux distribution during succinate production.

A. succinogenes belongs to the *Pasteurellaceae* family, which includes the genera *Actinobacillus, Haemophilus, Mannheimia*, and *Pasteurella*. Aside from *A. succinogenes*, twelve *Pasteurellaceae* genome sequences are publicly available (www.ncbi.nlm.nih.gov/genomes/MICROBES/microbial_taxtree.html; Accessed Nov. 2006). *A. succinogenes* and its close relative, *M. succiniciproducens*, collectively referred to as 'succinogens' in this chapter, are studied for their industrially attractive metabolisms. Other *Pasteurellaceae* are studied for their pathogenic traits. It will be important to confirm non-pathogenicity in the succinogens before they are used on an industrial scale. Without any reports of disease from *A. succinogenes* or *M. succiniciproducens*, their genome sequences are a logical starting point to assess their potential for non-pathogenicity. If *A. succinogenes* is non-pathogenic, comparing its genome sequence with those of pathogenic *Pasteurellaceae* could lead to further insights into *Pasteurellaceae* virulence mechanisms.

Here we present the first detailed analysis of the *A. succinogenes* draft genome sequence. Special attention is given to genes encoding metabolic enzymes from a biotechnological perspective. We also present possible opportunities for developing genetic tools based on characteristics of the genome sequence. Finally, the *A. succinogenes* and *M. succiniciproducens* genome sequences are examined for known *Pasteurellaceae* virulence genes.

5.3 MATERIALS AND METHODS

5.3.1 Source strain and genomic DNA purification. *A. succinogenes* type strain 130Z (ATCC 55618) was obtained from the American Type Culture Collection (Manassas, VA). *A. succinogenes* was grown in 100 ml of tryptic soy glucose (TSG; Becton Dickinson, Sparks, MD) broth with 25 mM $NaHCO_3$ in a 160-ml anaerobic serum vial at 37°C. The culture was harvested in log phase (~7.7 x 10^{10} cells) and washed twice in 45 ml of phosphate buffer containing (g/l): 15.5 K_2HPO_4, 8.5 $NaH_2PO_4*H_2O$, and 1 g/l NaCl. Genomic DNA was purified using a Qiagen genomic tip protocol with a Qiagen maxiprep column (Valencia, CA). Briefly, the cell pellet was lysed in 10 ml B1 buffer at 37°C for 1 h, then 4 ml B2 buffer was added, and the solution was incubated at 50°C for 1 h. The lysate was vortexed, then applied to a maxiprep column that was pre-equilibrated with QBT buffer. The column was washed twice with 15 ml QC buffer, then DNA was eluted with QF buffer (~30 ml) until the eluent was no longer viscous. Isopropanol (0.7 vol at 25°C) was added to the eluent to precipitate DNA. DNA was then pelleted at 10,000 rpm for 15 min, washed with 70% ethanol, dried under a stream of N_2, and dissolved in 10 mM Tris-HCl (pH 8.0) containing 1 mM EDTA.

5.3.2 Sequencing and automated annotation. Sequencing was performed by the Department of Energy Joint Genome Institute. Automated annotation was performed by the Oak Ridge National Laboratory. Open reading frames (ORFs) were identified using three gene caller programs: Critica, Generation, and Glimmer. Translated ORFs were subjected to an automated basic local alignment search tool (BLAST) for proteins (3) against Genbank's non-redundant database. The translated ORFs were also subjected to

searches against KEGG, InterPro (incorporating Pfam, PROSITE, PRINTS, ProDom, SmartHMM, and TIGRFam,), and Clusters of Orthologous Groups of proteins (COGs).

5.3.3 Manual annotation. BLAST alignments were examined to assess the correctness of the start codon. DNA sequences upstream of each ORF were examined for a ribosomal binding site (at least 3 nt of AAGGAGG, 5-10 nt upstream of the start codon) using the web Artemis tool. To assign product names to each ORF, results from BLAST, HMM searches (i.e., PFAM and TIGRFAM), and domain and motif searches were considered. Most importantly, efforts were made to find a citation of biological function for a homologous gene. If a translated ORF was at least 75% identical to a protein of known function, or if it belonged to a TIGRFAM equivalog, it was given the associated product name. If a translated ORFH was less than 75% identical to a protein of known function, the product name was modified as follows: 60-75% identity, putative product; 40-64% identity, probable product; 25-39% identity, possible product. If a translated ORF was at least 60% identical to a protein of unknown function, it was named a conserved hypothetical protein. If there was no adequate alignment with any protein, the translated ORF was named a hypothetical protein.

Uptake signal sequence (USS) 9 nt cores were counted and their surrounding sequences reported using our perl script, 'USS.pl.' The output was pasted into a Microsoft Excel (Redmond, WA) spreadsheet to calculate the frequency of each nucleotide occurring at each position, upstream and downstream of the USS core. The accuracy of USS.pl was confirmed by the fact that it identified the same number of USS in other *Pasteurellaceae* genome sequences as already reported (4).

5.4 RESULTS AND DISCUSSION

5.4.1 General features of the draft genome sequence. The *A. succinogenes* draft genome sequence is 2.04 Mb, spread over 117 contigs, making it one of the smallest industrially relevant genome sequences. The GC content is 44.9%. There is at least one prophage, which is comprised of 32 ORFs spanning 26 kb and possibly extending beyond the end of contig 166. Automatic annotation identified 1,884 ORFs, but failed to identify more ORFs, usually due to truncated sequences and poor sequence quality at the ends of contigs. Of the 1,884 ORFs, 91% were most similar to other proteobacterial genes, with 1,241 (66%) being most similar to *M. succiniciproducens* genes.

5.4.2 Metabolic reconstruction. *A. succinogenes* metabolism is of central interest to understand the pathways involved in succinate production. The central metabolic enzymes identified in the draft genome sequence are summarized in Table 5.1 and Figure 5.1. *A. succinogenes* metabolism has primarily been studied using fermentation balances, in vitro enzyme assays, and ^{13}C-metabolic flux analyses with glucose as the main carbon source (40, 41, 63). These studies indicated that glucose is catabolized to phosphoenolpyruvate (PEP) via glycolysis, with little involvement of the pentose phosphate pathway. PEP is then converted into fermentation products via the C_3 and C_4 pathways, with malic enzyme and OAA decarboxylase forming shunts between these pathways. All glycolytic and pentose phosphate pathway enzymes are encoded in the genome sequence. Two possible homologs to the Entner-Doudoroff enzyme 2-keto-3-deoxy-6-phosphogluconate aldolase were identified (AsucDRAFT_0727 and 1070). A

ORF(s) [a]	Function	E.C. #	Figure 5.1[b]
854-856	PEP:glucose phosphotransferase	2.7.1.69	1
1877	Glucokinase	2.7.1.2	2
146	Glucose-6-phosphate dehydrogenase	1.1.1.49	3
145	6-Phosphogluconolactonase	2.1.1.31	4
141	6-Phosphogluconate dehydrogenase	1.1.1.44	5
1544	Ribose-5-phosphate isomerase A	5.3.1.6	6
139	Ribulose-5-phosphate 4-epimerase	5.1.3.4	7
1787	Transketolase	2.2.1.1	8
413	Transaldolase	2.2.1.2	9
256	G6P isomerase	5.3.1.9	10
1282	6-Phosphofructokinase	2.7.1.11	11
458-9	Fructose-bisphosphate aldolase	4.1.2.13	12
899, 924, 1291	Triose phosphate isomerase	5.3.1.1	13
307	Glyceraldehyde-3-phosphate dehydrogenase	1.2.1.12	14
460	Phosphoglycerate kinase	2.7.2.3	15
373	Phosphoglycerate mutase	3.6.1.7	16
1030	Enolase	4.2.1.11	17
232	Pyruvate kinase	2.7.1.40	18
1849	Lactate dehydrogenase	1.1.1.28	19
C 126, ORF 1	Pyruvate formate-lyase	2.3.1.54	20
1404-1408	Formate dehydrogenase	1.2.1.2	21
1	Pyruvate dehydrogenase E1	1.2.4.1	22
2	Pyruvate dehydrogenase E2	2.3.1.12	22
3	Pyruvate dehydrogenase E3	1.8.1.4	22
405	Acetaldehyde dehydrogenase	1.2.1.10	23
405	Alcohol dehydrogenase	1.1.1.1	24
1768	Predicted aldehyde dehydrogenase	1.2.1.3	25
NA	Phosphotransacetylase	2.3.1.8	
NA	Acetate kinase	2.7.2.1	
1662	Predicted acylphosphatase	3.6.1.7	26
NA	Phosphoenolpyruvate carboxykinase	4.1.1.49	
1557-9	Oxaloacetate decarboxylase	4.1.1.3	27
NA	Malic enzyme	1.1.1.40	
1103	Malate dehydrogenase	1.1.1.37	28
1823	Fumarase	4.2.1.2	29
210-214	Fumarate reductase	1.3.99.1	30
889a,b	Succinyl-CoA synthetase	6.2.1.5	31
891	α-Ketoglutarate dehydrogenase E1	1.2.4.2	32
890	α-Ketoglutarate dehydrogenase E2	2.3.1.61	32
3	α-Ketoglutarate dehydrogenase E3	1.8.1.4	32
NA	Isocitrate dehydrogenase	1.1.1.42	
1809	Aconitase	4.2.1.3	33
388-90	Citrate lyase	4.1.3.6	34
1869	Possible aspartate aminotransferase	2.6.1.1	35
898	Aspartate aminotransferase	2.6.1.1	35
716	Aspartate ammonia-lyase	4.3.1.1	36
1393-7	Hydrogenase	1.12.7.2	37
393	Carbonic anhydrase	4.2.1.1	38
847-8	Transhydrogenase	1.6.1.2	39

Table 5.1. Central metabolic enzymes expected and identified in the draft genome sequence. [a] NA: no ORF found for the function. [b] Corresponding reaction in Figure 5.1.

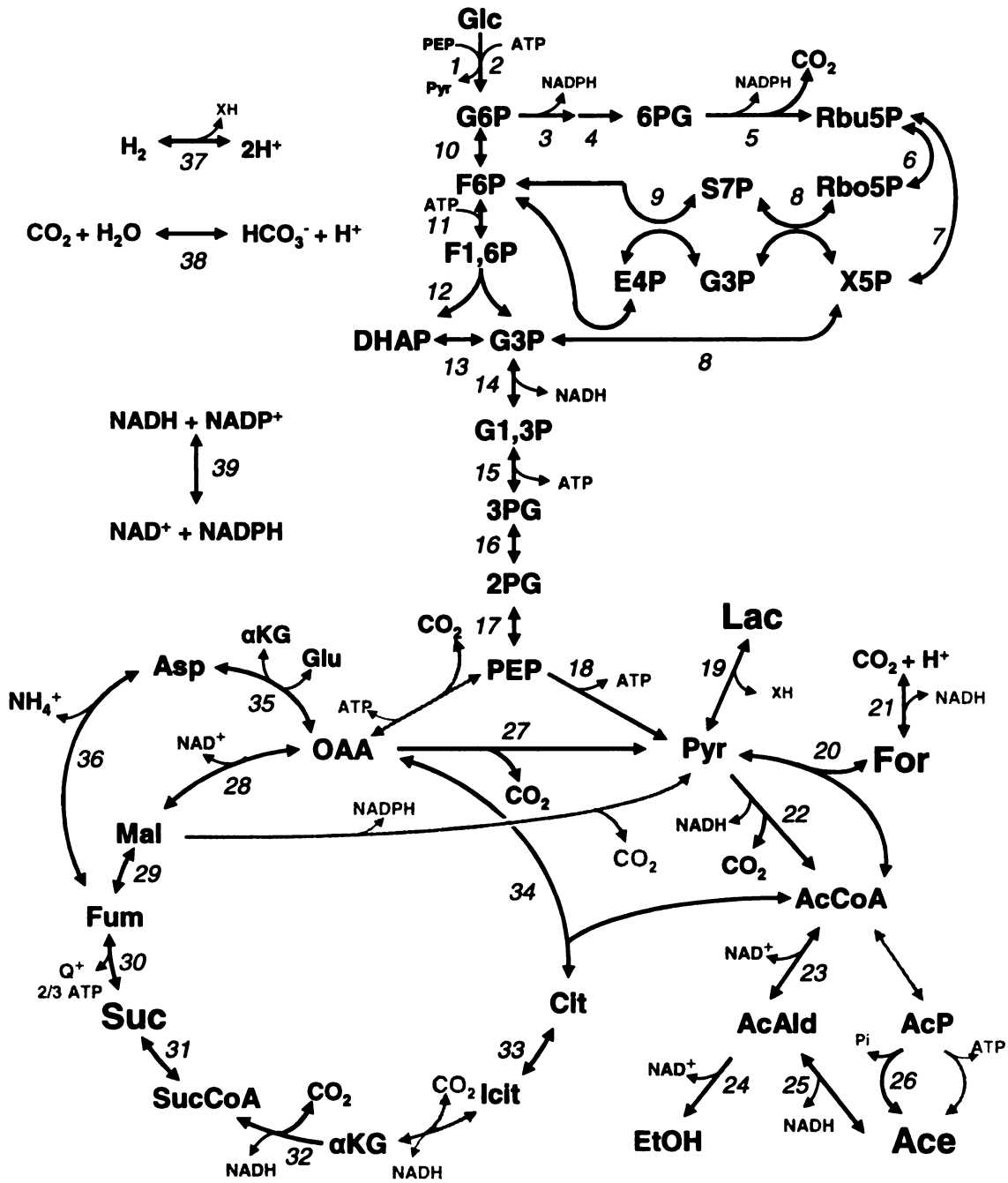

Figure 5.1. Central metabolism based on identified enzymes in the draft genome sequence. See Table 5.1 for reaction names. XH, unknown reduced cofactor. Q^+, menaquinone. Gray arrows indicate enzymes that were expected but not identified in the draft genome sequence. Numbers in italics refer to enzymes listed in Table 5.1.

possible homolog to the other Entner-Doudoroff enzyme, phosphogluconate dehydratase, was also identified (AsucDRAFT_0513). It is unlikely that this ORF encodes phosphogluconate dehydratase, though, because this ORF is located in an isoleucine synthesis operon and, correspondingly, is an equivalog for dihydroxy-acid dehydratase (EC 4.2.1.9).

Most of the expected C_3 and C_4 pathway proteins were identified, including pyruvate dehydrogenase and formate dehydrogenase, which ^{13}C-flux analyses indicated were important for generating reducing power for succinate production and anabolism (Chapters 3 and 4). A few genes were truncated at the ends of contigs including those encoding pyruvate formate-lyase (PFL) and succinyl-CoA synthetase. PEP carboxykinase (PEPCK) and malic enzyme were not identified. *A. succinogenes pckA* (encodes PEPCK) was previously cloned and sequenced (35), and cell extracts contain high levels of malic enzyme activity (Chapters 3 and 4). Both enzymes are expected to be identified in the complete genome sequence. Acetaldehyde dehydrogenase and alcohol dehydrogenase activities are likely due to a single multifunctional alcohol dehydrogenase (33) encoded by Asuc_DRAFT 305. Asuc_DRAFT 1306 is related to the *H. influenzae* and *M. succiniciproducens* ORFs annotated as alcohol dehydrogenase, however while this enzyme is classified as a class III alcohol dehydrogenase it functions as a formaldehyde dehydrogenase (E.C. 1.1.1.284) (37). Phosphotransacetylase and acetate kinase were not identified, but a conserved hypothetical protein with predicted acylphosphotransferase activity was identified. Phosphotransacetylase and acetate kinase are expected to be identified in the complete genome sequence, since their activities are detected in *A. succinogenes* cell extracts (63). However, a conserved hypothetical protein with predicted

aldehyde dehydrogenase activity may form an alternative route from acetyl-CoA to acetate without the formation of ATP (Fig. 5.1). All genes encoding TCA-cycle enzymes were identified with the exceptions of isocitrate dehydrogenase and citrate synthase. Isocitrate dehydrogenase activity was not detected in extracts of *A. succinogenes* grown under fermentative conditions (Chapter 3). Rather than citrate synthase, a citrate lyase gene was identified and is discussed in greater detail below. The α-ketoglutarate (αKG) dehydrogenase lipoamide dehydrogenase (E3) subunit is shared with pyruvate dehydrogenase. It is encoded in the pyruvate dehydrogenase operon, as it is in *E. coli* (60). It was reported that *A. succinogenes* glutamate auxotrophy was due to the absence or inactivity of TCA cycle-associated enzymes on either side of αKG. While αKG dehydrogenase and succinyl-CoA synthetase connect succinate and αKG, αKG dehydrogenase is generally considered to be a unidirectional enzyme going from αKG to succinyl-CoA. The reductive-TCA cycle counterpart to αKG dehydrogenase, αKG ferredoxin oxidoreductase, was not found in the draft genome sequence. As expected, the glyoxylate pathway enzymes, isocitrate lyase and malate synthase, were not found.

The draft genome sequence was also examined for gluconeogenic enzymes. Even though Asuc_DRAFT 855 is 26% identical to the *E. coli* PEP synthase, it is more likely a PEP phosphotransferase system (PTS) component, as it is part of a PTS operon and is 76% identical to an *E. coli* PTS protein. There are three known types of fructose-1,6-bisphosphatases. The draft genome sequence does not encode Type I or III fructose-1,6-bisphosphatases, but Asuc_DRAFT 1718 is 69% identical to *E. coli* fructose-1,6-bisphosphatase II. This gene is found in other *Pasteurellaceae* including *M. succiniciproducens*. In *E. coli* this type II enzyme is not the main gluconeogenic enzyme.

When the type I enzyme was knocked out in *E. coli*, the type II enzyme supported growth in conditions requiring gluconeogenesis only when it was overexpressed (21). Even if PEP synthase is not found in the complete genome sequence, *A. succinogenes* could generate a gluconeogenic flux by using PEPCK and fructose-1,6-bisphosphatase II. Gluconeogenesis is expected to be functional in *A. succinogenes*, because *A. succinogenes* can grow by anaerobic respiration using H_2 or electrically reduced neutral red as an electron source and using fumarate or malate as an electron acceptor/carbon source (45, 46, 63). Assuming rapid equilibrium between G3P and dihydroxyacetone phosphate, ^{13}C-metabolic flux analysis indicates that there is little gluconeogenic flux to glucose in *A. succinogenes* during mixed acid fermentation on glucose (Chapter 3).

Succinate production by *A. succinogenes* involves carboxylation of PEP and pyruvate, and fermentation balances are affected by CO_2 concentrations. No PEP-carboxylating enzymes were identified in the draft genome sequence, and *pckA* had been previously cloned and characterized (35). An ORF encoding pyruvate carboxylase was identified. Carbonic anhydrase, which interconverts CO_2 and HCO_3^- was identified. Since *A. succinogenes* succinate production is affected by CO_2 and HCO_3^- concentrations, carbonic anhydrase could be an important enzyme for succinate production. *A. succinogenes'* fermentation balances are constant within a pH range that affects the fermentation balance of the succinate-producing bacterium *Anaerobiospirillum succiniciproducens* (52, 63). Carbonic anhydrase may be important for making CO_2 or HCO_3^- available at different pH values. *A. succinogenes* will also utilize H_2 as a source of electrons for succinate production. A membrane-bound hydrogenase and a membrane-bound transhydrogenase were identified in the genome sequence (Table 5.1).

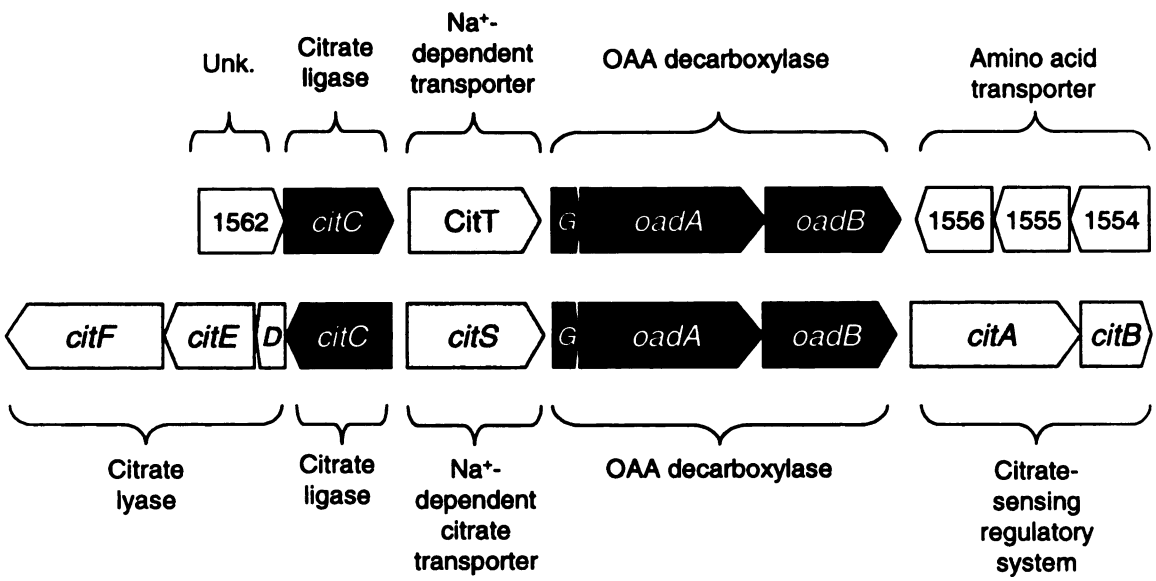

Figure 5.2. Physical map of the OAA decarboxylase operon region in the *A. succinogenes* (top) and *K. pneumoniae* (bottom) genomes. Genes in black highlight similarities between the genome topologies. Genes in gray highlight possible similarities in function (e.g., citrate fermentation) but differ between genomes by position or sequence. White genes are thought to have unrelated functions.

A. succinogenes OAA decarboxylase is also a Na^+-pump. Na^+-dependent OAA decarboxylase activity was detected in *A. succinogenes* extracts (Chapters 3 and 4). This enzyme is required for growth on citrate by other bacteria (18, 20, 71), but its role during *A. succinogenes* mixed acid fermentations is unclear. During citrate fermentation in other bacterial systems, citrate is taken up by a Na^+-dependent transporter, cleaved to OAA and acetyl-CoA by citrate lyase, then the Na^+-dependent OAA decarboxylase produces pyruvate for gluconeogenesis. The genes encoding the enzymes responsible for citrate fermentation in *Klebsiella pneumoniae* are arranged in an operon, with citrate lyase and ligase encoded furthest upstream, followed by the Na^+-dependent citrate transporter, OAA decarboxylase, and a two-component regulatory system involved in regulating citrate metabolism (57) (Fig. 5.2). Interestingly, *A. succinogenes* OAA decarboxylase is

encoded immediately downstream from a Na^+ symporter and a citrate ligase gene, but no two-component regulatory system is encoded downstream of OAA decarboxylase (Fig. 5.2). The citrate lyase genes are encoded on a separate contig. Citrate ligase acetylates and activates citrate lyase in an ATP-dependent reaction. The citrate ligase near the OAA decarboxylase operon was the only citrate ligase found in the draft genome sequence. This gene is in the opposite orientation to that in the *K. pneumoniae* genome (Fig. 5.2). Because this citrate ligase is most similar to that from *Fusobacterium nucleatum* (57% identitical), and because it is only 37% identical to the most closely related *Pasteurellaceae* homolog (*H. ducreyi*), it was likely acquired by horizontal gene transfer. The *A. succinogenes* Na^+-dependent symporter is not necessarily citrate-specific since it is not homologous to that in *K. pneumoniae*. Still, it belongs to the COG for di- and tri-carboxylic acid transport, CitT. Interestingly, OAA decarboxylase and citrate lyase activities were detected in extracts of *A. succinogenes* that were grown with glucose or with fumarate and H_2 (63). None of these conditions contained citrate and neither citrate nor isocitrate have been detected in *A. succinogenes* supernatants (data not shown). With some evidence of horizontal gene transfer and the lack of a two-component regulatory system, it is possible that OAA decarboxylase and citrate lyase are constitutively expressed in *A. succinogenes*. Both OAA decarboxylase and citrate lyases are most closely related to other *Pasteurellaceae* genes, suggesting that their activities during glucose fermentation and fumarate respiration are not unique to *A. succinogenes*.

A potential alternative route from OAA to fumarate was identified involving aspartate aminotransferase and aspartate ammonia-lyase (Fig. 5.1). While *M. succiniciproducens* also encodes aspartate aminotransferase and aspartate ammonia-

lyase, knocking out *fumC*, encoding fumarase, prevented growth in anaerobic conditions. Furthermore, aspartate ammonia-lyase activity was barely detectable in cell extracts from *A. succinogenes* grown under fermentative conditions (63). These observations suggest that this alternative route is not active under fermentative conditions.

A. succinogenes has never been reported to produce lactate, unlike its succinate-producing counterpart *M. succiniciproducens*. Surprisingly, an *A. succinogenes* lactate dehydrogenase was found that is 60% identical to the *E. coli* enzyme (1.1.1.28) that couples lactate oxidation to the transport of amino acids and sugars (7). To test whether *A. succinogenes* lactate dehydrogenase is active under anaerobic conditions, *A. succinogenes* was grown in AM3 with 100 mM $NaHCO_3$, 50 mM glucose, and 25 mM D,L-lactate. No lactate consumption was observed (data not shown).

As a producer of the dicarboxylate, succinate, it is interesting to note that the *A. succinogenes* draft genome sequence may encode at least nine anaerobic dicarboxylate transporters (Table 5.2). The closest *A. succinogenes* homolog to *E. coli*'s aerobic dicarboxylate transporter, DctA, is Asuc_DRAFT 6 (24% identical). Seven of the anaerobic transporters are similar to the tripartite ATP-independent periplasmic transporters (T.C. 2.A.56) encoded by *dctPQM* (32). These transporters have been characterized in *Rhodobacter capsulatus* and *Wolinella succinogenes* for their roles during fumarate respiration, where fumarate is transported by proton symport (24, 62). The other three anaerobic dicarboxylate transporters are related to DcuA, B, and C (T.C. 2.A.13). These transporters have been characterized during fumarate respiration by bacteria such as *E. coli* and *W. succinogenes* (59, 62, 75). They operate by exchanging an intracellular dicarboxylate (e.g., succinate) for an extracellular dicarboxylate (e.g.,

Asuc_DRAFT ORF#	Dicarboxylate transporter
901	Possible TRAP C4-dicarboxylate transporter, large permease component, DctM
902	Conserved hypothetical protein (TRAP, small permease component, DctQ)
903	Possible TRAP C4-dicarboxylate transporter solute receptor, DctP
1074	Possible TRAP C4-dicarboxylate transporter, large permease component, DctM
1075	Conserved hypothetical protein (TRAP, small permease component, DctQ)
1076	Possible TRAP C4-dicarboxylate transporter solute receptor, DctP
170	Possible TRAP C4-dicarboxylate transporter solute receptor, DctP
171	Possible TRAP C4-dicarboxylate transporter solute receptor, DctP
172	Possible TRAP C4-dicarboxylate transporter, large permease component, DctM
173	Conserved hypothetical protein (TRAP, small permease component, DctQ)
238	Possible TRAP C4-dicarboxylate transporter, large permease component, DctM
239	Possible TRAP C4-dicarboxylate transporter, small permease component, DctQ
240	Possible TRAP C4-dicarboxylate transporter solute receptor, DctP
721	Possible TRAP C4-dicarboxylate transporter solute receptor, DctP
722	Possible TRAP C4-dicarboxylate transporter, small permease component, DctQ
723	Possible TRAP C4-dicarboxylate transporter, large permease component, DctM
733	Possible TRAP C4-dicarboxylate transporter, large permease component, DctM
734	Conserved hypothetical protein (TRAP, small permease component, DctQ)
735	Possible TRAP C4-dicarboxylate transporter solute receptor, DctP
1737	Possible TRAP C4-dicarboxylate transporter, large permease component, DctM
717	Probable anaerobic C4-dicarboxylate transporter DcuB or DcuA
125	Putative anaerobic C4-dicarboxylate transporter DcuB
166b	Possible anaerobic C4-dicarboxylate transporter DcuC

Table 5.2. Dicarboxylate transporters identified in the draft genome sequence. TRAP: tripartite ATP-independent periplasmic.

fumarate, malate, or aspartate). DcuA and B may also transport Na^+ in symport with the dicarboxylates to avoid dissipating the proton motive force (62). DcuC may have preferential succinate efflux activity, since a *dcuC*$^-$ *E. coli* strain had increased dicarboxylate exchange and fumarate uptake activities (74). Glucose did not repress *dcuC* expression, suggesting that DcuC plays a role in succinate excretion during *E. coli* mixed acid fermentations (74). A microarray study examining *H. influenzae* gene expression

changes that occur as it becomes competent suggested that DcuA and B are important for *Pasteurellaceae* fermentation or fumarate respiration (50). In this study, 151 genes showed > 4-fold increase in transcript levels as *H. infleunzae* became competent, including transcripts for the C_4 pathway enzymes aspartate ammonia-lyase, malate dehydrogenase, fumarase, fumarate reductase, and a single dicarboxylate transporter. This *H. influenzae* transporter is 84% and 44% identical to the DcuB-type transporters, Asuc_DRAFT 717 and 125, respectively. *A. succinogenes dcuA*, *B*, and *C* are therefore attractive genes to investigate the importance of dicarboxylate transport during fumarate respiration and succinate fermentation.

A. succinogenes grows on a variety of industrially-relevant sugars including glucose, fructose, xylose, arabinose, and sucrose (26). Figure 5.3 and Table 5.3 summarize the sugar uptake and degradation pathways that were identified in the draft genome sequence. PTS systems were identified for glucose, fructose, mannose, and sorbitol, but biochemical testing is required to confirm their specificities. *A. succinogenes* produces acid from β-glucosides, including amygdalin, aesulin, arbutin, cellobiose, gentiobiose, and salicin (26). A β-glucoside PTS was identified but it is not clear whether this single transporter transports all β- glucosides. Galactose, maltose, arabinose, ribose, and xylose are taken up by ATP-dependent transporters. Xylose can also be transported by a H^+-symport mechanism. H^+-symport transporters were also identified for lactate, gluconate, and idonate. Operons for some transporters (e.g., for arabinose, maltose, ribose, xylose, and lactose or sucrose) include regulatory proteins, suggesting that uptake of these sugars is regulated (Table 5.3). Transporters were not found for sucrose, mannitol, or arabitol, which *A. succinogenes* can use, nor were some sugar degradation

enzymes (Fig. 5.3). These enzymes may be identified in the complete genome sequence and some transporters may transport multiple different sugars.

Asuc_DRAFT ORF #	Function	E.C. or T.C. #	Figure 5.3[a]
1833-4, 1667	Putative ATP-dependent galactoside transporter	3.A.1.2.3	1
1693	Galactokinase	2.7.1.6	2
1694	Galactose-1-phosphate uridylyltransferase	2.7.7.12	3
1229	Probable lactose permease	2.A.1.5.1	4
1228	Possible β-galactosidase	3.2.1.23	5
1230	Probable sucrose operon repressor (LacI?)		
1571,7	Probable α-amylase	3.2.1.1	
1578	Probable maltoporin		6
1572-6,9	Putative ATP-dependent maltose transporter	3.A.1.1.1	7
1568	Amylomaltase	2.4.1.25	8
1569	Probable maltodextrin phosphorylase	2.4.1.1	9
1877	Possible glucokinase	2.7.1.2	10
1570	Probable maltose regulon transcriptional regulator		
1050	Possible L-idonate or gluconate transport protein	2.A.8.1.2	11
1368	Possible L-idonate or gluconate transport protein	2.A.8.1.2	12
1048	Probable L-idonate 5-dehydrogenase	1.1.1.-	13
1049	Putative gluconate 5-dehydrogenase	1.1.1.69	14
1047	Probable gluconokinase	2.7.1.12	15
936-938	Putative high affinity ATP-dependent L-arabinose transporter	3.A.1.2.2	16
941	Probable L-arabinose isomerase	5.3.1.4	17
940	Conserved hypothetical protein (possible ribulokinase)	2.7.1.17	18
939	Probable arabinose operon regulatory protein		
308-311	Putative high affinity ATP-dependent ribose transporter	3.A.1.2.1	19
312	Probable ribokinase	2.7.1.15	20
313	Probable ribose operon repressor protein		
943	Probable low affinity D-xylose-proton symporter	2.A.1.1.3	21
944-946	Probable high affinity ATP-dependent xylose transporter	3.A.1.2.4	22
947	Putative xylose isomerase	5.3.1.5	23
948	Xylulose kinase	2.7.1.17	24
942	Putative xylose operon regulatory protein		
409-410, 53	Possible fructose-specific PTS	4.A.2.1.1	25
54	Probable 1-phosphofructokinase	2.7.1.56	26
46-48	Probable glucitol/sorbitol-specific PTS	4.A.4.1.1	27
44,45	Putative sorbitol-6-phosphate 2-dehydrogenase	1.1.1.140	28
273-275	Putative mannose-specific PTS	4.A.6.1.1	29
277	Mannose-6-phosphate isomerase, class I	5.3.1.8	30
730	Possible mannitol 2-dehydrogenase	1.1.1.67	31
1503	Probable ATP-dependent fructokinase	2.7.1.4	32
1504	Possible sucrose hydrolase	3.2.1.26	33
876	Probable β-glucoside-specific PTS, IIABC component	4.A.1.2.2	34
878	Probable 6-phospho-β-glucosidase	3.2.1.86	35

Table 5.3. *A. succinogenes* ORFs encoding uptake and degradation pathways for sugars other than glucose. [a] Corresponding reaction in Figure 5.3.

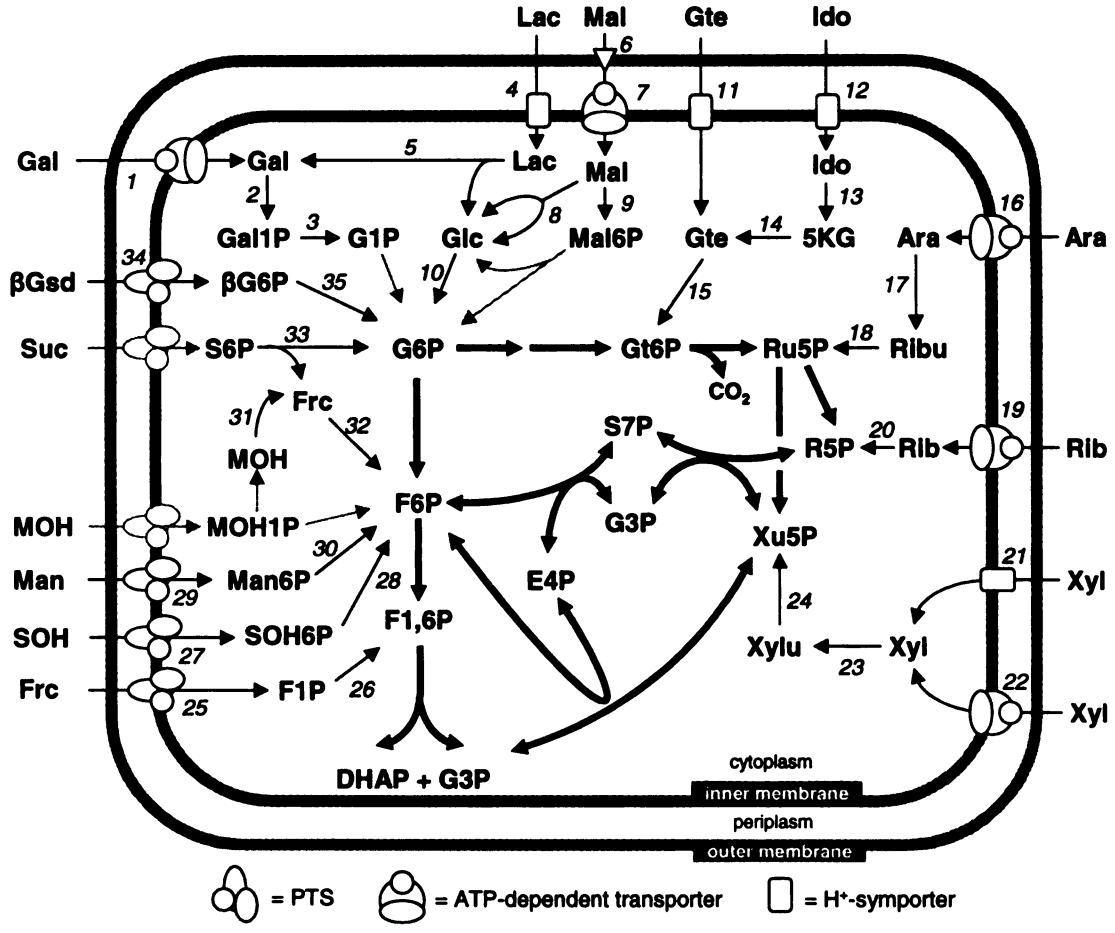

Figure 5.3. Uptake and degradation pathways for sugars other than glucose based on genes identified in the draft genome sequence. Bold arrows, glycolytic or pentose phosphate pathways as described in Figure 5.1 and Table 5.1; Gray arrows or symbols, no suitable sequence identified for function; dotted arrow, no sequence is known mannitol-1-phosphatase (E.C. 3.1.3.22); outer-membrane triangle, maltoporin. Numbers in italics refer to enzymes or transporters in Table 5.3.

5.4.3 Potential for engineering by natural transformation. Engineering *A. succinogenes* into an industrial biocatalyst requires genetic tools. Genetic tools for *A. succinogenes* are currently limited to an expression vector and transformation by electroporation (35). The ability to replace chromosomal DNA segments with engineered DNA is invaluable for making gene knockouts (e.g., of those encoding enzymes leading

Figure 5.3. Uptake and degradation ... **on genes identified in the dra**ft ... **phosphate pathways as descri**bed ... **no suitable sequence identi**fied ... **mannitol-1-phosphatase (E.C.** ... **in italics refer to enzymes** ...

5.4.3 Potential for engineering ...

saccharogenes into an industrial ...

saccharogenes are currently limited ...

electroporation (35). The ability ...

DNA is invaluable for making gene ...

to undesired products) and knock-ins (e.g., of a modified promoter to decrease or increase enzyme expression). One possible route for replacing *A. succinogenes* chromosomal DNA segments is through natural transformation. Under certain conditions (e.g., starvation or in the presence of elevated cAMP levels) many *Pasteurellaceae* become naturally competent, and can be transformed at frequencies as high as 10^{-3} to 10^{-2} (9, 11, 25, 29, 50, 66, 67). The mechanism behind *Pasteurellaceae* competence involves a coordinated response of several proteins that selectively uptake DNA molecules containing a specific uptake signal sequence (USS; AAGTGCGGT) (22, 50). If the DNA taken up is homologous to a section of chromosomal DNA then recombination can occur. This DNA uptake mechanism works best with linear DNA, making it well suited for strain engineering, since constructs can be easily generated by PCR and double recombination events are needed to integrate the linear DNA into the chromosome.

USS-containing DNA is also referred to as 'self-DNA' because the USS occurs as a repeat in *Pasteurellaceae* genomes. If *A. succinogenes* is capable of natural competence then its genome should contain USS repeats. The draft sequence contains 1,458 USSs, well within the range found in other *Pasteurellaceae* (i.e., from 927 in *P. multocida* to 1,760 in *A. actinomycetemcomitans*). Like with other *Pasteurellaceae* USS, the *A. succinogenes* 9-nt core sequence is usually preceded by 'AA' and followed by an AT-rich region (Fig. 5.4). One outstanding difference is that 70% of the *A. succinogenes* USS 9-nt cores are immediately followed by a 'C'. The frequency of 'C' in this position in other *Pasteurellaceae* USS is from 27% in *H. somnus* to 46% in *P. multocida*.

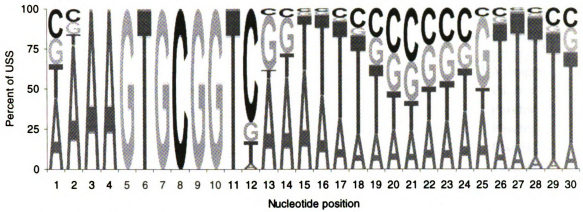

Figure 5.4. Nucleotide frequencies in 1,454 *A. succinogenes* uptake signal sequences.

Pasteurellaceae competence involves a specific set of proteins. A regulon of 25 genes encoding known competence proteins and proteins of unknown function was recently identified in a microarray study of *H. influenaze* competency (50). The regulon is regulated by the cAMP receptor protein, which was shown to bind to a newly discovered consensus sequence associated with the promoters of the regulon (50). The *A. succinogenes* draft genome sequence does not encode a cAMP receptor protein but most of the other competence proteins were identified (Table 5.4).

The number of USS repeats and competence proteins found in the *A. succinogenes* genome sequence suggests that it can be naturally transformed. However, it should be noted that the level of sequence identity between the *H. influenzae* and *A. succinogenes* competence proteins is often low. Of the nineteen *A. succinogenes* competence proteins idenified, seven were assigned probable function and six were assigned possible function (Table 5.4). It is also worth noting that, in a study of *A. actinomycetemcomitans* competency, only one of the 17 strains examined could be naturally transformed under the tested conditions (67).

H. influenzae ORF #	*H. influenzae* product description	Asuc_DRAFT ORF #	*A. succinogenes* modified product description[a]
HI0061	Recombination protein	336	NA (length)
HI0435	Competence protein E	1218	Putative
HI0436	Competence protein D	2125	Possible
HI0437	Competence protein C	1279	Possible
HI0438	Competence protein B	1278	Possible
HI0439	Competence protein A	1277	Possible
HI0365	Hypothetical protein HI0365	1009	Function
HI0296	Type 4 prepilin-like protein specific leader peptidase	580	Possible
HI0297	Protein transport protein	562	Probable
HI0298	Protein transport protein	561	Putative
HI0299	Prepilin peptidase-dependent protein D	560	Putative
HI0601	DNA transformation protein	1672	Probable
HI0659	Hypothetical protein HI0659	327	NA (length)
HI0660	Hypothetical HI0660		NA (No hits)
HI0938	Hypothetical protein HI0938	17	Probable
HI0939	Hypothetical protein HI0939	16	Probable
HI0940	Hypothetical protein HI0940	15	Possible
HI0941	Hypothetical protein HI0941	20	Probable
HI0985	DNA processing chain A	379	Probable
HI1117	Competence protein	952	Function
HI1182/83	DNA ligase	337	Putative
HI1631	Hypothetical protein HI1631	1163	NA (length)
HI0601	DNA transformation protein Sxy	1672	Probable

Table 5.4. *A. succinogenes* homologs of *H. influenzae* competency proteins. [a] Putative, 60-75% amino acid identity; Probable, 40-59% amino acid identity; Possible, 25-39% amino acid identity; NA, no suitable homolog was identified in the *A. succinogenes* draft genome sequence either due to insufficient alignment of length, or no hits were retrieved from the BLAST search.

5.4.4 Potential for non-pathogenicity. The natural *Pasteurellaceae* ecology is in association with a host (34). The host is usually mammalian, with some exceptions, such as *P. multocida* colonizing birds (34) or even amoebae (30). Most *Pasteurellaceae* have been isolated from healthy hosts and are considered to be part of the normal flora. However, in circumstances such as host stress, many *Pasteurellaceae* cause disease. As a result, *Pasteurellaceae* are generally considered to be opportunistic pathogens. All

members of the genus *Actinobacillus* are automatically classified as risk group 2 bacterial agents by the National Institute of Health and require handling under biosafety level 2 guidelines (1). Most *Pasteurellaceae* are isolated from the respiratory tract and cause respiratory type ailments (34). Others, though, have been isolated from the oral cavity (e.g., *A. actinomycetemcomitans* causing peridontitis [(28)]), the genital tract (e.g., *H. ducreyi* causing sexually transmitted chancroid (8)]), and cattle rumen (e.g., *A. lignieresii* causing "wooden toungue (47)]"). The two *Pasteurellaceae* receiving attention as potential industrial biocatalysts, *A. succinogenes* and *M. succiniciproducens*, collectively referred to as succinogens, were isolated from cow rumen. Virulence is an undesirable trait for an industrial organism, and the relatedness of *A. succinogenes* and *M. succiniciproducens* to several pathogens cannot be ignored. With no reports of disease caused by the succinogens, their genome sequences are a convenient and logical starting point to assess their potential for non-pathogenicity.

Pasteurellaceae are intensively studied due to their effects on human and animal health and, as a result, many virulence factors are known. Known *Pasteurellaceae* virulence genes (~250) were manually compilied and aligned against the of *A. succinogenes* and *M. succiniciproducens* protein databases. Global approaches used to identify *Pasteurellaceae* virulence factors, such as microarrays (13, 14, 72) and signature-tagged transposon mutagenesis (44, 58), show that global metabolic changes occur (e.g., expression of amino acid transporters, purine and pyrimidine biosynthesis enzymes, and metabolic enzymes for anaerobic metabolism). While expression of these genes may affect host health, they are not clear indicators of virulence. These genes were therefore excluded from the comparison. The comparison included gene products whose

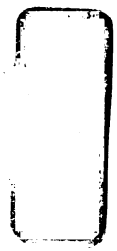

only role appears to be in virulence (e.g., toxins) and gene products involved in the synthesis of cell surface molecules and iron uptake. While most of the *A. succinogenes* genome is accounted for in the draft genome sequence, the absence of some genes may be due to sequence gaps.

Toxins. RTX leukotoxins are produced by many *Pasteurellaceae*, including *A. pleuropneumoniae* (54), *A. actinomycetemcomitans* (28), *M. haemolytica* (19), and *P. multocida* (55). The rumen bacterium *A. lignieresii* contains a full RTX toxin operon but lacks a promoter region to express it (55). The toxins are encoded by four genes: *A*, encoding the structural pretoxin; *C*, encoding the protein that activates the pretoxin; and *B* and *D*, encoding a type I secretion system for the toxin (55). The pretoxin is not encoded in either succinogen genome sequence, and only possible homologs to the other proteins are found, likely due to conserved sequences for ATP-dependent transport. *A. actinomycetemcomitans* also uses a cytolethal distending toxin that is encoded near a characteristic virulence-associated region (39). Neither succinogen genome sequence encodes a cytolethal distending toxin.

Cell surface structures. Virulence factors used by pathogenic *Pasteurellaceae* include cell surface structures such as pili, adhesions, lipopolysaccharides (LPS), and capsules. Even though the succinogens are rumen bacteria, large-scale culturing necessitates an analysis of the risk from aerosols, particularly since many *Pasteurellaceae* are respiratory pathogens. Adherence to respiratory epithelial cells is the first stage of colonization by respiratory *Pasteurellaceae* pathogens. Adherence requires a number of cell surface

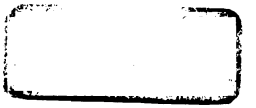

mechanisms (23). *H. influenzae's* hemagglutinating pili (*hifA-E*) are not found in the succinogen genome sequences, with the exceptions of a possible chaperonin-like HifB component in *M. succiniciproducens* and possible minor fimbrial subunit HifD precursor in *A. succinogenes*. Neither succinogen encodes *H. influenzae's* surface fibril protein, Hsf (61). Both succinogenes have putative, probable, and possible matches to all components of the type IV pilus (*pilABCD*) involved in *H. influenzae's* adherence to nasopharyngeal tissue (27). These pili are also part of the *H. influenzae* competence regulon (50). Both competence and pathogenicity are regulated in part by stress. *M. succiniciproducens* also has probable homologs of the *A. actinomycetemcomitans* pili needed for tight adherence, while *A. succinogenes* has possible homologs (48). These pili are widespread in bacteria and archaea (48). *H. influenzae* strains also use high molecular weight (HMW) adhesin proteins to colonize respiratory tissue (6, 23, 65). Aside from putative HmwC homologs in each genome, most *H. influenzae* HMW adhesions do not have significant sequence identity to any succinogen ORF. Each succinogen has several large ORFs that could encode HMW adhesions, including a possible homolog of the *A. actinomycetemcomitans* collagen adhesin, EmaA (42). Neither succinogen encodes a homolog of the *H. influenzae* adherence and penetration protein, Hap (23).

Gram-negative bacteria possess outer membrane LPS, which can act as endotoxin and play a role in evading the immune system. As expected, the succinogen genome sequences indicate that they make LPS, and that they are likely capable of LPS phase variation. Nontypeable *H. influenzae* are able to evade host immune defenses by incorporating host sialic acid and choline into their LPS, thereby mimicking host cell surfaces (2, 70). Both succinogenes lack the genes for choline incorporation (*licABCD*),

with the exception of a possible *licB* gene in *A. succinogenes*. Both succinogens also lack the genes for sialic acid incorporation (*lic3A2, siaB*) but they have a possible sialic acid transporter (*siaT*).

Pasteurellaceae, such as typeable *H. influenzae, P. multocida, A. pleuropneumoniae*, and *M. haemolytica*, produce capsule that is important for virulence (15, 16, 31, 36, 53, 68, 69). Both succinogens have possible homologs to, at most, two of the four capsule biosynthesis and export proteins, suggesting that they are not capsulated bacteria. However, nontypeable *H. influenzae* are non-capsulated, so capsule is not required for virulence in all *Pasteurellaceae*.

Iron uptake mechanisms. While iron acquisition is a well-documented *Pasteurellaceae* virulence trait, it is a common trait of most bacteria making it difficult to associate iron uptake with virulence. Nonetheless, some insight may be gained from the form of iron transported. For example, transferrin and hemoglobin are proteins that mammalian hosts use to bind iron. Unlike *A. pleuropneumoniae* (5, 31), *H. influenzae* (27), *M. haemolytica* (43), and *P. multocida* (10), the succinogens have possible homologs to only a few of the proteins required for transferin or hemoglobulin uptake.

Other virulence proteins. Both succinogens encode GroEL homologs. While GroEL is involved in bone resorption by *A. actinomycetemcomitans* (28), it is also a ubiquitous chaperonin that is important for the proper folding of proteins (17). Both succinogens have a putative homolog to an *A. actinomycetemcomitans* immunosuppressive factor (38) and a putative homolog to the inner membrane protein, ImpA, involved in

autoaggregation (28). Some *Pasteurellaceae* have urease activity, which is a known virulence factor of gastroduodenal and urinary tract pathogens (12), but the succinogens have no urease homologs, and *A. succinogenes* tested negative for urease activity (26). There is also no homolog in either succinogen genome sequence to *H. influenzae* immunoglobulin protease, Iga, which cleaves immunoglobulin, helping *H. influenzae* avoid host defenses at mucosal surfaces (49).

Non-pathogenicity cannot be concluded from the analysis of a genome sequence. However, it is encouraging that the succinogen genome sequences lack a considerable number of the virulence genes used by their relatives. Most *Pasteurellaceae* cause respiratory disease, while succinogens likely exist in the rumen. Therefore, if a succinogen-caused disease exists, the virulence factors involved could be different from those found in other *Pasteurellaceae*. Unfortunately, *A. lignieresii*, which can also be isolated from rumen and is the causative agent of 'wooden-tongue' disease, is not well-characterized (55). With the low prevalence of 'wooden-tongue' disease and no reports of disease caused by *A. succinogenes* or *M. succiniciproducens*, it is plausible that the succinogens are simply commensal organisms. Succinogen non-pathogenicity is an exciting prospect, not just for industrial purposes, but because comparisons of succinogens with other non-pathogenic (i.e., *H. influenzae* KW20) and pathogenic *Pasteurellaceae* could lead to a better understanding of *Pasteurellaceae* virulence.

5.5 REFERENCES.

1. 2002. NIH guidelines for research involving recombinant DNA molecules (NIH guidelines). National Institute of Health.

2. Allen, S., A. Zaleski, J. W. Johnston, B. W. Gibson, and M. A. Apicella. 2005. Novel sialic acid transporter of *Haemophilus influenzae*. Infect. Immun. 73:5291-5300.

3. Altschul, S. F., T. L. Madden, A. A. Schaffer, J. Zhang, Z. Zhang, W. Miller, and D. J. Lipman. 1997. Gapped BLAST and PSI-BLAST: a new generation of protein database search programs. Nucleic Acids Res. 25:3389-3402.

4. Bakkali, M., T. Y. Chen, H. C. Lee, and R. J. Redfield. 2004. Evolutionary stability of DNA uptake signal sequences in the Pasteurellaceae. Proc. Natl. Acad. Sci. USA 101:4513-4518.

5. Baltes, N., I. Hennig-Pauka, and G.-F. Gerlach. 2002. Both transferrin binding proteins are virulence factors in *Actinobacillus pleuropneumoniae* serotype 7 infection. FEMS Microbiol. Lett. 209:283-287.

6. Barenkamp, S. J., and J. W. St Geme, 3rd. 1996. Identification of a second family of high-molecular-weight adhesion proteins expressed by non-typable *Haemophilus influenzae*. Mol. Microbiol. 19:1215-1223.

7. Barnes, E. M., Jr., and H. R. Kaback. 1971. Mechanisms of active transport in isolated membrane vesicles. I. The site of energy coupling between D-lactic dehydrogenase and beta-galactoside transport in *Escherichia coli* membrane vesicles. J. Biol. Chem. 246:5518-5522.

8. Bauer, B. A., M. K. Stevens, and E. J. Hansen. 1998. Involvement of the *Haemophilus ducreyi gmhA* gene product in lipooligosaccharide expression and virulence. Infect. Immun. 66:4290-4298.

9. Bigas, A., M. E. Garrido, A. M. de Rozas, I. Badiola, J. Barbe, and M. Llagostera. 2005. Development of a genetic manipulation system for *Haemophilus parasuis*. Vet. Microbiol. 105:223-228.

10. Bosch, M., M. E. Garrido, M. Llagostera, A. M. Perez De Rozas, I. Badiola, and J. Barbe. 2002. Characterization of the *Pasteurella multocida hgbA* gene encoding a hemoglobin-binding protein. Infect. Immun. 70:5955-5964.

11. Bosse, J. T., J. H. E. Nash, J. S. Kroll, and P. R. Langford. 2004. Harnessing natural transformation in *Actinobacillus pleuropneumoniae*: a simple method for allelic replacements. FEMS Microbiol. Lett. 233:277-281.

12. Bosse, J. T., and J. I. MacInnes. 1997. Genetic and biochemical analyses of *Actinobacillus pleuropneumoniae* urease. Infect. Immun. 65:4389-4394.

13. Boyce, J. B., I. Wilkie, M. Harper, M. L. Paustian, V. Kapur, and B. Adler. 2004. Genomic-scale analysis of *Pasteurella multocida* gene expression during growth within liver tissue of chickens with fowl cholera. Microb. Infect. 6:290-298.

14. Boyce, J. B., I. Wilkie, M. Harper, M. L. Paustian, V. Kapur, and B. Adler. 2002. Genomic scale analysis of *Pasteurella multocida* gene expression during growth within the natural chicken host. Infect. Immun. 70:6871-6879.

15. Boyce, J. D., and B. Adler. 2000. The capsule is a virulence determinant in the pathogenesis of *Pasteurella multocida* M1404 (B:2). Infect. Immun. 68:3463-3468.

16. Boyce, J. D., J. Y. Chung, and B. Adler. 2000. Genetic organisation of the capsule biosynthesis locus of *Pasteurella multocida* M1404 (B:2). Vet. Microbiol. 72:121-134.

17. Chapman, E., G. W. Farr, R. Usaite, K. Furtak, W. A. Fenton, T. K. Chaudhuri, E. R. Hondorp, R. G. Matthews, S. G. Wolf, J. R. Yates, M. Pypaert, and A. L. Horwich. 2006. Global aggregation of newly translated proteins in an *Escherichia coli* strain deficient of the chaperonin GroEL. Proc. Natl. Acad. Sci. U S A 103:15800-15805.

18. Dahinden, P., Y. Auchli, T. Granjon, M. Taralczak, M. Wild, and P. Dimroth. 2005. Oxaloacetate decarboxylase of *Vibrio cholerae*: purification, characterization, and expression of the genes in *Escherichia coli*. Arch. Microbiol. 183:121-129.

19. Davies, R. L., T. S. Whittam, and R. K. Selander. 2001. Sequence diversity and molecular evolution of the leukotoxin (*lktA*) gene in bovine and ovine strains of *Mannheimia* (*Pasteurella*) *haemolytica*. J. Bacteriol. 183:1394-1404.

20. Dimroth, P. 1980. A new sodium-transport system energized by the decarboxylation of oxaloacetate. FEBS Lett. 122:234-236.

21. Donahue, J. L., J. L. Bownas, W. G. Niehaus, and T. J. Larson. 2000. Purification and characterization of *glpX*-encoded fructose 1,6-bisphosphatase, a new enzyme of the glycerol 3-phosphate regulon of *Escherichia coli*. J. Bacteriol. 182:5624-5627.

22. Dubnau, D. 1999. DNA uptake in bacteria. Annu. Rev. Microbiol. 53:217-244.

23. Ecevit, I. Z., K. W. McCrea, M. M. Pettigrew, A. Sen, C. F. Marrs, and J. R. Gilsdorf. 2004. Prevalence of the *hifBC*, *hmw1A*, *hmw2A*, *hmw2C*, and *hia* genes in *Haemophilus influenzae* isolates. J. Clin. Microbiol. 42:3065-3072.

24. Forward, J. A., M. C. Behrendt, N. R. Wyborn, R. Cross, and D. J. Kelly. 1997. TRAP transporters: a new family of periplasmic solute transport systems encoded by

the *dctPQM* genes of *Rhodobacter capsulatus* and by homologs in diverse gram-negative bacteria. J. Bacteriol. 179:5482-5493.

25. Gioia, J., X. Qin, H. Jiang, K. Clinkenbeard, R. Lo, Y. Liu, G. E. Fox, S. Yerrapragada, M. P. McLeoad, T. Z. McNeill, L. Hemphill, E. Sodergren, Q. Wang, D. M. Muzny, F. J. Homsi, G. M. Weinstock, and S. K. Highlander. 2006. The genome sequence of *Mannheimia haemolytica* A1: Insights into virulence, natural competence, and *Pasteurellaceae* phylogeny. J. Bacteriol. 188:7257-7266.

26. Guettler, M. V., D. Rumler, and M. K. Jain. 1999. *Actinobacillus succinogenes* sp. nov., a novel succinic-acid-producing strain from the bovine rumen. Int. J. Syst. Bacteriol. 49:207-216.

27. Harrison, A., D. W. Dyer, A. Gillaspy, W. C. Ray, R. Mungur, M. B. Carson, H. Zhong, J. Gipson, M. Gipson, L. S. Johnson, L. Lewis, L. O. Bakaletz, and R. S. Munson Jr. 2005. Genomic sequence of an otitis media isolate of nontypeable *Haemophilus influenzae*: Comparative study with *H. influenzae* serotype d, strain KW20. J. Bacteriol. 187:4627-4636.

28. Henderson, B., S. P. Nair, J. M. Ward, and M. Wilson. 2003. Molecular pathogenicity of the oral opportunistic pathogen *Actinobacillus actinomycemcomitans*. Annu. Rev. Microbiol. 57:29-55.

29. Herroitt, R. M., E. M. Meyer, and M. Vogt. 1970. Defined nongrowth media for stage II development of competence in *Haemophilus influenzae*. J. Bacteriol. 101:517-524.

30. Hundt, M. J., and C. G. Ruffolo. 2005. Interaction of *Pasteurella multocida* with free-living amoebae. Appl. Environ. Microbiol. 71:5485-5464.

31. Jacques, M. 2004. Surface polysaccharides and iron-uptake systems of *Actinobacillus pleuropneumoniae*. Can. J. Vet. Res. 68:81-85.

32. Kelly, D. J., and G. H. Thomas. 2001. The tripartite ATP-independent periplasmic (TRAP) transporters of bacteria and archaea. FEMS Microbiol. Rev. 25:405-424.

33. Kessler, D., I. Leibrecht, and J. Knappe. 1991. Pyruvate-formate-lyase-deactivase and acetyl-CoA reductase activities of *Escherichia coli* reside on a polymeric protein particle encoded by *adhE*. FEBS Lett. 281:59-63.

34. Killian, M., W. Frederiksen, and E. L. Biberstein. 1981. *Haemophilus, Pasteurella,* and *Actinobacillus*. Academic Press Inc., New York.

35. Kim, P., M. Laivenieks, J. McKinlay, C. Vieille, and J. G. Zeikus. 2004. Construction of a shuttle vector for the overexpression of recombinant proteins in *Actinobacillus succinogenes*. Plasmid 51:108-115.

36. Kroll, J. S., B. Loynds, L. N. Brophy, and E. R. Moxon. 1990. The *bex* locus in encapsulated *Haemophilus influenzae*: a chromosomal region involved in capsule polysaccharide export. Mol. Microbiol. 4:1853-1862.

37. Kummerle, N., H. H. Feucht, and P. M. Kaulfers. 1996. Plasmid-mediated formaldehyde resistance in *Escherichia coli*: characterization of resistance gene. Antimicrob. Agents Chemother. 40:2276-2279.

38. Kurita-Ochiai, T., and K. Ochiai. 1996. Immunosuppressive factor from *Actinobacillus actinomycetemcomitans* down regulates cytokine production. Infect. Immun. 64:50-54.

39. Mayer, M. P. A., L. C. Bueno, E. J. Hansen, and J. M. DiRienzo. 1999. Identification of a cytolethal distending toxin gene locus and features of a virulence associated region in *Actinobacillus actinomycetemcomitans*. Infect. Immun. 67:1227-1237.

40. McKinlay, J. B., Y. Shachar-Hill, J. G. Zeikus, and C. Vieille. 2006. Determining *Actinobacillus succinogenes* metabolic pathways and fluxes by NMR and GC-MS analyses of ^{13}C-labeled metabolic product isotopomers. Metab. Eng. doi:10.1016/j.ymben.2006.10.006.

41. McKinlay, J. B., J. G. Zeikus, and C. Vieille. 2005. Insights into *Actinobacillus succinogenes* fermentative metabolism in a chemically defined growth medium. Appl. Environ. Microbiol. 71:6651-6656.

42. Mintz, K. P. 2004. Identification of an extracellular matrix protein adhesin, EmaA, which mediates the adhesion of *Actinobacillus actinomycetemcomitans* to collagen. Microbiol. 150:2677-2688.

43. Ogunnariwo, J. A., T. K. Woo, R. Y. Lo, G. C. Gonzalez, and A. B. Schryvers. 1997. Characterization of the *Pasteurella haemolytica* transferrin receptor genes and the recombinant receptor proteins. Microb. Pathog. 23:273-284.

44. Ojha, S., M. Sirois, and J. I. Macinnes. 2005. Identification of *Actinobacillus suis* genes essential for the colonization of the upper respiratory tract of swine. Infect. Immun. 73:7032-7039.

45. Park, D. H., M. Laivenieks, M. V. Guettler, M. K. Jain, and J. G. Zeikus. 1999. Microbial utilization of electrically reduced neutral red as the sole electron donor for growth and metabolite production. Appl. Environ. Microbiol. 65:2912-2917.

46. Park, D. H., and J. G. Zeikus. 1999. Utilization of electrically reduced neutral red by *Actinobacillus succinogenes*: physiological function of neutral red in membrane-driven fumarate reduction and energy conservation. J. Bacteriol. 181:2403-2410.

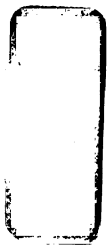

47. Phillips, J. E. 1981. The genus *Actinobacillus*, p. 1393-1398. *In* M. P. Starr, H. Stolp, H. G. Truper, A. Balows, and H. G. Schlegel (ed.), The Prokaryotes, vol. II. Springer-Verlag, Berlin.

48. Planet, P. J., S. C. Kachlany, D. H. Fine, R. DeSalle, and D. H. Figurski. 2003. The widespread colonization island of *Actinobacillus actinomycetemcomitans*. Nat. Genet. 34:193-198.

49. Plaut, A. G. 1983. The IgA1 proteases of pathogenic bacteria. Annu. Rev. Microbiol. 37:603-622.

50. Redfield, R. J., A. D. Cameron, Q. Qian, J. Hinds, T. R. Ali, J. S. Kroll, and P. R. Langford. 2005. A novel CRP-dependent regulon controls expression of competence genes in *Haemophilus influenzae*. J. Mol. Biol. 347:735-747.

51. Samuelov, N. S., R. Datta, M. K. Jain, and J. G. Zeikus. 1999. Whey fermentation by *Anaerobiospirillum succiniciproducens* for production of a succinate-based animal feed additive. Appl. Environ. Microbiol. 65:2260-2263.

52. Samuelov, N. S., R. Lamed, S. Lowe, and J. G. Zeikus. 1991. Influence of CO_2-HCO_3 levels and pH on growth, succinate production, and enzyme activities of *Anaerobiospirillum succiniciproducens*. Appl. Environ. Microbiol. 57:3013-3019.

53. Satola, S. W., P. L. Schirmer, and M. M. Farley. 2003. Complete sequence of the cap locus of *Haemophilus influenzae* serotype b and nonencapsulated b capsule-negative variants. Infect. Immun. 71:3639-3644.

54. Schaller, A., R. Kuhn, P. Kuhnert, J. Nicolet, T. J. Anderson, J. I. MacInnes, R. P. A. M. Segers, and J. Frey. 1999. Characterization of *apxIVA*, a new RTX determinant of *Actinobacillus pleuropneumoniae*. Microbiol. 145:2105-2116.

55. Schaller, A., P. Kuhnert, V. A. de la Puente-Redondo, J. Nicolet, and J. Frey. 2000. Apx toxins in *Pasteurellaceae* species from animals. Vet. Microbiol. 74:365-376.

56. Scheifinger, C. C., and M. J. Wolin. 1973. Propionate formation from cellulose and soluble sugars by combined cultures of *Bacteroides succinogenes* and *Selenomonas ruminantium*. Appl. Environ. Microbiol. 26:789-795.

57. Schneider, K., C. N. Kastner, M. Meyer, M. Wessel, P. Dimroth, and M. Bott. 2002. Identification of a gene cluster in *Klebsiella pneumoniae* which includes *citX*, a gene required for biosynthesis of the citrate lyase prosthetic group. J. Bacteriol. 184:2439-2446.

58. Sheehan, B. J., J. T. Bosse, A. J. Beddek, A. N. Rycroft, J. S. Kroll, and P. R. Langford. 2003. Identification of *Actinobacillus pleuropneumoniae* genes important for survival during infection in its natural host. Infect. Immun. 71:3960-3970.

59. Six, S., S. C. Andrews, G. Unden, and J. R. Guest. 1994. *Escherichia coli* possesses two homologous anaerobic C_4-dicarboxylate membrane transporters (DcuA and DcuB) distinct from the aerobic dicarboxylate transport system (Dct). J. Bacteriol. 176:6470-6478.

60. Spencer, M. E., and J. R. Guest. 1985. Transcription analysis of the *sucAB*, *aceEF* and *lpd* genes of *Escherichia coli*. Mol. Gen. Genet. 200:145-154.

61. St Geme, J. W., 3rd, D. Cutter, and S. J. Barenkamp. 1996. Characterization of the genetic locus encoding *Haemophilus influenzae* type b surface fibrils. J. Bacteriol. 178:6281-6287.

62. Ullmann, R., R. Gross, J. Simon, G. Unden, and A. Kroger. 2000. Transport of C_4-dicarboxylates in *Wolinella succinogenes*. J. Bacteriol. 182:5757-5764.

63. van der Werf, M. J., M. V. Guettler, M. K. Jain, and J. G. Zeikus. 1997. Environmental and physiological factors affecting the succinate product ratio during carbohydrate fermentation by *Actinobacillus sp.* 130Z. Arch. Microbiol. 167:332-342.

64. van Gylswyk, N. O. 1995. *Succiniclasticum ruminis* gen. nov., sp. nov., a ruminal bacterium convering succinate to propionate as the sole energy-yielding mechanism. Int. J. Syst. Bacteriol. 45:297-300.

65. van Schilfgaarde, M., P. van Ulsen, P. Eijk, M. Brand, M. Stam, J. Kouame, L. van Alphen, and J. Dankert. 2000. Characterization of adherence of nontypeable *Haemophilus influenzae* to human epithelial cells. Infect. Immun. 68:4658-4665.

66. Wang, Y., J. Orvis, D. Dyer, and C. Chen. 2006. Genomic distribution and functions of uptake signal sequences in *Actinobacillus actinomycetemcomitans*. Microbiol. 152:3319-3325.

67. Wang, Y., S.D. Goodman, R.J. Redfield, and C. Chen. 2002. Natural transformation and DNA uptake signal sequences in *Actinobacillus actinomycetemcomitans*. J. Bacteriol. 184:3442-3449.

68. Ward, C. K., and T. J. Inzana. 1997. Identification and characterization of a DNA region involved in the export of capsular polysaccharide by *Actinobacillus pleuropneumoniae* serotype 5a. Infect. Immun. 65:2491-2496.

69. Ward, C. K., M. L. Lawrence, H. P. Veit, and T. J. Inzana. 1998. Cloning and mutagenesis of a serotype-specific DNA region involved in encapsulation and virulence of *Actinobacillus pleuropneumoniae* serotype 5a: concomitant expression of serotype 5a and 1 capsular polysaccharides in recombinant *A. pleuropneumoniae* serotype 1. Infect. Immun. 66:3326-3336.

70. West-Barnette, S., A. Rockel, and W. E. Swords. 2006. Biofilm growth increases phosphorylcholine content and decreases potency of nontypable *Haemophilus influenzae* endotoxins. Infect. Immun. 74:1828-1836.

71. Woehlke, G., and P. Dimroth. 1994. Anaerobic growth of *Salmonella typhimurium* on L(+)- and D(-)-tartrate involves an oxaloacetate decarboxylase Na^+ pump. Arch. Microbiol. 162:233-237.

72. Wong, S. M., and B. J. Akerley. 2005. Environmental and genetic regulation of the phosphorylcholine epitope of *Haemophilus influenzae* lipooligosaccharide. Mol. Microbiol. 55:724-738.

73. Zeikus, J. G., M. K. Jain, and P. Elankovan. 1999. Biotechnology of succinic acid production and markets for derived industrial products. Appl. Environ. Microbiol. 51:545-552.

74. Zientz, E., I. G. Janausch, S. Six, and G. Unden. 1999. Functioning of DcuC as the C_4-dicarboxylate carrier during glucose fermentation by *Escherichia coli*. J. Bacteriol. 181:3716-3720.

75. Zientz, E., S. Six, and G. Unden. 1996. Identification of a third secondary carrier (DcuC) for anaerobic C_4-dicarboxylate transport in *Escherichia coli*: roles of the three Dcu carriers in uptake and exchange. J. Bacteriol. 178:7241-7247.

Chapter 6.

CONCLUSIONS and FUTURE DIRECTIONS.

6.1 The current understanding of *A. succinogenes* fermentative metabolism. *A. succinogenes* produces some of the highest succinate titers ever reported, making it a promising biocatalyst for industrial succinate production (3, 4). However, in addition to producing succinate, *A. succinogenes* also produces unwanted formate, acetate, and ethanol. While *A. succinogenes* produces more succinate with increasing CO_2 or reductant (i.e., H_2 or a more-reduced carbon source than glucose) concentrations, formate and acetate are always produced as major fermentation products. Therefore, *A. succinogenes* must be engineered to increase flux to succinate and decrease flux to alternative fermentation products.

Metabolic engineering strategies are unlikely to succeed without an understanding of the metabolism under study. *A. succinogenes* metabolism was first characterized by in vitro enzyme assays and fermentation balances (5, 19). These data indicated that *A. succinogenes* catabolizes glucose to phosphoenolpyruvate (PEP) by glycolysis and the oxidative pentose phosphate pathway (OPPP) (19). Metabolism was then thought to split at PEP to form the acetate-, formate-, and ethanol-producing C_3 pathway, and the succinate-producing C_4 pathway. Succinate production from PEP involves one CO_2 fixation step by PEP carboxykinase (PEPCK), and two reduction steps by malate dehydrogenase and fumarate reductase (Chapter 3, Fig.1). The positive effects of increased CO_2 and reductant concentrations on succinate production were therefore

thought to be due to the increased availability of these substrates for PEPCK and the C_4 pathway dehydrogenases (19).

Metabolic engineering also requires genetic tools. An *A. succinogenes-Escherichia coli* shuttle vector was developed to overexpress proteins in *A. succinogenes* (10). *A. succinogenes* PEPCK was overexpressed and was expected to increase succinate production because PEPCK is the CO_2-fixing, first reaction of the C_4 pathway. *E. coli* NADP-dependent and *Bacillus subtilis* NAD-dependent malic enzymes were also overexpressed, and were expected to increase succinate production through pyruvate (Pyr) carboxylation, as they did for *E. coli* (8, 17). In each case, enzyme activity levels increased 2 – 5 fold, but fermentation balances were unaffected (Kim et al., unpublished data).

The inability to affect *A. succinogenes* fermentation balances by overexpressing PEPCK and malic enzymes indicated that there was insufficient knowledge on *A. succingenes* metabolism to predict the metabolic effects of genetic manipulations. In fact, several enzyme activities detected in *A. succinogenes* cell extracts suggested a more complex metabolism than a simple branched fermentation (19): (i) high citrate lyase activity levels suggested that TCA-cycle associated fluxes could bridge the C_3 and C_4 pathways; (ii) low Entner-Doudoroff pathway enzyme activity levels suggested an alternative to the pentose phosphate pathway for NADPH generation; (iii) low isocitrate lyase activity levels suggested that the glyoxylate pathway could bridge the C_3 and C_4 pathways; and (iv) oxaloacetate (OAA) decarboxylase and malic enzyme activities suggested shunts from the C_4 pathway to the C_3 pathway.

^{13}C-metabolic flux analysis (MFA) methods were chosen to obtain a detailed understanding of *A. succinogenes* fermentative metabolism. Unlike in vitro enzyme activity levels, which do not necessarily correlate with in vivo fluxes, results from MFA can provide a global picture of active pathways and the fluxes through these pathways. Further insight into the roles of metabolic fluxes can be obtained by repeating MFA experiments under various growth conditions. MFA involves the analysis of ^{13}C incorporated into metabolic products, with most information usually obtained from labeling patterns in proteinaceous amino acids. To ensure that *A. succinogenes* proteins are synthesized from ^{13}C-labeled substrate, a chemically defined growth medium had to be developed.

In Chapter 2, *A. succinogenes* fermentations were characterized in a chemically defined growth medium, called AM3, and compared to those in a comlex medium. Succinate yields were similar in each medium, but C_3-pathway product yields were higher in the complex medium. These high C_3-pathway product yields may be due to decreased pyruvate and acetyl-CoA requirements for biosynthesis, since biosynthetic precursors are abundant in yeast extract. More pyruvate and acetyl-CoA are used for biosynthesis than any other intermediates during growth in AM3 (Chapter 3). The ratio of succinate:(acetate plus ethanol) increased with the $NaHCO_3$ concentration between 5 mM and 75 mM $NaHCO_3$ in AM3, indicating that the $NaHCO_3$ effects observed in complex media are also observed in AM3. Fermentation balances were similar between 75 and 150 mM $NaHCO_3$ in AM3, defining an upper range for the effects of $NaHCO_3$ on the fermentation balance. AM3 contained Cys, Met, and Glu, which were required for growth. Aspartate:glutamate transaminase activity was previously detected in *A.*

succinogenes extracts (19), suggesting that *A. succinogenes* could synthesize Glu from α-ketoglutarate (αKG). αKG supported growth in place of Glu when NH_4Cl or aspartate was supplied as a nitrogen source. Therefore, Glu-auxotrophy was due to an inability to synthesize αKG from glucose. This inability indicated that at least one TCA cycle activity and one reductive TCA-cycle activity are missing or inactive under fermentative conditions in AM3. Thus, while citrate lyase is detected in *A. succinogenes* cell extracts (19), it is not involved in bridging the C_3 and C_4 pathways by known TCA-cycle associated reactions.

Chapter 3 described the first ^{13}C-labeling study of *A. succinogenes* metabolism, in which *A. succinogenes* was fed [1-^{13}C]glucose in batch AM3 fermentations with 150 mM $NaHCO_3$ to determine active (3, 13)metabolic pathways and to quantify metabolic fluxes. Pseudo-metabolic steady state was confirmed by comparing extracellular fluxes and isotopic enrichments at different cell densities. When Entner-Doudoroff and glyoxylate pathways were included in metabolic models, they were shown to carry no flux. The OPPP flux was only 5% that of the glucose uptake rate, not nearly enough to meet anabolic NADPH demands. More acetate and ethanol were produced than formate, indicating formate dehydrogenase (ForDH) and/or Pyr dehydrogenase (PyrDH) activity. Both activities were detected in vitro and the flux through these enzymes contributed to a net NADH flux. Transhydrogenase could convert this net NADH flux to NADPH, and in vitro transhydrogenase activity was detected. Pyruvate dehydrogenase activity may also explain how *A. succinogenes* mutants with defective pyruvate formate lyase activity (3, 13) produce essential acetyl-CoA. Another potential NADPH source was malic enzyme. The isotopomer data indicated a significant C_4-decarboxylating flux forming a shunt from

the C_4 to the C_3 pathways. This flux was probably due to both malic enzyme and OAA decarboxylase, and both activities were detected in cell extracts. Since PEPCK can feed both the C_4 and C_3 pathways in the presence of the C_4-decarboxylating flux, overexpressing PEPCK alone is likely not enough to increase flux to succinate. OAA decarboxylase activity was an intriguing finding as its sequence and Na^+-dependent activity indicated that it was also a Na^+-pump.

In Chapter 4, an informative substrate isotopomer mixture composed of [1-^{13}C]glucose, [U-^{13}C]glucose, and unlabeled $NaHCO_3$, was used for a series of ^{13}C-MFA studies. This isotopomer mixture revealed that there is not only a C_4-decarboxylating flux, but a Pyr-carboxylating flux as well. Exchange flux was also revealed in the C_3 pathway, through pyruvate formate-lyase (PFL), ForDH and possibly through PyrDH. Chapter 4 also provided further insight into the roles of the C_4-decarboxylating flux and the C_3 pathway dehydrogenases by examining the flux changes that occur in response to different $NaHCO_3$ and H_2 concentrations. While the environmental perturbations affected the fermentation balance, the growth rate and biomass yield were not affected, indicating that the resulting flux changes were to maintain growth parameters. The results indicated that CO_2 concentration does not necessarily affect PEPCK flux as was previously hypothesized. Instead, increased $NaHCO_3$ concentration decreased the flux shunted from the C_4 to the C_3 pathway and increased the flux in the opposite direction. With more flux committed to the C_4 pathway, more succinate was excreted. To meet the reductant demands of the increased flux to succinate, C_3 pathway dehydrogenases responded by decreasing the NADH-oxidizing flux to ethanol and increasing the NADH-producing flux through ForDH and/or PyrDH. Supplying H_2 partially alleviated the need for NADH-

production by the C_3 pathway, as indicated by a slight decrease in the total C_3 pathway flux, and a larger decrease in the ForDH and/or PyrDH flux.

Chapter 5 described industrially relevant features of the *A. succinogenes* draft genome sequence. The metabolic enzymes identified in the genome sequence generally support the findings of the metabolic flux analyses. Dicarboxylate transporters were identified that could be involved in succinate excretion. Numerous transporters of industrially relevant sugars were also identified. There is some evidence that *A. succinogenes* is, or was, capable of natural transformation, as indicated by a nearly complete set of competence proteins and 1,458 DNA uptake signal sequences. The *A. succinogenes* genome sequence does not encode many of the virulence factors used by its pathogenic relatives.

The results in this dissertation have re-shaped our understanding of *A. succinogenes* fermentative metabolism. Instead of a simple branched fermentation, flux is distributed between the C_3 and C_4 pathways at four metabolic nodes: PEP, Pyr, OAA, and malate, due to the activities of OAA decarboxylase and malic enzyme. NADPH is produced by C_3 pathway dehydrogenases coupled with transhydrogenase, and possibly by malic enzyme, rather than by the OPPP. The mechanisms by which $NaHCO_3$ and H_2 affect *A. succinogenes* fermentation balances are not limited to their roles as substrates for succinate production in the C_4 pathway. $NaHCO_3$ concentration may affect the amount of flux shunted between the C_4 and the C_3 pathways. By changing the metabolic reductant demands, $NaHCO_3$ also affects the distribution of fluxes within the C_3 pathway. H_2 also affects C_3 pathway fluxes by serving as an alternative source of reductant and alleviating the need for reductant generation by ForDH and/or PyrDH.

6.2 Future research and development of *A. succinogenes* metabolism. The described discoveries have raised important considerations for the metabolic engineering of *A. succinogenes* and important questions about *A. succinogenes* metabolism. The following sections address the future work needed to understand and engineer *A. succinogenes* fermentative metabolism.

6.2.1 Oxaloacetate decarboxylase and malic enzyme. OAA decarboxylase and malic enzyme are shunts between the C_4 and the C_3 pathways. Since these enzymes can divert flux away from succinate, it is desirable to decrease the flux through these enzymes from OAA and malate to Pyr). However, each enzyme potentially serves an important physiological role, and could affect the outcome of engineering strategies if not taken into accout.

As a Na^+-pump, OAA decarboxylase may be important for maintaining a Na^+ gradient used for cell processes such dicarboxylate transport (e.g., glutamate and succinate) (6, 18). Furthermore, OAA decarboxylase flux could be important for maintaining osmotic balance. In AM3, with 150 mM $NaHCO_3$, the total Na^+ concentration is ~230 mM. If OAA decarboxylase functions to maintain osmotic balance, then decreasing the Na^+ concentration in the medium could result in decreased OAA decarboxylase flux. High Na^+ concentrations are also harmful to industrial bioreactors. To test whether OAA decarboxylase flux responds to Na^+ concentrations, a low Na^+ medium must first be developed. In AM3, the phosphate buffer (NaH_2PO_4) and $NaHCO_3$ are the main Na^+ sources. Using K^+ media components is not suitable because *A.*

succinogenes growth rates decrease at a K^+ concentration above 75 mM. A suitable alternative might be to use poorly soluble $MgCO_3$ with only enough phosphate buffer to provide adequate PO_4^{2-} for growth. *A. succinogenes* can grow and produce high succinate titers with $MgCO_3$ concentrations as high as 80 g/l (~950 mM if all were dissolved) (4). Acid produced during the fermentation dissolves more $MgCO_3$ and moderates the pH decline. The main disadvantage to using $MgCO_3$ is that growth measurements are less convenient since they can no longer be performed by optical density. Samples would have to be taken during growth to determine biomass concentrations by protein assays, and taking multiple samples necessitates larger culture volumes. Preliminary experiments would involve culturing *A. succinogenes* in this medium with different NaCl (treatment) and KCl (control) concentrations. The effects of cation concentrations on the succinate:(acetate + ethanol) ratio would then be determined by HPLC, and OAA decarboxylase activity would be quantified in cell extracts from each condition. ^{13}C-labeling experiments could be used to determine whether the C_4-decarboxylating flux decreases in response to a decrease in Na^+ concentrations. However, even in the absence of H_2, this flux is not well determined and changes in OAA decarboxylase flux may not be observed against a high malic enzyme flux. Ultimately, it would be desirable to knock out OAA decarboxylase and determine whether the mutant strain has a decreased Na^+ tolerance. In the absence of genetic tools, the importance of OAA decarboxylase for Na^+ tolerance could potentially be assessed by using limiting amounts of biotin. OAA decarboxylase is a biotin-containing enzyme. Biotin is also required for essential enzymes such as acetyl-CoA carboxylase for lipid synthesis, and *A. succinogenes* may require biotin (biotin is supplied in the AM3 vitamin mix). If *A. succinogenes* requires

biotin, and if OAA decarboxylase is responsible for Na^+ tolerance, then *A. succinogenes* should grow to higher final ODs at low Na^+ concentrations than at high Na^+ concentrations when biotin is limiting. These experiments should show whether OAA decarboxylase and the Na^+ concentration are important for distributing flux between succinate and alternative products. These experiments should also establish a Na^+ concentration for maximum succinate production without adversely affecting cell growth.

Malic enzyme was hypothesized to be important for NADPH production based on the C_4-decarboxylating fluxes observed. However, its contribution to NADPH production could not be determined for several reasons: (i), C_4 decarboxylating flux confidence intervals were large; (ii) the individual contributions of OAA decarboxylase and malic enzyme to the C_4 decarboxylating flux is unknown; and (iii) the NADPH requirement could be satisfied entirely by OPPP flux plus ForDH/PyrDH flux coupled with transhydrogenase. Since pyruvate carboxylating flux increased and the C_4dec flux decreased in conditions with high reductant demands (i.e., high succinate production rates in the presence of 100 mM $NaHCO_3$; Chapter 4), transhydrogenase is likely more important than malic enzyme for NADPH production. If malic enzyme is important for NADPH production, then inactivating malic enzyme should be compensated for by other fluxes (i.e., increased PyrDH/ForDH or OPPP fluxes). Knocking out OAA decarboxylase or malic enzyme individually would also be useful for determining the contribution of each enzyme to the total C_4-decarboxylating flux in a ^{13}C-labeling experiment. It is possible that malic enzyme carries a net pyruvate carboxylating flux under the high CO_2 concentrations used in this dissertation. Malic enzyme carboxylates pyruvate to malate in succinate producing *E. coli* strains overexpressing malic enzyme (8, 17). With either

enzyme inactivated, in vivo exchange fluxes for each enzyme could be determined with reasonable confidence (Chapter 4). With both C_4-decarboxylating enzymes inactivated, the in vivo contribution of enzymes like PEPCK and pyruvate kinase to the total C_4-decarboxylating flux could be determined. These enzymes can have OAA decarboxylase activity, as discussed in Chapter 3.

6.2.2 The effects of CO_2 concentration on PEPCK and C_4-decarboxylating fluxes.

The prevailing hypothesis for how CO_2 concentrations affect *A. succinogenes* succinate production is through its role as a substrate for PEPCK. The results in Chapter 4 do not show a significant difference in PEPCK flux at 25 and 100 mM $NaHCO_3$, but it could not be concluded that the $NaHCO_3$ concentration does not affect PEPCK flux due to large confidence intervals. The results in Chapter 4 did indicate that the $NaHCO_3$ concentration affects the amount of flux shunted to the C_3-pathway. These results provide an alternative (or an additional) hypothesis for how CO_2 concentration affects *A. succinogenes* fermentation balances. OAA decarboxylase and malic enzyme knockouts would certainly be useful for determining the extent to which CO_2 concentration affects fermentation balances in the absence of one or both C_4-decarboxylating activities. The mechanisms by which CO_2 affects flux distributions could also be addressed without genetic tools. When *A. succinogenes* was grown in anaerobic respiration conditions with fumarate and H_2, significant formate and acetate were still produced (19). In vitro OAA decarboxylase and malic enzyme activities were also detected, leading to the hypothesis that these enzymes divert flux to the C_3 pathway during fumarate respiration as well (19). During fumarate respiration, PEPCK should carry gluconeogenic flux, so the succinate formation rate

should not depend on PEP-carboxylating PEPCK flux. A decrease in formate and acetate yields in response to high $NaHCO_3$ concentrations during fumarate respiration would support the hypothesis that $NaHCO_3$ concentrations affect the amount of flux shunted through malic enzyme and OAA decarboxylase. The main drawback to this experiment is that the findings may not apply to fermentative conditions.

A potential experiment for testing the effect of $NaHCO_3$ concentration on PEPCK flux would be to grow *A. succinogenes* on fructose at different $NaHCO_3$ concentrations. This experiment operates on the assumption that fructose is transported only by a PEP:fructose phosphotransferase system (PTS). If high $NaHCO_3$ concentrations cause PEPCK flux to increase, then PEPCK could potentially compete with the PTS for PEP, resulting in a decreased growth rate. Alternatively, PTS flux could increase in response to the increased PEPCK flux, resulting in an increased growth rate. Using ^{13}C-fructose isotopomers would be useful for this experiment to confirm that the observed effects are related to PEPCK flux changes. Characterizing metabolic fluxes on fructose is also industrially relevant since fructose is a highly abundant plant sugar, especially in sugarcane, which is a feedstock for industrial fermentations in tropical countries.

6.2.3 Pyruvate dehydrogenase and formate dehydrogenase. MFA experiments indicated that PyrDH and/or ForDH fluxes were important for generating reducing power in the absence of H_2. However, the fluxes through each enzyme could not be distinguished. Although the final engineering goal is to decrease the flux through both enzymes, being able to quantify fluxes through the individual enzymes is of interest to the study of microbial metabolism. Chapter 4 presented methods for quantifying C_3 pathway exchanges fluxes. PyrDH is generally considered to be a unidirectional enzyme,

but the high CO_2 environment used to grow *A. succinogenes* may influence PyrDH reversibility. Knocking out PFL would prevent formate production, thereby preventing ForDH fluxes, and leaving PyrDH as the only enzyme activity connecting Pyr and acetyl-CoA. The methods in Chapter 4 could then be applied to the mutant strain to determine the extent to which $NaHCO_3$ concentration affects PyrDH exchange flux, if at all.

6.2.4 The C_3 pathway. The C_3 pathway has three important functions: (i) synthesis of Pyr and acetyl-CoA for biosynthesis; (ii) ATP production (by acetate kinase); and (iii) NADH production for succinate production and biosynthesis (or NADH oxidation at low CO_2 concentrations). Knowing the C_3 pathway functions is important for designing effective metabolic engineering strategies to increase flux to succinate, for example by forcing *A. succinogenes* to fulfill the C_3 pathway functions by other means. Since pyruvate and acetyl-CoA synthesis is useful to avoid adding potentially expensive alternatives, engineering efforts should focus on generating ATP and/or NADH by other means. For example, supplying H_2 partially alleviated the need for reductant generation in the C_3 pathway (Chapter 4). Supplying H_2 also decreased fumarate excretion rate, suggesting that fumarate reductase flux is limited by reductant availability. Achieving a homosuccinate fermentation requires the addition of extra reductant (Chapter 1). H_2 may be a suitable source of reductant for industrial succinate production provided that it can be obtained or produced inexpensively (e.g., from phostosynthetic bacteria). C_3 pathway flux could decrease and flux to succinate could increase by increasing the rate of H_2 oxidation. Increased H_2 oxidation could be achieved to some extent by using reactors that can increase the dissolved H_2 concentration. However, it may be more beneficial to force

high H_2 oxidation rates in *A. succinogenes*. H_2 oxidation in *A. succinogenes* is coupled to quinone reduction (14). By overexpressing hydrogenase in *A. succinogenes*, high H_2 oxidation rates could be achieved and would maintain a reduced quinone pool leading to increased succinate production rates. Repeated culturing of hydrogenase-overexpressing *A. succinogenes* strains, may lead to mutants with an increased ability to couple quinone oxidation to succinate production, since these mutants would have the energetic advantage of increased ATP formation rates by ATPase utilizing the H^+ gradient generated by quinone oxidation. Repeated culturing may also lead to mutants with increased flux to succinate through the C_4 pathway by overcoming allosteric regulatory mechanisms such as ATP concentration inhibiting PEPCK activity. Sequencing enzymes such as PEPCK in evolved strains would then provide further insights into the amino acid residues important for allosteric regulation. The energetic advantage of increasing flux to succinate to compensate for the increased H_2 oxidation rates may be enough to significantly favor C_4 pathway flux over C_3 pathway flux without gene knockouts. High H_2 oxidation rates could be complemented by overexpressing NADH oxidase to further reduce the quinone pool. The increased NADH oxidizing flux may stimulate higher glycolytic flux to compensate, resulting in a higher glucose consumption rate, and a higher succinate formation rate. Since ethanol production relies on NADH oxidation rather than quinone oxidation, succinate production would be favored over ethanol production in hydrogenase-overexpressing strains. However, to ensure that NADH from glycolytic flux is used for succinate production, and converted to NADPH for biomass, it may be necessary to knockout acetaldehyde/alchohol dehydrogenase. Knocking out acetate kinase would also force the bacterium to rely on the C_4 pathway for ATP

production. Potentially, with the C_3 pathway terminating at Acetyl-CoA, there would be only enough C_3 pathway flux to supply pyruvate and acetyl-CoA for biosynthesis. However, inactivating central C_3 pathway enzymes may also be useful. For example, inactivating PFL has already been shown to increase succinate yields for *A. succinogenes* (3) and result in decreased growth rates, perhaps due to decreased flux to acetyl-CoA with pyruvate dehydrogenase acting alone. These decreased growth rates may be useful for diverting more carbon to succinate rather than biomass.

The engineering strategies described above illustrate how knowledge of pathway function can influence engineering strategies. However, strategies made with the current understanding of *A. succinogens* metabolism could be ineffective since the physiological importance of the C_4-decarboxylating fluxes is unknown. OAA decarboxylase flux may be influenced entirely by Na^+ concentrations and not by reductant and ATP demands. Malic enzyme may even carry a net pyruvate carboxylating flux that can't be observed against a high OAA decarboxylase flux. The strategies described above could result in excess pyruvate as is observed for *A. succinogenes* mutants with inactive PFL (3). A better understanding of how CO_2 concentrations influence the direction of malic enzyme could therefore be useful to divert excess pyruvate to succinate. It is currently unknown which of malic enzyme, OAA decarboxylase, PTS, or pyruvate kinase carries the most flux to pyruvate. Thus, the benefits of knocking out any single one of these enzymes for succinate production cannot be reasonably predicted. Determining the functions of the C_4-decarboxylating fluxes and the individual fluxes leading into pyruvate will undoubtedly be useful for developing effective metabolic engineering strategies.

6.2.5 Importance of the *A. succinogenes* genome sequence. While MFA measures fluxes through a metabolic network, it does not necessarily identify the enzymes responsible for these fluxes. In fact, the accuracy of MFA is dependent on the accuracy of the metabolic model. A genome sequence is an excellent resource by which to shape and constrain a metabolic network. A genomic sequence therefore complements MFA by indicating which enzymes may be responsible for observed fluxes, by suggesting pathways that could generate unusual labeling patterns, and by decreasing the number of labeling experiments needed to address the activity of certain pathways.

The analysis of sugar uptake and degradation pathways in Chapter 5 points to potentially important targets for metabolic engineering. Xylose and arabinose are abundant plant pentoses and as such are industrially relevant carbon sources. *A. succinogenes* encodes two xylose transporters: (i) a low affinity H^+-symporter, and (ii) a high affinity, ATP-dependent transporter. To conserve energy, it may be beneficial to ensure xylose transport through the H^+-symporter by knocking out the ATP-dependent transporter. An *E. coli* PFL knockout strain did not grow fermentatively on xylose by using an ATP-dependent transporter, but grew when a H^+-symporter was expressed (7). Additionally, only an ATP-dependent arabinose transporter has been identified in the *A. succinogenes* draft genome sequence. If an arabinose H^+-symporter is not found in the complete genome sequence, it may be important to introduce a gene encoding one. Constitutively expressing the xylose H^+-symporter could also lead to arabinose uptake since pentose H^+-symporters can have low substrate specificity (7).

To produce succinate industrially using *A. succinogenes* in an inexpensive chemically defined medium, cysteine auxotrophy must be eliminated. While glutamate

and methionine are relatively inexpensive, being produced from large scale fermentations, cysteine is expensive. When the *A. succinogenes* genome sequence is complete, it will be important to determine which cysteine pathway enzymes are not encoded, and introduce them into the genome. If cysteine, or methionine, auxotrophy can be eliminated by introducing a single enzyme activity, the genes encoding these enzymes could also be useful as alternative *A. succinogenes* selective markers to antibiotic resistance cassettes.

The *A. succinogenes* genome sequence opens the door to using functional genomics for studying *A. succinogenes* metabolism. Microarray and proteomic analyses can complement MFA studies to gain a better understanding of the factors controlling *A. succinogenes* metabolism. By shifting *A. succinogenes* from one growth condition to another, and sampling for microarrays at different time points during this transition, coordinately regulated genes can be identified. Such a microarray experiment was done for *Haemophilus influenzae* by transitioning it from growth conditions to starvation conditions to induce competence (15). An interesting outcome from this study was that many C_4 pathway genes were coordinately expressed as part of a regulon regulated by the cAMP receptor protein. This protein has not been identified in the *A. succinogenes* genome sequence, but the idea of a regulatory protein controlling all the C_4 pathway genes as a regulon is an exciting prospect. Kacser and Acerenza (9) proposed a 'universal method' for increasing flux to a desired product, which, in short, involves overexpressing every enzyme in a pathway leading to the desired product. This approach was tested by overexpressing different combinations of the five enzymes involved in tryptophan synthesis in *Saccharomyces cerevisiae* (12). The highest flux to tryptophan was observed

when all five enzymes were overexpressed (12). If all enzymes in the C_4 pathway are part of the same regulon, then it may be possible to affect their expression through the regulator (e.g., by constitutively expressing the regulator or by mutating allosteric binding sites), or through engineering the promoters. This approach would be more convenient, and likely more stable, than overexpressing all C_4 pathway genes from a plasmid.

6.2.6 Developing genetic tools for replacing *A. succinogenes* chromosomal DNA segments. Many of the future directions described in the previous sections rely on the ability to knock out genes. This technology has not been developed yet for *A. succinogenes*. This technology is not only important for studying *A. succinogenes* metabolism, but is essential for its metabolic engineering. Knocking out genes is the most commonly used method for preventing flux to unwanted products and diverting flux to the product of interest. However, in some cases, preventing flux to an unwanted product could be detrimental to cell health, or even lethal. Although the goal for developing an *A. succinogenes* homosuccinate fermentation involves decreasing the C_3 pathway flux, the C_3 pathway produces pyruvate and acetyl-CoA, which are essential intermediates for biosynthesis. Without C_3 pathway flux, the medium must contain alternative compounds to pyruvate and acetyl-CoA to support growth. The most economical source of these compounds would likely be an uncharacterized mixture of an agricultural product or waste stream. The problem with using these uncharacterized mixtures is that they make purifying succinate from fermentation broths more difficult and more expensive. If succinate is to be produced in an inexpensive defined medium, then some C_3 pathway

flux must remain to produce enough pyruvate and acetyl-CoA for growth. Achieving low C_3 pathway flux for biosynthesis without product excretion will require genetic tools capable of making minor flux adjustments. Such genetic tools will likely rely on the same technology as that for gene knockouts. Rather than replacing a gene for an enzyme with an interrupted or partially deleted gene, a gene could be replaced with one encoding a less active enzyme. Alternatively, promoters could be re-engineered to decrease enzyme expression. Clearly there is much need for technology to make specific chromosomal alterations in *A. succinogenes*.

Prospects for developing genetic tools for chromosomal alterations in *A. succinogenes* are not discouraging. As described in Chapter 5, many *Pasteurellaceae* have specific mechanisms taking up linear fragments of DNA. Natural transformation has been used to replace chromosomal segments in at least four different *Pasteurellaceae* (1, 2, 15, 20). The *A. succinogenes* genome sequence has several indicators that it is capable of natural transformation, or at least was capable in the past. However, it is important to note that, in a study of natural competence in *A. actinomycetemcomitans*, only one of seventeen isolates tested could be naturally transformed (20).

A more promising method for replacing *A. succinogenes* chromosomal segments is to use a sucrose counter selection system. This technology was recently used to knock out seven different genes in *M. succiniciproducens* (11), the closest known relative of *A. succinogenes*. This technology works by using a suicide vector containing the mutant gene of interest (e.g., a gene interrupted with an ampicillin resistance cassette) and *sacB*, encoding *B. subtilis* levansucrase. Sucrose is toxic to Gram-negative bacteria expressing levansucrase, likely due the accumulation of levans in the persiplasmic space (16). The

suicide vector is introduced to the cells (e.g., by electroporation) then the cells are plated on media with ampicillin. Cells incorporating the plasmid into their genomes, most likely by a single-recombination event, will grow on the selective media. Single recombinants are then grown in liquid media. The greater cell population increases the chance of a second single-recombination event between the wild-type gene and the mutant gene that can splice out the wild-type gene and the *sacB*-containing suicide vector. Cells are then plated on media with ampicillin and sucrose, and only those cells that retained the mutant gene and lost the *sacB* gene should survive.

In establishing a knockout method for *A. succinogenes* it is important that the target be a non-essential enzyme. PFL is not expected to be essential because *A. succinogenes* mutants with no PFL activity and *M. succiniciproducens pflB::Cm*^{R} strains are viable (11, 13). Furthermore, a PFL knockout strain should have better ratios of succinate to alternative endproducts making it industrially attractive (11, 13). A PFL knockout strain would also be useful for assessing the reversibility of PyrDH, as described in section 6.2.3.

In summary, this dissertation has refined our understanding of *A. succinogenes* metabolism by analyzing its fermentations with and without ^{13}C-substrates, and by analyzing the its draft genome sequence. *A. succinogenes* metabolism was revealed to be complex, with multiple branchpoints for distributing flux to succinate versus alternative fermentation products. Furthermore, the classical environmental perturbations used to affect *A. succinogenes* fermentation balances, CO_2 and reductant concentrations, were shown to affect metabolism by other mechanisms than just their roles as substrates for the C_4 pathway. The future of *A. succinogenes* research and development will benefit from

'16

2(

further characterizations of its metabolism using environmental perturbations, such as different Na^+ concentrations, and different $NaHCO_3$ concentrations during fermentative growth on fructose or during respiration with fumarate. The *A. succinogenes* genome sequence greatly expands the experimental opportunities for using system-wide approaches to study its metabolism. The ability to make chromosomal modifications in would further increase the experimental opportunities for studying *A. succinogenes* metabolism and is crucial for engineering a homosuccinate fermentation.

6.3 REFERENCES

1. Bigas, A., M. E. Garrido, A. M. de Rozas, I. Badiola, J. Barbe, and M. Llagostera. 2005. Development of a genetic manipulation system for *Haemophilus parasuis*. Vet. Microbiol. 105:223-228.

2. Bosse, J. T., J. H. E. Nash, J. S. Kroll, and P. R. Langford. 2004. Harnessing natural transformation in *Actinobacillus pleuropneumoniae*: a simple method for allelic replacements. FEMS Microbiol. Lett. 233:277-281.

3. Guettler, M. V., M. K. Jain, and D. Rumler. 1996. Method for making succinic acid, bacterial variants for use in the process, and methods for obtaining variants. U.S. patent 5,573,931.

4. Guettler, M. V., M. K. Jain, and B. K. Soni. 1996. Process for making succinic acid, microorganisms for use in the process and methods of obtaining the microorganisms. U.S. patent 5,504,004.

5. Guettler, M. V., D. Rumler, and M. K. Jain. 1999. *Actinobacillus succinogenes* sp. nov., a novel succinic-acid-producing strain from the bovine rumen. Int. J. Syst. Bacteriol. 49:207-216.

6. Hase, C. C., N. D. Fedorova, M. Y. Galperin, and P. A. Dibrov. 2001. Sodium ion cycle in bacterial pathogens: evidence from cross-genome comparisons. Microbiol. Mol. Biol. Rev. 65:353-370.

7. Hasona, A., Y. Kim, F. G. Healy, L. O. Ingram, and K. T. Shanmugam. 2004. Pyruvate formate lyase and acetate kinase are essential for anaerobic growth of *Escherichia coli* on xylose. J. Bacteriol. 186:7593-7600.

8. Hong, S. H., and S.Y. Lee. 2001. Metabolic flux analysis for succinic acid production by recombinant *Escherichia coli* with amplified malic enzyme activity. Biotechnol. Bioeng. 74:89-95.

9. Kacser, H., and L. Acerenza. 1993. A universal method for achieving increases in metabolite production. Eur. J. Biochem. 216:361-367.

10. Kim, P., M. Laivenieks, J. McKinlay, C. Vieille, and J. G. Zeikus. 2004. Construction of a shuttle vector for the overexpression of recombinant proteins in *Actinobacillus succinogenes*. Plasmid 51:108-115.

11. Lee, S. J., H. Song, and S. Y. Lee. 2006. Genome-based metabolic engineering of *Mannheimia succiniciproducens* for succinic acid production. Appl. Environ. Microbiol. 72:1939-1948.

12. Niederberger, P., R. Prasad, G. Miozzari, and H. Kacser. 1992. A strategy for increasing an in vivo flux by genetic manipulations. The tryptophan system of yeast. Biochem. J. 287:473-479.

13. Park, D. H., M. Laivenieks, M. V. Guettler, M. K. Jain, and J. G. Zeikus. 1999. Microbial utilization of electrically reduced neutral red as the sole electron donor for growth and metabolite production. Appl. Environ. Microbiol. 65:2912-2917.

14. Park, D. H., and J. G. Zeikus. 1999. Utilization of electrically reduced neutral red by *Actinobacillus succinogenes*: physiological function of neutral red in membrane-driven fumarate reduction and energy conservation. J. Bacteriol. 181:2403-2410.

15. Redfield, R. J., A. D. Cameron, Q. Qian, J. Hinds, T. R. Ali, J. S. Kroll, and P. R. Langford. 2005. A novel CRP-dependent regulon controls expression of competence genes in *Haemophilus influenzae*. J. Mol. Biol. 347:735-747.

16. Reyrat, J. M., V. Pelicic, B. Gicquel, and R. Rappuoli. 1998. Counterselectable markers: untapped tools for bacterial genetics and pathogenesis. Infect. Immun. 66:4011-4017.

17. Stols, L., and M. I. Donnelly. 1997. Production of succinic acid through overexpression of NAD^+-dependent malic enzyme in an *Escherichia coli* mutant. Appl. Environ. Microbiol. 63:2695-2701.

18. Ullmann, R., R. Gross, J. Simon, G. Unden, and A. Kroger. 2000. Transport of C_4-dicarboxylates in *Wolinella succinogenes*. J. Bacteriol. 182:5757-5764.

19. van der Werf, M. J., M. V. Guettler, M. K. Jain, and J. G. Zeikus. 1997. Environmental and physiological factors affecting the succinate product ratio during carbohydrate fermentation by *Actinobacillus sp.* 130Z. Arch. Microbiol. 167:332-342.

20. Wang, Y., S.D. Goodman, R.J. Redfield, and C. Chen. 2002. Natural transformation and DNA uptake signal sequences in *Actinobacillus actinomycetemcomitans*. J. Bacteriol. 184:3442-3449.